Fungi for Future
Biotechnological application of anaerobic fungi

Zur Erlangung des akademischen Grades eines

DOKTORS DER NATURWISSENSCHAFTEN

von der KIT-Fakultät für Chemieingenieurwesen und Verfahrenstechnik des
Karlsruher Instituts für Technologie (KIT)
genehmigte

DISSERTATION

von

M. Sc. Marcus Stabel
aus Otterstadt

Tag der mündlichen Prüfung: 20.12.2021

Erstgutachter: Prof. Dr. Christoph Syldatk

Zweitgutachterin: PD Dr.-Ing Katrin Ochsenreither

For those who were with me since the beginning,

For those who accompanied me on this part of my path,

In remembrance of those who would have liked to witness this moment with me.

Preamble

This doctoral thesis explores the isolation and biotechnological implementation of anaerobic fungi from the phylum *Neocallimastigomycota*. Parts of this text have been published as peer review research articles. Relevant chapters have been indicated as such at the beginning and their content might be identical to the content of the corresponding publication. Citation style, layout, figures, formatting and parts of the text have been modified accordingly to fit the style of this thesis. All articles were drafted during this work and describe major results of it.

Chapter 3 describes the isolation of a novel genus and species of the phylum *Neocallimastigomycota* and has been published as:

***"Aestipascuomyces dupliciliberans gen. nov, sp. nov.*, the first cultured representative of the uncultured SK4 clade from aoudad sheep and alpaca"** by Marcus Stabel, Radwa Hanafy, Tabea Schweitzer, Meike Greif, Habibu Aliyu, Veronika Flad, Diana Young, Michael Lebuhn, Mostafa Elshahed, Katrin Ochsenreither and Noha H. Youssef in *Microorganisms* 2020, *8*, 1734, doi:10.3390/microorganisms8111734

The fourth chapter describes the isolation of five additional anaerobic fungal strains and the biochemical characterization of those as well as of the isolate described in Chapter 3. The obtained results were published as:

"Isolation and Biochemical Characterization of Six Anaerobic Fungal Strains from Zoo Animal Feces" by Marcus Stabel, Tabea Schweitzer, Karoline Haack, Pascal Gorenflo, Habibu Aliyu and Katrin Ochsenreither in *Microorganisms* 2021, 9, 1655. https://doi.org/10.3390/microorganisms9081655.

The establishment of a stirred tank reactor batch-process of one of the isolates and further examination of its metabolism is content of chapter 5. This content was also published as:

"Metabolic shift towards increased biohydrogen production during dark fermentation in the anaerobic fungus Neocallimastix cameroonii G341" by Marcus Stabel, Karoline Haack, Hannah Lübbert, Meike Greif, Pascal Gorenflo, Habibu Aliyu and Katrin Ochsenreither in *Biotechnology for Biofuels and Bioproducts* 2022, 15, 96. doi:10.1186/s13068-022-02193-z

Chapter 6 deals with the heterologous expression of enzymes from anaerobic fungi for xylan degradation and has been published as:

"Characterization and phylogenetic analysis of a novel GH43 β-xylosidase from *Neocallimastix californiae*" by Marcus Stabel, Julia Hagemeister, Zacharias Heck, Habibu Aliyu and Katrin Ochsenreither in *Front. Fungal Biol.* 2021, *2*, 23, doi:10.3389/ffunb.2021.692804.

Acknowledgements

I´m grateful to have been allowed to research and learn these past years of my doctoral thesis in the group of Prof. Dr. Christoph Syldatk. I especially want to thank my supervisor PD Dr.-Ing Katrin Ochsenreither for her continuous support during this thesis, her advice, the discussions and, of course, for sharing her addiction to tea with me. You taught me a lot and without you and your enthusiasm for fungi, this thesis would never have been possible.

I thank Dr. Habibu Aliyu for introducing me to and teaching me everything I know about bioinformatics and phylogeny. Thank you for all the on- and off topic discussions over theses last years. It has been a real pleasure to work with you.

I´m grateful to Dr. Veronika Flad, Diana Young, Dr. Michael Lebuhn and the rest of the group of the LfL Freising for kindly welcoming me at their institute and introducing me into the culture of anaerobic fungi.

I thank the staff members of TeBi for their continued help and support. Especially, I would like to thank Michaela (Minerva) Kugel, for her help with the bioreactor systems, Pascal Gorenflo(w), for his support during HPLC measurements and lunch procurement, and Daniela Rambow, for her enthusiasm for anaerobic fungal cultures. Another special thanks goes to Susanne Warth and Beate Skolik, without your help I wouldn’t have managed to navigate through all the bureaucracy and formalities.

I thank my PhD colleagues for their help, their support and the willingness to start drinking beer in the middle of a bad day. Thank you for being with me in this insanity!

I want to thank my students, Julia Hagemeister, Tabea Schweitzer, Meike Greif, Hannah Lübbert, Zacharias Heck and Karoline Haack. Without you guys, the sheer workload of this thesis wouldn’t have been possible. Thank you for your motivation, intelligence and cheerfulness. It was a pleasure to supervise you.

I want to give a special thanks to my family for always supporting me during these past years. Without you, I wouldn´t have made it this far.

Last but not least I want to thank Carolin Lohmann. Your love, support and belief in me kept me going when nothing else could.

List of publications

Peer review publications implied in this thesis:

1. *Aestipascuomyces dupliciliberans gen. nov, sp. nov.*, the first cultured representative of the uncultured SK4 clade from aoudad sheep and alpaca

Marcus Stabel*, Radwa Hanafy*, Tabea Schweitzer, Meike Greif, Habibu Aliyu, Veronika Flad, Diana Young, Michael Lebuhn, Mostafa Elshahed, Katrin Ochsenreither and Noha H. Youssef *Microorganisms* **2020**, *8*, 1734, doi:10.3390/microorganisms8111734

*shared first authorship

2. Characterization and phylogenetic analysis of a novel GH43 β-xylosidase from *Neocallimastix californiae*

Marcus Stabel, Julia Hagemeister, Zacharias Heck, Habibu Aliyu and Katrin Ochsenreither *Front. Fungal Biol.* **2021**, *2*, 23, doi:10.3389/ffunb.2021.692804.

3. Isolation and Biochemical Characterization of Six Anaerobic Fungal Strains from Zoo Animal Feces

Marcus Stabel, Julia Hagemeister, Zacharias Heck, Habibu Aliyu and Katrin Ochsenreither *Microorganisms* **2021**, 9, 1655, doi:10.3390/microorganisms9081655.

4. Metabolic shift towards increased biohydrogen production during dark fermentation in the anaerobic fungus Neocallimastix cameroonii G341

Marcus Stabel, Karoline Haack, Hannah Lübbert, Meike Greif, Pascal Gorenflo, Habibu Aliyu and Katrin Ochsenreither *Biotechnology for Biofuels and Bioproducts* **2022**, 15, 96. doi:10.1186/s13068-022-02193-z

Abstract

Utilization of lignocellulose containing materials will play an essential role in the transition from a fossil-based to a bio-based economy. However, due to the required pretreatment the biotechnological conversion of lignocellulose is energy intensive and/or produces toxic wastes and by-products. Hydrogen could be a promising green energy carrier in a future bio-based economy but is currently mainly produced from fossil materials. An alternative option might be the biological hydrogen production from lignocellulose, however, this technique is limited by the energy requirements for lignocellulose conversion.

Anaerobic fungi of the phylum *Neocallimastigomycota* are able to grow directly on lignocellulosic biomass employing a wide array of lignocellulolytic enzymes. Hydrogen is produced as a metabolic end-product, along other valuable products like acetate, formate, lactate, ethanol and succinate. Despite their high biotechnological potential, general knowledge about these organisms or their enzymes is limited. Basic growth requirements are understudied and metabolic pathways and their regulation remain to be elucidated. This thesis aims to address this situation and establishes the principles for anaerobic fungi biotechnological application.

One of the challenges to overcome when working with anaerobic fungi is the unavailability to obtain these microorganisms from culture collections. Therefore, an isolation from feces of different zoo animals was performed and a total of six different isolates were obtained. A strain isolated from alpaca feces proved to be a fungus that was only known from environmental sequences as SK4 clade. Interestingly, the same fungus was isolated from an aoudad sheep rumen sample by a group from Texas, USA at the same time. This finding was published in a cooperation between both institutes and is described in chapter 3. Isolates from both locations showed nearly identical morphological and microscopic features, forming medium-sized (2-5 mm) white filamentous colonies with a white center of sporangia on agar roll tubes and a heavy biofilm in liquid media. Microscopic analysis revealed monocentric thalli, and spherical poly-flagellated zoospores with 7–20 flagella. Zoospore release occurred through an apical pore as well as by sporangial wall rupturing, a duality that is unique amongst described anaerobic gut fungal strains. Phylogenetic assessment based on the D1-D2 28S large rRNA gene subunit (LSU) and internal transcribed spacer-1 (ITS-1) regions demonstrated high sequence identity (minimum identity of 99.07 % and 96.96 %, respectively) between all isolates; but low sequence identity (92.4 % and 86.7 %, respectively) to their closest cultured relatives. LSU phylogenetic trees grouped the isolates as a new monophyletic clade within the *Orpinomyces-Neocallimastix-Pecoramyces-Feramyces-Ghazallamyces* supragenus group. LSU and ITS-1 sequences recovered from the obtained isolates were either identical, or displayed extremely high sequence similarity to sequences recovered from the same aoudad sheep sample on which isolation was conducted, as well as several sequences recovered from domestic sheep and few other herbivores. Interestingly, members of the SK4 clade seem to be encountered preferably in animals grazing on summer pasture. Consequently, the novel isolates were accommodated in a new genus, *Aestipascuomyces* (derived from the Latin word for "summer pasture"), and a new species, *A. dupliciliberans*.

The other obtained isolates could be assigned to the existing *Neocallimastigomycota* genera and species *Neocallimastix cameroonii*, *Caecomyces spec.*, *Orpinomyces joyonii*, *Pecoramyces ruminantium*, and *Khoyollomyces ramosus* as described in chapter 4. During the phylogenetic assignation of the isolates a high similarity between species of the genus *Neocallimastix* was noticed, leading to the reassignment of *Neocallimastix californiae* and *Neocallimastix lanati* to *Neocallimastix cameroonii*. Similarly, the phylogeny pointed towards a redesignation of the genus *Cyllamyces* as a species of *Caecomyces*. Chapter 4 further describes the biochemical analysis of all isolates including the one described in chapter 3. The fungi were grown on different carbon sources and the produced metabolites were analyzed with hydrogen, acetate, formate, lactate, ethanol and succinate being the main products. *Orpinomyces joyonii* was lacking succinate production and *Khoyollomyces ramosus* was not able to produce lactate under the studied conditions. The results further suggested a sequential production of metabolites with a preference for hydrogen, acetate, and formate. By comparing fungal growth on

monosaccharides and wheat straw, a higher hydrogen production was noticed on the latter hinting a possible reaction to elevated sugar concentrations.

The most robust isolate, *Neocallimastix cameroonii* G341, was further studied for implementation in dark fermentation, which is described in chapter 5. While testing different nitrogen sources only glutamine and ammonium led to growth of this isolate. The fungus grew optimally in a temperature range between 38.5 °C and 41.5 °C and preferred an initial pH range of pH 6.6-6.8 in bottle experiments. The highest hydrogen production was achieved at slightly lower pH value between 6.4 and 6.6. Addition of hydrogen at the beginning of the experiment led to a decrease in hydrogen production. In contrast increasing the volume of the gas phase or agitation of the bottle resulted in an increase of hydrogen production and in most cases to a decrease of lactate and ethanol amounts. By combination of both parameters, ethanol and lactate production were strongly decreased leaving hydrogen, acetate and formate as only products. Succinate, if detected, was only present in traces. After establishing the bioreactor process in a stirred tank reactor system, the effects on hydrogen production could be confirmed as hydrogen production increased with the stirrer speed. While an increase from 0 rpm to 250 rpm also increased the speed of hydrogen production, increasing it further to 600 rpm delayed the production of hydrogen. A similar effect was observed when comparing pH regulated vs. unregulated bioprocesses: a constant pH of 6.8 resulted in a doubling of all metabolites except lactate. These results led to the conclusion that hydrogen might be the preferred way of electron disposal in *Neocallimastix cameroonii* and lactate and ethanol are only produced when hydrogen production is thermodynamically impaired. The highest hydrogen yield (2.406 mmol/g = 58.84 ml/g) achieved with straw as sole carbon source was obtained in bottle experiments using 5 g/l straw with increased head space volume and agitation. In comparison to literature references this corresponds roughly to 33%-50% of reported dark fermentation yields. However, those literature results were obtained only after extensive substrate pretreatment unnecessary for the fungal process that has furthermore not been optimized yet.

Although the biomass degrading capabilities of anaerobic fungi are widely known and a variety of the lignocellulose degrading enzymes have been expressed heterologously, knowledge on the biochemical properties of these enzymes is limited, particularly for enzymes degrading hemicellulose which have received less attention compared to enzymes for cellulose degradation. Therefore, chapter 6 describes the heterologous expression of a *Neocallimastigomycota* hemicellulases and their biochemical characterization. A GH43 xylosidase, Xyl43Nc, and a GH11 endoxylanase, X11Nc, from the anaerobic fungus *Neocallimastix californiae* were heterologously expressed in *Escherichia coli* after being identified by screening the putative proteome. Xyl43Nc was highly active against 4-Nitrophenol-xylopyranosides with a K_m of 0.72 mM, a k_{cat} of 29.28 s^{-1}, exhibiting a temperature optimum of 32 °C and a pH optimum of 6. When combined, Xyl43Nc and X11Nc released xylose from beechwood xylan and arabinoxylan from wheat. Phylogenetic analysis revealed that Xyl43Nc shares common ancestry with enzymes from *Spirochaetes* and groups separately from Ascomycete sequences in the phylogeny, indicating an acquisition through horizontal gene transfer.

In summary this thesis lays the foundation for a future biotechnological application of anaerobic fungi and their enzymes.

Zusammenfassung

Der Verwendung Lignocellulose-haltiger Rohstoffe wird eine essentielle Rolle beim Übergang von einer auf fossilen Rohstoffen basierenden zu einer biobasierten Ökonomie beigemessen. Die für die biotechnologische und chemische Nutzbarmachung von Lignocellulose als Ausgangssubstrat nötige Vorbehandlung ist jedoch energieintensiv und/oder produziert toxische Abfälle und Nebenprodukte. Wasserstoff ist ein vielversprechender Energieträger für eine zukünftige Bioökonomie, der jedoch zurzeit hauptsächlich aus fossilen Rohstoffen gewonnen wird. Eine Alternative bietet die biologische Wasserstoffproduktion auf Basis von Lignocellulose, die jedoch zurzeit durch den hohen Energiebedarf der Lignocellulose-Vorbehandlung sowie niedriger Ausbeuten bisher eher unbedeutend ist.

Anaerobe Pilze des Phylums *Neocallimastigomycota* können durch die Sekretion einer Vielzahl von Lignocellulose abbauenden Enzymen auf unvorbehandelter Biomasse wachsen und produzieren hierbei Wasserstoff und andere Plattformchemikalien wie Acetat, Formiat, Lactat, Ethanol und Succinat als metabolische Endprodukte. Trotz des hohen biotechnologischen Potenzials sind diese Organismen und ihre Enzyme weitgehend unerforscht. So sind grundlegende Wachstumsvoraussetzungen nahezu unbekannt und Kenntnisse über ihre Stoffwechselwege und deren Regulierung sind noch begrenzt. Durch Untersuchung dieser Aspekte soll diese Arbeit den Grundstein für eine biotechnologische Anwendung von anaeroben Pilzen legen.

Die Nichtverfügbarkeit anaerober Pilz-Stämme in Stammsammlungen stellt eine der Herausforderungen bei der Arbeit mit diesen Organismen da. Der erste Schritt war daher eine Isolation aus dem Kot unterschiedlicher Zootiere, was zum Erhalt von sechs verschiedenen Isolaten führte. Ein aus Alpakakot isolierter Stamm stellte sich als eine neue Pilzgattung und -art heraus, die zuvor nur als SK4-Klade von sequenzierten Umweltproben bekannt war. Interessanterweise wurde der gleiche Stamm gleichzeitig aus dem Pansen eines Mähnenspringers in Texas, USA isoliert. Die Kooperation unserer Forschergruppen mündete in einer gemeinsamen Publikation, welche Kapitel 3 bildet. Isolate von beiden Orten waren nahezu identisch. Sie bildeten mittelgroße (2-5 mm) Kolonien mit einem weißen Zentrum aus Sporangien auf Agar und einen Biofilm aus Myzel in flüssigem Medium. Mikroskopisch waren monozentrische Thalli und sphärische poly-flagellierte Zoosporen mit 7-20 Flagellen zu erkennen. Sowohl die Öffnung einer apikalen Pore des Sporangiums wie auch das Aufbrechen der sporangialen Zellwand führten zur Freisetzung der Zoosporen. Dieser duale Mechanismus ist bisher einzigartig unter allen derzeit beschriebenen anaeroben Pilz-Stämmen. Ein phylogenetischer Vergleich anhand der Sequenzen der D1-D2 28S Untereinheit des rRNA Gens (LSU) und des *internal transcribed spacer 1* (ITS1) wies hohe Identitätsübereinstimmungen zwischen allen Isolaten (geringste Identität jeweils 99,07 % und 96,96 %) aber geringe Übereinstimmung zu den nächsten Verwandten auf (jeweils 92,4 % und 86.7 %). Anhand der LSU konstruierte phylogenetische Bäume ordneten die Isolate als neue monophyletische Gruppe in der *Orpinomyces-Neocallimastix-Pecoramyces-Feramyces-Ghazallamyces* Klade ein. Sowohl die LSU wie auch die ITS1 Sequenzen der Isolate wiesen eine hohe Sequenzidentität zu Umweltproben aus Schafen und verschiedenen anderen Herbivoren auf. Interessanterweise wurden diese Proben der SK4-Klade hauptsächlich bei Tieren gefunden, die auf Sommerweiden grasten, woraus sich die Benennung der neuen Gattung, *Aestipascuomyces* (abgeleitet vom lateinischen Wort für „Sommerweide“), und der Spezies, *A. dubliciliberans*, ableitete.

Die übrigen fünf Isolate konnten, wie in Kapitel 4 beschrieben, den bereits bekannten *Neocallimastigomycota* Gattungen und Spezies *Neocallimastix cameroonii*, *Caecomyces spec.*, *Orpinomyces joyonii*, *Pecoramyces ruminantium*, und *Khoyollomyces ramosus* zugeordnet werden. Während der phylogenetischen Analyse wurde eine hohe Ähnlichkeit zwischen Spezies der Gattung *Neocallimastix* bemerkt, was zur Neuzuweisung von *Neocallimastix californiae* und *Neocallimastix lanati* zu *Neocallimastix cameroonii* führte. Die Daten befürworteten ebenfalls eine Neuzuweisung der Gattung *Cyllamyces* als Spezies der Gattung *Caecomyces*. Kapitel 4 beschreibt ebenfalls die biochemische Charakterisierung aller Isolate inklusive des in Kapitel 3 beschriebenen. Die Pilze wurden auf verschiedenen Kohlenstoffquellen kultiviert und die Produktion der Metabolite Wasserstoff, Acetat, Formiat, Lactat, Ethanol und Succinat, analysiert. Unter den getesteten

Bedingungen produzierte *Orpinomyces joyonii* kein Succinat und *Khoyollomyces ramosus* kein Lactat. Die Ergebnisse wiesen des Weiteren auf eine sequenzielle Produktion der Metabolite unter Bevorzugung von Wasserstoff, Acetat und Formiat hin. Beim Vergleich der Metabolitproduktion während des Wachstum auf Monosacchariden und auf Stroh fiel eine höhere Wasserstoffproduktion bei letzterem auf. Dies könnte auf eine Reaktion des Metabolismus auf erhöhte Zuckerkonzentrationen hindeuten.

Für das robusteste Isolat, *Neocallimastix cameroonii* G341, wurde ein Dunkelfermentationsprozess im Rührkessel-Bioreaktor entwickelt, was in Kapitel 5 beschrieben ist. Dazu wurden im Vorfeld weitere Optimierungen bezüglich Medienzusammensetzung und Kultivierungsbedingungen vorgenommen. Beim Testen verschiedener Stickstoffquellen führten nur Glutamin und Ammonium zum Wachstum des Isolates. Der Pilz wuchs optimal in einem Temperaturbereich von 38,5 °C bis 41,5 °C und präferierte initiale pH-Werte zwischen 6,6 und 6,8. Die höchste Wasserstoffproduktion fand jedoch bei einem initialen pH-Wert von 6,4 bis 6,6 statt. Zugabe von Wasserstoff zu Beginn des Experiments verringerte die Wasserstoffproduktion. Im Gegensatz dazu konnte durch Erhöhung des Kopfraumvolumens oder durch Agitation die Wasserstoffproduktion erhöht werden, was mit einem Abfall der gebildeten Lactat- und Ethanol-Konzentrationen einherging. Durch Kombination beider Parameter sanken Lactat- und Ethanolproduktion soweit, dass Wasserstoff, Acetat und Formiat nahezu die einzigen Produkte waren. Succinat konnte, wenn überhaupt, nur in Spuren nachgewiesen werden. Nach Etablierung des Prozesses im Rührkesselreaktor konnten die Ergebnisse aus dem Flaschenversuch bestätigt werden. Die Wasserstoffproduktion stieg mit steigender Rührgeschwindigkeit an. Während der Anstieg von 0 rpm auf 250 rpm mit einem Anstieg der Geschwindigkeit der Wasserstoffproduktion einherging, verlangsamte eine weitere Steigerung auf 600 rpm dessen Produktion. Ein ähnlicher Effekt trat beim Vergleich von Fermentationsprozessen mit und ohne pH Regulation auf. Wurde der pH-Wert konstant bei 6,8 gehalten, verdoppelte sich im direkten Vergleich zu nicht-pH regulierten Prozessen die Produktion aller Metabolite mit Ausnahme von Lactat. Diese Ergebnisse führten zu dem Schluss, dass Wasserstoff der präferierte Elektronenendakzeptor von *Neocallimastix cameroonii* sein könnte. In diesem Fall würden Lactat und Ethanol nur produziert, falls eine thermodynamische Beeinträchtigung der Wasserstoffbildung vorliegt. Die höchste Wasserstoffausbeute (2,406 mmol/g = 58,84 ml/g) resultierte aus Flaschenversuchen mit 5 g/l Stroh als einziger Kohlenstoffquelle mit erhöhtem Kopfraumvolumen und Agitation. Im Literaturvergleich entspricht dies ungefähr 33-50 % der für die Dunkelfermentation angegebenen Wasserstoffausbeuten auf Basis von Stroh. Allerdings wurden bei diesen Studien diese Ausbeuten nur nach einer intensiven Vorbehandlung des Strohs erzielt. Weiterhin ist der hier beschriebene Prozess mit anaeroben Pilzen noch nicht optimiert.

Auch wenn das Potential anaerober Pilze, lignocellulose-haltige Biomasse effizient zu hydrolysieren, weithin bekannt ist, und eine Vielzahl ihrer Enzyme bereits heterolog exprimiert wurden, sind die wenigsten biochemisch charakterisiert. Dies betrifft besonders hemicellulolytische Enzyme, welche verglichen mit cellulolytischen Enzymen weit weniger erforscht sind. Kapitel 6 behandelt daher die Expression von *Neocallimastigomycota* Hemicellulasen und deren biochemische Charakterisierung. Nach ihrer Identifikation im Pilzproteom von *Neocallimastix californiae* konnten die GH43 Xylosidase Xyl43Nc und die GH11 Endoxylanase X11Nc in *Escherichia coli* exprimiert werden. Xyl43Nc wies eine hohe Aktivität gegen 4-Nitrophenol-Xylopyranosid (K_m = 0,72 mM und k_{cat} = 29,28 s^{-1}) bei einem Temperaturoptimum von 32 °C und einem pH Optimum von 6 auf. Bei gemeinsamer Verwendung von Xyl43Nc und X11Nc konnte Xylose aus Buchenholzxylan und Weizen-Arabinoxylan freigesetzt werden. Phylogenetische Analysen von Xyl43Nc zeigten einen gemeinsamen Ursprung mit Enzymen aus Spirochaeten. Das Enzym bildete eine monophyletische Gruppe abseits der Sequenzen von Ascomyceten im phylogenetischen Baum. Hieraus ließ sich ein Ursprung des Enzyms aus horizontalem Gentransfer ableiten.

Zusammengefasst legt diese Arbeit den Grundstein für eine zukünftige biotechnologische Anwendung anaerober Pilze und deren Enzyme.

Table of contents

1 Introduction

The effects of human made climate change [1] have been recognized by most governments. Several nations have developed strategies for the transition from a fossil fuel based economy towards a circular bio-based economy to reduce these effects with an example being the German national bio-economy strategy [2]. The concept of a bio-based economy is based on the fixation of CO_2 by plant growth enabled by sun light. When fuels produced from plant biomass are combusted, only the previously sequestered CO_2 is released, resulting in an overall balance of zero CO_2 emissions. Substrates for the production of biofuels have been categorized into generations [3]. The first generation consisted of potentially edible crops, thereby being in direct competition with food production. This leads to the "food vs fuel" dilemma that raises moral issues of investing agricultural resources in fuel production potentially jeopardizing the world wide food security [4]. In addition to the ethical issue, first generation biofuels have a high production cost because of the resources expended in their growth [3]. Second generation substrates are agricultural waste products, forest residues and other side streams, thereby avoiding the competition with food production [3]. As waste product and being coproduced with other products these substrates are cheap(er). The main setback is the energy input required for their conversion to fuel. While this work focuses on the second generation of biofuel substrates it is worth mentioning that further generations exist. The third generation encompasses the use of macro- and microalgae for fuel production [3]. While growth of these is cheap and fast, the processing costs are high. The fourth generation tries to remedy the problems of the other generations by genetic modification, whereby also focusing on algae.

The main problem of using second generation biofuel substrates is the energy input required for its conversion due to the high lignocellulose content. Lignocellulose is a complex component of plant cell walls that is composed of three main factions: cellulose, hemicellulose and lignin. The relative quantities of these components vary greatly from plant to plant [5]. The main component cellulose is a linear polymer of glucose molecules linked by β-1,4-glycosidic bonds [6]. These chains attach to each other via hydrogen and Van der Waals bonds forming microfibrils. The hemicellulose fraction enveloping these fibrils is much more heterogeneous. While it also consists of a backbone of saccharides linked by β-1,4-glycosidic bonds, the composition of these saccharides varies greatly [7]. Another difference to cellulose is the further substitution of the backbone. Some of those substituents are other saccharides, acetylations and methylations. The saccharides can vary in length from monosaccharides to entire side chains. Several different hemicellulose-types can be defined depending on the constitution of the backbone with the main types being xyloglucans, xylans, mannans, glucomannans and β-1,3-1,4-glucans. These can be further differentiated depending on the substituents of the backbone. Which types are present in the respective lignocellulose depends on the plant species. When broken down to monosaccharides the hemicellulose fraction consists of glucose, xylose, mannose, galactose, glucuronic acid, arabinose, fucose and rhamnose with the exact composition depending on the respective hemicellulose type. Lignin is built up by the three monolignols p-coumaryl alcohol, coniferyl alcohol, and sinapyl alcohol [8]. These three components are randomly cross-linked and their relative composition varies between plants. Hemicelluloses and cellulose are linked through hydrogen bonding, while hemicelluloses and lignin form covalent bonds [9]. Due to this bonding a three-dimensional structure is formed with hemicelluloses and lignin being wrapped around the cellulose microfibrils. The complex structure leads to the high resistance of lignocellulose against degradation. For thermal conversion to fuel high pressures and/or temperatures are required [10] explaining the aforementioned high energy demand. Biological conversion in contrast only requires ambient pressures and temperatures decreasing the energy demand with the setback of being rather slow. Therefore, pretreatment of lignocellulose before biotechnological use is indispensable. The high interest in the use of lignocellulose for industrial purposes has led to a wide research area and the development of a plentitude of methods that can be roughly classified in chemical, physicochemical, physical and biological. These methods have been reviewed in detail by several authors [5,11]. Until now all methods have several setbacks [5] mainly high cost, high energy input, environmental hazard or the production of toxic byproducts making fuel production from lignocellulose unfeasible.

One possible second generation fuel is bio-based hydrogen. Up to now hydrogen is mainly used for refining, ammonia production, methanol production and direct reduced steal production with a total demand of around 70 million tons in 2018 [12]. A lot of "green" strategies focus on hydrogen as a future fuel [13,14] which will increase the demand eventually. Currently, hydrogen is produced mainly from fossil fuels with the main substrates being natural gas, coal and oil [12]. These substrates are converted by reforming or gasification producing between 10 and 19 tons of CO_2 per ton of hydrogen. The most known non-fossil-based alternative is electrolysis. While the hydrogen production through water-electrolysis is marginal (<0.1%) around 2 % of the total global hydrogen are produced as side product during chlor-alkali electrolysis [12]. Apart from established processes other experimental procedures like the biological hydrogen production exist. The main advantage of these processes when compared to the other possibilities of hydrogen production is the lower energy cost due to lower reaction temperatures and lower pressure requirements [15]. A further advantage over chemical production is the low catalyst cost with microorganisms regenerating through growth while chemical catalysts are deactivated during the process. The setback of the fermentative ways of bio hydrogen production is the concurrence with agriculture for producing the required substrates or the pretreatment if using lignocellulose containing waste products, both having been described above. A possible solution for the general use of lignocellulose in biotechnology and specifically for hydrogen production are the anaerobic fungi of the phylum *Neocallimastigomycota*.

Neocallimastigomycota inhabit the gut of a variety of herbivores [16], playing an essential role in the degradation of ingested plant material. Due to their natural function they can grow on a variety of unpretreated biomasses and show the highest variety of lignocellulose degrading enzymes of the fungal kingdom [17]. During growth hydrogen is produced accompanied with other valuable products like acetate, formate, lactate and ethanol [18,19]. Despite this prominent attributes for biotechnological exploitation they remain widely understudied. The exact requirements for their growth are unknown [20] and their strict anaerobic nature impedes the utilization of most standard procedures for microorganisms. In contrast to model microorganisms, like *Escherichia coli* or *Saccharomyces cerevisiae*, strains have to be isolated and can´t be ordered from culture collections. Despite some studies investigating their application in biogas production [21], their culture in laboratories remains limited to culture bottles and no attempt of growing pure fungal cultures in stirred tank reactors has been made so far. While some of the lignocellulolytic enzymes of anaerobic fungi have been expressed heterologously [17,22], in most cases the biochemical characterization is lacking. Over the last years several genomes have been published, but a big portion of their genes remain without annotation, e.g. accounting for around 48 % in a recent study [19]. Furthermore, no techniques for genetic modification exist with exception of transient siRNA knock down in zoospores [23]. In this thesis, some of these issues will be addressed by isolation of *Neocallimastigomycota* from animal feces followed by biochemical characterization. Fungal culture in stirred tank reactors for biological hydrogen production shall be established and evaluated. In parallel, lignocellulolytic enzymes detected in the genome of an anaerobic fungus will be expressed heterologously and their properties characterized.

2 Theory and research proposal

2.1 Biological hydrogen production

Biological hydrogen production can be achieved by several mechanisms including biophotolysis, photofermentation, dark fermentation, microbial electrolysis and biological water-gas shift reaction.

Biophotolysis is a process available to cyanobacteria and green algae. It can be further devided into two separate processes called direct and indirect biophotolysis. Direct biophotolysis is a process similar to photosynthesis in higher plants [24]. In addition to reduction of CO_2 cyanobacteria and green algae are able to produce hydrogen through a hydrogenase [24], which is missing in higher plants. This alternative pathway is used if carbon fixation by photosynthesis is impaired for instance by a lack of O_2 and is thought to be an outlet for excessive electrons [25,26]. It is possible to achieve sustained H_2 production through a two-step process [27]. In a first step the organisms are grown under aerobic conditions while in the second step they are deprived of sulfur. Due to the deprivation Photosystem II is inactivated thereby obstructing photosynthetic O_2 evolution leading to the depletion of O_2 from the culture by oxidative respiration inducing H_2 production.

Indirect biophotolysis is a process mainly know from cyanobacteria [26]. Carbohydrates are produced by photosynthesis and stored [28]. In a second fermentative step produced carbohydrates are converted to H_2 and CO_2. Due to the oxygen sensitivity of hydrogenases the second step is separated from the oxygen producing photosynthesis either temporally or spatially [25]. Another hydrogen production option of some cyanobacteria is by the enzyme nitrogenase [26]. This enzyme enables the fixation of molecular nitrogen into ammonia and produces hydrogen as a by-product. If nitrogen is depleted from the atmosphere the reaction produces additional hydrogen [26,29].

Photofermentation occurs in purple non-sulfur bacteria. In contrast to the biophotolysis processes an organic substrate like, but not exclusively, acetate, lactate, malate or succinate is required [30]. These substrates act as both carbon source and electron donors entering the metabolism through the TCA cycle. Gained electrons enter the anoxygenic photosynthesis cycle where they are used to reduce quinone Q. Quinone Q translocates electrons together with protons from the cytoplasma to a cytochrome complex, which in turn releases the protons to the periplasma and transfers the electrons to the next complex of the chain. With the help of light, electrons are reduced and transferred back to quinone Q. ATP is generated though an ATPase using the proton gradient produced by the cycle between cytoplasma and periplasma. Due to the cycling the same electrons are re-used several times [31]. Hydrogen is generated through a nitrogenase in a similar process as described above, with the electrons from the anoxygenic photosynthesis cycle being transferred first to ferredoxin and then to the nitrogenase. In absence of nitrogen the process is used as an outlet for excessive reducing equivalents generating additional hydrogen [30].

Dark fermentation involves the production of hydrogen through fermentation of a carbon source without light being required. The best investigated bacteria performing this type of reaction are facultative anaerobes belonging to the genus *Enterobacteria* and obligate anaerobes belonging to the genus *Clostridia*. There are two differences between both types of dark fermentation with the first being the enzyme used to convert pyruvate to Acetyl-CoA. *Enterobacteria* catalyze the reaction through a pyruvate formate lyase (PFL) producing formate as side-product which is further metabolized to hydrogen and CO_2 by a formate hydrogen lyase (FHL) [32,33]. *Clostridia* use a pyruvate ferredoxin oxidoreductase (PFO) which reduces ferredoxin in the process forming CO_2 as a side-product. The reduced ferredoxin is then reoxidized through the hydrogenase HydA with the electrons being transferred to protons generating hydrogen. The second and main difference between both bacterial types is the ability to oxidize NADH under hydrogen formation. The NADH:ferredoxin oxidoreductase (NFOR) oxidizes NADH by transferring the electrons to ferredoxin which in turn can be oxidized under hydrogen formation as described above. Further hydrogenases like hnd directly oxidize NADH under hydrogen formation. In bifurcating hydrogenases like hydABC both ferredoxin and NADH are used for hydrogen generation at the same time. While *Clostridia* use these pathways having a theoretical

maximum hydrogen yield of 4 mol/mol glucose, *Enterobacteria* tend to lack both NFOR and hnd lowering their maximal theoretical hydrogen yield to 2 mol/mol glucose. These yields can only be achieved if no other by-products like alcohols are formed while the formation of such products lead to a loss in reducing power that could otherwise be used for hydrogen generation.

Microbial electrolysis enables conversions of substrates to hydrogen which are thermodynamically impossible under normal biological conditions. The most common substrate is acetate but other organic acids and sugars have also been successfully applied [34]. Bacteria are grown on the anode of an electrolysis cell and an external voltage is supplied to overcome the endothermic barrier of the reaction [35,36]. The substrate is oxidized to CO_2 by the bacteria. Electrons produced during this process are transferred to the anode whereas the produced protons are released to the medium. An external circuit transfers the electrons from the anode to the cathode where hydrogen is produced by reaction with the protons in the medium. When compared to the direct electrolysis of water the energy yield is roughly a factor 10 higher in microbial electrolysis because the required input energy is a factor 10 lower [37].

The biological water-gas shift reaction uses the low redox potential of CO to reduce ferredoxin [38] catalyzed by the enzyme CO dehydrogenase. The reduced ferredoxin is then used by a complex to generate a proton gradient. Hereby ferredoxin is oxidized and the electrons are transferred to protons generating hydrogen. Energy is gained through the generated proton gradient which fuels an ATP synthase.

All the described processes are still in developmental stages and to the best of my knowledge none has been commercialized yet. The technology readiness level is reported to be low e.g. 5 for dark fermentation, 4 for photofermentation and 2-4 for microbial electrolysis [15]. This is reflected in most of the economic assessments of these methods with the potential hydrogen price being highly variable even when using the same technology [39]. The main problem for these processes is the low yield coupled with being expensive up to date. A more specific overview of the challenges faced by each process is given in Table 1. To conclude, while promising the implementation of these technologies is still a mid to long term project.

Table 1: Problems and challenges of different processes for biological hydrogen production. Adopted from [15,40]

Process	**Problems and challenges**
Direct bio-photolysis	• Low yield • Low light conversion efficiency • O_2 generation
Indirect bio-photolysis	• Low yield • Low light conversion efficiency
Photofermentation	• Low yield • Low light conversion efficiency • High energy demand
Darkfermentation	• Low yield • Therodynamical limitation to 4 mol H_2/mol glucose • High by-products generation • Pretreatment (if using biomass)
Microbial electrolysis	• Expensive catalysts
Biological water-gas shift reaction	• Low growth rate • Gas-liquid mass transfer limitations

2.2 Anaerobic Fungi

As implied by their name, anaerobic fungi (AF) are obligate anaerobes which have diverged early in evolution from the rest of the fungal kingdom. Despite their biotechnological potential, general knowledge about them is scarce. The following chapters shall summarize what is known of their phylogeny, lifestyle, abilities and biotechnological potential.

2.2.1 Phylogeny of anaerobic fungi

AF were first described as flagellated protozoa based on their zoospores [41]. Orpin contradicted this with his observations in 1975 [42] and demonstrated by the occurrence of chitin in the cell walls of the zoospores that AF were effectively fungi [43]. While being placed with the related *Chytridiomycota* in the beginning, AF are forming their own phylum *Neocallimastigomycota* since 2007 [44]. The phylum *Neocallimastigomycota* contains a single class, *Neocallimastigomycetes*, with a single order, *Neocallimastigales*. The exact position of the phylum is still under debate as some authors place it as a sister clade to *Chytridiomycota* [45,46] and others place it as a distinctive phylum inside *Chytridiomycota* [47]. Recently, a novel subkingdom, *Chytridiomyceta*, was proposed inside the fungal kingdom [48]. *Chytridiomyceta* contains the related *Neocallimastigomycota*, *Monoblepharomycota* and *Chytridiomycota* as sister clades. Independent from these uncertainties AF belong to the basal clades of the fungal kingdom. The radiation of AF into distinct genera is a relatively recent event (around 66 million years ago) which coincides with the appearance of grasses (*Poaceae*) and a dietary change of mammals from insectivore to herbivore/omnivore [49]. This suggests an important role of AF in the dietary transition of their hosts to grasses. Horizontal gene transfer has played an important role in this coevolution as 2-3.46 % of AF genes originate from other organisms, mainly gut inhabitants [50].

To the best of my knowledge 20 *Neocallimastigomycota* genera have been described based on isolation up to this date, namely: *Neocallimastix*, *Piromyces*, *Caecomyces*, *Cyllamyces*, *Anaeromyces*, *Orpinomyces*, *Oontomyces*, *Buwchfawromyces*, *Pecoramyces*, *Liebetanzomyces*, *Feramyces*, *Agrisomyces*, *Aklioshmyces*, *Capellomyces*, *Ghazallomyces*, *Joblinomyces*, *Khoyollomyces*, *Tahromyces*, *Aestipascuomyces* and *Paucimyces* [51–63]. An overview of isolated AF genera and species is given in Table 2. In addition to the described isolated genera several non-cultured clades have been identified based on DNA amplicons gained from environmental sequences [64,65].

Table 2: Genera of *Neocallimastigomycota* with their assigned species. *original publication could not be obtained

Genus	Species	Description history
Neocallimastix [51]	*N. frontalis*	Described as *Callimastix frontalis* Braune 1913 [51]* Renamed as *N. frontalis* Vavra and Joyon 1966 [51]* Taxonomical assignation [51] Described as *N. patriciarum* [66]; identical with *N. frontalis* [67,68] Described as *N. variabilis* [69]; identical with *N. frontalis* [67] Described as *N. hurleyensis* [70]; identical with *N. frontalis* [68]
	N. cameroonii	Described [71] Described as *N. californiae* [72]; identical with *N. cameroonii* [73] Described as *N. lanati* [19]; identical with *N. cameroonii* [73]
Piromyces [52]	*P. communis*	Described as *Piromonas communis* [74] Renamed as *Piromyces communis* [52] Detailed morphological description [58]
	P. mae	Described [75]
	P. dumbonica	Described [75]
	P. rhizinflata	Described [76]
	P. citronii	Described [77]
	P. polycephalus	Described [78]

	P. irregularis	Described [71]
	P. finnis	Described [72]
Caecomyces [52]	*C. equi*	Described [52]; maybe identical to *C. communis* [67]
	C. communis	Described as *Sphaeromonas communis* [79] Renamed as *Caecomyces communis* [52]
	C. churrovis	Described [80]
	C. sympodialis	Described [81]
Cyllamyces [56]	*C. aberrensis*	Described [56]
Anaeromyces [57]	*A. mucronatus*	Described [57]
	A. elegans	Described as *Ruminomyces elegans* Ho et al. 1990 in Mycotaxon 39 [67]* Renamed as *Anaeromyces elegans* Ho et al. 1993 in Mycotaxon 47 [67]*
	A. robustus	Described [72]
	A. contortus	Described [82]
Orpinomyces [58]	*O. joyonii*	Described as *Neocallimastix joyonii* [83] and *O. bovis* [58] Combined to *O. joyonii* [84]
	O. intercalaris	Described Ho et al. 1994 in Mycotaxon 50 [67]*
Oontomyces [59]	*O. anksri*	Described [59]
Buwchfawromyces [60]	*B. eastonii*	Clade SK2 from environmental DNA sequences [64] Described [60]
Pecoramyces [61]	*P. ruminantium*	First described as *Orpinomyces* spec. C1A [85] Identified as *gen. nov. sp. nov* [61]
Liebetanzomyces [62]	*L. polymorphus*	Described [62]
Feramyces [63]	*F. austinii*	Clade AL6 known from environmental DNA sequences [64] Described [63]
Agriosomyces [53]	*A. longus*	Described [53]
Aklioshbomyces [53]	*A. papillarum*	Described [53]
Capellomyces [53]	*C. foraminis*	Described [53]
	C. elongatus	Described [53]
Ghazallomyces [53]	*G. constrictus*	Described [53]
Joblinomyces [53]	*J. apicalis*	Clade AL5 from environmental DNA sequences [64] Described [53]
Khoyollomyces [53]	*K. ramosus*	Clade AL1 from environmental DNA sequences [64] Described [53]
Tahromyces [53]	*T. munnarensis*	Described [53]
Aestipascuomyces [54]	*A. dubliciliberans*	Clade SK4 from environmental sequences [64] Described [54]
Paucimyces [55]	*P. polynucleatus*	Described [55]

The first descriptions of AF were based on morphological characteristics, like flagella number of the zoospores, growth form of the rhizoid or the number of reproductive centers, to determine genus and species [67]. In chapter 2.2.3 the morphological diversity of AF is discussed in more detail. Because of great variations of the morphology even within the same species, DNA barcoding has emerged as a new technique to identify AF. Through this barcoding, the genus *Piromyces* was shown to be polyphyletic [86–88], and *Pecoramyces,* which has been a member of the *Orpinomyces* clade, was separated as a distinct genus [61]. The most used barcode marker is the internal transcribed spacer region 1 (ITS1) from the ribosomal RNA operon. Because of considerable sequence variation even within a single strain [60], differences of the region length [89,90] and general heterogeneity of the region, phylogenetic analyses based on the ITS1 region can lead to inconclusive results. Koetschan *et al.* (2014) tried to remedy this by improving the alignment through secondary structure information [91], but over the last years, the D1/D2-domain from the large ribosomal subunit (LSU) has emerged as a more consistent

phylogenetic marker for AF [60,92]. The main current weakness of AF LSU phylogeny is the lack of sequences for several clades only known by their ITS1 sequences. Linking the known ITS1 and LSU sequences has recently been started to be addressed [65] and a community effort is ongoing to create a new database based on the whole ribosomal RNA operon (personal communication).

2.2.2 Ecology and effect on the host

AF have been detected in feces, saliva and/or the gut of a wide variety of domesticated and undomesticated herbivores with some examples being cattle, horses, sheep, elephant, giraffe, deer, buffalo, kangaroo and iguana [90,93,94]. A more extensive overview of AF hosts from both culture dependent and independent studies is given by Gruninger et al. [16]. The authors hypothesized that two prerequisites are required for the presence of AF in an herbivore: A specialized digestive chamber and a high retention time of ingested plant material. The composition of the AF community inside a host is mainly dependent from the host family and the feed or lifestyle of the host animal [64,65,90] (Figure 1). Geography doesn´t seem to have a big influence on the AF population of animals [16], with cases of the same fungal species being isolated on opposite sides of the world [54].

Inside of their hosts AF play an essential role in the digestion of ingested biomass. Depletion of the fungi from the rumen of sheep led to lower digestibility of the ingested biomass and less voluntary uptake of feed [95]. In contrast, the beneficial effect of AF addition to domesticated animals has been reported in several studies in sheep, cattle calves, buffalo calves and adult buffalo [96–101]. The effects included higher feedstock digestibility, more efficient nutrient utilization, increased body weight gain, higher milk production and increased fat content of the milk. Recently the positive effects of AF on

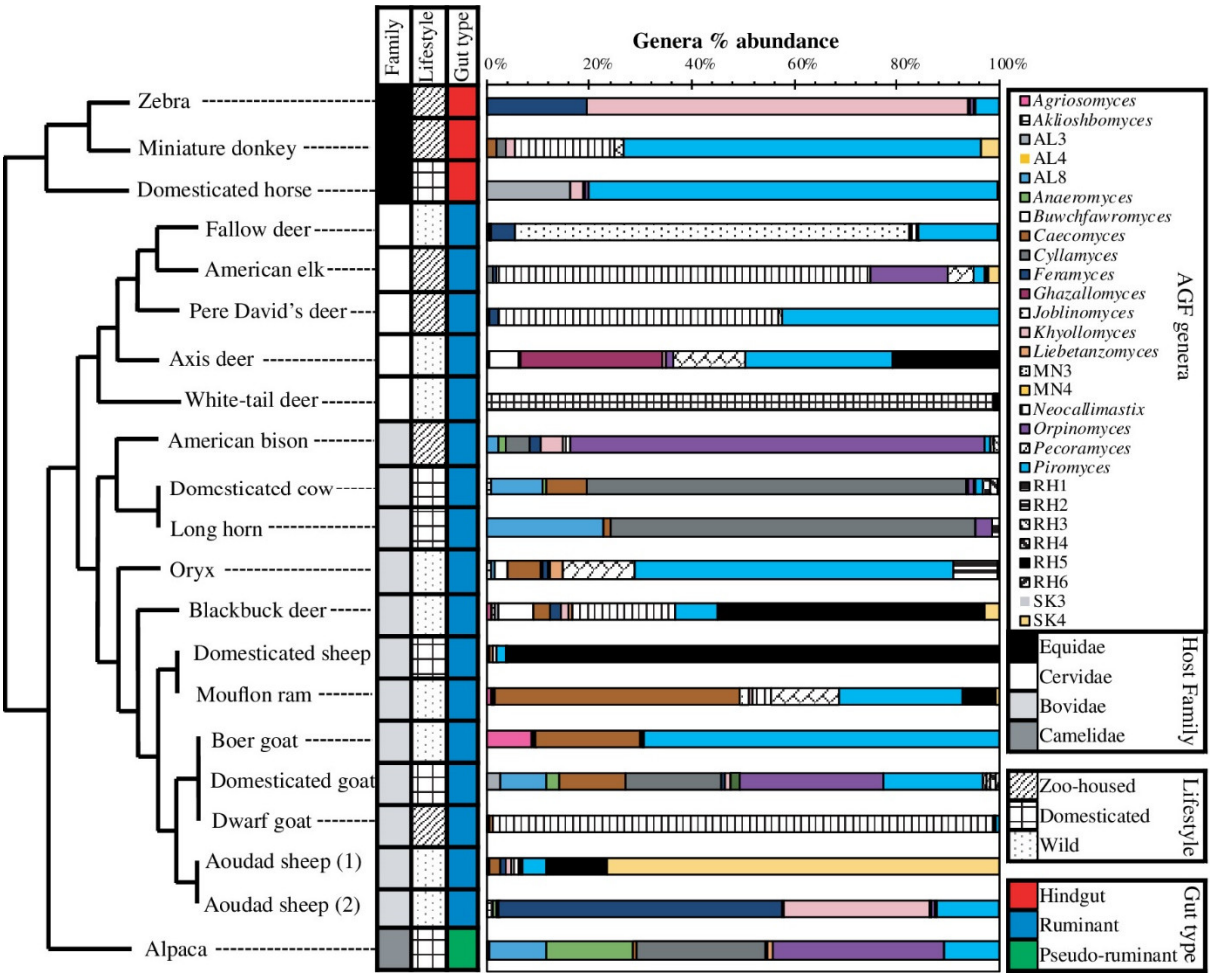

Figure 1: Distribution of AF in different host animals with comparison of gut type, lifestyle and host family. Adopted from [65]. © 2020 Society for Applied Microbiology and John Wiley & Sons Ltd., Environmental Microbiology, 22, 3883–3908.

animals and the potential use of AF as food additive for animal husbandry have been reviewed extensively [102].

2.2.3 Morphology and life cycle

AF go through a cycle of two life stages, a motile zoospore and a vegetative rhizoid stage with sporangia (Figure 2). Zoospores are round and have one or several flagella. The number of flagella is dependent from the species. AF having one to four flagella are determined as monoflagellated and fungi having more flagella as polyflagellated [67]. After the ingestion of fresh plant material zoospores are released from sporangia, the latter being described later in this text. Zoospores localize injured plant material through chemotaxis to released sugars [103]. Zoospore chemotaxis to phenolic compounds occurring in plants has also been shown [104]. Zoospores move through the beating of their flagella or in a amoeboid fashion with a switch between the two forms being possible [42,74]. The attachment to the substrate seems to happen preferably at weak spots of the plant material like ruptures or stomata [74,105]. The zoospore encysts by growing a germ tube opposite to the flagella and shedding these [42,74,79]. The development of the vegetative form at this point varies depending on the genus and can be classified into rhizoid forming or bulbous growth forms (Figure 3).

Rhizoid forming fungi form an extensive and branched rhizoid which penetrates the plant material beginning with the germ tube from the encysted zoospore. The penetration and degradation of the material is mediated mechanically through appressoria formation [106,107] and biochemically by a multitude of enzymes. Lignocellulolytic enzymes of AF are further elucidated in chapter 2.2.4. Rhizoid forming fungi can be further categorized into monocentric and polycentric fungi depending on the number of centers of reproduction [67]. In monocentric fungi (one reproductive center) the nucleus stays at the former zoospore leading to a rhizoid devoid of nuclei. There are two different growth forms of monocentric fungi. In case of endogenous development/growth a sporangium forms directly from the former zoospore. Alternatively, it is also possible for the nucleus to migrate in the opposite direction of the forming rhizoid sometimes leaving a swelling at the place of the former zoospore. This is called exogenous development/growth. After the migration of the nucleus the fungus forms a sporangium. The hypha between the former zoospore and the sporangium is called sporangiophore or sporangial stalk. Sporangiophores can be differentiated from other hyphae by two main characteristics, the afore mentioned swelling at the former zoospore location and their inability to branch. Further less specific characteristics are sporangiophores being wider than the rhizoid, swelling just beneath the sporangium or having a different shape than the rhizoid [53,60–63]. In both endogenous and exogenous development, the nuclei are located in one place and only one sporangium can be formed per former zoospore. In polycentric fungi the nucleus migrates inside the germ tube, where it divides repeatedly forming an rhizomycelium similar to other filamentous fungi [67]. The presence of several nuclei leads to the possibility of several sporangia forming at different places of the rhizoid and thus multiple reproductive centers.

Bulbous fungi form a round cell from their germ tube [52,79], which in more recent literature is called holdfast [56,80,81]. Further bulbous rhizoids and sporangiophores with sporangia grow attached to the holdfast [52,56,79,81]. The number of rhizoids and sporangiophores is determined by genus and species. While fungi of the genus *Caecomyces* develop sporangiophores carrying single sporangia, sporangiophores of the genus *Cyllamyces* are branched with several sporangia [56]. Narrow rhizoids emanating from the holdfast have also been described [52]. The distribution of nuclei is less clear then in rhizoid growing fungi. Even within the same species a variation between the nuclei being limited to the sporangia and also being present in the rest of the fungus has been reported [108]. Generally, it seems to be accepted that Caecomyces is monocentric, producing mostly one sporangium per holdfast and nuclei only being seen rarely in the holdfast. Cyllamyces in contrast is considered polycentric because of the occurrence of multiple nuclei in holdfast and sporangiophores and the usual production of several sporangia per holdfast. Recently, Cyllamyces has been suggested to be reassigned to the Caecomyces genus [73]. Taken together, a differentiation between mono- and polycentric growth in bulbous fungi is doubtable as it is at the moment. Especially when looking at the newest advances in the field, it is

possible that the differentiating morphologies of the bulbous fungi are due to differences in cultivation in dependence of the laboratory. When looking at AF in general, differences in morphology due to culture conditions have been reported [62,67].

The shape and size of the sporangia vary with genus, species and the used culture conditions. Zoospores are released as a reaction to the food ingestion of the host animal [42,74,79]. The release can also be induced by addition of oat extract or haemin to the rumen of the host [109]. How zoospores are released varies from species to species. Some fungi dissolve or rupture the sporangial cell wall yielding in the release of the zoospores [51,53,56,58] while other release their zoospores through a pore with the sporangial wall staying intact [53,61,63]. A mix of both mechanisms with a pore release followed by sporangial collapse is also known [53].

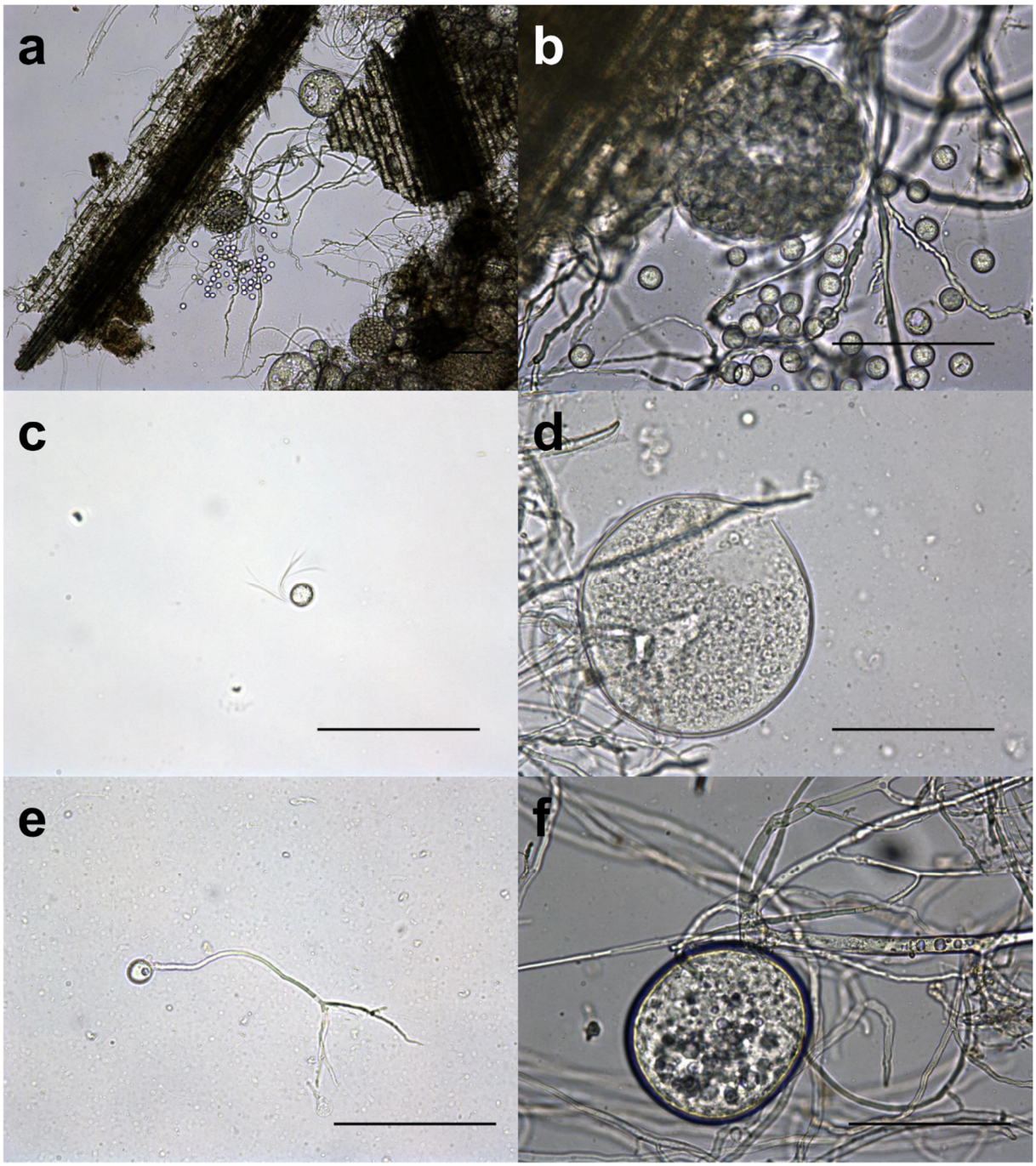

Figure 2: Life cycle of the anaerobic fungus *Aestipascuomyces dubliciliberans* strain A252. a, zoospore release from a sporangium; c, free swimming zoospore; d, sporangium after zoospore release; e, germinating zoospore; f, grown sporangium. All scale bars are 100 µm.

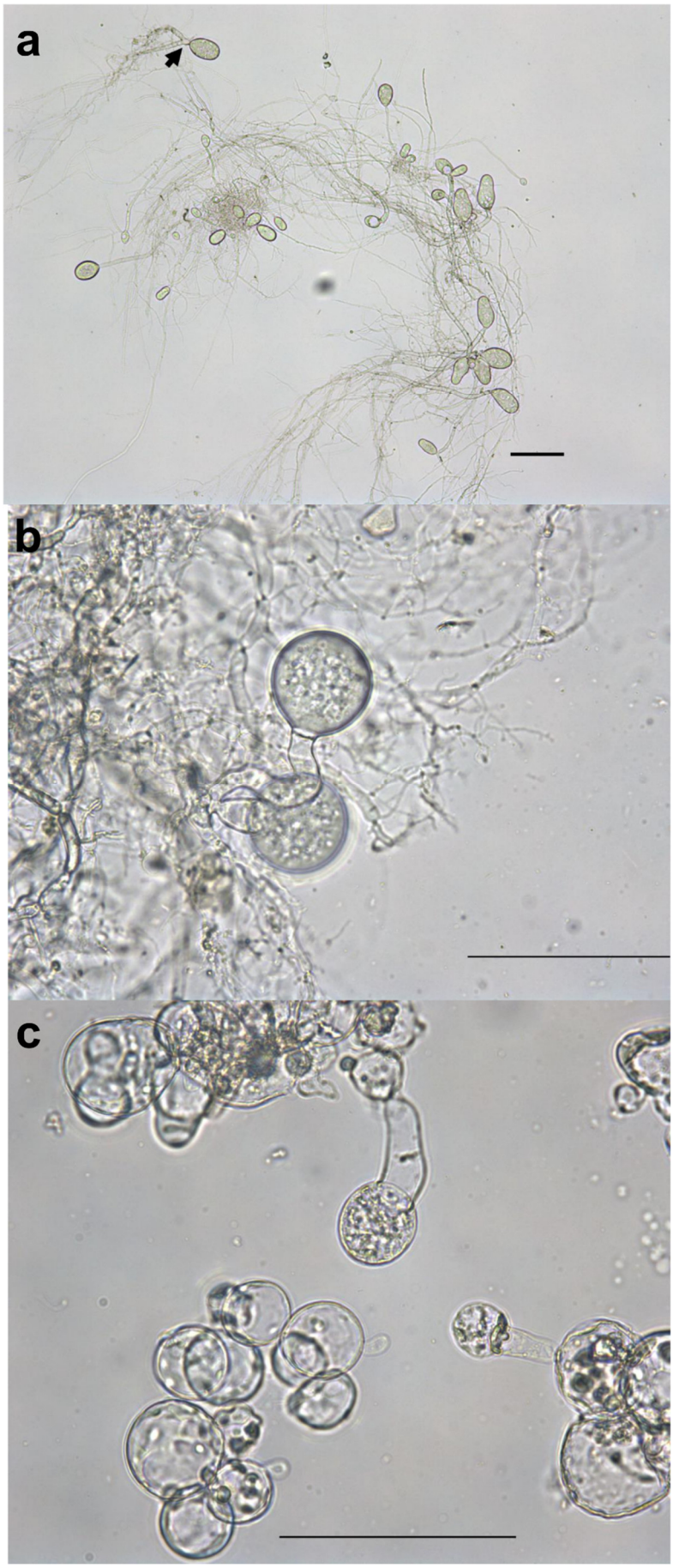

Figure 3: Growth forms of AF. a, monocentric growth of *Aestipascuomyces dubliciliberans* strain A252; b, polycentric growth of *Orpinomyces joyonii* strain W212; c, bulbuos growth of *Caecomyces spec*. strain PP313. All scale bars are 100 µm.

The described life stages are highly susceptible to oxygen exposure. The tolerance towards oxygen seems to vary between culture conditions and observed species with reports of 5 minutes [110], 12-18 hours [93] and 13.5-168 hours [111] of exposure necessary to kill the culture. In contrast, isolation from feces up to 63 days after defecation was possible with the feces being kept under natural conditions [112]. The environmental conditions seem to play a role in the survival as the same experiment performed in summer instead of winter concluded with the isolation being impossible after 7 days. Isolation of AF from feces kept up to 128 days at 20 °C or 39 °C has also been reported [93]. As mechanisms for the propagation of AF between hosts both saliva and feces have been suggested [113]. The aforementioned difference in the survival between cultures and the survival in feces implies the existence of a third life stage dedicated to survival and propagation. Production of spores is well established in other fungal phyla. A shift from the production of zoospores to melanin containing structures has been described in older cultures [114], but the structures could not be brought to germination. Sporangia found on plant material recovered from feces lead to a viable culture of AF [115]. Chambered structures in cultures of *Anaeromyces sp*. seemed to be related to a longer viability of the cultures and inoculation from older cultures showed a longer lag phase typical for inoculation with spores [116]. Despite this evidence a definite proof for the existence of the third life stage remains to be provided.

2.2.4 Biomass degradation

AF are capable degraders of unpretreated lignocellulolytic materials like wheat straw, corn stover, reed canary grass, sorghum, energy cane, alfalfa [73,85,117]. This process is mostly mediated by a multitude of enzymes. Enzymes involved in the degradation of carbohydrates are often called CAZymes (**c**arbohydrate **a**ctive en**zymes**). Within the fungal kingdom, AF contain the most CAZymes genes both in terms of amount and diversity [17] and secrete enzymes of redundant activity for optimal biomass degradation [118]. In addition AF CAZymes have been shown to be highly active and even competitive with established and optimized commercial enzymes [117,119]. Horizontal gene transfer has played an important role in the evolution of the impressive biomass degrading capability with most of AF CAZymes being of prokaryotic origin [50]. While the degradation capabilities for cellulose and hemicellulose are wide, AF seem to be lacking the ability to degrade lignin [85].

CAZymes secreted by AF can be categorized into two groups: free enzymes and cellulosome bound enzymes. The ratio of free to bound enzymes varies with 15 % - 31.4 % being cellulosome bound depending on the species [80]. Cellulosomes are enzyme complexes of several CAZymes, carbohydrate binding modules (CBM) and scaffoldin proteins. They show a higher biomass degradability than free enzymes due to the CBM mediated targeting of the substrate and the synergistic enzyme organization inside the complex [120]. The occurrence of cellulosomes in AF was described first by [121]. AF cellulosomes were shown to have evolved separately from the bacterial ones by sequence heterology [122]. The central part of the cellulosome is a scaffoldin protein with several cohesin domains [122]. These domains bind the dockerin domains of the CAZymes and the CBM mediates the cellulosome assembly. In contrast to bacteria, AF scaffoldins are conserved between species and are able to bind dockerins from different AF species enabling multispecies cellulosome complexes [122]. Interestingly, while the dockerin part of the AF CAZymes is of pure fungal origin, the catalytic part is often bacterial [122]. These attributes make the AF dockerin/cohesin system an excellent candidate for the design of artificial cellulosomes. By adding a dockerin domain from *Piromyces finnis* to an endoglucanase and an endoxylanase from *Thermotoga maritima* the enzymes retained their activity and were able to bind to the *Piromyces finnis* cellulosome [123].

Transcription of AF CAZyme genes has been reported both to be constitutive [118] and substrate regulated [117,124]. Latter authors suggest the constitutive base level expression of CAZyme genes to release the needed inductors from the substrate, which in turn trigger a substrate specific response [117,124]. Antisense transcripts seem to play an important regulative role [125] and catabolites of lignocellulose degradation repress the expression of CAZymes [126].

2.2.5 Metabolism

The following described sugar metabolism is only based on reports of *Piromyces* and *Neocallimastix*, being the only two genera with detailed information available (Figure 4). While details like the ability to use certain carbon sources may vary, the metabolism of different AF is highly similar [19]. Hexoses enter the metabolism directly via glycolysis [127,128]. Pentoses, like xylose, are isomerized, phosphorylated and then enter glycolysis via the pentose phosphate pathway [129,130]. AF contain the genes for an unclosed citric acid cycle, with succinate being product from the reductive branch and α-ketoglutarat being the product of the oxidative branch [128,131]. Citrate and Malate are products of this pathway that also have been detected during AF growth [131–133]. In addition, the cytosol contains a lactate dehydrogenase and a pyruvate formate lyase (PFL) [127]. While the first enzyme enables the fermentation of pyruvate to lactate, the second catalyzes the reaction of pyruvate to formate and acetyl coenzyme A (Acetyl-CoA). Acetyl-CoA can be further fermented to ethanol by alcohol dehydrogenase E (ADHE), an enzyme combining both aldehyde dehydrogenase and alcohol dehydrogenase activity [18]. Both PFL and ADHE from AF are of bacterial origin [18], which is in accordance with the postulated importance of horizontal gene transfer in AF evolution [50].

Instead of mitochondria AF contain hydrogenosomes. These organelles have evolved from mitochondria and opposed to them lack an own genome [134–136]. Malate from the reductive branch of the citric acid

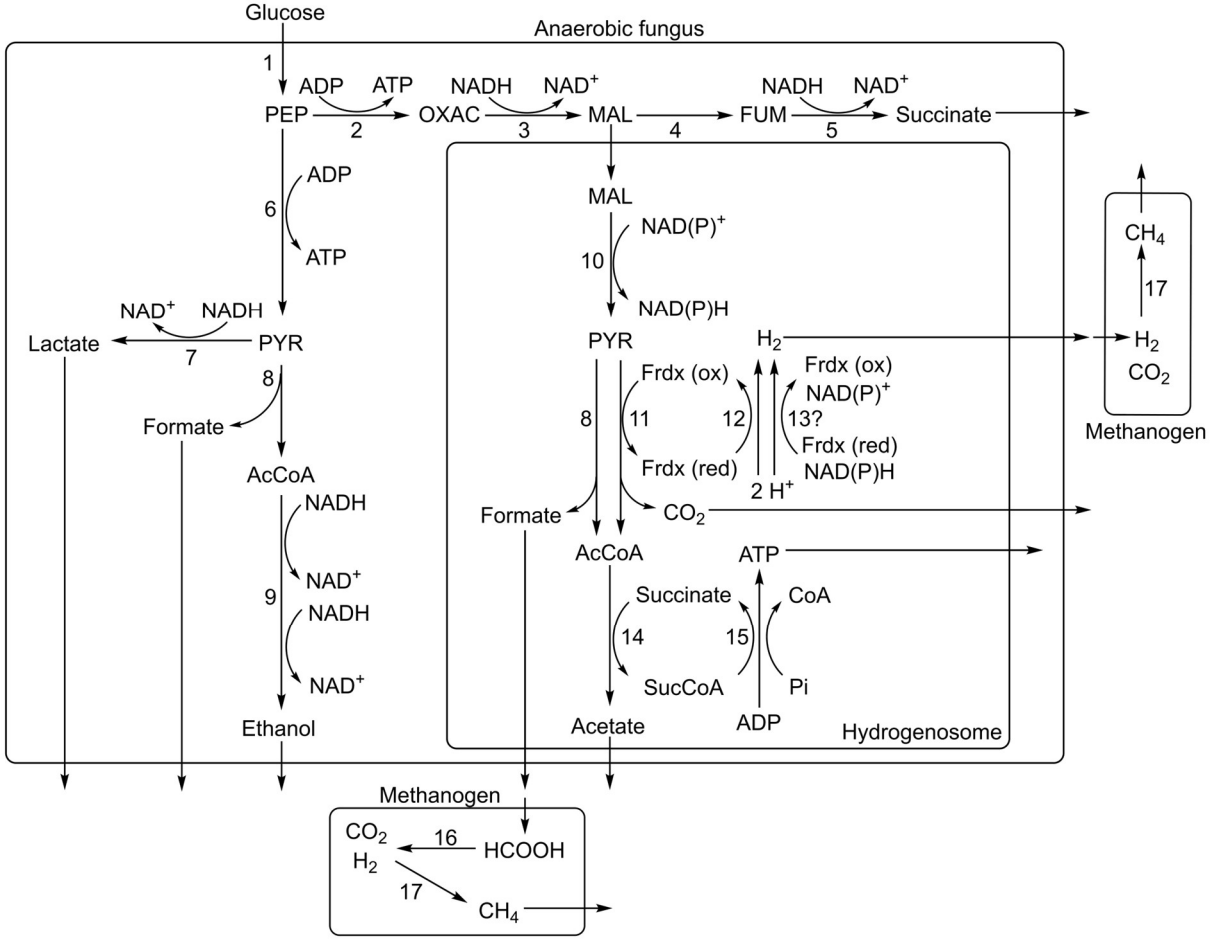

Figure 4: Metabolism of anaerobic fungi and interaction with methanogens from the current point of understanding. Adopted from [18,19,133]. Enzymes are marked as numbers: 1. Embden-Meyer pathway, 2. phosphoenolpyruvate carboxykinase, 3. Malate dehydrogenase, 4. Fumarase, 5. Fumarate reductase, 6. Pyruvate kinase, 7. Lactate dehydrogenase, 8. Pyruvate formate lyase, 9. Alcohol dehydrogenase E, 10. Malic enzyme, 11. Pyruvate ferredoxin oxidoreductase, 12. Ferredoxin hydrogenase, 13?. Possible bifurcating hydrogenase, 14. Acetate:succinate CoA tranferase, 15. succinylCoA synthetase, 16. Formate dehydrogenae, 17. Methyl coenzyme-M reductase, PEP, phosphoenolpyruvate; OXAC, oxaloacetate; MAL, malate; FUM, fumarate; PYR, pyruvate; AcCoA, acetyl coenzyme A; CoA, coenzyme A; Frdx, ferredoxin; SucCoA, succinyl coenzyme A.

cycle is transported inside the hydrogenosomes and converted to pyruvate [127]. This reaction catalyzed by the malic enzyme requires the reduction of NAD(P) to NAD(P)H. In addition to malate, pyruvate can also be transported into the hydrogenosome [18,19]. The enzyme which catalyzes the subsequent conversion of pyruvate to Acetyl-CoA was long debated. Marvin-Sikkema et al. 1993 were able to detect pyruvate:ferredoxin oxidoreductase (PFO) activity in activity assays with isolated hydrogenosomes [127]. Other studies reported the production of the PFL byproduct formate and thereby propose PFL as the responsible enzyme [18,137]. While transcriptome sequences for PFL have been reported [137], there is only protein activity based information for the existence of a PFO [127,138]. Recently, a study comparing several *Neocallimastigomycota* genomes reported that both enzymes are available to the metabolism [19]. While PFL seemed to carry the majority of the flux, PFO appeared responsible for hydrogen production. PFO catalyzes the reaction from pyruvate to Acetyl-CoA by reducing ferredoxin and producing CO_2. Ferredoxin is reoxidized by a ferredoxin hydrogenase under hydrogen production. Several other pathways have been postulated for the regeneration of the reducing equivalents ferredoxin and NAD(P)H. Activity of a NAD(P)H:ferredoxin oxidoreductase was detected in enzyme assays from isolated hydrogenosomes [127]. This enzyme oxidizes NAD(P)H by reduction of ferredoxin. Ferredoxin in turn is reoxidized as described above. Other authors also suspected hydrogen production via a reverse working hydrogen dehydrogenase catalyzing the oxidation of NAD(P)H [18], but this reaction is energetically unfavorable [19]. Recently, sequences homologous to a bifurcating hydrogenase were found in the genome of *Neocallimastix lanati* [19]. Bifurcating hydrogenases oxidize reduced ferredoxin and NAD(P)H in a combined step under hydrogen formation. In any case, energy in hydrogenosomes is gained by substrate level phosphorylation of Acetyl-CoA to Succinyl-CoA and acetate [127]. The required succinate is then regenerated via a Succinyl-CoA synthetase in a ATP producing step. Additionaly, ATPase activity was detected in hydrogenosomal extract [138] and several studies report genomic and transcriptomic sequences of ATPase subunits [19,139]. In contrast, modelling of the metabolism of *Neocallimastix lanati* showed only low flux through this ATPase system from the current point of understanding [19].

In their natural habitat AF live in a close relationship with methanogens, which attach to their rhizoid [140,141] and metabolize their fermentation products formate and hydrogen [133]. Such end product depletion allows the AF metabolism to switch to the energetically more favorable disposal of electrons via the hydrogenosomal pathway with hydrogen, formate and acetate as endproducts [133]. This leads to an increase of acetate and a decrease of the cytosomal fermentation products lactate, succinate, citrate and malate during the coculture of AF with methanogens when compared to AF monoculture [129,132,133,142]. A decrease in ethanol production is reported in some studies [142] while others report no difference [129,132]. In coculture AF show enhanced biomass formation, faster carbon source consumption and elevated secretion of lignocellulose degrading enzymes [129,132,133,143].

2.2.6 Future biotechnological applications and challenges

Up to date biotechnological application of AF was focussed on their rich diversity of CAZymes which have been already described in chapter 2.2.4. Therefore, a multitude of studies exist expressing these enzymes in different hosts (Table 3) and native expression in a continuous flow system has also been investigated [144]. Heterologous expression of anaerobic fungal CAZyme genes in microbes native to farm animals and their follow up use as probiotics has been suggested [145]. *Lactobacillus reuteri* isolated from broiler chicks was modified to express a xylanase and a cellulase from AF gaining the ability to digest cellulose and xylan. The addition of such probiotics to the feed might increase the performance of the animals. Similarly, the direct addition of AF as probiotic is also an option with the positive effects on their host being described in chapter 2.2.1 and having been reviewed recently [102]. Another usage of microbes heterologously expressing anaerobic fungal CAZyme genes is the production of biofuels from lignocellulosic feedstock. Expression of CAZymes in the yeast *Kluyveromyces marxianus* led to a higher, faster and cheaper ethanol production from rice straw [146]. AF can also be used directly for the pretreatment of lignocellulose containing biomass. In a first step *Pecoramyces ruminantium* was grown on alkaline pretreated corn stover to produce CAZymes [147].

Table 3: Heterologously expressed lingocellulolytic enzymes from anerobic fungi. Adopted from [17,22].

Enzyme	From	Expressed in	Source
Xylanase xynA	*N. patriciarum*	*Bacillus subtilis*	[149]
Xylanase xynA	*N. patriciarum*	*Escherichia coli*	[150]
Xylanase	*N. patriciarum*	*Escherichia coli*	[151]
Xylanase xynR8	Unpurified AF culture	*Lactobacillus reuteri*	[152]
Xylanase xynCDBFV	*N. patriciarum*	*Lactobacillus reuteri*	[145]
Cellulase eglA	*Piromyces rhizinflata*	*Lactobacillus reuteri*	[145]
GH celA	*N. patriciarum*	*Clostridium beijerinckii*	[153]
GH celD	*N. patriciarum*	*Clostridium beijerinckii*	[153]
GH celD	*N. patriciarum*	*Escherichia coli*	[154]
Xylanase xynA	*N. patriciarum*	*Butyrivibrio fibrisolvens*	[155]
Endoxylanase xyn3	*N. frontalis*	*Kluyveromyces lactis* *Penicillium roqueforti*	[156]
β-glucosidase cel1A	*Piromyces* sp. E2	*Pichia pastoris*	[157]
β-glucosidase BglA	*Orpinomyces* PC-2	*Saccharomyces cerevisiae*	[158]
bglA, cel48A, celpin, xylA, xylB	*Piromyces sp.* E2	*Saccharomyces cerevisiae*	[159]
Hydrogen. Malic enzyme	*N. frontalis*	*Hansenula polymorpha*	[160]
Xylanase xynA	*Orpinomyces*	*Hypocrea jecorina*	[161]
Cinnamoyl Esterase EstA	*Piromyces equi*	*Trichoderma reesei*	[162]
Xylanase xynC	*N. patriciarum*	*Brassica napus*	[163]
CBM domain	Piromyces equi	*Nicotiana tabacum*	[164]
Cellulase celA	*N. patriciarum*	*Escherichia coli*	[165]
β-1,3-1,4 glucanase *bglA13*, *bglA16*, *bglA51*, *bglM2*	*N. patriciarum* J11	*Escherichia coli*	[166]
Bgxg1 (xylosidase/Glucosidase/galactosidase)	*Orpinomyces sp.* C1A	*Escherichia coli*	[167]
Endoglucanase celB29	*Orpinomyces joyonii* SG4	*Escherichia coli*	[168]
Endoglucanase celB2	*Orpinomyces joyonii* SG4	*Escherichia coli*	[168]
Endoglucanase GH5	*Piromyces rhizinflata*	*Escherichia coli*	[169]
Cellobiohydrolase celA	*N. patriciarum*	*Escherichia coli*	[170]
Endoglucanases celB, celC	*N. patriciarum*	*Escherichia coli*	[170]
Endoglucanase celB	*N. patriciarum*	*Escherichia coli*	[171]
Acetyl xylan esterase axeA	*Orpinomyces* PC-2	*Escherichia coli*	[172]
Acetyl xylan esterase BnaA	*N. patriciarum*	*Escherichia coli*	[173]
Acetyl xylan esterase bnaA, bnaB, bnaC	*N. patriciarum*	*Escherichia coli*	[174]
Xylanase xynA	*Piromyces*	*Escherichia coli*	[175]
Mannanase manA	*Piromyces*	*Escherichia coli*	[175]
Mannase manA, manC	*Piromyces*	*Escherichia coli*	[176]
Acetyl xylan esterase XynS20E	*N. patriciarum*	*Escherichia coli*	[177]
Xylanase	*N. patriciarum*	*Escherichia coli*	[178]
β-glucosidase NpaBGS	*N. patriciarum* W5	*Pichia pastoris*	[179]
Endoglucanase EG5	*Orpinomyces* C1A	*Escherichia coli*	[119]
Exoglucanase Cel6A	*Orpinomyces* C1A	*Escherichia coli*	[119]
Exoglucanase Cel48	*Orpinomyces* C1A	*Escherichia coli*	[119]
Xylanase XYL11	*Orpinomyces* C1A	*Escherichia coli*	[119]
β-glucosidase BGL1	*Orpinomyces* C1A	*Escherichia coli*	[119]
β-glucosidase BGL3	*Orpinomyces* C1A	*Escherichia coli*	[119]
Xylose isomerase + d-xylulokinase	*Piromyces sp.* E2	*Saccharomyces cerevisiae*	[130]
β-glucosidase Cel3A	*Piromyces sp.* E2	*Escherichia coli*	[180]
Cellulases (10x)	*N. patriciarum* W5	*Pichia pastoris*	[181]
Cellulase Cel6A	*N. patriciarum*	*Escherichia coli*	[182]
Endo-β-1,4-glucanase celE	*Orpinomyces* PC-2	*Pichia pastoris*	[183]
Endoglucanase	*Orpinomyces* PC-2	*Escherichia coli*	[184]
Endoglucanases Cel5B + Cel6A	*Piromyces rhizinflata*	*Escherichia coli*	[185]
Endoglucanases cel5A + Cel45A	*Piromyces equi*	*Escherichia coli*	[186]
Cellulases CelAcd	*Piromyces rhizinflata*	*Escherichia coli*	[187]
β-glucanase CbhYW23-2	*Piromyces rhizinflatus*	*Escherichia coli*	[188]
Xylanase OpX	*Orpinomyces* PC-2	*Escherichia coli*	[189]
Xylanase xynS20	*N. patriciarum*	*Escherichia coli*	[190]
Xylanase XynR8	Unpurified AF	*Escherichia coli*	[191]
Mannase ManA	*Orpinomyces* PC-2	*Saccharomyces cerevisiae*	[192]
Xylose isomerase	*Orpinomyces*	*Saccharomyces cerevisiae*	[193]
Ferulic acid esterase Fae1A	*A. mucronatus*	*Escherichia coli*	[194,195]
Cinnamoyl esterase EstA	*Piromyces equi*	*Escherichia coli*	[196]

Afterwards, fungal growth was inhibited and ethanol was produced from the released sugars with *Escherichia coli* K011. A similar system was used with *Piromyces indianae* and *Kluyveromyces marxianus* to produce ethyl acetate, isoamyl alcohol and phenyl ethanol from different feedstocks [148].

In chapter 2.2.5 the close interaction between fungi and methanogens was mentioned and *Neocallimastigomycota* were detected in several German biogas plants operated with cattle manure [197] suggesting importance for the biogas process. Addition of AF increased the methane production in batch and fed-batch anaerobic digestion, but a semi-continuous process led to a fast decrease in fungal biomass [198]. In a later study, AF improved the degradation of biomass and accelerated the initial biogas production, but didn't survive for a prolonged time in the community of the digester [21]. To maximize the biogas yield and the digestion of the used biomass, the anaerobic digestion was divided into two temporally separated steps: Hydrolysis and biogas production. AF were grown on straw until hydrogen production ceased and the methanogens were inoculated afterwards [199]. This led to an increase in the biogas yield when compared to a single batch procedure. While the idea of biogas production with AF has received some attention, the idea of darkfermentation has just been formulated lately [200] and no experimental data exists. Just recently the production of secondary metabolites by AF has started to be addressed [201] and further research will have to evaluate the value of these.

Several challenges with the biotechnological implementation of AF exist. Foremost, the exact nutritional requirements of the organisms are still not known, studies use different media and the reports of the used experimental parameters often lack sufficient detail [20]. Although several sequenced genomes exist these contain gaps and nearly half of the putative genes remain to be annotated [19]. Methods of genetic manipulation have to be developed and only a transient expression following biolistic transformation has been achieved [202]. Preliminary studies on the use of RNA interference to knock down the expression of certain genes [23] seem promising and could be used while further tools are under development.

2.3 Research proposal

In a world of advancing climate change the transition from a fossil based to a renewable economy is necessary. Despite lignocellulose containing waste products being cheap and widely available, their usage has been restricted by the high energy demand required for their conversion. The anaerobic fungi of the phylum *Neocallimastigomycota* are able to grow on such materials and produce the next generation energy carrier hydrogen together with other valuable side products. Despite the high biotechnological potential, little is known of their requirements and metabolic pathways. Their rich diversity of highly active lignocellulolytic enzymes, despite some having been expressed in different hosts, remains widely uncharacterized. This thesis aims to help to overcome some of these limitations paving the way for a biotechnological implementation of anaerobic fungi.

In a first step, the culture of anaerobic fungi was established in the laboratory and the obtained culture were characterized as follows:

- Isolation of anaerobic fungi from different animal feces provided by the Zoo Karlsruhe.
- Identification and phylogenetic classification of the isolates using the sequenced ITS1 and LSU regions.
- Analysis of metabolites produced by the isolates during growth on different carbon sources.

Following up, the growth of the most robust isolate was tested for dark fermentative hydrogen production by:

- Identification of possible nitrogen sources for the isolate.
- Studying the effects of temperature and pH on the metabolite production.
- Testing for possible product inhibition of the process by hydrogen.
- Establishment of a bioreactor process in a stirred tank reactor system.
- Assessment of the influence of the parameters stirring speed and pH regulation on the metabolite production.

In parallel work, the lacking biochemical knowledge of anaerobic fungal enzymes was started to be addressed by:

- Bioinformatic identification of lignocellulolytic enzymes from a published *Neocallimastigomycota* genome.
- External gene synthesis of the identified enzymes and cloning into a suitable host.
- Expression and purification of the cloned enzymes.
- Characterization of the purified enzymes.

3 Isolation of a novel fungus: *Aestipascuomyces dupliciliberans*

This chapter is based on the publication:

Aestipascuomyces dupliciliberans gen. nov, sp. nov., the first cultured representative of the uncultured SK4 clade from aoudad sheep and alpaca

Marcus Stabel[1]*, Radwa Hanafy[2]*, Tabea Schweitzer[1], Meike Greif[1], Habibu Aliyu[1], Veronika Flad[3], Diana Young[3], Michael Lebuhn[3], Mostafa Elshahed[2], Katrin Ochsenreither[1] and Noha H. Youssef[2]

[1] Karlsruhe Institute of Technology, Process Engineering in Life Sciences 2: Technical Biology, Karlsruhe, Germany

[2] Department of Microbiology and Molecular Genetics, Oklahoma State University, Stillwater, OK 74074

[3] Bavarian State Research Center for Agriculture, Central Department for Quality Assurance and Analytics, Micro- and Molecular Biology, Freising, Germany

*shared first authorship

Publishing details:

Microorganisms

Volume 8 Article 1734

Published on 5 November 2020

DOI: https://doi.org/10.3390/microorganisms8111734

Author Contributions: Conceptualization, M.S.E., N.H.Y., and K.O.; methodology and formal analysis, M.S. T.S., M.G., H. A., and R.H.; resources, M.S.E., N.H.Y., and K.O.; writing—original draft preparation, M.S. and R.H.; writing—review and editing, V.F., D.Y., M.L., M.S.E., N.H.Y., and K.O.; supervision, M.S.E, N.H.Y., D.Y., V.F., M.L., and K.O.; project administration, M.S.E., N.H.Y., M.L., and K.O.

3.1 Introduction

The herbivorous gut harbors a wide range of bacterial, archaeal, protozoan, and fungal communities that collectively mediate the transformation of plant biomass into fermentable sugars and short-chain fatty acids [16]. Within such complex assemblages, members of the anaerobic gut fungi (AF, phylum *Neocallimastigomycota*) remain the most enigmatic group [85,203]. During the last few decades, an increased understanding of the AF diversity, ecology, and metabolic capabilities has been accumulating, and it is now broadly agreed that AF play an integral role in the anaerobic degradation of recalcitrant lignocellulosic material [204,205] through hyphal penetration of plant material and production of a wide array of polysaccharide-degrading enzymes [16,85,122].

To date, eighteen different cultured AF genera have been described, the majority of which were isolated in the last few years [51–53,56–61,63,67,71,76]. Generally, AF genera are distinguished morphologically based on several structural features such as thallus development pattern [58,67], zoospore flagellation, and thallus morphology. Monocentric thallus development (i.e. zoospore cyst germination is not accompanied by nucleus migration into the germ tube, resulting in anucleated rhizoidal system) is the most abundant among AF genera, as opposed to polycentric thallus development (i.e. nucleus enters the germ tube, developing a nucleated rhizomycelium) that is thus far only observed in three genera, *Anaeromyces* [57], *Orpinomyces* [58] and *Cyllamyces* [56]. Additionally, the majority of AF genera produce monoflagellated zoospores (with 1-4 flagella), with only four genera thus far (*Orpinomyces* [58], *Neocallimastix* [67], *Feramyces* [63], and *Ghazallomyces* [53]) known to produce polyflagellated zoospores (7-30 flagella). Finally, all currently described genera exhibit filamentous thalli, except for the phylogenetically-related genera *Cyllamyces* [56] and *Caecomyces* [52], both known to display bulbous thallus morphology.

Culture-independent diversity surveys have clearly demonstrated that AF diversity is much broader than previously inferred from culture-based approaches. Such studies have identified several novel yet-uncultured lineages, mostly through the use of the ITS1 and D1/D2 LSU regions as phylogenetic markers [64,65,90,91,206]. Despite multiple recent efforts to isolate and characterize novel AF lineages [53,59–61,63], many candidate genera remain uncultured. A recent study combining amplicon-based diversity survey with isolation efforts suggested that the success of isolation of an AF taxon is positively correlated to its relative abundance in a sample, and negatively correlated to the sample evenness [65]. Further, multiple culture-based [53,59], and culture-independent [65,90] studies have provided evidence that poorly sampled animal hosts harbor a wide range of hitherto uncharacterized AF taxa. Based on these observations, we adopted two strategies to isolate novel AF taxa: a targeted sequence-guided isolation strategy, where samples harboring relatively high proportions of yet-uncultured genera are prioritized for AF isolation efforts, and a sampling strategy targeting animals from which no prior isolation efforts have been reported. Intriguingly, these efforts, driven by two different hypotheses, and sampling different animals (a wild aoudad sheep and a zoo-housed alpaca) from two different geographical locations (Texas, USA, and Baden-Württemberg, Germany) have yielded almost identical strains of a hitherto uncultured AF lineage (SK4, originally identified in samples from New Zealand (NZ)). This study demonstrates the global distribution of AF lineages across multiple continents, suggests that some yet-uncultured AF genera are not refractive to isolation given the right sampling and isolation conditions, and highlights the value of implementing a sequence-guided culturing approach as well as directing isolation efforts to poorly sampled animals.

3.2 Materials and Methods

3.2.1 Samples

Fresh fecal and rumen contents were collected in sterile 50-ml falcon tubes from a wild aoudad sheep (*Ammoragus lervia*) during a hunting trip in Sutton County, Texas, USA in April 2018. Fecal samples were collected from an alpaca (*Vicugna pacos*) at the Karlsruhe Zoo, Germany in August 2019. Tubes were filled completely to ensure the absence of oxygen. Aoudad sheep samples were stored on ice and transferred to the laboratory within 24 hours, where they were either directly utilized for DNA extraction

or stored at -20 °C. Alpaca fecal samples were stored at room temperature until the next day, on which they were used for isolation.

3.2.2 Isolation

The aoudad sheep sample exhibited a relatively high abundance (76.6 %) of the yet-uncultured SK4 lineage in a prior study [65], and hence was chosen for targeted enrichment and isolation. Isolation efforts were conducted on fecal, as well as rumen samples. Rumen samples used in the isolation process were stored unopened at -20 °C. Fecal samples were opened once in an anaerobic chamber (Coy laboratories, Grass Lake, Michigan, USA) to obtain 0.5 g for use in culture-independent diversity survey efforts, and then stored at -20 °C. Isolation efforts were conducted 22 months post sample collection and DNA extraction. Samples were enriched in autoclaved rumen fluid-cellobiose (RFC) medium [207] for 24 h at 39 °C. Enriched tubes were serially diluted into anaerobic rumen fluid medium (RF) supplemented with either 1 % w/v cellulose or a (1:1) mixture of cellobiose and switchgrass (1 % w/v), and an antibiotics mixture of 50 µg/ml kanamycin, 50 µg/ml penicillin, 20 µg/ml streptomycin, and 50 µg/ml chloramphenicol. Following enrichment, serial dilutions up to 10-5 were performed, and the dilution tubes were incubated for 3 days at 39 °C. Dilutions showing visible signs of growth (change in the color of cellulose, clumping and floating of the switch grass, and production of gas bubbles) were used to prepare roll tubes [208] using RFC medium with 2 % agar. Roll tubes were incubated for 2-3 days at 39 °C, after which single colonies were transferred into RFC medium. Roll tube preparation and colony picking were repeated at least 3 times to ensure the purity of the obtained isolates. Obtained isolates are being maintained via bi-weekly sub-culturing into RFC media. Cultures are stored on agar medium for long-term preservation as previously described [207].

Isolation efforts from the alpaca sample were conducted by suspending 1 g of fecal material in a 1:1 mixture of anoxic salt solutions A (g/l: KH_2PO_4 (3.0), $(NH_4)_2SO_4$ (6.0), NaCl (6.0), $MgSO_4 \bullet 7H_20$ (0.6) and $CaCl_2 \bullet 2H_2O$ (0.6)) and B (g/l: K_2HPO_4 (3.0)), followed by inoculation in serum bottles with Enriched Rumen Fluid medium (ERF) adapted from the basal medium described in [60], and supplemented with dissolved xylan solution (0.2 % w/v), cellobiose (0.2 % w/v), and wheat straw milled to a particle size of 1 mm (0.5 % w/v), and an antibiotics solution of 60 µg/ml each penicillin sodium salt, ampicillin sodium salt, and streptomycin sulfate. Inoculated serum bottles were then incubated for 7 days at 39 °C in the dark. Fungal growth was monitored by light microscopy and serum bottles with signs of anaerobic fungal growth were then used to inoculate roll tubes followed by incubation for 4 days at 39 °C in the dark. Single colonies were transferred into fresh medium. Roll tube preparation and colony picking were repeated at least 3 times to ensure the purity of the obtained isolates.

3.2.3 Morphological characterization

For aoudad sheep isolates, both light and scanning electron microscopy were utilized to observe various microscopic features at different growth stages. For light microscopy, fungal biomass was collected from an actively growing 2-3 days old culture in RFC medium. Fungal biomass was stained with lactophenol cotton blue for examination of various thallus features including: hyphae, sporangia, zoospores, and other specific microscopic structures as previously described [53,61,63]. For nuclear localization, samples were stained with DNA-binding dye 4, 6 diamidino-2-phenylindole (DAPI, final concentration of 10 µg/ml), followed by incubation in the dark for 10 min at room temperature. All light microscopy examinations were conducted using an Olympus® BX51 microscope (Olympus, Center Valley, PA, USA) equipped with a Brightline DAPI high contrast filter set for DAPI fluorescence and a DP71 digital camera (Olympus, Center Valley, PA, USA). Sample preparation and fixation for scanning electron microscopy was conducted as previously described [61]. The prepared samples were then examined on a FEI Quanta 600 scanning electron microscope (FEI Technologies Inc., Hillsboro, Oregon, USA).

For alpaca isolates, light microscopy was performed using a Nikon® Eclipse E200 with a DFK 23U274 camera (Imaging Source®), while fluorescence microscopy (to visualize DAPI staining) was performed

using a Zeiss® Axio Imager Z1 at an excitation wavelength of 353 nm. Differential interference contrast microscopy (DIC) was used for generating image overlay.

3.2.4 Substrate utilization

Growth of the type strain (R4) obtained from aoudad sheep was assessed by replacing the cellobiose in RFC medium with glucose, xylose, mannose, fructose, glucuronic acid, arabinose, ribose, galactose, sucrose, maltose, trehalose, lactose, cellulose, xylan, starch, inulin, raffinose, polygalacturonate, chitin, alginate, pectin, peptone, or tryptone at a final concentration of 0.5 % w/v [61,63]. To assess substrate utilization in the alpaca isolate, the strain was grown in defined media adapted from [60] with omission of clarified rumen fluid and addition of trace metal (prepared according to [209]), vitamin solution (prepared according to [210]) and replacement of the cellobiose with 0.05 % of hemicellulose, xylan, starch, crystalline cellulose, inulin, chitin, pectin, cellobiose, maltose, trehalose, lactose, sucrose, glucose, xylose, mannose, fructose, arabinose, ribose, galactose, or glucuronic acid, or 0.5 % of wheat straw. The ability of a strain to utilize a specific substrate was considered positive if it exhibited viable growth on the tested substrate after four successive transfer events [57,61,63]. All results were compared to substrate-free medium.

3.2.5 Phylogenetic analysis and ecological distribution

For the aoudad sheep isolates, DNA was extracted from 10 ml of 2-3 days old RFC-grown cultures of five strains using DNeasy PowerPlant Pro Kit (Qiagen Corp., Germantown, MD) according to the manufacturer's instructions. For the alpaca isolate, DNA was extracted from 1-week old cultures grown in rumen-free medium supplemented with 0.5 % w/v cellobiose using the Quick-DNA Fecal/Soil Microbe DNA Miniprep Kit (Zymo Research). The extracted DNA was used as a template to amplify the region encompassing ITS1, 5.8S rRNA, ITS-2, and the D1/D2 domains of the 28S (LSU) rRNA gene using the primers ITS5F (5'-GGAAGTAAAAGTCGTAACAAGG-3') and NL4R (5′-GGTCCGTGTTTCAAGACGG-3′) [53,63] with the following PCR protocols: For the aoudad sheep samples: Initial denaturation at 94 °C for 5 min followed by 39 cycles of denaturation at 94 °C for 1 min, annealing at 55° C for 1 min, and elongation at 72 °C for 2 min, and a final elongation step at 72 °C for 10 min. For the alpaca samples: Initial denaturation at 98 °C for 30 sec followed by 30 cycles of denaturation at 98 °C for 10 sec, annealing at 62 °C for 30 sec, and elongation at 72 °C for 90 sec, and a final elongation step at 72 °C for 2 min. PCR amplicons were cloned into a TOPO-TA cloning vector (Life Technologies®, Carlsbad, CA, USA) or using a PCR Cloning Kit (NEB) following the manufacturers' instructions, and were Sanger-sequenced at the Oklahoma State University DNA sequencing core facility (22 clones from 5 aoudad sheep strains), or Eurofins Genomics (14 clones from 1 alpaca strain). For every clone sequence obtained, the ITS1, and the D1/D2-LSU regions were extracted in Mega7 [211] by trimming using the sequence of the ITS1 reverse primer MNGM2 (CTGCGTTCTTCATCGTTGCG), and the sequence of the LSU forward primer NL1 (GCATATCAATAAGCGGAGGAAAAG), respectively. The trimmed sequences were aligned to anaerobic fungal reference ITS1 and D1/D2-LSU sequences using MAFFT v7.471 [212], and the alignments were manually curated in BioEdit [213]. The refined alignments were used to construct maximum likelihood trees to assess the phylogenetic position of the obtained sequences using IQ-TREE v2.0.3 [214]. The best model was selected using ModelFinder [215] and 1000 ultrafast bootstraps [216] were applied. *Gonopodya prolifera* was used as the outgroup (NR_132861 for ITS1, JN874506 for LSU).

To assess the ecological distribution of this novel lineage, we queried the trimmed ITS1 sequences against a manually curated *Neocallimastigomycota* ITS1 database encompassing all known cultured genera, as well as yet-uncultured taxa previously identified in culture-independent studies [64,65,90,91,217,218] using BLASTN. Hits with significant sequence similarity (>87 %) were evaluated by insertion into ITS1 phylogenetic trees. We also queried the D1/D2 LSU dataset generated in our prior effort [65], and hits with >93 % sequence similarity were further evaluated by insertion into D1/D2-LSU phylogenetic trees.

3.2.6 Data and culture accession

Clone sequences are deposited in GenBank under accession numbers MW019479-MW019500 for the aoudad sheep strains R1-R5, and MW049132-MW049145 for the alpaca strain A252.

3.3 Results

3.3.1 Obtained isolates

Five rumen isolates (R1-R5) were obtained from a single wild aoudad sheep in Texas, USA. Concurrently one isolate, A252, was obtained from fecal samples of alpaca in Baden-Württemberg, Germany. Preliminary morphological and microscopic characterization as well as phylogenetic analysis (see chapter 3.3.5) showed identical attributes for strains R1-R5 and only minimal differences between the R strains and strain A252. One isolate (strain R4) was chosen as the type strain for detailed characterization. Below, we present a detailed characterization of the putative novel genus, and we report on the morphology and phylogenetic affiliation of the isolates highlighting differences between strains R4 and A252 when appropriate.

3.3.2 Colony morphology and liquid growth pattern

On solid media, strain R4 formed circular, white filamentous colonies with a white center of sporangia (Figure 5a). Colony size ranged between 2-5 mm. In liquid media, strain R4 produced a heavy fungal biofilm-like growth that loosely attached to the tube's glass surface (Figure 5b).

3.3.3 Microscopic features

Strain R4 produced globose zoospores with an average diameter of 9.3 ± 2.1 µm (standard deviation for 60 zoospores, range: 5–14 µm) (Figure 6a). All zoospores were polyflagellated, with 7-20 flagella and an average flagellum length of 28.1 ± 4.8 µm (average ± standard deviation from 60 zoospores, range:

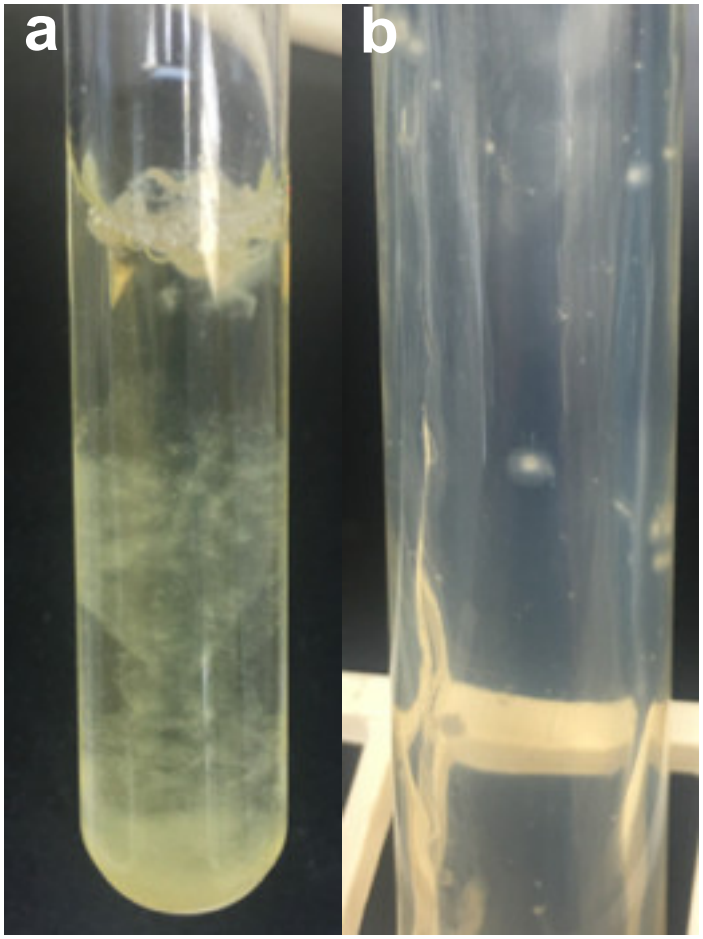

Figure 5: Macroscopic features of *Aestipascuomyces dupliciliberans* type strain R4. (a) Heavy fungal biofilm-like growth in liquid medium. (b) Circular, white filamentous colonies with a white center of sporangia on cellobiose agar roll tube

19–36 µm). Strain A252 produced slightly larger spherical zoospores (10–20 µm, average 14 µm) with slightly longer flagella (35–49 µm, average 42 µm) (Figure 7a).

Zoospores germination in strain R4 resulted in monocentric thalli with highly branched anucleated rhizoids (Figure 6b-e). Strain R4 displayed both endogenous and exogenous thallus development. Endogenous thalli were developed as a result of enlargement of zoospore cysts into sporangia with one (Figure 6f), or two adjacent (Figure 6g) rhizoidal systems. Endogenous sporangia displayed different shapes and sizes including ovoid (20–70 µm L x 15–45 µm W) (Figure 6f), rhomboid (30–70 µm L x 40–85 µm W) (Figure 6g), and elongated (25–90 µm L x 15–40 µm W) (Figure 6h). No intercalary or pseudo-intercalary sporangia (sporangia present between two main rhizoidal systems) were observed.

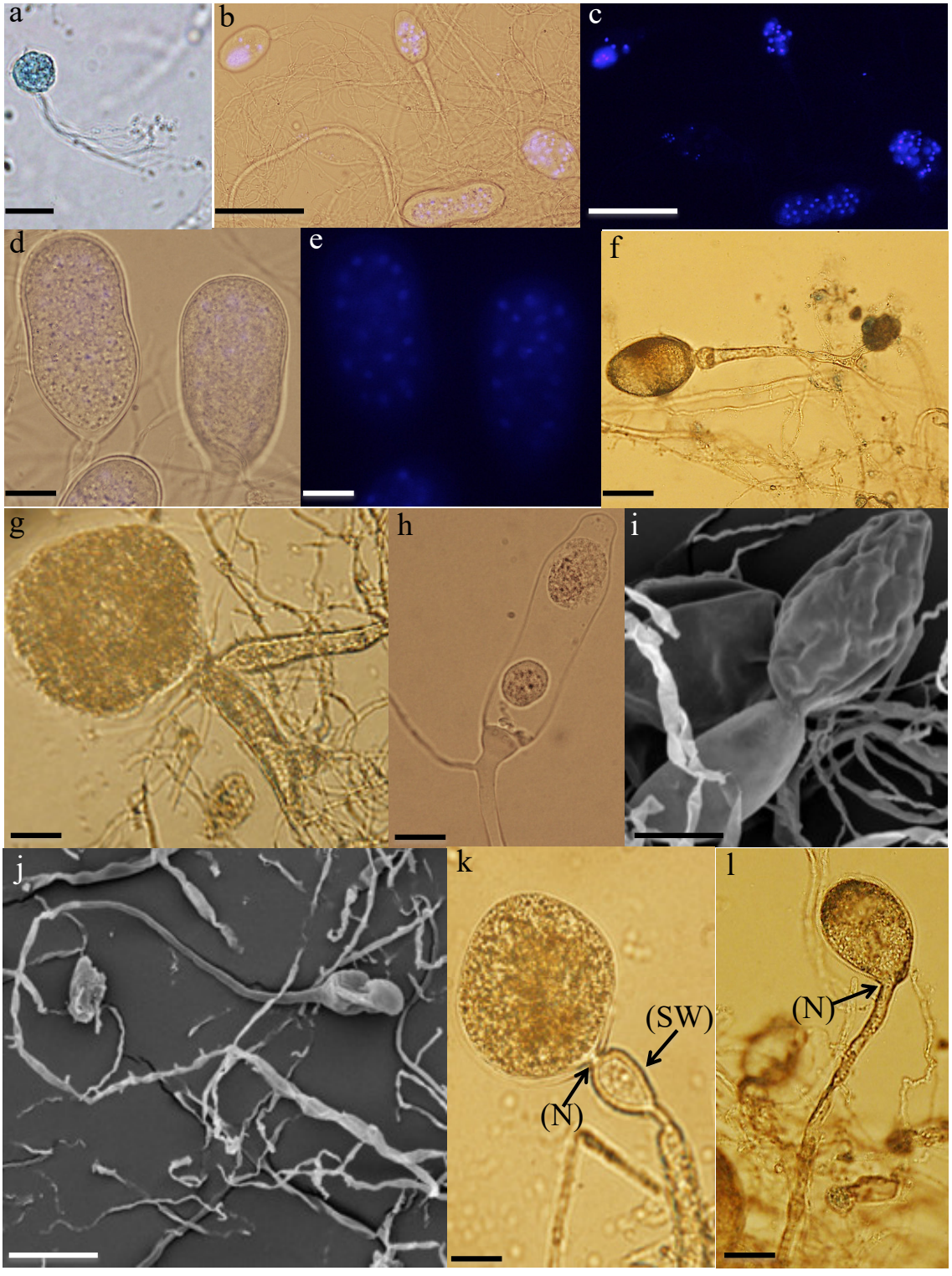

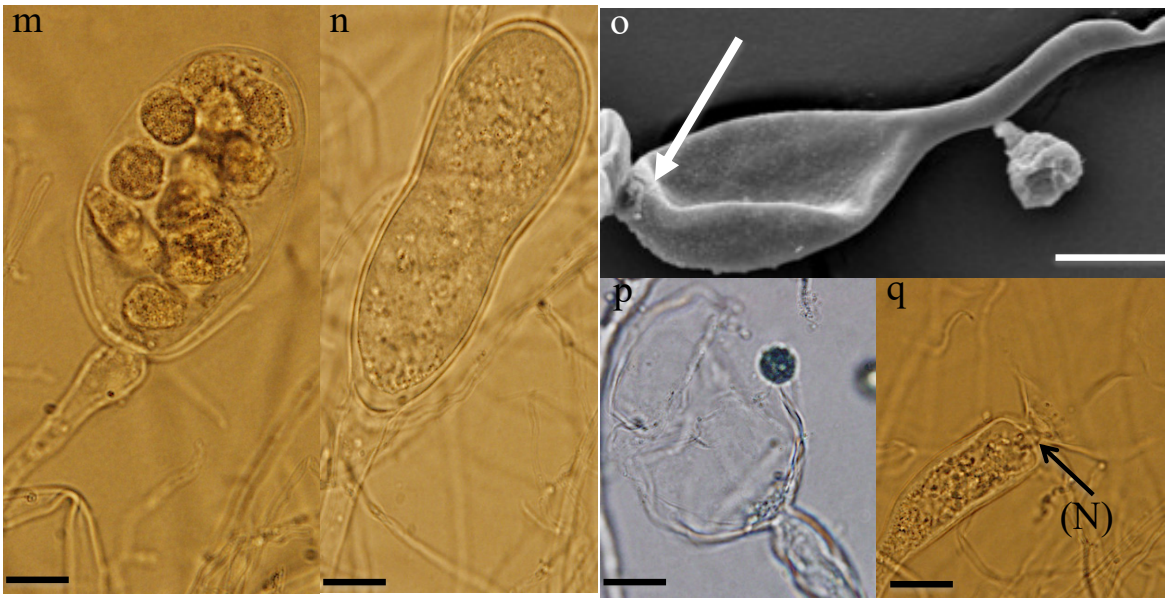

Figure 6: Microscopic features of *Aestipascuomyces dupliciliberans* type strain R4. Light (a-h, k-n and p-q), fluorescence (c and e) and scanning electron (i, j and o) micrographs are shown. (b-c) and (d-e) each depict the same field with c and e showing the fluorescence field, and b and d showing the overlay of fluorescence and phase contrast micrographs. (a) A spherical polyflagellated zoospore. (b-e) Monocentric thalli; nuclei were observed in sporangia, not in rhizoids or sporangiophore. (f-h) Endogenous sporangia: (f) Ovoid sporangium with single rhizoidal system, (g) rhomboid sporangium with two adjacent rhizoidal systems, (h) elongated sporangium. (i-n) Exogenous sporangia: (i) obpyriform sporangium on a flattened sporangiophore, (j) ellipsoidal sporangium on a long sporangiophore, (k) globose sporangium with sub-sporangial swelling and tightly constricted neck, (l) Ovoid sporangium with broad neck and wide port, (m) mature ovoid sporangium full of zoospores, (n) constricted ellipsoidal sporangium. (o-q) Zoospore release mechanisms: (o) An empty sporangium with intact wall after zoospore release through an apical pore (arrow), (p) zoospore release through rupturing the sporangial wall, (q) collapse and disintegration of the sporangial wall after zoospore release. (SW), sub-sporangial swelling; (N), neck. Bar =20 µm (a, f-h, k-n, p-q). Bar =50 µm (b-e, i and o). Bar =100 µm (j).

Exogenous sporangia were mainly developed at the end of unbranched sporangiophores that ranged in length between 10–300 µm (Figure 6i-j). Wide flattened sporangiophores (Figure 6i) and sporangiophores ending with sub-sporangial swellings (Figure 6k) were also frequently encountered. Mature exogenous sporangia ranged in size between (40–90 µm L x 15–35 µm W), and exhibited different morphologies including obpyriform (Figure 6i), ellipsoid (Figure 6j), globose (Figure 6k), ovoid (Figure 6m), and constricted ellipsoid (Figure 6n). Sporangial necks (point between sporangia and rhizoids) were either tightly constricted (Figures 6f, 6k, and 6q), or broad (Figure 6j, 6l, 6n, and 6o). The neck opening, port, was either narrow (Figure 6k), or wide (Figure 6l).

On the other hand, only endogenous sporangia were observed for strain A252, with one (Figure 7b), or less frequently two adjacent (Figure 7c) rhizoidal systems. Endogenous sporangia were mainly globose (diameter up to 145 µm) (Figure 7d), and ellipsoidal (up to 76 µm L x 48 µm W) (Figure 7e).

Zoospore release in strain R4 was achieved through two mechanisms, either from an apical pore (Figure 6o) as previously observed in Feramyces [63]), or through rupturing of the sporangial wall (Figure 6p) as commonly observed in Neocallimastix [67]. To our knowledge, the simultaneous utilization of both mechanisms by a single strain has not been previously reported in other AF taxa. Sporangial walls either stayed intact (Figure 6o) or completely disintegrated after zoospore discharge (Figure 6q).

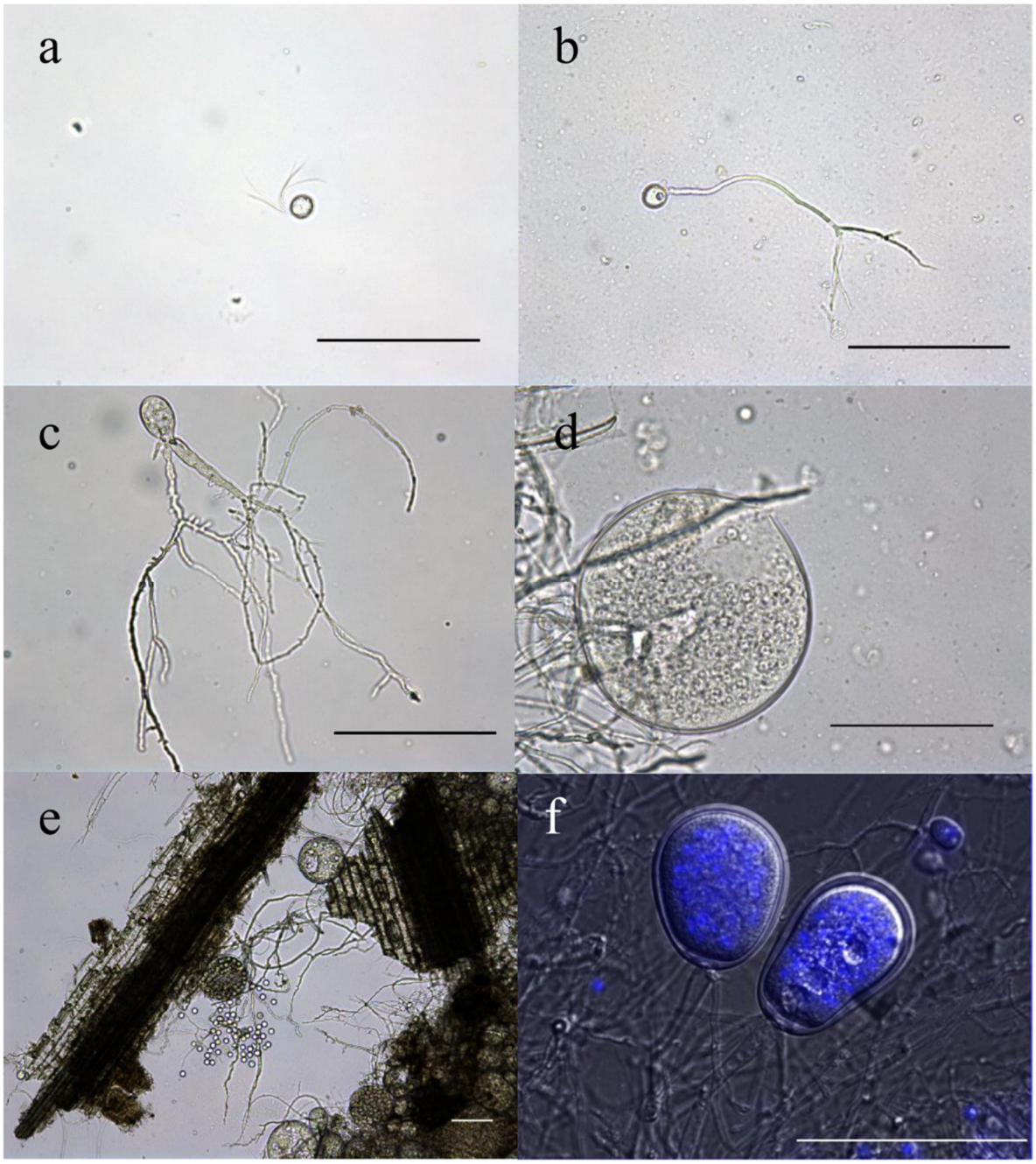

Figure 7: Microscopic features of *Aestipascuomyces dupliciliberans* type strain A252. Light (a-e) and DIC (f) micrographs. (a) A spherical polyflagellated zoospore with long flagella. (b-e) Endogenous sporangia: (b) young globose sporangium with a single rhizoidal system, (c) ovoid sporangium with two rhizoidal systems, (d) large globose sporangium with an apical pore for zoospore release, (e) sporangium during zoospore release, (f) DAPI stained mature ellipsoid sporangia. All scale bars are 100 µm.

3.3.4 Substrate utilization

Strain R4 utilized a wide range of substrates as the sole carbon and energy source. These included monosaccharides, e.g., glucose, fructose, mannose, xylose, and glucuronic acid, but not arabinose, galactose, or ribose. Strain R4 was able to metabolize and vigorously grow on all disaccharides tested including cellobiose, lactose, maltose, sucrose, and trehalose. Among the polymers tested, strain R4 was able to grow on cellulose, xylan, starch, inulin, and raffinose, but not alginate, chitin, pectin, poly-galacturonate, peptone, or tryptone.

On the other hand, strain A252 grew on polysaccharides including wheat straw, hemicellulose, xylan, starch, and inulin, but did not grow on chitin, pectin, or crystalline cellulose. The disaccharides cellobiose, maltose, lactose, and sucrose supported the growth of strain A252, but trehalose was not utilized. Strain A252 was capable of utilizing the monosaccharides glucose, xylose, and fructose, but not mannose, arabinose, ribose, galactose, or glucuronic acid.

3.3.5 Phylogenetic analysis and ecological distribution

Phylogenetic analysis using the D1/D2 domains of 28S rRNA gene (D1/D2 LSU) reproducibly grouped all six isolates in a single, monophyletic cluster within the *Orpinomyces-Neocallimastix-Pecoramyces-Feramyces-Ghazallamyces* supragenic clade (Figure 8a). The isolates obtained in the present study showed very low D1/D2 LSU inter-sequence length heterogeneity (749–751 bp long, average 750 bp), low within-strain divergence between copies (0–1.74 %) as well as low inter-sequence divergence between strains (0–1.6 %). The closest cultured representative to the obtained isolates *was Feramyces austinii* (MG584193; 92.4 % similarity). When compared to amplicon sequences, D1/D2 LSU sequences of the isolates showed highest similarity (93-100 %) to amplicon sequences assigned to the uncultured lineage SK4 [65], originating from fecal material of the same aoudad sheep individual whose rumen sample was used for the US isolation (n=1,338 sequences), as well as to sequences recovered from blackbuck deer (n=4), elk (n=2), domesticated horse (n=1), miniature donkey (n=2), mouflon ram (n=2), and oryx (n=2).

On the other hand, the obtained isolates showed a slightly higher ITS1 length heterogeneity (196–200 bp; average 197.5 bp), within-strain divergence between copies (0–4.38 %) as well as inter-sequence divergence between strains (0–5.84 %). ITS1 phylogeny (Figure 8b) placed the obtained isolates again close to the genus *Feramyces*. BLASTN search against our custom ITS1 database identified 1,327 sequences with ≥87 % sequence similarity. All hits were affiliated with the SK4 clade (originally identified in domesticated sheep and red deer samples in New Zealand (NZ) [64,206]). The majority of hits were from the same wild aoudad sheep samples from which the US isolates were obtained (n=1,311), domesticated sheep (n=5) previously reported in NZ [64], as well as oryx, blackbuck deer, horse, miniature donkey, mouflon, and elk (n=11). Analysis of all available SK4-affiliated sequences obtained from prior studies [64,65,206], and the current study indicates a clade ITS1 sequence divergence range of 0–13.2 %, with two well-defined subclades. Interestingly, divergent ITS1 sequences originating from one isolate routinely clustered within both clades (Figure 8b), precluding their allocation to two distinct species and highlighting the difficulty associated with species-level OTU assignments using only ITS1 data in the *Neocallimastigomycota*.

Notably, it seems that members of the SK4 clade exhibit higher abundance when animals graze on summer pasture. For example, in New Zealand's domesticated sheep, SK4 was only identified as part of the AF community when the animals were grazing on summer but not winter pasture [64,206], suggesting a potential relationship between the enrichment of SK4 in the AF community and the season feed type.


a
0.01
Orpinomyces
Ghazallomyces
Pecoramyces
Neocallimastix
Feramyces
Isolate A252 CloneB1.14 MW049138
Isolate R3 CloneB4 MW019492
Uncultured Blackbuck deer amplicon BBDoe 31581
Isolate A252 CloneB1.15 MW049139
Isolate R2 CloneA7 MW019482
Uncultured Elk amplicon Elk 133008
Uncultured Blackbuck deer amplicon BBDoe 137157
Isolate R1 CloneA2 MW019486
Isolate R5 CloneC2 MW019489
Isolate R3 CloneB1 MW019488
Isolate R2 CloneA8 MW019487
Isolate R1 CloneA6 MW019481
Uncultured Miniature donkey amplicon MinDon 39441
Isolate R1 CloneA5 MW019485
Isolate R5 CloneC1 MW019498
Isolate R5 CloneC5 MW019500
Uncultured Horse 13197
Uncultured Aoudad sheep amplicon Aoud18 141177
Uncultured Elk amplicon Elk 140354
Isolate R1 CloneA4 MW019484
Isolate R4 CloneB10 MW019497
Isolate R5 CloneC3 MW019499
Isolate R3 CloneB2 MW019490
Isolate R1 CloneA3 MW019483
Isolate R5 CloneC4 MW019479
Isolate R4 CloneB7 MW019494
Uncultured Miniature donkey amplicon MinDon 20638
Isolate R4 CloneB8 MW019495
Isolate A252 CloneB2.7 MW049142
Uncultured Aoudad sheep amplicon Aoud18 17687
Isolate A252 CloneB1.4 MW049135
Isolate A252 CloneB1.12 MW049137
Isolate A252 CloneB1.5 MW049136
Uncultured Mouflon amplicon Mouf 40280
Uncultured Aoudad sheep amplicon Aoud18 42651
Uncultured Aoudad sheep amplicon Aoud18 143123
Isolate R1 CloneA1 MW019480
Isolate R4 CloneB9 MW019496
Isolate R3 CloneB3 MW019491
Isolate R3 CloneB5 MW019493
Uncultured Oryx amplicon Oryx 21426
Uncultured Oryx amplicon Oryx 7228
Isolate A252 CloneB1.1 MW049132
Isolate A252 CloneB1.2 MW049133
Isolate A252 CloneB5.1 MW049144
Isolate A252 CloneB2.1 MW049140
Isolate A252 CloneB1.3 MW049134
Isolate A252 CloneB4.8 MW049143
Isolate A252 CloneB5.2 MW049145
Isolate A252 CloneB2.3 MW049141
Aestipascuomyces
Caecomyces
Cyllamyces
Piromyces
Aklioshbomyces
Khyollomyces
Agriosomyces
Liebetanzomyces
Capellomyces
Oontomyces
Anaeromyces
Buwchfawromyces
Tahromyces
Joblinomyces
Gonapodya

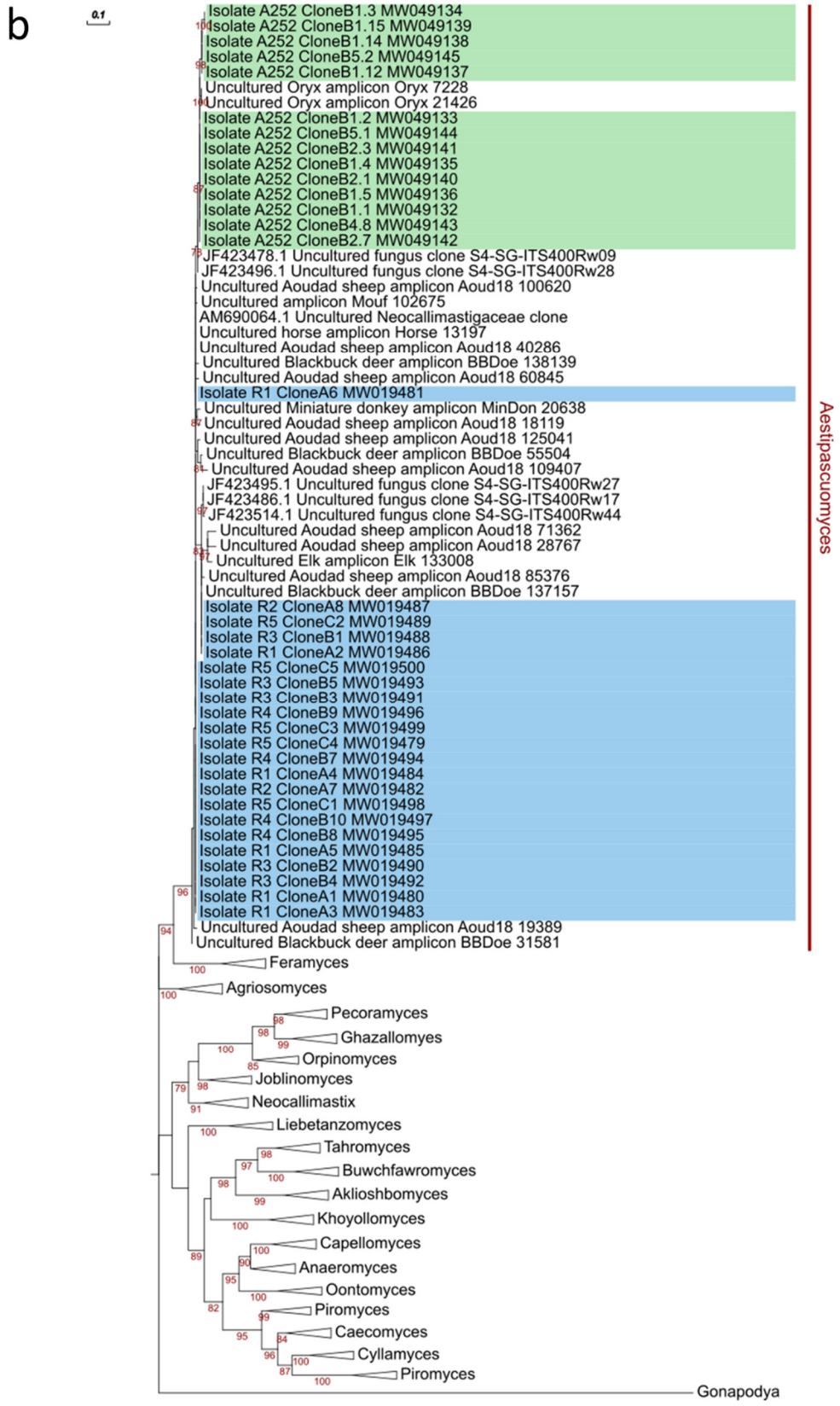

Figure 8: Phylogenetic affiliation of the *Aestipascuomyces* genus to other AF genera based on the nucleotide sequences of the D1–D2 domains of 28S rRNA gene (a), and partial ITS1 sequences (b). Sequences were aligned in MAFFT [212] and manually curated in BioEdit [213]. Curated alignments (LSU: 677 characters, 209 sequences; ITS1: 295 characters, 126 sequences) were used to construct ML-trees using IQTREE with the predicted models TN+F+R2 (28S rDNA) or HKY+F+G4 (ITS1) and –bb 1,000. Bootstrap values are shown for nodes with more than 70 % bootstrap support. Background color indicates the origin of the isolate (blue: Texas, USA; green: Baden-Württemberg, Germany).

3.4 Discussion

Here, we report on the isolation and characterization of the previously uncultured *Neocallimastigomycota* lineage SK4 from the rumen contents of a wild aoudad sheep and feces of a zoo-housed alpaca. Phylogenetic analysis using the D1/D2-LSU region showed that the six isolates obtained formed a single, monophyletic cluster within the *Orpinomyces-Neocallimastix-Pecoramyces-Feramyces-Ghazallamyces* supragenus clade [49,65]. All hitherto described members in this clade are characterized by the production of polyflagellated zoospores, with the notable and peculiar exception of the genus *Pecoramyces*, which produces monoflagellated zoospores. This suggests an acquisition pattern of zoospore polyflagellation at ~ 46.3 Mya (the most current estimate of this clade emergence per [49]), followed by a recent loss and reverting to zoospore monoflagellation for the relatively recently-evolved genus *Pecoramyces* (current estimates of emergence at 19.1 Mya, [49]). Similarly, all members of this supragenus clade form monocentric thalli, with the exception of the genus *Orpinomyces* that is known to develop polycentric thalli, suggesting that the development of polycentric thalli is a recent independent event that happened multiple times in the *Neocallimastigomycota* (for example with the emergence of *Orpinomyces*, *Anaeromyces*, and *Cyllamyces*). The closest cultured representatives of the SK4 clade are the genera *Feramyces* and *Neocallimastix*. While the three genera share similar morphological and growth patterns (e.g. polyflagellated zoospores and monocentric thalli development), they exhibit several distinct macroscopic and microscopic features. For example, members of the SK4 genus produce zoospores with 7-20 flagella, as opposed to 7-16 for *Feramyces* [63] and 7-30 for *Neocallimastix* [67]. Additionally, SK4 members produce terminal sporangia, while the *Feramyces* genus members produce terminal, pseudo-intercalary, and sessile sporangia [63]. Also, and perhaps most notably, members of the SK4 genus show two zoospore release mechanisms; either through an apical pore or via rupturing of the sporangial wall. On the other hand, the majority of *Neocallimastix* genus members are known to release zoospores through complete rupturing and lysis of the sporangial wall (Figure 25 in [67], with only a few exceptions (e.g. [70,219]), while *Feramyces* members release zoospores through apical pores (Figure 2x in [63]). To our knowledge, the dual zoospore release mechanism has not been encountered before in any of the cultured AF genera members and hence appears to be highly characteristic of the SK4 genus.

Within the microbial world, a large fraction of organisms remains uncultured. This is more commonly encountered within the bacterial and archaeal domains, although a similar pattern has been suggested for the Fungi [48,220–222]. Within the anaerobic fungal phylum *Neocallimastigomycota*, multiple putative novel genera were identified in culture-independent studies [64,90,217]. Failure to obtain these taxa in pure culture could be attributed to several reasons. First, some AF taxa are extremely fastidious and might require special nutritional and culturing requirements, and hence would not grow using routinely utilized isolation and enrichment protocols [16,62]. Second, some AF taxa might exhibit a very limited ecological distribution pattern and could be confined to few phylogenetically-related animal hosts. Indeed, many novel genera recently isolated appear to be of limited distribution, being observed only in very few samples from which they have been successfully isolated (e.g. *Aklioshbomyces* from white-tailed deer, *Ghazallomyces* from axis deer, and *Khyollomyces* (AL1) in the *Equidae* [53]). We argue that, in addition to mere presence, the relative abundance of the target lineage in the sample could be an important determinant for isolation success in the AF. Our recent efforts [65] suggest that while some AF genera are generalists, present in low abundance in a large number of samples and are often readily recovered from these samples, e.g. *Orpinomyces*, and *Anaeromyces*, others show a clear correlation between the success of their isolation and their relative abundance within a sample, especially in samples where one or a few lineages make up the majority (>90 %) of the AF community.

While information on the AF community in the alpaca sample that was used for isolation in Germany is currently lacking, we believe that the success of obtaining a cultured SK4 representative was largely dependent on its presence in high relative abundance in the samples used for isolation. Therefore, this study clearly demonstrates the value of the sequence-guided isolation strategy that was employed here, whereby samples are initially prescreened using culture-independent approaches followed by targeting promising samples exhibiting a high proportion of novel/wanted genera for isolation efforts using a wide

range of substrates, sample types, and growth conditions. Evidently, this approach will unfortunately involve storing the samples at -20 °C for a certain amount of time to allow for sequencing and data analysis to be conducted. Nevertheless, while some AF taxa might not survive prolonged freezing, we have been successful in recovering isolates from samples stored frozen, especially when tubes were unopened, or at least where repeated freezing and thawing cycles were avoided, and where tubes were filled to the top with little to no space for air [63]. Isolates obtained from aoudad sheep and alpaca were very similar morphologically and phylogenetically despite the differences in geographical locations (Texas, USA versus Baden-Württemberg, Germany) and handling procedures, samples used (rumen versus fecal samples), and animal host phylogeny (*Bovidae* versus *Camelidae*) and gut type (ruminant versus pseudo-ruminant). This demonstrates the global distribution of AF lineages across multiple continents, and suggests that some yet-uncultured AF genera are not refractive to isolation, given the right sampling and isolation conditions.

Based on morphological, physiological, microscopic, and phylogenetic characteristics, we propose accommodating these new isolates into a new genus, for which the name *Aestipascuomyces* (from *aestas*, Latin for summer, and *pastura*, Latin for pasture, to indicate the apparent enrichment of the clade during animal feeding on summer pasture) is proposed. The type species is *Aestipascuomyces dupliciliberans* (to indicate the two zoospore release mechanisms exhibited by members of the clade), and the type strain is *Aestipascuomyces dupliciliberans* strain R4.

3.5 Taxonomy

Aestipascuomyces Marcus Stabel, Radwa Hanafy, Tabea Schweitzer, Meike Greif, Habibu Aliyu, Veronika Flad, Diana Young, Michael Lebuhn, Mostafa Elshahed, Katrin Ochsenreither & Noha Youssef, *gen. nov.*

MycoBank ID: MB837524

Typification: *Aestipascuomyces dupliciliberans* Marcus Stabel, Radwa Hanafy, Tabea Schweitzer, Meike Greif, Habibu Aliyu, Veronika Flad, Diana Young, Michael Lebuhn, Mostafa Elshahed, Katrin Ochsenreither & Noha Youssef (holotype).

Etymology: *Aestipascuo* = derived from *aestas*, Latin for summer, and *pastura*, Latin for pasture; *myces* = the Greek name for fungus.

Obligate anaerobic fungus that produces globose polyflagellated zoospores (7-20 flagella). Zoospores germinate into determinate monocentric thalli with highly branched anucleated rhizoids that lack constriction and intercalary swellings. The clade is defined by the sequences MW019479- MW019500 and MW049132-MW049145 (ITS1, 5.8S rDNA, ITS2, D1-D2 28S rDNA). The most genetically similar genera are *Feramyces*, which is characterized by its polyflagellated zoospores (7-16) and monocentric thalli that usually produce a single terminal sporangium, and in some occasions produce pseudo-intercalary and sessile sporangia, and *Neocallimastix*, which is characterized by the production of polyflagellated zoospores (7-30), monocentric thalli, and empty zoospore cysts that remain at the base of sporangiophores.

Aestipascuomyces dupliciliberans Marcus Stabel, Radwa Hanafy, Tabea Schweitzer, Meike Greif, Habibu Aliyu, Veronika Flad, Diana Young, Michael Lebuhn, Mostafa Elshahed, Katrin Ochsenreither & Noha Youssef, sp. nov.

Mycobank ID: MB837526

Typification: The holotype shown in Figure 6 in this manuscript is derived from the following: U.S.A. TEXAS: Sutton county, 30.591 N and 100.138 W ~300 m above sea level, 3d old culture of strain R4, which is isolated from the frozen rumen content of a female aoudad sheep (*Ammotragus lervia*), collected in April 2018 by Mr. Jim Austin. Ex-type strain R4 is stored on solid agar media at 39 °C at Oklahoma State University, Department of Microbiology and Molecular Genetics.

Etymology: *duplicus* = Latin for double, *liberans* = Latin for liberating or releasing. The species epithet highlights the dual zoospore release mechanisms.

An obligate anaerobic fungus that produces globose (5–14 µm in diameter) zoospores with 7-20 flagella (19–36 µm long). Zoospores germinate into determinate monocentric thalli with highly branched anucleated rhizoids that lack constriction and intercalary swellings. Both endogenous and exogenous thalli developments are observed. Mature endogenous sporangia are mainly rhomboid (30–70 µm L x 40–85 µm W) and elongated (25–90 µm L x 15–40 µm W). Mature exogenous sporangia range in size between (40–90 µm L x 15–35 µm W), and display a variety of shapes including obpyriform, ellipsoid, globose, constricted ellipsoid, and ovoid. Sporangiophores vary in length between 10–300 µm. Wide flattened sporangiophores and sporangiophores ending with sub-sporangial swellings are occasionally encountered. Zoospores are released either through an apical pore or through the lysis of the sporangial wall. Sporangial walls remain intact or are completely collapsed after zoospore release. Produces white filamentous colonies with a white center of sporangia (2-5 mm diam.) on agar roll tubes and heavy fungal biofilm-like growth that doesn't attach to the tube's glass surface in liquid media. The strain is defined by the sequences MW019494- MW019497 (for ITS1, 5.8S rDNA, ITS2, D1-D2 28S rDNA).

Additional specimens examined: Radwa Hanafy strains R1 (MW019480, MW019481, MW019483, MW019484, MW019485, MW019486), R2 (MW019482, MW019487), R3 (MW019488, MW019490, MW019491, MW019492, MW019494), and R5 (MW019498, MW019489, MW019499, MW019479, MW019500) (GenBank accession number of clones in parenthesis), isolated from the same frozen rumen content of a female aoudad sheep (*Ammotragus lervia*) from which the type strain was isolated, in April 2018. Marcus Stabel strain A252 (MW049132-MW049145) (GenBank accession number of clones in parenthesis), isolated from the feces of an alpaca (*Vicugna pacos*) from the Karlsruhe Zoo, Karlsruhe, Germany in August 2019.

4 Biochemical characterization of anaerobic fungi

This chapter is based on the publication:

Isolation and Biochemical Characterization of Six Anaerobic Fungal Strains from Zoo Animal Feces

Marcus Stabel[1], Tabea Schweitzer[1], Karoline Haack[1], Pascal Gorenflo[1], Habibu Aliyu[1] and Katrin Ochsenreither[1]

[1] Karlsruhe Institute of Technology, Process Engineering in Life Sciences 2: Technical Biology, Karlsruhe, Germany

Publishing details:

Microorganisms

Volume 9 Article 1655

Published on 3 August 2021

DOI: https://doi.org/10.3390/microorganisms9081655

Author Contributions: Conceptualization, M.S.; methodology, M.S. and H.A.; software, H.A.; validation, M.S., H.A. and K.O.; formal analysis, M.S. and H.A.; investigation, M.S., T.S., K.H., P.G. and H.A.; resources, K.O.; data curation, M.S. and H.A.; writing—original draft preparation, M.S.; writing—review and editing, H.A and K.O; visualization, M.S.; supervision, K.O.; project administration, M.S. and K.O.; funding acquisition, K.O.

4.1 Introduction

The reduction of greenhouse gas emissions to limit global warming is one of the biggest challenges scientists need to address. Using renewables like lignocellulosic materials instead of fossil resources for the production of energy carriers and materials is one option to lower the CO_2 footprint. However, the usage of agricultural waste products like straw as carbon source for microorganisms requires pretreatment to make carbohydrates accessible due to the recalcitrance of lignocellulose. These pretreatments are expensive, energy intensive and/or ineffective [223]. Additionally, toxic substances like furfural and 5-hydroxymethyl furfural are produced by some methods inhibiting microbial growth and product formation [224]. Anaerobic fungi (AF), which inhabit the gut of a great variety of herbivores [16], do not require pretreatment of lignocellulose to use it as substrate [225], making them excellent candidates for biofuel production. As demonstrated recently, they were used together with *Escherichia coli* in a two stage process to produce ethanol from corn stover [147]. AF mediate the breakdown of ingested lignocellulose in their host, using a mix of mechanical disruption [106,226] and secretion of a big variety of hemicellulases and cellulases [85]. These enzymes often form multi enzyme complexes called cellulosomes [227,228]. Enzyme preparations from AF have shown similar activities as commercial formulations [119] which makes them excellent candidates for the screening of lignocellulose degrading enzymes. Despite their potential, AF seem to be lacking lignin degrading capabilities [85,229].

Historically, AF were first described as flagellated protozoans [41], which was contradicted by Orpin in 1975 [42] by demonstrating the occurrence of chitin in the cell walls of zoospores [43]. In 2007, anaerobic fungi were unified in a new phylum, *Neocallimastigomycota,* before being placed systematically with the closely related *Chytridiomycot*a [44]. To the best of our knowledge, 20 genera of anaerobic fungi have been described until now: *Neocallimastix*, *Piromyces*, *Caecomyces*, *Cyllamyces*, *Anaeromyces*, *Orpinomyces*, *Oontomyces*, *Buwchfawromyces*, *Pecoramyces*, *Liebetanzomyces*, *Feramyces*, *Agrisomyces*, *Aklioshmyces*, *Capellomyces*, *Ghazallomyces*, *Joblinomyces*, *Khoyollomyces*, *Tahromyces*, *Aestipascuomyces*, and *Paucimyces* [51–63]. While in the past morphological features played a major role in describing AF [67], nowadays DNA barcoding plays a decisive role. Lately, the D1/D2-domain of the large ribosomal subunit (LSU) has been used as marker, being more consistent than the previously-used internal transcribed spacer region 1 (ITS1)[60,92].

Anaerobic fungi gain energy through mixed acid fermentation, with acetate, formate, succinate, lactate, ethanol, and hydrogen being the main products [18,19]. Production of hydrogen, acetate, and formate occurs mainly in the hydrogenosomes, organelles which have evolved from mitochondria lacking in AF [135]. Studies analyzing the metabolites produced during AF growth are scarce and are mainly focused on the genera *Piromyces* and *Neocallimastix*. With the exact nutritional needs of AF being unknown but highly relevant for the biotechnological use of these promising organisms [20], such studies are of high importance. To the best of our knowledge any study has so far compared the produced metabolites from several AF species during growth on multiple carbon sources. Here, the isolation of five strains of AF belonging to the genera *Neocallimastix*, *Orpinomyces*, *Caecomyces*, *Pecoramyces*, and *Khoyollomyces* is reported. The biochemical characterization of these isolates as well as of isolate A252, which was previously identified [54], was also performed.

4.2 Materials and Methods

4.2.1 Media

Enriched medium was adapted from the basal medium as previously described [60]. One liter contained 150 mL salt solution A, 150 mL salt solution B, 3 g yeast extract, 10 g tryptone, 2 mL hemin solution, and 2 mL resazurin solution. Distilled water was added to a total weight of 850 g, and the solution was boiled by microwaving to reduce the oxygen content, as indicated by the color change of resazurin to red. After readjusting the weight to 850 g with distilled water, the solution was cooled on ice, and 150 mL clarified rumen fluid, 6 g $NaHCO_3$ and 1 g cysteine hydrochloride monohydrate were added. Subsequently, enriched medium was supplemented with the following carbon sources: dissolved xylan solution with 2 g dry weight/l, 2 g/L cellobiose and 5 g/L wheat straw (milled to a particle size of 1 mm

with a Pulverisette 25, Fitsch, Idar-Oberstein, Germany). The medium was deoxygenated by gassing with 100% CO_2 until turning yellow. Afterwards the pH was adjusted to 6.9 with 5M NaOH, and 50 mL of the medium was dispensed into serum bottles (118 mL) prior flushed with CO_2. These were closed with a butyl stopper, fastened with an aluminum crimp seal, and subsequently sterilized by autoclaving at 121 °C for 20 min. The medium for the roll tube isolation technique was prepared identically except the addition of 0.9 g agar to each serum bottle and different carbon sources. Here, no straw and 3 g/L cellobiose instead of 2 g/L were used. The roll tubes were stored at 60 °C after autoclaving to avoid agar solidification. Before inoculation of any media, 0.5 mL of antibiotics solution was added to each serum bottle.

Salt solution A contained KH_2PO_4 (3.0 g/L), $(NH4)_2SO_4$ (6.0 g/L), NaCl (6.0 g/L), $MgSO_4$ $7H_20$ (0.6 g/L), and $CaCl_2$ $2H_2O$ (0.6 g/L) in distilled water. Salt solution B contained K_2HPO_4 (3.0 g/L) in distilled water. Hemin solution was prepared by dissolving 0.05 g hemin in 50 mL ethanol and then adding 50 mL of 0.05 M NaOH. The resazurin solution was made by dissolving 1 g/L resazurin in distilled water. Dissolved xylan was prepared according to [230] by adding 50 g of beechwood xylan (Carl Roth) to 1 L of distilled water, adjusting the pH value to 10 with 5M NaOH, and incubating at room temperature for 1 h. The solution was centrifuged for 10min at 10,000 ×*g*, the supernatant was transferred to a beaker, and the pH value was adjusted to 7 with 1 M acetic acid. The quantity of dissolved xylan was determined by freeze drying 10 mL of the solution and weighing the dried substance. The antibiotics solution contained 120 g/L of each penicillin sodium salt, ampicillin sodium salt, and streptomycin sulfate dissolved in distilled water, and was filter sterilized.

Defined medium was prepared similarly to enriched medium with the following changes: clarified rumen fluid was replaced by 140 mL distilled water, yeast extract and tryptone were omitted, 10 mL of the trace elements solution were added during medium deoxygenation, and 0.5 mL of the vitamin solution was added just before fungal inoculation. When using insoluble carbon sources (wheat straw, agarose, xylan, starch, inulin, chitin, pectin, alginate, or crystalline cellulose), 0.25 g of each substrate was added to a serum bottle flushed with 100% CO_2 and subsequently, aliquots of 49.5 mL media were added to achieve a final concentration of 5 g/L of each carbon source. When using soluble carbon sources (cellobiose, maltose, trehalose, lactose, sucrose, glucose, xylose, mannose, fructose, arabinose, ribose, galactose, or glucuronic acid), the aliquots consisted of 44.5 mL media, and 5 mL carbon source were added from a 50 g/L stock to each serum bottle for a final concentration of 5 g/L before fungal inoculation.

The vitamin solution was prepared in distilled water and contained 0.01 g/L thiamine, 0.2 g/L riboflavin, 0.6 g/L calcium pantothenate, 0.6 g/L nicotinic acid, 1.0 g/L nicotinamide, 0.05 g/L folic acid, 0.02 g/L vitamine B12, 0.2 g/L biotin, 0.1 g/L pyridoxamine, and 0.05 g/L p-aminobenzoic acid [210] and was filter sterilized after preparation. The trace elements solution was prepared according to Lowe et al. 1985 [209] and contained 0.25 g/L $MnCl_2$ $4H_2O$, 0.25 g/L $NiCl_2$ $6H_2O$, 0.25 g/L $NaMoO_4$ $2H_2O$, 0.25 g/L H_3BO_3, 0.20 g/L $FeSO_4$ $7H_2O$, 0.05 g/L $CoCl_2$ $6H_2O$, 0.05 g/L Na_2SeO_3 $5H_2O$, 0.05 g/L $NaVO_3$ $4H_2O$, 0.025 g/L $ZnSO_4$, 0.025 g/L $CuSO_4$ $2H_2O$ in 0.2 M HCl.

4.2.2 Isolation of AF

Feces from reticulated giraffe (*Giraffa reticulata* "G"), watussi cattle (*Bos primigenius f. taurus,* "W"), Przewalski's horse (*Equus ferus,* "PP"*),* and scimitar oryx (*Oryx dammah,* "SA") were collected by personal from the Karlsruhe Zoo (Germany) in the afternoon (08.04.2019) and stored at room temperature in plastic sample beakers until the next day. Feces of horse (*Equus caballus,* "X") was collected in a barn in Reilingen, Baden Württemberg, Germany (25.01.2019) and used directly for isolation as described below. A 1:1 mixture of salt solution A and salt solution B was deoxygenated by gassing with 100% CO_2 for 30 min. One gram of feces was added to the solution and dispersed by further gassing. Enriched medium was inoculated with 5 mL of this suspension and incubated for 7 days at 39 °C in darkness in a BBD 6220 incubator (Heraeus Deutschland GmbH & Co., Hanau, Germany). Inoculations were carried out by transferring 5 mL of culture with a syringe to the recipient vessel. After

the incubation, fungal growth was monitored by light microscopy. Serum bottles with visible anaerobic fungal growth were chosen to inoculate roll tubes which had been prepared as described above. After inoculation, the bottle was placed on ice and rolled to achieve a fine layer of solidified medium on the inner surface of the serum bottle. The roll tubes were incubated for 4 days at 39 °C in darkness. By picking different colony types from the roll tubes, various strains of AF were separated from other microorganisms. Picked colonies were transferred to fresh enriched medium and incubated for another 7 days followed by another passage of roll-tubing. After 3 passages of roll-tubing and observation by light microscopy, all cultures were considered as pure fungal isolates.

4.2.3 Identification of AF

Genomic DNA was isolated from the entire mycelium of one-week old cultures grown in 50 mL defined medium with cellobiose as C-source using the Quick-DNA Fecal/Soil Microbe DNA Miniprep Kit (Zymo Research, Orange County, CA, USA) following the instructions of the manufacturer. The amount of isolated gDNA was determined using a microplate spectrophotometer (Epoch, BioTek Instruments GmbH, Bad Friedrichshall, Germany). The part of the ribosomal operon between the 18S small ribosomal subunit and the D1/D2 region of the 28S large ribosomal subunit was amplified as described by Wang et al. (2017)[68] using the ITS5 [231] and NL4 [232] primers (NL4: GGTCCGTGTTTCAAGACGG; ITS5: GGAAGTAAAAGTCGTAACAAGG). The PCR reaction was composed of 12.5 µL of Q5 High-Fidelity 2X Master Mix (New England Biolabs (NEB), Ipswich,MA, USA), 0.5 µL of each primer (10 µM stock) and 20 ng gDNA in 25 µL reaction volume. The PCR program consisted of 30 sec initial denaturation at 98 °C, 30 cycles of 10 sec denaturation at 98 °C, 30 sec annealing at 62 °C, 90 sec elongation at 72 °C and a final extension step at 72 °C for 2 min. The resulting 1.5 kb fragments were separated in a 2% agarose gel run at 120 V and stained with ROTI®GelStain (Carl Roth, Karlsruhe, Germany). Bands were cut out from the gel and the DNA was eluted with a Monarch Gel Extraction Kit (NEB). Recovered DNA fragments were cloned using a PCR Cloning Kit (NEB) and transformed into NEB 10-beta *Escherichia coli* following the supplier's instructions. Transformants were selected by streaking on LB-agar containing 10 g/L NaCl, 10 g/L trypton, 5 g/L yeast extract, 20 g/L agar, and 0.05 g/L ampicillin sodium salt. The agar-plates were incubated overnight at 37 °C. Colonies were picked and grown overnight in LB-media as described above (no agar) at 37 °C under shaking at 210 rpm in a Multitron Shaker (Infors, Bottmingen, Switzerland). Plasmids were extracted using the Monarch Plasmid Miniprep Kit (NEB) and sequenced by the Supreme Run Sanger Sequencing Service from Eurofins Genomics using the sequencing primer from the PCR Cloning Kit. The obtained sequences were uploaded to genbank with following accession numbers: Isolate G341 MW175298-175304, Isolate W212 MW175312-175318, Isolate SA222 MW175305-MW175311, Isolate X2152 MW175319-MW175325 and Isolate PP313 MW175289-175297. The ribosomal operon between the 18S small ribosomal subunit and the D1/D2 region of the 28S large ribosomal subunit for *Neocallimastix californiae*, *Neocallimastix lanati*, and *Caecomyces churrovis* was extracted from the respective published genomes [19,122,233] using BioEdit V. 7.0.5.3 [213]. For the LSU analysis, a database with *Neocallimastigomycota* sequences, the sequences of our isolates and the sequences extracted from the genomes were used encompassing a total of 244 sequences. *Gonopodya prolifera* (JN874506) was included as outgroup. Phylogenetic analysis was performed by aligning the sequences from the isolates with the databases using MAFFT v7.471 [212] at https://mafft.cbrc.jp/alignment/server/ (Accessed on 10 June 2021). The resultant alignments were manually curated and trimmed using BioEdit. Phylogenies were reconstructed using IQ-TREE v2.0.3 [214] with model selection [215] and 1000 ultrafast bootstraps [216]. The obtained trees were visualized and edited with Evolview V.3 [234]. Sequence identity matrices were calculated using BioEdit.

4.2.4 Carbon Source Usage and Analytics

Five mL of culture liquid from the isolates and *Aestipascuomyces dubliciliberans* strain A252 [54] were inoculated into defined media prepared as described above with 5 g/L of one of the following carbon sources: wheat straw, xylan, starch, inulin, chitin, pectin, alginate, crystalline cellulose, cellobiose, maltose, trehalose, lactose, sucrose, glucose, xylose, mannose, fructose, arabinose, ribose, galactose, or

glucuronic acid. Incubation followed at 39 °C in the dark. After five to seven days, they were transferred into fresh defined media. After three passages, biomass formation was evaluated by eye, light microscopy, and pressure measurement through a manometer. Cultures with visible growth were inoculated into a fourth passage of seven days growth in triplicate. The composition of the liquid phase was measured by HPLC by taking 1 mL samples directly after inoculation and on the seventh day. Samples were prepared for HPLC by centrifuging at 10,000 g for 10 s and filtering the supernatant with 0.22 µm cellulose acetate syringe filters (Restek). Subsequently, 10 µL of supernatant were injected to a Rezex ROAorganic acid H + (8%) column from Phenomex in a 1100 Series System from Agilent Technologies with 5 mM sulfuric acid as eluent at a flow rate of 0.5 mL/min and a column temperature of 50 °C. Sugars and ethanol were detected with a refractive index detector and organic acids by a diode array detector at 220 nm. The gaseous phase was analyzed by GC by taking 5 mL of sample from the gaseous phase with a syringe after measuring the pressure on the fifth day. This sample was injected manually into a 3000 Micro GC System from Inficon with a CP-Molsieve 5 Å column and a PoraPLOT Q column at 80 °C.

4.3 Results

4.3.1 Isolation and Phylogeny

From each host animal a single fungal isolate was obtained: G341 from giraffe (*Giraffa reticulata*), PP313 from Przewalski's horse (*Equus ferus)*, W212 from watussi cattle (*Bos primigenius f. taurus*), SA222 from scimitar oryx (*Oryx dammah*), and X2152 from horse (*Equus caballus*). The LSU phylogeny was inferred in IQtree based on 245 sequences (alignment: 691 characters) from the above isolates (G341, PP313, W212, SA222, and X2152), and other AF using *Gonapodya prolifera* strain ATCC MYA-4800 as outgroup. All isolates could be assigned at least on genus level to previously described AF genera (Figure 9) in well-supported monophyletic groups. The sequences from G341 grouped into the sequences assigned to *Neocallimastix cameroonii*, W212 into sequences of *Orpinomyces joyoonii*, SA222 into the ones from *Pecoramyces ruminantium* and X2152 into sequences of *Khoyollomyces ramosus*. According to our phylogeny, the sequences from the genomes of *Neocallimastix californiae* and *Neocallimastix lanati* grouped inside the *Neocallimastix cameroonii* clade. The identity of the aligned and trimmed sequences to the assigned species were 99.0–100% for G341, 99.0–99.6% for W212, 97.8–100% for SA222, and 98.9–99.6% for X2152 (Table S1, available from https://www.mdpi.com/2076-2607/9/8/1655/s1), respectively. The genomic sequences from *Neocallimastix californiae* shared 99.6% and the ones from *Neocallimastix lanati* shared 99.5–100% identity with the sequences from *Neocallimastix cameroonii*.

However, the affiliation by LSU phylogeny of the isolate PP313 was less clear. The PP313 sequences grouped into a clade consisting of sequences from *Caecomyces communis*, *Cyllamyces aberensis* and *Caecomyces churrovis*. The sequences of PP313 and those extracted from the *Caecomyces churrovis* genome cluster distinctly in two subclades. PP313 shared 98.7–99.0% sequence identity with *Caecomyces communis*, 98.4–99.8% with *Caecomyces churrovis* and 96.7–98.7% with *Cyllamyces aberensis*. Interestingly, the sequences from *Cyllamyces aberensis* grouped inside the *Caecomyces* sequences forming a group with sequences from *Caecomyces communis* and sharing 97.5–98.6% sequence identity. The sequence identity between *Caecomyces churrovis* and *Cyllamyces aberensis* was 98.1–98.7%.

As for the whole bulbous clade, sequences of the D1/D2 region were either highly similar and/or LSU sequences were not available. ITS1 region was therefore used to study the clade. In the ITS phylogeny sequences from PP313 were placed together with published (MF460993) and genome extracted sequences from *Caecomyces churrovis* (Figure 24, Appendix). In the corresponding identity matrix, the sequences from the genome shared 98.3–100% identity with MF460993 (Table S2, available from https://www.mdpi.com/2076-2607/9/8/1655/s1). PP313 shared 99.1% identity with both MF460993 and the genomic sequences. *Cyllamyces aberrensis* grouped outside the *Caecomyces* clade in this ITS1 phylogeny (Figure 24, Appendix).

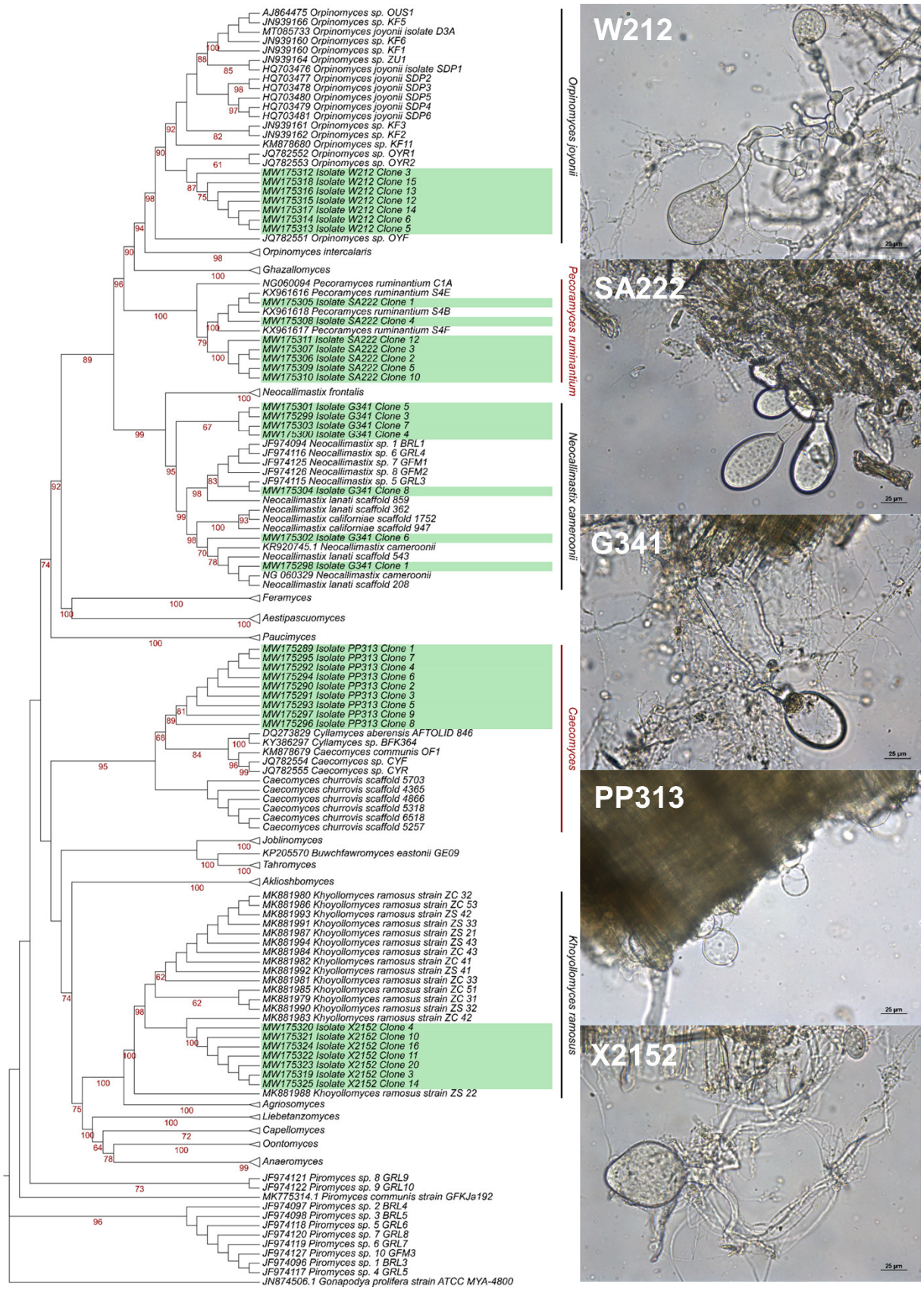

Figure 9: Left: Phylogenetic affiliation of the isolated strains to other AF genera based on the nucleotide sequences of the D1–D2 domains of the LSU from the ribosomal operon. MAFFT [212] was used for alignment and BioEdit [213] was used for manual curation of the sequences. The ML-tree was constructed using IQTREE [214] with the predicted model TN + F + R2 and –bb 1000. Bootstrap values higher than 50% are shown at the nodes. Right: Isolates growing in defined media with straw as c-source.

4.3.2 Carbon Source Usage

The substrate utilization range by isolates, as well as the *Aestipascuomyces dubliciliberans* strain A252, was analyzed and evaluated by quantification of the produced metabolites. Ethanol, while being detected during the growth of all strains, could not be quantified reliably due to sample preparation which facilitated evaporation. Therefore, ethanol amounts are not detailed further. Furthermore, if the total amount of produced metabolites was lower than 1 mmol in the fourth passage, growth was considered as low. The total amount of produced metabolites on the different C-sources excluding ethanol is given in Table 4. None of the fungi was able to grow on chitin, alginate, arabinose, ribose, galactose, and glucuronic acid.

G341 grew on wheat straw, xylan, starch, inulin, pectin, cellulose, cellobiose, maltose, lactose, sucrose, glucose, xylose, mannose, and fructose. The isolate showed low growth on trehalose (0.008 ± 0.003 mmol).

PP313 grew on wheat straw, xylan, cellobiose, lactose, glucose, xylose, and fructose. Low growth was observed on starch (0.204 ± 0.152 mmol), pectin (0.352 ± 0.155 mmol), cellulose (0.093 ± 0.047 mmol), and maltose (0.080 ± 0.038 mmol).

W212 utilized wheat straw, xylan, starch, cellulose, cellobiose, maltose, lactose, sucrose, glucose, xylose, and fructose while showing low growth on pectin (0.269 ± 0.085 mmol).

SA222 could use wheat straw, xylan, starch, cellulose, cellobiose, maltose, lactose, sucrose, glucose, xylose, mannose, and fructose. Low growth was observed on pectin (0.393 ± 0.027 mmol) and trehalose (0.005 ± 0.000 mmol).

X2152 grew on wheat straw, xylan, cellulose, cellobiose, lactose, glucose, xylose, and fructose. In addition, low usage of starch (0.008 ± 0.001 mmol), pectin (0.408 ± 0.063 mmol), maltose (0.035 ± 0.002 mmol), trehalose (0.006 ± 0.000 mmol), and sucrose (0.246 ± 0.042 mmol) was observed.

A252 grew on wheat straw, xylan, starch, cellulose, cellobiose, maltose, lactose, sucrose, glucose, xylose, mannose, and fructose. Low growth was observed on inulin (0.315 ± 0.419 mmol), pectin (0.444 ± 0.150 mmol) and trehalose (0.007 ± 0.005 mmol).

Table 4: Total metabolites (mmol) without ethanol produced by the isolates during growth on different C-sources.

	Total Metabolites [mmol]					
	G341	**PP313**	**W212**	**SA222**	**X2152**	**A252**
Cellobiose	4.015±0.079	3.741±0.12	3.606±0.154	3.519±0.218	3.983±0.052	4.434±0.07
Cellulose	3.85±0.069	0.093±0.047	4.061±0.015	1.181±0.112	3.409±0.159	3.238±0.321
Fructose	3.85±0.15	3.31±0.247	3.608±0.043	3.286±0.09	3.865±0.361	3.868±0.184
Glucose	3.736±0.02	3.167±0.287	3.347±0.192	3.399±0.087	3.926±0.085	4.039±0.14
Inulin	3.153±0.436	X	X	X	X	0.315±0.419
Lactose	1.3±0.104	2.146±0.122	2.428±0.035	2.168±0.055	2.403±0.418	3.759±0.15
Maltose	3.83±0.132	0.08±0.038	3.542±0.084	3.279±0.087	0.035±0.002	4.201±0.187
Mannose	3.265±0.35	X	X	3.339±0.058	X	3.498±0.268
Pectin	0.16±0.007	0.352±0.155	0.269±0.085	0.393±0.027	0.408±0.063	0.444±0.15
Starch	3.578±0.397	0.204±0.152	3.934±0.293	3.521±0.695	0.008±0.001	4.032±0.33
Wheat straw	2.29±0.024	1.565±0.021	2.312±0.071	1.709±0.025	1.707±0.096	2.682±0.08
Sucrose	4.125±0.077	X	3.978±0.232	3.721±0.066	0.246±0.042	4.309±0.134
Trehalose	0.008±0.003	X	X	0.005±0	0.006±0	0.007±0.005
Xylan	2.627±0.02	2.841±0.061	2.557±0.04	2.54±0.101	2.781±0.226	3.201±0.415
Xylose	3.925±0.273	3.23±0.061	3.271±0.156	3.357±0.108	3.478±0.209	3.664±0.397

Table 5: Calculated carbon balance without ethanol of the isolates during growth on the C-sources cellobiose, fructose, glucose, maltose, mannose, and xylose. Ø is the average of these sugars. "Lactose" stands for the C-balance during growth on lactose with regard to the hydrolyzed amount of lactose, but not taking into account the actual consumption of released monosaccharides. "Lactose*" is the C-balance including residual galactose.

	C-Balance					
	G341	**PP313**	**W212**	**SA222**	**X2152**	**A252**
Cellobiose	0.787±0.026	0.702±0.035	0.597±0.027	0.659±0.050	0.633±0.053	0.795±0.008
Fructose	0.828±0.052	0.679±0.060	0.675±0.023	0.654±0.033	0.784±0.062	0.781±0.037
Glucose	0.772±0.009	0.628±0.064	0.584±0.032	0.700±0.034	0.730±0.023	0.778±0.030
Maltose	0.775±0.028	X	0.604±0.017	0.621±0.016	X	0.804±0.033
Mannose	0.626±0.074	X	X	0.762±0.017	X	0.771±0.046
Xylose	0.841±0.043	0.692±0.038	0.687±0.026	0.691±0.035	0.677±0.036	0.725±0.090
Ø	0.772±0.083	0.675±0.059	0.629±0.05	0.681±0.055	0.713±0.071	0.776±0.054
Lactose	0.472±0.017	0.385±0.022	0.423±0.011	0.432±0.029	0.394±0.097	0.805±0.023
Lactose*	0.966±0.027	0.828±0.044	0.889±0.017	0.885±0.039	0.699±0.152	0.841±0.027

As the number of detected metabolites on trehalose was low for all isolates, it might be considered as an experimental artefact and will not be discussed further. The overall highest cumulated metabolite concentration was detected for A252 growing on cellobiose (4.434 ± 0.070 mmol), but it also consistently produced the highest metabolite concentrations with most of the C-sources (Table 4) except when growing on cellulose (W212) and inulin or xylose which were best utilized by G341.

Table 5 displays the carbon balance excluding the not quantifiable ethanol for the soluble C-sources. For PP313, the number of produced metabolites on maltose was so low and variant that a precise calculation of the carbon balance was not conclusive. The total carbon balance was calculated from the samples of cellobiose, fructose, glucose, maltose, mannose, and xylose. When one of the C-sources was not usable by an isolate, it was omitted in the calculation. On lactose, the carbon balance was seemingly much lower for all isolates than on other carbon sources except for strain A252. It was observed that most strains consumed preferably the released glucose from lactose but the residual galactose only to a much lower extent. When the residual galactose was added to the product side of the carbon balance relatively high values were achieved compared to the average carbon balance (Table 5). The amount of residual galactose varied highly between isolates (Table 13, Appendix) with the lowest amount being 0.043 ± 0.008 mmol for A252, but for all tested fungi a small decrease in galactose was determined while growing on lactose.

4.3.3 Metabolite Production

Figure 10 shows the total amount of metabolites in mmol, including their relative distribution. The main detected metabolites were hydrogen, acetate, and formate, which were produced by all isolates. Lactate production was observed for all fungi but X2152, where it was only detected in one of three samples of sucrose cultures. Succinate was produced by all isolates but W212, while for SA222 its production was lower compared to the other isolates and restricted to fructose, glucose, starch, sucrose, and xylan cultures. Citrate was only detected in traces in samples of xylan, straw, or pectin cultures of strain SA222. Next, the dependence of the metabolite composition from the C-source was analyzed. Therefore, the number of single metabolites was compared to the total amount of produced metabolites (Figure 11). Although no big changes were apparent between C-sources that yielded in roughly the same total amount of metabolites, prominent differences were noticeable when compared to C-sources which only yielded in a small total amount of metabolites. Here, less metabolite diversity was observed. As the total amount increased, not only did the diversity of metabolites increase, but the metabolites seemed to be produced in a specific order. Hydrogen was always present with formate and acetate appearing with increasing total metabolite amount followed by lactate. Strain PP313 was an exception as it produced lactate subsequent to hydrogen, then acetate and finally formate. Succinate seems to be produced only when an abundant production of other metabolites occurred (Figure 10), although it remained a marginal metabolite (Figure 11). Another factor influencing the composition of the metabolites seemed to be the

complexity of the C-source, as the most complex C-source (wheat straw) resulted in a high relative (Figure 10) as well as absolute (Figure 11) amount of produced hydrogen. The analysis below will focus on straw and the monosaccharides fructose, glucose, and xylose as these enabled good growth for all tested fungi. Both absolute and relative values for all strains on all C-sources are given in the supplementary Tables 14–25 (Appendix).

G341 produced 0.352 mmol of hydrogen while growing on straw followed by 0.312 mmol on glucose, 0.232 mmol on fructose, and 0.278 mmol on xylose, although the total amount of metabolites being 2.290 mmol on straw compared to 3.736–3.925 mmol for the monosaccharides. In relation to the total amount of metabolites, 15.4% hydrogen were produced on straw in comparison to 6.1–8.4% on monomeric sugars. Strain G341 grown on straw also produced lower portions of lactate (6.1%) and succinate (ND) compared to growth on xylose, glucose, or fructose (18.2–19.7% lactate and 3.0–3.4% succinate). For formate, concentrations were slightly higher in straw cultures (44.4%) than in cultures using monomeric sugars (37.0–39.1%), whereas acetate concentrations were comparable (33.6% vs. 31.4–34.7%).

Isolate PP313 produced less hydrogen when grown on straw (0.322 mmol) than on the monosaccharides (0.400–0.488 mmol). Although in relation to the total amount of metabolites hydrogen was more elevated on straw than on monosaccharides (20.6% vs. 12.4–15.5%), the differences between the C-sources were not as pronounced as for the other isolates and might be explained by the incrementing diversity explained above.

Metabolite production by strain W212 and G341 followed a similar pattern. Hydrogen increased significantly while growing on straw (0.375 mmol) in comparison to monosaccharides (0.097–0.194 mmol) despite a lesser number of total metabolites (2.312 mmol vs. 3.271–3.608 mmol) being produced. On straw lactate amounted to 6.2%, while acetate and formate yielded in 39.3% and 37.7% of the total metabolites, respectively. In comparison, cultivation with monosaccharides resulted in increased formate (48.3–56.8%) and decreased acetate (29.0–33.34%) levels. The relative lactate amount spanned a range between 6.4% (glucose) and 19.7% (xylose) and seemed to be increasing with the decreasing relative amount of formate. As described above, succinate could not be detected for W212.

Strain SA222 also produced the highest amount of hydrogen when growing on straw (0.303 mmol) compared to the monosaccharides (0.193–0.260 mmol) despite the differences in total metabolite amount (1.709 mmol for straw vs. 3.286–3.399 mmol for monosaccharides). While the portion of acetate when growing on straw (35.7%) was higher compared to the monosaccharides (25.3–27.8%), the portion of lactate was lower (3.4% on straw vs. 17.6–25.6% on monosaccharides). While growing on straw and xylose, succinate was not detected, and it amounted to 0.9% on glucose and 2.0% on fructose. When comparing the monosaccharides, a relation between a higher percentage of succinate (2.0% for fructose vs. ND for xylose) and a lower percentage of lactate (17.6% on fructose vs. 25.6% on xylose) as well as hydrogen (5.9% on fructose vs. 7.8% on xylose) was observed. No correlations were found for the relative amount of formate which varied independently from the complexity of the C-source between 40.8% and 46.7%.

Isolate X2152 produced 0.411 mmol of hydrogen while growing on straw which was comparatively high in relation to 0.236–0.321 mmol for growth on monosaccharides, although the total amount of metabolites was considerably higher on sugars (3.5–3.9% vs. 1.7%). On straw, the relative amount of formate was slightly higher (53.8%) and the relative amount of acetate was lower (21.4%) when compared to growth on monosaccharides (49.3–50.6% formate and 35.1–36.7 acetate). No succinate was detected on straw, whereas it ranged between 5.3% and 8.3% for growth with monosaccharides. Lactate was not detected in any of the samples, as described above.

For strain A252, the highest total amounts of hydrogen (0.543 mmol) were observed in straw cultures, although total amount of metabolites (2.682 mmol) was relatively low when compared to growth on monosaccharides (0.430–0.500 mmol hydrogen of 3.664–4.039 mmol total metabolites). The relative

amount of acetate was higher on straw (39.3%) compared to the growth with monosaccharides (29.4–31.0%). All other metabolites were produced in lower portions on straw (33.6% formate, 3.2% lactate, 3.1% succinate) than when growing on monosaccharides (37.7–38.6% formate, 14.2–15.9% lactate, 4.2–5.1% succinate). In all samples with straw as C-source a small amount of citrate was detected, ranging between 0.2% (SA222) to 0.6% (X2152) of the total metabolites.

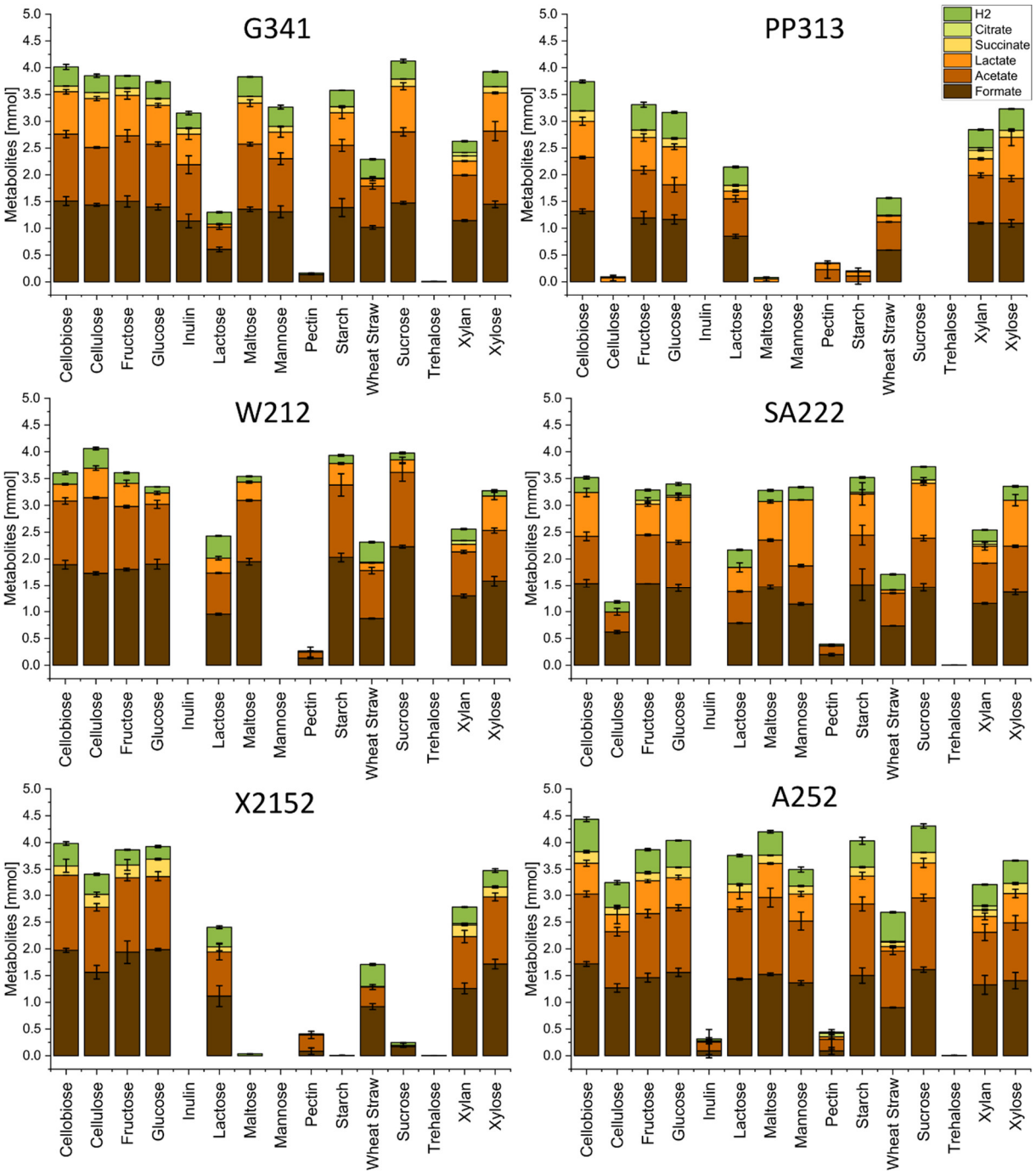

Figure 10: Produced metabolites (mmol) of the strains G341, PP313, W212, SA222, X2152 and A252 during growth on different C-sources. Ethanol is excluded. Values shown represent averages of triplicate experiments and standard deviations.

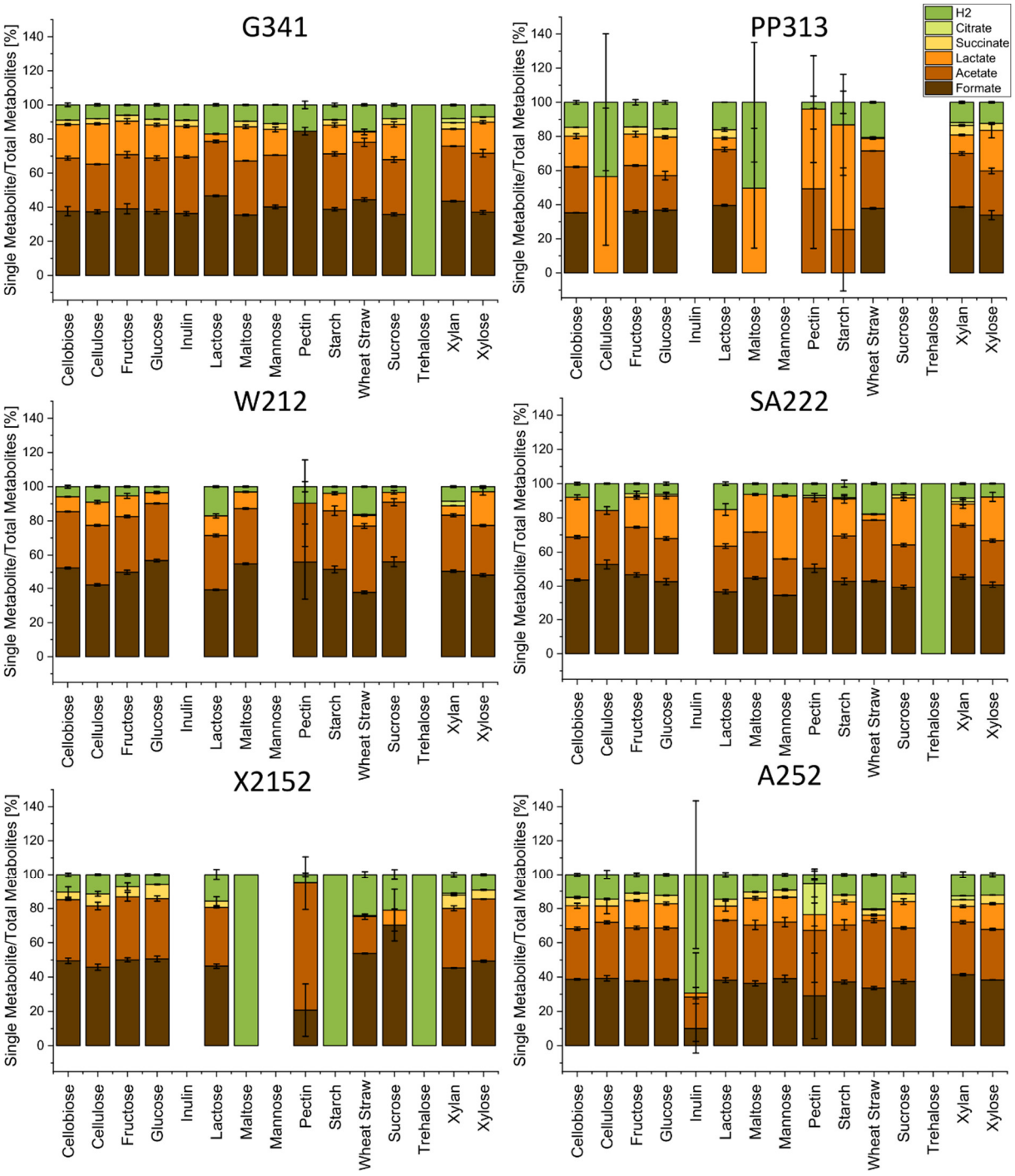

Figure 11: Relative amount of each produced metabolite when compared to the total of produced metabolites (%) of the strains G341, PP313, W212, SA222, X2152, and A252 during growth on different C-sources. Ethanol is excluded. Values shown represent averages of triplicate experiments and standard deviations.

4.4 Discussion

4.4.1 Phylogeny

In this study five different fungal species of *Neocallimastigomycota* from fecal sample of different zoo animals were isolated. Four of the isolates could be assigned to known anaerobic fungal species: isolate G341 to *Neocallimastix cameroonii*, isolate W212 to *Orpinomyces joyoonii*, isolate SA222 to *Pecoramyces ruminantium*, and isolate X2152 to *Khoyollomyces ramosus*. Our phylogeny showed clustering of isolate G341 together with *Neocallimastix californiae* and *Neocallimastix lanati* and *Neocallimastix cameroonii* in a well-supported clade and shared high sequence identity, indicating that *Neocallimastix californiae*, *N. lanati*, and *N. cameroonii* may be conspecific. The description of

Neocallimastix cameroonii [71] preceded *N. californiae* [72] and *N. lanati* [19] and hence should have taxonomic preference as the species name. This would reduce the number of described *Neocallimastix* species to two: *Neocallimastix frontalis* and *Neocallimastix cameroonii*. The *Neocallimastix* species *N. patriciarum*, *N. variabilis* and *N. hurleyensis* [66,69,70] described in the past were later also shown to be part of the already described species *N. frontalis* [67,68]. This highlights the need for a more robust phylogenetic framework that may include multiple genetic markers or whole genome sequences to resolve the phylogeny of AF.

Isolate PP313 clustered inside a clade of sequences from both *Caecomyces* and *Cyllamyces* in the LSU phylogeny. While sharing the highest sequence identity with *Caecomyces churrovis* the sequences of PP313 clustered separately as an own clade. In contrast, when using the ITS1 region as a phylogenetic marker PP313 clustered together with sequences of *Caecomyces churrovis*. The genera of *Caecomyces* and *Cyllamyces* are the only AF with bulbous growth pattern compared to the other genera which are forming rhizoids [56,102]. The two genera *Caecomyces* and *Cyllamyces* are thought to be closely related and their taxonomic status has been the subject of debate. For instance, Wang et al. previously recommended more LSU sequencing to resolve the affiliations of the two genera [68]. To the best of our knowledge no phylogeny of the D1/D2 LSU region, including *Caecomyces churrovis*, has been reported so far. According to previous reports [60,68], *Cyllamyces* grouped in a clade together with different *Caecomyces* species in our LSU phylogeny. Conversely, but in accordance to previous reports [53,54,218], *Cyllamyces* grouped outside of the *Caecomyces* sequences in the ITS1 phylogeny. The ITS1 region is highly divergent even within the same strain and *Caecomyces* and *Cyllamyces* have an especially high sequence divergence in the ITS1 region [65]. The lower heterogeneity of the D1/D2 region and the respective placement of *Cyllamyces* in the corresponding phylogeny, we suggest the reassignment of *Cyllamyces* as a species of *Caecomyces*. Because of the discrepancy between ITS and LSU phylogenies and the questions raised above concerning the *Caecomyces* clade, we assign PP313 to the genus *Caecomyces* but avoid affiliating to a species. The inclusion of additional taxonomic markers could help resolve the highlighted discrepancies.

Interestingly, only one fungal strain was isolated from each sample. It has been shown before that the frequency of isolation of an AF strain correlates with its abundance in the sample [65]. The same study reports that special effort was invested in obtaining several strains from the same sample. As the objective of this study was to isolate more robust species for a possible future biotechnological application, no special effort was undertaken for isolating as many strains as possible from each sample in contrast to the aforementioned study. Therefore, it is highly probable that only the most abundant or most robust species of each sample was isolated.

4.4.2 Carbon Source Usage

Of all isolates, strain G341 used the widest substrate range. Whereas no information concerning the substrate usage of the *Neocallimastix cameroonii* type strain was available, N. *californiae* was reported to be able to grow on glucose, cellobiose, cellulose, fructose, maltose, and different grasses [117,124]. The most extensive analysis on the carbon source usage has been performed recently for N. *lanati* [19]. In accordance with these experiments, isolate G341 was able to grow on glucose, cellobiose, fructose, maltose, cellulose, and xylan. Wilken et al. also used a model to predict further usable carbon sources, i.e., galactose, mannose, and xylose, which could not be confirmed in growth experiments [19]. In contrast, G341 was able to grow on most of these substrates confirming the model prediction. The difference between the two experiments is probably due to variances in media or experimental handling. The exception was galactose. While G341 did not grow on pure galactose, it seemed to be partly co-consumed when growing on lactose. Interestingly, N. *californiae* has been reported to lack the required genes for galactose usage [124].

Of all tested isolates, substrate usage range of strain PP313 was the narrowest. In accordance to literature, it was able to grow on all carbon sources reported previously for *Caecomyces churrovis* [80] including cellobiose, glucose, fructose, and xylan. *Caecomyces churrovis* was also reported to grow on

different types of grass. While we did not test grasses, PP313 was able to grow on wheat straw, affirming the ability to grow on complex lignocellulosic substrates. While in accordance with *Caecomyces churrovis* not being able to utilize arabinose, galactose, and mannose, PP313 was able to grow on lactose. In lactose cultures, a slight consumption of galactose could be measured. As reported and discussed previously for *Caecomyces churrovis* [80], PP313 showed a preference for soluble carbon sources and growth on cellulose was low.

The metabolic information about *Orpinomyces joyonii* is particularly scarce as only one publication was found describing it [83]. Similar to isolate W212, *O. joyonii* was reported to grow on cellulose, xylan, starch, glucose, cellobiose, fructose, maltose, lactose, and shows only poor growth on pectin. Interestingly, growth on galactose was also reported. In our case, strain W212 was only able to co-utilize galactose when it was applied as component of lactose, and even then it consumed the lowest amount of all tested fungi.

Isolate SA222 differed in the carbon source usage from *Pecoramyces ruminantium* [61]. Contrary to previous reports, SA222 was not able to grow on inulin and barely survived on trehalose. On the contrary, it was able to utilize both lactose and pectin which was not reported before. In accordance with previous publications, SA222 grew on xylan, starch, cellulose, cellobiose, maltose, sucrose, glucose, xylose, mannose, and fructose. Although previously no growth on wheat straw was reported, growth on different lignocellulose containing materials has extensively been studied.

Up to date and to the best of our knowledge, information about the substrate usage of *Khoyollomyces ramosus* has not been published yet, as both genus and species were just described recently [53]. This renders our characterization of isolate X2152 the first report in this field.

Strain A252 was able to grow on cellulose, mannose, and pectin in addition to the C-sources reported previously [54], probably due to the tenfold increase of C-source concentration. While the other *Aestipascuomyces dubliciliberans* isolate R4 was also able to grow on glucuronic acid, this still was not the case for A252. Similar to the other tested fungi, A252 was not able to grow on galactose, but when grown on lactose it metabolized nearly all of it, even leading to a similar C-balance as on other C-sources with good growth.

4.4.3 Metabolite Production

The main fermentation products reported up to date for AF are hydrogen, formate, acetate, ethanol, lactate, and succinate [18], although production of citrate and malate has also been reported [131,133]. Our study confirmed these findings, although some of the tested fungal isolates were only producing some of the mentioned metabolites, i.e., only traces of citrate and no malate were detected. *Orpinomyces joyonii* isolate W212, for example, did not produce any succinate, confirming previous studies in which the production of formate, acetate, lactate, ethanol, and hydrogen was reported [83]. Similarly, *Khoyollomyces ramosus* isolate X2152 did not produce lactate, while this was a common metabolite for the other tested strains. However, generally only scarce information is available about metabolic data for AF. Available reports focus on the genera *Piromyces* and *Neocallimastix* and little is known of other AF. When comparing metabolite production of different fungi growing on different C-sources yielding either in high or low total metabolite production we noticed a sequential appearance of different metabolites with increasing total metabolite concentration. Although we just sampled at the beginning and at the end of the experiment, we can speculate about a preference for certain end products: first hydrogen, then acetate and formate, lactate, and finally succinate. A possible exception from this rule could be PP313 for which lactate was detected in samples lacking formate and acetate. Future studies should address this hypothesis with more sampling points between start and end. As it is possible that low total metabolite concentrations on some carbon sources are due to delayed fungal growth, elongating the duration of the experiments could also be considered.

Another difference in the fermentation pattern appears when comparing the growth on wheat straw to the growth on different monosaccharides. Despite the total sum of produced metabolites being much

higher during monosaccharide growth, the amount of hydrogen was higher when growing on straw. When looking on the relative parts of other metabolites, they varied greatly between growth on monosaccharides and straw with the exact pattern depending on the observed species. An exception was PP313, which showed a strong general preference for soluble C-sources as mentioned above. Past studies showed a repression of biomass degrading enzymes by free sugars [126], indicating a reaction of AF towards these conditions. Anaerobic fungi have been reported to contain both pyruvate formate lyase (PFL) and pyruvate ferredoxin oxidoreductase (PFO) [18,127]. Recently it was shown that while both enzymes are present, the main metabolic flux is carried by PFL [19]. The authors also speculated that during growth on high sugar concentrations PFL could be used and under more complex conditions, like lignocellulose, it could switch to PFO. A higher PFO flux would lead to a higher hydrogen concentration [19], which would confirm our findings of higher hydrogen concentrations when growing on straw. If the flux through PFO increases, the relative amount of produced formate should decrease. This could only be observed for the strains A252, W212 and X2152 whereas the relative concentrations were comparable for SA222 and even slightly increased for G341. A common reaction to high sugar concentrations is the effect known as overflow metabolism, Crabtree effect or Warburg effect, known from a multitude of organisms including *Escherichia coli* [235], *Lactobacillus plantarum* [236], *Bacillus subtilis* [237], *Saccharomyces cerevisiae* [238], and mammalian cells [238]. Under high sugar/fast growth conditions these organisms switch from energy efficient respiration to energy inefficient fermentation. Despite the oxygen dependent pathways not being present in AF, a proton gradient has been observed in the hydrogenosomes through which an ATPase could work [19]. A shift from this hydrogenosomal pathway, analogous to the respiratory chain, towards the cytosolic mixed acid fermentation in response to high sugar concentrations similar to an overflow metabolism could be possible. A reason for the discrepancy between the amounts of produced hydrogen independent of C-source type could also be the reabsorption of the produced hydrogen into the metabolism at later fermentation stages. Past studies showed the presence of a hydrogen dehydrogenase that under physiological conditions would catalyze the reaction from $NAD(P)^+$ and H_2 towards H^+ and NAD(P)H [19]. If this enzyme would be expressed only at later growth stages, it could explain the relative decrease in hydrogen at higher total metabolite concentrations.

5 Establishing of fermentation procedures for *Neocallimastigomycota*

This chapter is based on the draft for the publication:

Metabolic shift towards increased biohydrogen production during dark fermentation in the anaerobic fungus *Neocallimastix cameroonii* G341

Marcus Stabel[1], Karoline Haack[1], Hannah Lübbert[1], Meike Greif[1], Pascal Gorenflo[1], Habibu Aliyu[1], Katrin Ochsenreither[1]

[1] Karlsruhe Institute of Technology, Process Engineering in Life Sciences 2: Technical Biology, Karlsruhe, Germany

Publishing details:

Biotechnology for Biofuels and Bioproducts

Volume 15 Article 96

Published on 19 September 2022

DOI: https://doi.org/10.1186/s13068-022-02193-z

Author Contributions: Conceptualization, M.S.; methodology, M.S.; validation, M.S., H.A. and K.O.; formal analysis, M.S.; investigation, M.S., K.H., H.L., M.G., P.G.; resources, K.O.; data curation, M.S.; writing—original draft preparation, M.S.; writing—review and editing, H.A and K.O; visualization, M.S.; supervision, K.O.; project administration, M.S. and K.O.; funding acquisition, K.O.

5.1 Introduction

As consequences of global warming and climate change become more and more apparent, the necessity of establishing a circular bio-based economy seems inevitable. Hydrogen is considered as a possible green energy carrier in such a bio-based economy and is already highly demanded in different industries today [12,239]. Up to date, hydrogen is mostly produced from fossil fuels. Lignocellulose containing waste is a cheap and widely available alternative with the main drawback being its recalcitrance against degradation. While several pathways for thermochemical lignocellulose conversion to hydrogen exist these require a high energy investment [15]. In contrast, biological processes only require relatively low temperatures and pressures thereby reducing energy cost. Having no need for catalyst regeneration further reduces costs. The main known processes are biophotolysis, photofermentation, bioelectrolysis, biological water-shift reaction and dark fermentation, which have been reviewed recently [15]. Dark fermentation enables the conversion of residual biomass to hydrogen through microorganisms without the need for an external light or electricity source. Normally the use of biomass by microorganisms requires extensive pretreatment for the breakdown of lignocellulose to fermentable sugars which comes along with several drawbacks mainly high cost, high energy input, environmental hazard and/or the production of fermentation inhibiting compounds [5]. Anaerobic fungi (AF) of the phylum *Neocallimastigomycota* have been shown to grow on unpretreated biomass [225]. Originating from the gut of a variety of herbivores [16] AF are known degraders of lignocellulose with a wide range of cellulases and hemicellulases [17].

During growth mainly hydrogen, acetate, formate, lactate and ethanol are produced in a bacterial like mixed acid fermentation [18,19]. Interestingly, both pyruvate ferredoxin oxidoreductase (PFO) and pyruvate formate lyase (PFL) are available to the fungal metabolism [19]. A central piece of this metabolism is the hydrogenosome, an organelle *Neocallimastigomycota* contain instead of mitochondria. These organelles are thought to have evolved from mitochondria but do not contain an organelle genome [136,240]. A detailed insight into anaerobic fungal hydrogenosomes is given by [241].

Despite their biotechnological potential the knowledge of the culture conditions of AF is lacking [20]. Up to now experiments with pure cultures of *Neocallimastigomycota* have been conducted in still standing, air tight bottles. Recent studies on basic growth parameters like pH, influence of agitation or product inhibition on growth are widely missing and stirred tank reactors have not been used to the best of our knowledge for studying pure fungal cultures. The idea of applying AF in dark fermentation has just been reported recently [200]. *Neocallimastix cameroonii* (*N. cameroonii*) strain G341 has been isolated previously from giraffe feces[73]. Among all isolated strains it showed the highest carbon source diversity and the highest robustness. *Neocallimastix* is one of the best described genera of AF, enhancing the comparison of G341 to other studies in a research area where much is unknown. Here, we report the first adaptation of the culture of strain G341 to dark fermentation and the establishment in a small scale stirred tank reactor giving novel insights into the fungal metabolism.

5.2 Methods

5.2.1 Fungal culture and bottle experiments

The used medium, media components and the fungal strain were described recently [73]. *Neocallimastix cameroonii* strain G341 was maintained by subculture every six to seven days. Therefore, 5 ml of grown culture were inoculated with a syringe into 50 ml of fresh defined medium in a 118 ml serum bottle with 5 g/l wheat straw or cellobiose as carbon source. The cultures were incubated still standing at 39 °C in the dark in a Multitron Shaker (Infors, Bottmingen, Switzerland). These culture conditions were also applied for the experiments described below if not specified otherwise.

Determination of temperature optimum: A bottle of defined medium with 5 g/l cellobiose as carbon source was complemented with vitamin and antibiotic solution. 5 ml of complemented medium was transferred to a 16 ml hungate tube with a CO_2 atmosphere through a syringe. Prepared hungate tubes were inoculated with 0.5 ml of preculture and incubated for 6 days in triplicate at 35 °C, 37 °C, 39 °C, 41°C, 43 °C and 45 °C in a BioShake IQ (Analytic Jena). The exact temperature was determined by

measurement of an identical setup with water instead of culture in the same shaker as the samples with a submersion thermometer. Pressure was measured daily and hydrogen content was determined at the end of the incubation period.

Determination of pH optimum: 50 ml of defined medium with a pH of 6.2, 6.4, 6.6, 6.8 or 7.0 was inoculated in triplicate with 1 ml of well grown culture and incubated at 39 °C in the dark for 6 days. 5 g/l cellobiose was used as sole carbon source. Samples of liquid and gas phase were taken after inoculation and at the end of the experiment. Gas phase samples were analyzed by GC, while analysis of liquid samples were performed by HPLC.

Influence of agitation, carbon source concentration and headspace volume: 50 ml of defined medium was filled either in 250 ml or 118 ml serum bottles and contained 5 g/l or 20 g/l of either cellobiose or straw. After inoculation with 5 ml of culture the bottles were incubated with shaking (200 rpm) or without (0 rpm) for 4 days at 39 °C in the dark. Each combination was tested in triplicate. Pressure was determined at a daily basis. The components of both liquid and gas phase were analyzed respectively by HPLC or GC after inoculation and at the end of the experiment.

Hydrogen inhibition: Prior to inoculation 0 ml, 2.5 ml, 5 ml, 7.5 ml, 10 ml, 12.5 ml, 15 ml or 20 ml of hydrogen were added to the headspace of the serum bottle with a syringe at 1 bar. The bottle contained 50 ml of defined medium with 5 g/l cellobiose and was inoculated with 5 ml of preculture. Pressure was measured post inoculation and after 4 days of incubation and samples from both liquid and gas phase were taken. Samples were analyzed with HPLC or GC.

Pressure inhibition: Prior to inoculation the pressure was adjusted to 1.2 bar, 1.4 bar, 1.6 bar, 1.8 bar, 2.0 bar, 2.2 bar or 2.4 bar by addition of 100 % nitrogen through a syringe with manometer. The bottle contained 50 ml of defined medium with 5 g/l cellobiose. All conditions were inoculated with 5 ml of culture and incubated for 4 days. Pressure was determined on daily basis and samples from the gas phase were analyzed by GC at the beginning and the end of the experiment.

Alternative reducing agent and nitrogen sources: Na_2S was tested as an alternative reducing agent to replace cysteine and was applied in concentrations of 0 mM, 3 mM and 5 mM. Subsequently, 0.5 mM Na_2S was used to substitute cysteine when testing alternative nitrogen sources. Here, 5 g/l cellobiose were used as carbon source. All nitrogen sources were added to the medium post autoclaving with final concentration of 19.966 mmol nitrogen from 10x stock solutions. These were prepared by dissolving the desired nitrogen source in ddH_2O, adjusting the pH to 6.9 with NaOH/HCl and filter sterilizing. The exact concentrations in g/l for the stock solutions can be found in Table 26 (Appendix). After inoculation *N. cameroonii* was grown for 5 days before passaging to fresh media, which was repeated twice. In the fourth passage triplicates of each condition were cultivated for 7 days. The pressure was measured on daily basis and samples of the gas phase were taken at the end of the experiment.

5.2.2 Bioreactor fermentation

A multi-minifermenter system consisting of six 500 ml vessels (“SixFors”, Infors, Bottmingen, Switzerland) was used for bioreactor cultivations. Each bioreactor contained sensors for temperature and pH regulation, sample tubes for liquid and gas phase, a stirrer and a sparger. Tygon®-LMT-55 tubes were used for all connections to keep the system air-tight. The temperature was regulated through external heating plates and the pH by addition of anaerobic 4 M H_3PO_4 and 1 M NaOH, automatically controlled by the software IRIS 6 (Infors, Bottmingen, Switzerland). Before autoclaving vessels were filled with 300 ml of defined medium containing 20 g/l wheat straw. When 5 g/l cellobiose was used as a carbon source instead of wheat straw, it was added from a 50 g/l stock under a sterile hood post autoclaving. In this case the volume and the concentration of the other medium components were adapted accordingly. After autoclaving, the medium was complemented by addition of 3 ml of each vitamin solution and antibiotic solution. The whole system was subsequently anaerobized by sparging with 100 % CO_2 while stirring at 250 rpm. After gassing, 3 ml of sterile cysteine HCl solution (100 g/l) was added to each bioreactor. After one hour the pH was set to 7.1. When this pH value was reached

both the gas entry and gas exit of the fermenter were closed, sealing off the fermenter, and the pH was readjusted to 6.8 afterwards. Once the parameters were stable the pressure inside the fermenter was adjusted to 1.1 bar with CO_2 by using a syringe with manometer. Inoculation followed with 30 ml of *N. cameroonii* culture grown with 5 g/l cellobiose for 4-5 days. If not specified otherwise all fermentations were performed at 39 °C, pH 6.8 and 250 rpm with daily sampling of 2 ml liquid phase for HPLC. The pressure was measured with a manometer and 5 ml samples of the headspace were taken with a syringe. Special care was taken to avoid leaching of the gas phase. Sampling was repeated every 24 h. Following parameters were tested in experiments: Rotation velocity of the stirrer (0 rpm, 250 rpm, 600 rpm), turned on vs turned off pH regulation during the fermentation. All reactor experiments were performed in duplicate and the fermentation with cellobiose was performed in quadruplicate.

5.2.3 Analytics

While sample preparation and measurements were performed as described recently [73], special care was taken during sampling to avoid evaporation of volatile compounds. Therefore, samples were kept on ice at all times or stored at -20 °C when analyses were not performed immediately.

5.2.4 Statistics

Multiple linear regression analysis was performed with Origin 2019b V.9.65(OriginLab, Northampton, USA).

5.3 Results

Here we describe the first characterization of the growth conditions of the anaerobic fungus *N. cameroonii* and their effects on metabolite production. Culture pressure correlates with biomass production [242] and increases due to H_2 and CO_2 produced by the organism and CO_2 liberated from the carbonate buffer due to acidification of the media by the produced organic acids. Hence, it was used as a fast and qualitative measure for metabolic activity in initial experiments.

5.3.1 Temperature and pH effects on G341

To determine the optimal growth temperature *N. cameroonii* was cultured at temperatures between 34 and 45 °C in Hungate-Tubes. Analysis of the cumulative pressure revealed a sustained pressure build-up between 36.5 °C and 41.5 °C with the maximum of 1.617±0.017 bar at 41.5 °C (Figure 12a). Outside this range, the metabolism of the organism was suppressed greatly, as indicated by sharply decreased pressure values of 1.113±0.017 bar at 44 °C and 1.123±0.033 bar at 34.5 °C (Figure 12a).

Pressure development (Figure 12b) and metabolite production (Figures 12c and 12d) were investigated for different initial pH values in the range of pH 6.2 to 7.0. The highest final pressure was determined at an initial pH of 6.8 (2.003±0.005 bar) and the lowest at pH 6.2 (1.633±0.021 bar) (Figure 12b), a trend which was also reflected in carbon source consumption. The carbon source cellobiose was completely hydrolyzed to glucose monomers under all conditions. However, at initial pH values of 6.6 and 6.8, the carbon source was completely consumed as no residual glucose was detectable, whereas some glucose remained unused at pH 6.2 (0.537±0.020 mmol), 6.4 (0.192±0.011 mmol) and 7.0 (0.067±0.048 mmol). Similarly, the highest total metabolite production (4.685±0.048 mmol) was achieved at an initial pH of 6.8 (Figure. 12c). Due to the correlation between pressure increase (Figure 12b) and total metabolite production (Figure 12c), and the focus of this study on fungal metabolism, inferences will be made based upon the metabolites.

Additionally, initial pH also affected total amount (Figure 12c) and ratio (Figure 12d) of the produced metabolites. The highest cumulative hydrogen level (0.218±0.002 mmol) was observed in cultures growing at pH 6.4, followed by pH 6.6 (0.212±0.002 mmol). At pH 6.8 the highest amounts of formate (1.945±0.079 mmol), acetate (1.207±0.015 mmol), ethanol (0.711±0.060 mmol) and succinate (0.097±0.009 mmol) were observed but the lowest hydrogen production (0.166±0.020 mmol). The highest production of lactate took place at an initial pH of 6.6 (1.022±0.045 mmol) followed by pH 6.4 (0.950±0.004 mmol). When comparing the ratio of the single metabolites to the total amount of

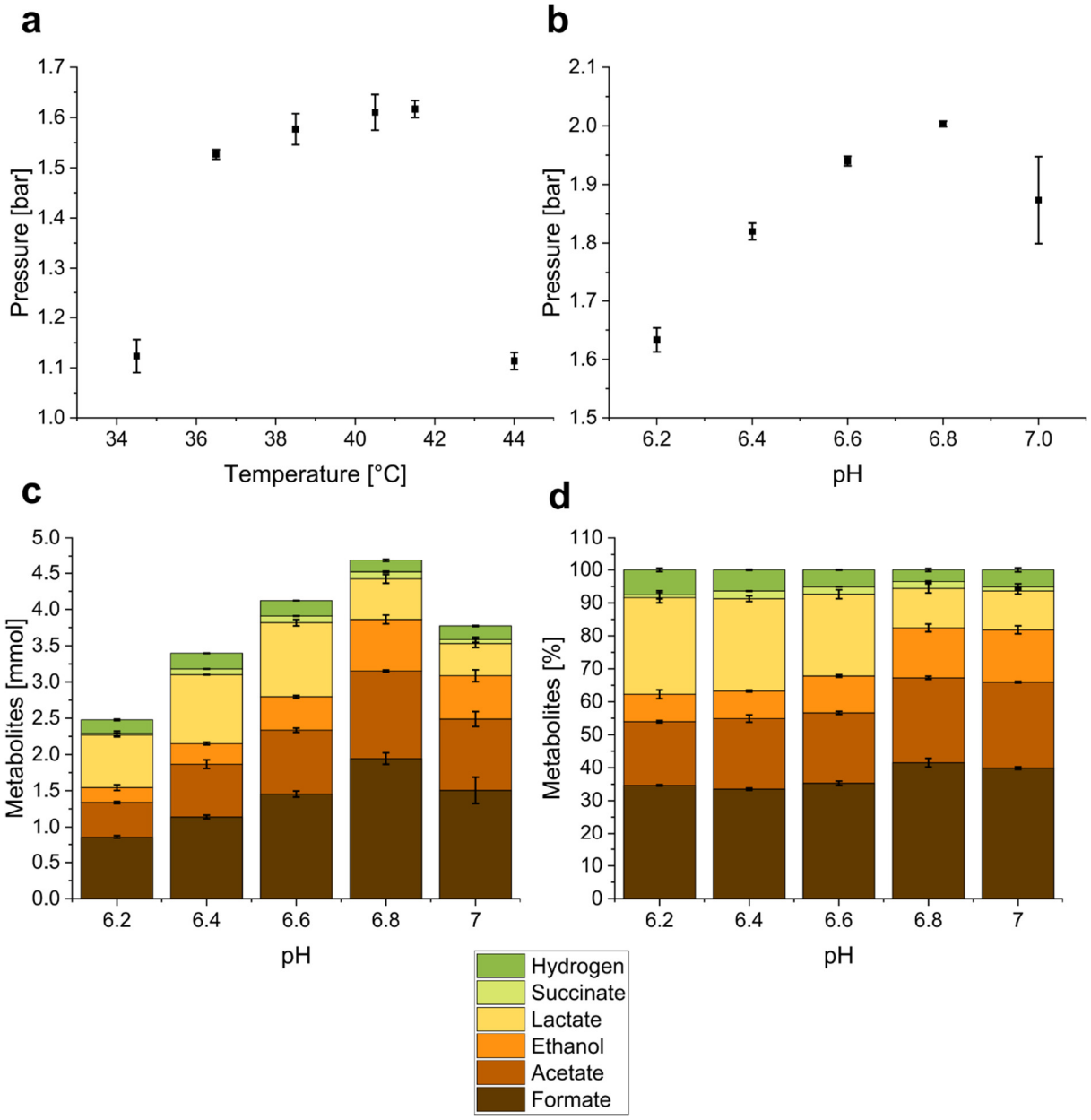

Figure 12: Influence of temperature and pH on growth and metabolite production of *N. cameroonii*. a: influence of the temperature on the pressure during growth; b: influence of pH on the pressure during growth; c: influence of pH on the total amount produced metabolites during growth; d: influence of pH on the relative amounts of produced metabolites compared to the total metabolite amount during growth.

produced metabolites (Figure 12d) a shift from acetate, formate and ethanol at higher initial pH (6.8) towards lactate and hydrogen at lower pH (6.2-6.6) could be observed. However, at an initial pH of 7 the relative hydrogen values were elevated when compared to pH 6.8.

5.3.2 Volumetric and bottle agitation effects on metabolite production.

To evaluate the influence of culture agitation on metabolic activities, *N. cameroonii* was cultivated with 5 g/L and 20 g/L of either wheat straw or cellobiose combined with an agitation of either 0 or 200 rpm. Gas to liquid ratio effects on net anaerobic metabolism was studied by comparing produced metabolites in cultures cultivated in 118 and 250 ml bottles. The results indicated that no fungal growth occurred in 20 g/L cellobiose culture under all conditions. By contrast, varying metabolic patterns were observed in cultures grown with 5 g/L cellobiose and both straw amounts. However, bottle agitation changed culture morphology from mat aggregates formed under still cultivation to pellet like aggregates in agitated cellobiose cultures (Figure 25, Appendix). For straw cultures no aggregation was observed during agitation. Overall, higher H_2 yields were observed under agitation and/or in larger bottles compared to

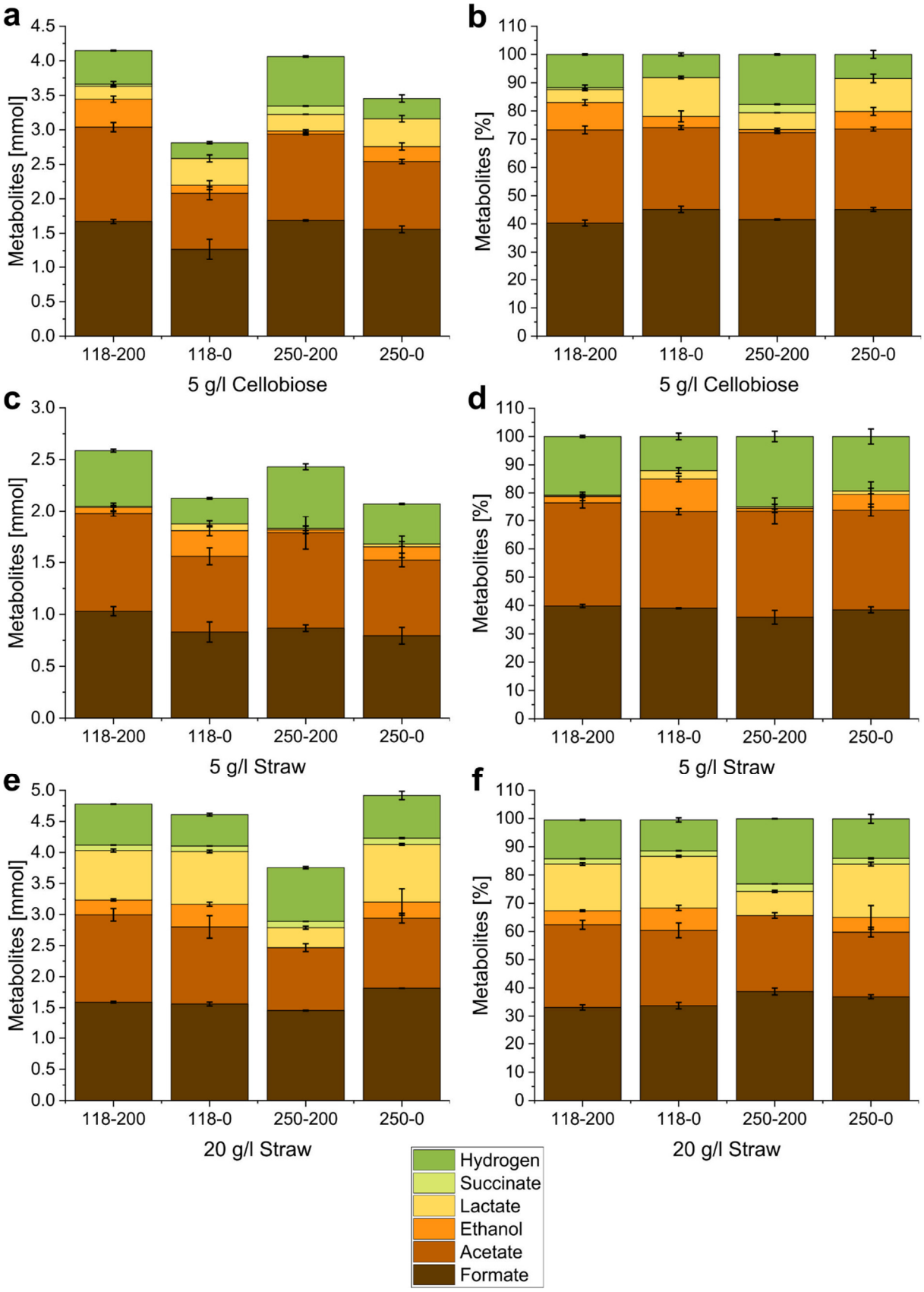

Figure 13: Effect of bottle volume and agitation on metabolite production of *N. cameroonii* growing on different carbon sources. a, c and e show the absolute metabolite amounts produced and b, d and f the relative amount of each metabolite to the totalt amount of produced metabolites. The samples are named after the bottle volume in ml (118 vs 250) and the agitation in rpm (0 vs 200). Please mind the differences of the y-axis between the different carbon sources.

the still and/or smaller culture bottles (Figure 13). The effect of bottle volume was smaller than the effect of agitation and the highest amounts of hydrogen were always observed when both conditions applied, i.e. in agitated 250 ml bottles.

The increase of hydrogen production was accompanied with a decrease in lactate and in most cases also a decrease of ethanol amount (Figure 13). For 250 ml bottles with 5 g/l (Figures 13c, 13d) or 20 g/l straw (Figures 13e, 13f) the values of ethanol were so low, that no change to net production could be observed. Only when using 5 g/l cellobiose in 118 ml bottles more ethanol was produced with agitation than without agitation (Figures 13a, 13b) leading to the highest total ethanol amounts (0.404±0.045 mmol) of the whole experiment. Furthermore, it represents the only exception to the observed inverse relation of hydrogen and ethanol production. Lactate was detected only in low amounts (0.011±0.009 mmol - 0.065±0.029 mmol) in cultures with 5 g/l straw, in comparison to the other conditions and highest with 20 g/l straw (0.322±0.024 mmol - 0.929±0.016 mmol). Citrate was only detected in traces in samples of 20 g/l straw cultures. Succinate was produced in the lowest amounts after citrate only being detected in agitated culture with cellobiose (0.000 mmol – 0.120±0.004 mmol) and 20 g/l straw (0.089±0.001 mmol – 0.101±0.008 mmol). In the latter succinate values seemed not to be influenced by agitation but were slightly higher in 250 ml serum bottles. Both formate and acetate production behaviors varied depending on the carbon source. During growth on cellobiose, both metabolites were produced in a similar pattern as hydrogen both increasing with agitation and a higher gas phase volume. For 5 g/l straw cultures acetate and formate increased with agitation and formate amounts seemed to decrease slightly with the higher headspace volume. In 20 g/l straw cultures acetate amounts were higher in the smaller bottles, but no conclusions could be drawn for formate production. Some conditions, like 20 g/l straw in 250 ml bottle with agitation, showed high deviations of the total amount of produced metabolites when compared to the conditions of the same amount of carbon source suggesting differences in the growth state.

In order to verify whether an increase in headspace volume is indeed causative for higher hydrogen production, for instance due to dilution effects or the reduction of hydrogen partial pressure, experiments were conducted with several different initial hydrogen concentrations. The increase of the initial hydrogen concentration led to an increase in both carbon source consumption (Table 27, Appendix) and total metabolite production (Figure 26a, Appendix) with the exception of hydrogen itself (Figure 26a, Figure 27a, both Appendix). When looking at the relative metabolite distribution (Figure 26b, Appendix), an increase of lactate and ethanol, and a decrease of formate production could be observed with increasing initial hydrogen concentration. As the addition of hydrogen also increases total pressure, the influence of elevated initial pressure on hydrogen production was investigated by the addition of nitrogen. Although a pressure increase decreased the hydrogen production (Figure 27b, Appendix), the effect was, however, significantly smaller than by the corresponding hydrogen partial pressure as revealed by multiple linear regression with $p < 0.05$ (Table 28, Appendix). While increasing the pressure (bar) had a coefficient of -0.053 in the analysis, increasing the corresponding initial hydrogen amount (mmol) had a coefficient of -0.142. During the addition of hydrogen to the bottle the maximal difference of initial bottle pressure was 0.226 bar (Table 27, Appendix). Thereby, the reduction of the produced hydrogen by pressure should not surpass 0.012 mmol. The maximal reduction of hydrogen production by hydrogen addition was 0.109 mmol, thereby, exceeding this value.

5.3.3 Alternative reducing agent and nitrogen sources

In order to evaluate alternative nitrogen sources, the standard reducing agent cysteine, which might also be a usable nitrogen source, had to be replaced by another non-nitrogen containing reducing agent, for example with Na_2S. However, in literature contradicting results on Na_2S being usable as reducing agent for anaerobic fungal growth have been reported. While [243] confirmed its suitability, other groups found it to be toxic [19]. In the presented study growth was achieved with both 0.3 mM and 0.5 mM of Na_2S. Omitting the reducing agent completely led to inconsistent results, with growth being detected in some replicates and in others not. By applying Na_2S as reducing agent different nitrogen sources were tested for sustaining the growth of *N. cameroonii* using pressure and produced hydrogen as growth

indicators. The fungus grew on glutamine, ammonium sulfate and ammonium nitrate but not on urea, sodium nitrate, arginine, cysteine, glycine and straw. When comparing Na_2S to cysteine as reducing agent, the variation in growth seemed to be higher (Table 29, Appendix). As cysteine is also a reducing agent, its toxicity was also tested: *N. cameroonii* grew up to a concentration of 2 g/l of cysteine, but at concentrations of 3 g/l no growth was detected.

5.3.4 Stirring enhances fermentative hydrogen production

Following up on the agitation experiments in bottles the effect of stirring on the growth of *N. cameroonii* with straw was further investigated in a bioreactor. Figure 14a shows the amount of hydrogen in the headspace for two fermentation setups. In the first set-up differences between no stirring and stirring at 250 rpm were tested, while in the second set-up the differences between 250 rpm and 600 rpm stirring rate were compared. The cultivation length was determined by the duration of hydrogen production, i.e. 6 days and 10 days for the first and second setup, respectively. Hydrogen production was lowest without stirring (1.821±0.302 mmol after 7 days). While stirring at 250 rpm led to the fastest hydrogen production with 2.641±0.345 mmol after 6 days, it was surpassed on day 8 when stirring at 600 rpm (2.795±0.034 mmol). When comparing the other produced metabolites in the second setup (Figures 14b, 14c), at 250 rpm (Figure 14b) 17.497±3.570 mmol of formate was present after the first 6 days and its amount increased further to 21.125±0.419 mmol at the end of the fermentation. In contrast,

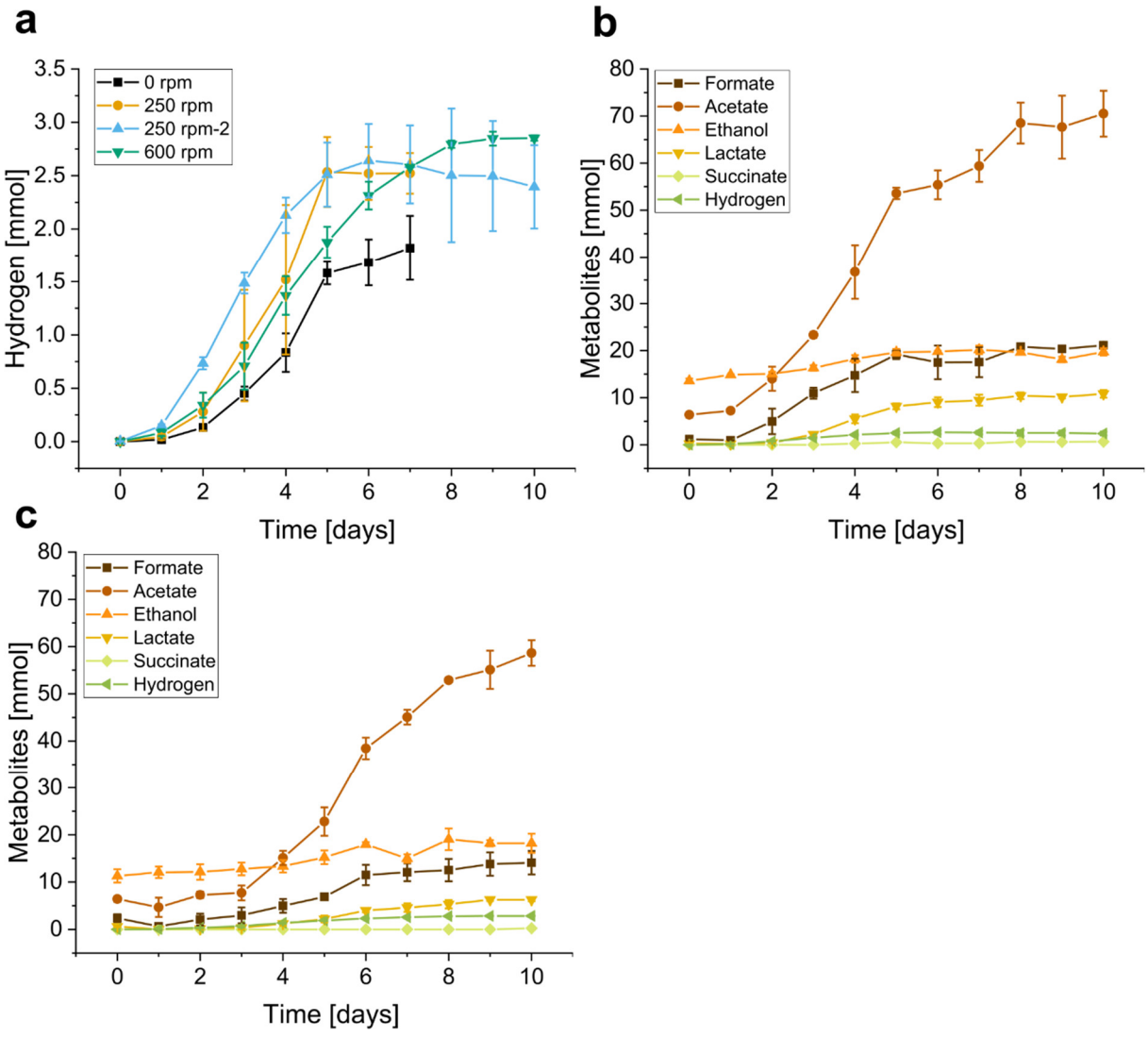

Figure 14: Effect of stirrer velocity on the metabolite production of *N. cameroonii* during growth in a stirred tank reactor with straw as sole carbon source. a: Hydrogen evolution during two different setups comparing 0 rpm (black) vs 250 rpm (yellow) and 250 rpm (blue) vs 600 rpm (green). b: Metabolite production during the second setup with 250 rpm. c: Metabolite production during the second setup with 600 rpm.

9.056±1.043 mmol lactate and 20.164±0.919 mmol ethanol were detected after the first 6 days and both amounts changed only marginally to 10.835±0.821 mmol and 19.728±0.762 mmol afterwards, respectively. Acetate amounts continued to increase from 55.386±3.065 mmol to 70.519±4.870 mmol independent of hydrogen production. Succinate could only be detected in trace amounts (0.642±0.049 mmol at day 10) and no relation could be drawn. While at 250 rpm the metabolite production seemed to have reached a stationary phase after the 10 days of fermentation, with 600 rpm (Figure 14c) the metabolites continued to accumulate until the last day with 2.852±0.026 mmol hydrogen, 58.650±2.701 mmol acetate, 14.100±2.480 mmol formate, 18.202±0.302 mmol ethanol, 6.280±0.302 mmol lactate and 0.232±0.232 succinate being detected. This suggests an overall slower growth of the fungus at higher stirrer velocities. An overview of the produced amounts of each metabolite is presented in Table 6.

Table 6: Metabolites produced during stirred tank reactor fermentation of *N. cameroonii* G341 with straw as sole carbon source depending on of the stirrer velocities 250 rpm and 600 rpm. Displayed are the final amount after 6 days (250 rpm) and 10 days (600 rpm) of cultiviation. Ø is the mean value of the duplicate and SD the corresponding standard deviation.

		ΔHydrogen [mmol]	**ΔAcetate [mmol]**	**ΔFormate [mmol]**	**ΔEthanol [mmol]**	**ΔLactate [mmol]**	**ΔSuccinate [mmol]**	**Total [mmol]**
250 rpm	**Ø**	2.392	64.154	19.918	6.164	10.589	0.642	103.859
	SD	0.393	5.438	0.820	0.249	1.067	0.049	2.860
600 rpm	**Ø**	2.852	52.231	11.706	6.913	5.641	0.232	79.575
	SD	0.026	3.243	3.283	3.440	0.136	0.232	3.157

5.3.5 pH regulation improves metabolite production

To determine the effects of pH regulation on the growth and metabolite production of *N. cameroonii* a fermentation omitting pH regulation was performed and compared to a fermentation with constant optimal pH. Without regulation the pH decreased gradually from pH 6.8 to 5.65±0.05 on day 8 while the regulation kept the pH constant at 6.8 (Figure 15). The amounts of all produced metabolites were higher with pH regulation than without (Table 7). The production of hydrogen also seemed dependent on the pH. After reaching pH 5.85±0.05, hydrogen increased marginally from 1.539±0.235 mmol to 1.568±0.254 mmol on day 7 and decreased to 1.509±0.259 mmol on day 8 post inoculation (Figure 15a). Similar to the second setup of the stirring experiment (250 rpm vs. 600 rpm), the amount of formate also increased from 10.612±2.478 mmol to 12.733±0.750 mmol on days 6 and 8, respectively. In contrast to the previous observations, lactate continued to increase independent of hydrogen production and pH starting between day 2 and 3 (Figure 15b) with a total amount of 6.517±0.325 mmol and 7.189±0.426 mmol under unregulated and regulated conditions, respectively. Similarly, ethanol production without pH control seemed to start around day 4 reaching 7.638±0.021 mmol at the end of the fermentation. With pH regulation (Figure 15c) ethanol was produced constantly from the start reaching 10.849±0.086 mmol at day 7 and decreased slightly on day 8. By contrast, acetate amounts increased both without and with pH regulation reaching 24.402±0.167 mmol and 53.765±2.770 mmol, respectively. Under both conditions, succinate was produced in comparable small amounts (0.706±0.051 mmol vs 0.685±0.082 mmol).

Table 7: Metabolites produced during pH unregulated (reg-) and pH regulated (reg+) stirred tank reactor fermentation of *N. cameroonii.* Ø is the mean valueof the duplicate and SD the corresponding standard deviation.

		ΔHydrogen [mmol]	**ΔAcetate [mmol]**	**ΔFormate [mmol]**	**ΔEthanol [mmol]**	**ΔLactate [mmol]**	**ΔSuccinate [mmol]**	**Total [mmol]**
reg -	Ø	1.509	17.490	5.785	1.520	6.238	0.706	33.247
	SD	0.259	0.243	0.831	0.227	0.319	0.051	1.411
reg +	Ø	2.972	46.898	12.261	3.841	6.926	0.685	73.583
	SD	0.016	2.662	0.035	0.023	0.454	0.082	3.194

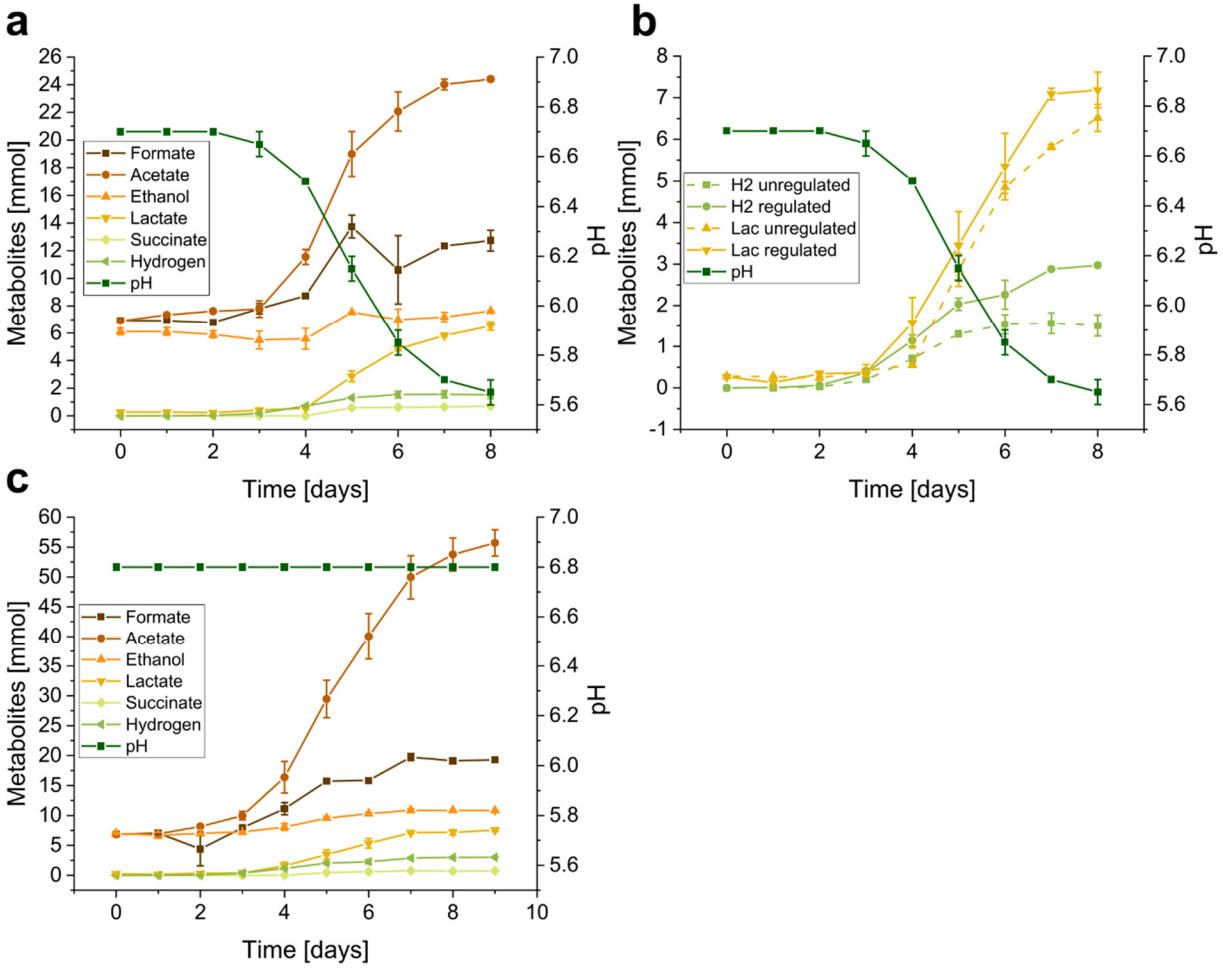

Figure 15: Effect of pH regulation on the metabolite production of *N. cameroonii* G341 during growth in a stirred tank reactor with straw as sole carbon source. a: Metabolite production and pH development during growth without pH regulation; b: Comparison of pH regulated and unregulated lactate and hydrogen production. pH from the unregulated fermenters is shown and pH for the regulated was kept constantly at 6.8; c: Metabolite production and pH development during growth with pH regulation.

5.3.6 Cellobiose as carbon source

As the application of straw as carbon source complicates the calculation of molar yields, bioreactor fermentations with 5 g/l cellobiose as sole carbon source were performed. Overall, metabolite production was much faster compared to straw, but ceased at day 3 (Figure 16a). In contrast to the other bioreactor experiments with straw, formate was the metabolite produced in the highest amounts (9.503±0.123 mmol) followed by acetate (7.065±0.288 mmol). Ethanol and lactate production amounted to 3.308±1.156 mmol and 3.754±0.316 mmol, respectively. Succinate was only detected in trace amounts (0.585±0.016 mmol). The calculated yields for each metabolite are given in Table 9 and the carbon recovery rate was 0.838±0.052. As observed in the bottle experiments, the fungus formed pellets (Figure 16b) when grown in cellobiose with stirring at 250 rpm in the Sixfors reactors.

5.3.7 Yields

To compare the performance of bottle and reactor experiments, yields for the conditions with the highest hydrogen production for each carbon source were calculated (Table 8, Table 9), i.e. bottles with 250 ml volume and grown at 200 rpm vs. reactor cultivations with straw and 600 rpm stirring. When using straw as carbon source, the calculation of the yields proved to be difficult as a separation of fungal cell mass and residual straw at the end of the fermentation was impossible, preventing the determination of substrate consumption. Therefore, the presented yields assume complete consumption, which was not the case and led most likely to underestimation. Nevertheless, when comparing the same carbon sources within the different cultivation set-ups the yield for hydrogen was higher in bottles, while lactate and ethanol yields were higher in the reactor fermentations. While the acetate and formate yields were

similar with cellobiose as carbon source, using 20 g/l straw led to higher formate and much higher acetate yields in the reactor. No reactor experiment using 5 g/l of straw was performed but in bottle experiments the yield for all metabolites except lactate was higher when compared to 20 g/l straw.

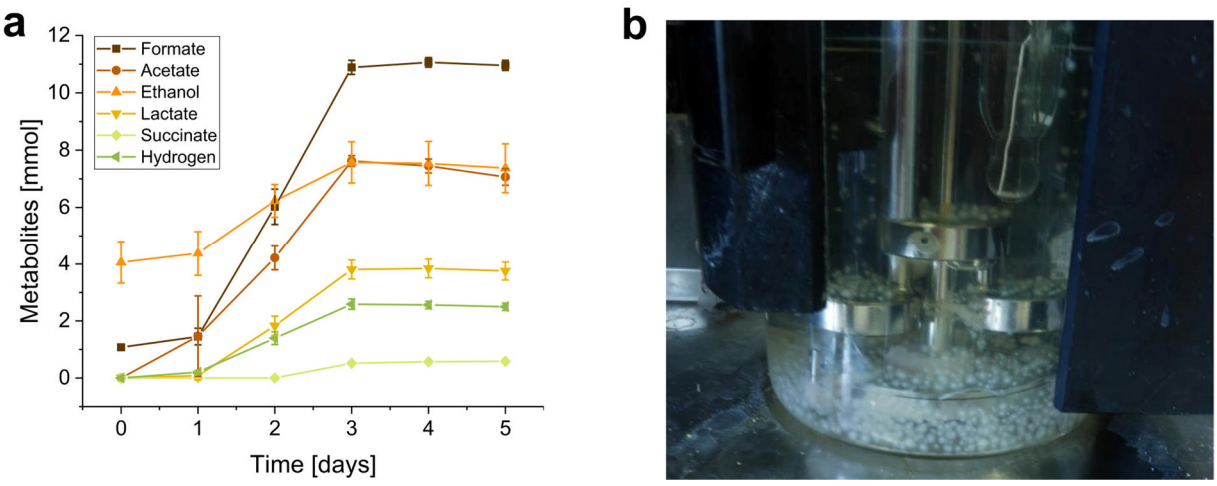

Figure 16: Stirred tank reactor fermentation *of N. cameroonii* with cellobiose as carbon source. a: Metabolite production. b: Fungal pellets in the reactor at the end of fermentation.

Table 8: Highest yields recorded for each carbon source during bottle experiments. Ø is the mean value of the duplicate and SD the corresponding standard deviation.

5 g/l Cellobiose: Yield Metabolite/equivalent Glucose [mmol/mmol]						
Metabolite	**Hydrogen**	**Acetate**	**Formate**	**Ethanol**	**Lactate**	**Succinate**
Ø	0.491	0.855	1.155	0.031	0.165	0.082
SD	0.007	0.009	0.006	0.012	0.001	0.003
5 g/l straw: Yield Metabolite/Straw [mmol/g]						
Metabolite	**Hydrogen**	**Acetate**	**Formate**	**Ethanol**	**Lactate**	**Succinate**
Ø	2.406	3.679	3.470	0.107	0.058	0.000
SD	0.114	0.633	0.127	0.151	0.082	0.000
20 g/l straw: Yield Metabolite/Straw [mmol/g]						
Metabolite	**Hydrogen**	**Acetate**	**Formate**	**Ethanol**	**Lactate**	**Succinate**
Ø	0.866	1.013	1.454	0.000	0.322	0.100
SD	0.019	0.064	0.007	0.000	0.024	0.000

Table 9: Highest yields recorded for each carbon source during stirred tank reactor experiments. Ø is the mean value of the duplicate and SD the corresponding standard deviation.

5 g/l Cellobiose: Yield Metabolite/equivalent Glucose [mmol/mmol]						
Metabolite	**Hydrogen**	**Acetate**	**Formate**	**Ethanol**	**Lactate**	**Succinate**
Ø	0.285	0.806	1.084	0.377	0.428	0.067
SD	0.014	0.033	0.014	0.132	0.036	0.002
20 g/l straw: Yield Metabolite/Straw [mmol/g]						
Metabolite	**Hydrogen**	**Acetate**	**Formate**	**Ethanol**	**Lactate**	**Succinate**
Ø	0.475	8.705	1.951	1.152	0.940	0.039
SD	0.004	0.541	0.547	0.573	0.023	0.039

5.4 Discussion

Knowledge on the nutritional needs of *Neocallimastigomycota* fungi is generally scarce [20]. Despite the discovery of novel genera and species over the last years, no efforts have been invested in characterizing the basic needs, like pH or temperature range, of these fungi. Here, we were able to show the pronounced influence of pH and hydrogen partial pressure on the metabolism of the fungus and to establish the cultivation in a stirred tank reactor system for the first time. Finally, the hydrogen yields of other dark fermentation studies are compared highlighting the potential of AF for hydrogen production.

5.4.1 Growth conditions influence metabolite production

Our analysis showed that *N. cameroonii* strain G431 grows optimally at temperatures between 38.5 °C and 41.5 °C, conforming to previous description of the genus *Neocallimastix* [243,244]. In contrast, the majority of studies dealing with cultivation of other *Neocallimastigomycota* species were conducted only around 39 °C [20], which is in the optimal range of *N. cameroonii* but slightly below the temperatures (40.5-41.5 °C) under which the highest hydrogen production and pressure were observed from the current study. Our data highlight the temperature sensitivity of *N. cameroonii* as suggested by the rapid decrease in growth observed outside the optimum temperature range. More studies could help to elucidate if the generally used 39 °C are truly optimal for all species of AF, especially with a future biotechnological application of the organisms in mind. Initial pH values of 6.6 and 6.8 are considered as optimal, as these were the only conditions with a full consumption of the carbon source. Other *Neocallimastix* species were reported to grow optimally at pH 6.5-7.5 [243] or optimally germinate at pH 5.5-6.4 [244].

At lower pH values the dynamics switched from production of acetate, formate and ethanol to lactate and hydrogen. Similar dynamics were also observed in bioreactor experiments with pH control. While all metabolites were produced in much lower amounts without pH regulation, lactate production was fairly stable. Furthermore, our experiments revealed a pH modulation of hydrogen production. Both initial pH values of 6.4 and 6.6 in bottles and a constant pH of 6.8 in bioreactors resulted in higher hydrogen amounts. In bioreactors without pH regulation, hydrogen production declined considerably when the pH dropped below 6.6. However, the exact modulation by pH will have to be elucidated in future studies. In contrast to bottle experiments bioreactor fermentations allow a much closer control of parameters as pH and will therefore be helpful in subsequent studies.

5.4.2 Hydrogen is the main influence on metabolite production

Up to now AF were cultivated exclusively in still standing bottles [20]. In this study we showed that increasing the ratio of gas-phase to liquid-phase as well as bottle agitation enhanced hydrogen production and in most parts, also end-product yields in bottle fermentations. This was confirmed in bioreactor experiments where the hydrogen production increased with stirrer velocity. Previous studies have revealed the influence of partial pressure on dark fermentative hydrogen production [245–247]. High hydrogen partial pressures shift the metabolic flux from hydrogen to other fermentation products. Here, this influence could be shown for *N. cameroonii* in bottle experiments with addition of hydrogen lowering the amount of produced hydrogen (Figure 17). However, agitation appears to compensate the effect of the partial pressure in two ways as seen by the influence of agitation in the bottle experiments. Firstly, it increases the mass transfer between liquid and gaseous phase which in turn decreases the concentration of dissolved and inhibiting hydrogen. Secondly, the typical mat formation of the fungus is prevented. Under still standing conditions produced gas can accumulate under the matt which causes local high hydrogen concentrations in near vicinity to the growing fungus, thereby inhibiting the hydrogen production. In the reactor experiments the applied stirring regime did not disrupt fungal cell matts completely. In these fermentations only a single rushton turbine near the vessel bottom was used. For better morphology control and general optimization of the process several stirrer types should be tested at different heights of the reactor.

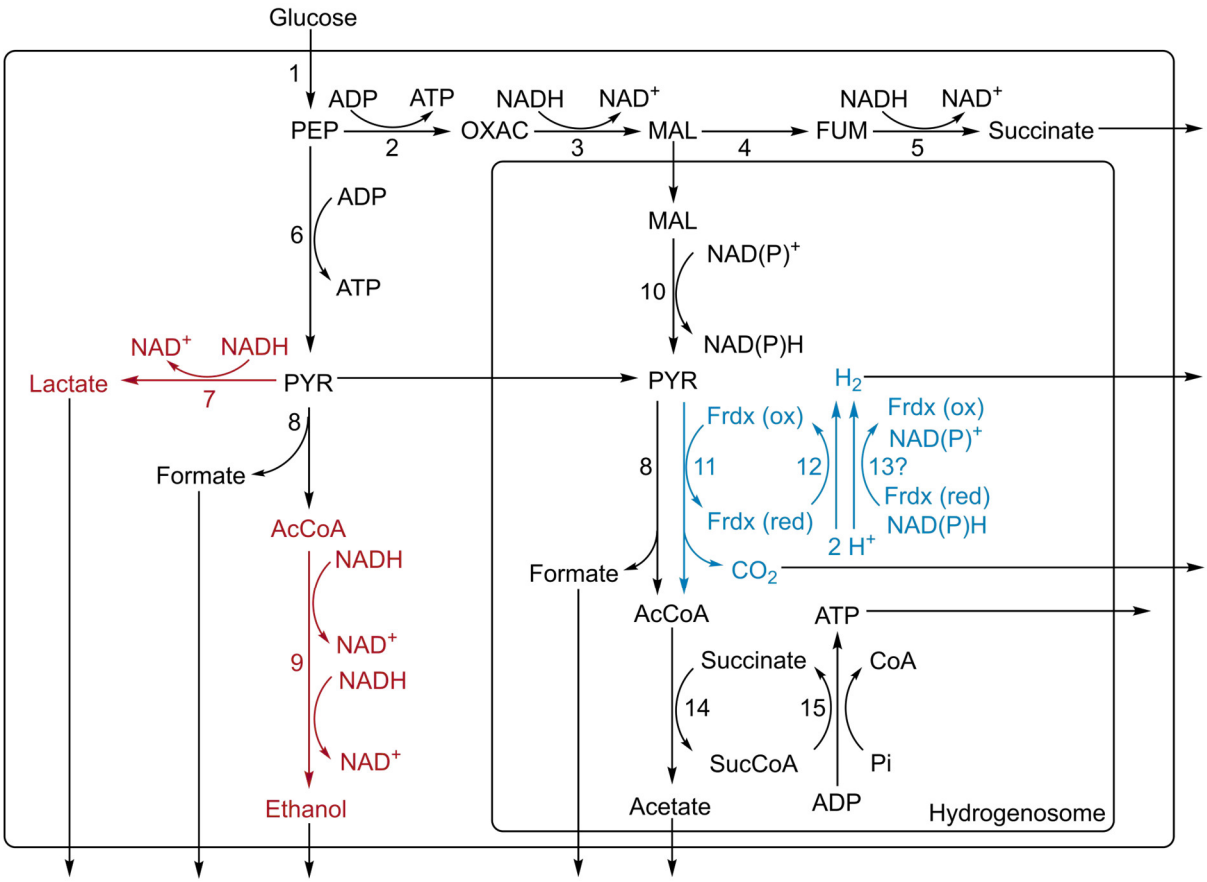

Figure 17: Metabolic pathways from *N. cameroonii*. Adopted from [18,19]. Primary and preferential electron disposal for hydrogen production marked blue. Secondary cytosolic electron disposal marked red. Enzymes are marked as numbers: 1. Embden-Meyer pathway, 2. phosphoenolpyruvate carboxykinase, 3. Malate dehydrogenase, 4. Fumarase, 5. Fumarate reductase, 6. Pyruvate kinase, 7. Lactate dehydrogenase, 8. Pyruvate formate lyase, 9. Alcohol dehydrogenase E, 10. Malic enzyme, 11. Pyruvate ferredoxin oxidoreductase, 12. Ferredoxin hydrogenase, 13?. Possible bifurcating hydrogenase, 14. Acetate:succinate CoA tranferase, 15. succinylCoA synthetase. PEP, phosphoenolpyruvate; OXAC, oxaloacetate; MAL, malate; FUM, fumarate; PYR, pyruvate; AcCoA, acetyl coenzyme A; CoA, coenzyme A; Frdx, ferredoxin; SucCoA, succinyl coenzyme A.

5.4.3 Hydrogenosomal metabolism

Previous studies [18,19] showed that the amount of produced formate molecules is equal to the sum of the produced ethanol and acetate molecules. While [18] used *Pyromyces* as organism and fructose as carbon source, [19] used a related *Neocallimastix* strain and 5 g/l cellobiose as carbon source. In AF pyruvate is converted to Acetyl-CoA through a pyruvate formate lyase (PFL), thereby producing one molecule formate for each molecule of Acetyl-CoA. PFL is located in both cytosol and hydrogenosome [137]. In further pathways Acetyl-CoA is then converted to ethanol or acetate. In this study exceptions to the ratio between formate, acetate and ethanol appeared. In bioreactor experiments with straw the amount of produced acetate alone tripled the amount of formate. However, when the carbon source in the same setup was 5 g/l cellobiose the equimolar ratio was approximated. Similarly, equimolar ratio of formate to ethanol and acetate were observed in most of the bottle experiments. These results highlight a probable dependency of the metabolite ratio on the culture conditions.

Recently, more insights into the metabolic pathways of AF have been given [19]. In addition to the PFL anaerobic fungi also contain a pyruvate ferredoxin oxidoreductase (PFO), located in the hydrogenosome, which catalyzes the conversion of pyruvate to Acetyl-CoA. The usage of one enzyme over the other carries no energetic cost [19]. While PFL produces formate as a by- product, PFO produces not only CO_2 but also reduced ferredoxin. Reduced ferredoxin is used to produce hydrogen through a ferredoxin hydrogenase or a bifurcating hydrogenase. For the latter only homologous sequences have been found in *Neocallimastix* [19]. The advantage of using PFO over PFL would be the disposal of electrons through

hydrogen production, under the prerequisite of the presence of a bifurcating hydrogenase. If all electrons were disposed this way, only hydrogen, formate and acetate would be metabolic end-products and alternative options of electron disposal, like production of ethanol and lactate, would not be necessary. This was observed for the shaken 250 ml bottle with 5 g/l straw as carbon source which barely produced lactate and ethanol when compared to the total of metabolites. In contrast, culture conditions resulting in relatively low hydrogen production, like the still standing bottles, showed increased production of lactate and ethanol. A similar phenomenon is also known from the co-culture of AF with methanogens. The latter attach to the fungal rhizoid [140] and consume produced formate and hydrogen [133]. The consumption of the hydrogenosomal end-products leads to an increase in the hydrogenosomal pathways and an decrease in the cytosolic pathways like lactate fermentation [129]. Interestingly the same study reported no differences in ethanol production between fungal mono-culture and co-culture with methanogens in contrast to our results.

5.4.4 Secondary electron disposal in *N. cameroonii*

As mentioned above, the increase of hydrogen production during agitation or a by providing bigger headspace volume in the bottle experiments were accompanied by a decrease in lactate and ethanol production. Hydrogen, lactate and ethanol production are all options to dispose electrons. The increase/decrease of both lactate and ethanol amounts dependent on hydrogen production suggest a switch from hydrogen to lactate and ethanol if hydrogen production becomes energetically unavailable. In the bioreactor experiments we saw both a dependency and an independency between lactate and hydrogen production, varying with the experiment. In the stirring experiment it seemed that the production of all metabolites was stopping at the same time point as lactate and hydrogen production. This suggests that the lactate production did not stop because of the ceasing hydrogen production, but because the growth of the fungus ended. Conformingly, the lactate production in bioreactor cultivations testing pH regulation continued long after discontinuation of the hydrogen production. Here, lactate production was similar between both conditions (pH regulated vs unregulated) despite one producing more than twice the amount of total metabolites, suggesting a continuous production of lactate independent of the conditions. In contrast, in the same experiment we noticed that both lactate and ethanol production did not start on the first day as for the other metabolites. During the agitation bottle experiments almost no lactate was produced under some conditions. Previously, it was suggested that the production of anaerobic fungal metabolites is sequential with lactate, ethanol and succinate being produced later than hydrogen, formate and acetate [73]. Future studies will have to elucidate if and how lactate production is regulated. We are inclined to speculate that lactate is used as a secondary electron acceptor in case of the unavailability of the hydrogen producing pathways and might be regulated accordingly. The other metabolites used for alternative electron disposal, ethanol and succinate, seem to have a lesser importance to the metabolism. While succinate was only detected in traces the amount of ethanol was lower than lactate in nearly all experiments. While lactate can be derived directly from pyruvate, ethanol is derived from Acetyl-CoA requiring one additional catalytic step. Electron disposal through ethanol synthesis could compete directly with energy production through acetate synthesis, with Acetyl-CoA being the substrate for both processes. This higher catalytic effort combined with the concurrence of electron disposal with energy production could explain the preference for lactate in *N. cameroonii* G341.

5.4.5 Dark fermentation

With this being the first report of the establishment of AF as organisms for dark fermentation, the procedure still requires a lot of refinement. One such factor is the observed high deviation of produced metabolites in some cases, which may be due to differences in the growth state of the inoculum. As the fungus growths forming a dense rhizoid, a completely homogeneous inoculation is impossible. When using other fungi, the spore number tends to serve as a method to guaranty homogeneous inoculation. AF reproduce via zoospores and a harvesting method for those has been reported [207]. Using a defined amount of zoospores could be the first step towards an inoculum standardization for AF, similar to the ones used for fungi outside the phylum.

Table 10: Comparison of pretreatment, used organisms and hydrogen yields of different studies using dark fermentation of wheat straw. *conversion of mmol to ml hydrogen following the ideal gas law with temperature 21 °C and pressure 1 bar.

Pretreatment	Organism	H_2 Yield	Publication
Steam acid + enzymatic hydrolysis	*Caldicellulosiruptor saccharolyticus*	3.43 mol/mol sugar	[248]
CaO hydrolysis	Thermal pretreated anaerobic sludge	114 ml/g total solid	[249]
Dilute acid	*Escherichia coli* WDHL	140.1 ml/g total sugars	[250]
Dilute acid + enzymatic hydrolysis	Mixed sludge	141 ml/g volatile solids	[251]
None	*Neocallimastix cameroonii*	2.406 mmol/g = 58.84 ml/g*	This study

While the yields for hydrogen were higher in the bottle experiments, the yields for lactate and ethanol were generally higher in bioreactor experiments. As described above increasing gas-phase/liquid-phase ratio and/or disrupting the mat formation of the fungus increased the hydrogen production. In serum bottles this ratio was bigger than in the reactors. In addition, mat formation couldn´t be completely prevented by stirring. Combining both effects, the metabolic shift from hydrogen to lactate and ethanol can be explained. Above we discussed the effect of pH regulation on the metabolite production. The highest yield (Table 10) was calculated for the bottle experiments and therefore without pH regulation. By optimizing the procedure in the reactor potentially much higher yields could be achieved. Previous studies showed that continuous flow culture increases the substrate consumption by *Neocallimastix hurleyensis* (later reclassified as *Neocallimastix frontalis* [68]) at high substrate concentrations [252]. Here, we similarly noticed a decrease in yield with the higher substrate concentrations of 20 g/l. An older study reported a stimulation of zoospore germination and growth by acetate, iso-butyrate and 2-methylbutyrate [244]. In contrast, an inhibitory effect of fermentation products, including acetate, from AF on their growth was also published [253]. While the inhibitory effect of hydrogen was studied here, the effect of other produced metabolites and the reason for growth inhibition at higher substrate concentrations remains to be investigated.

Table 10 gives an overview of the hydrogen yields from wheat straw of different studies and compares the used pretreatment methods. A comparison between the studies proofed to be hard due to differences in pretreatment and the application of different pretreatment fractions in the subsequent fermentation. While other studies used extensive pretreatment, breaking down complex biomass-derived substrates to their sugar monomers in a lot of cases, in this study straw was only milled to smaller particles. Similarly, while the yields of other studies were calculated on basis of the total solids, volatile solids or sugar content of the straw, our yield is derived directly from the mass of the applied straw. Even like this, roughly half to one third of the yield reported in other studies was obtained. Apart from optimizations of fungal growth conditions, this yield could be further increased by follow up processes using the acids produced by the fungus for additional hydrogen production. A potential integration of anaerobic fungal dark fermentation with photofermentation and biological electrolysis has been discussed recently [200]. Photofermentation is a process of purple non-sulfur bacteria which are able to gain energy through light but require a carbon source consisting of organic acids like acetate, lactate or succinate [30]. Hydrogen is generated through a nitrogenase which during absence of nitrogen is used as an outlet for excessive electrons. In biological electrolysis organic acids are oxidized to CO_2, electrons and protons by bacteria attached to the anode of a electrolysis cell [35,254]. The anode is the electron acceptor and the electrons are transferred to the cathode via an external circuit. At the cathode the protons react with the electrons to form hydrogen. The endothermic barrier of these reactions is overcome by supplying an external voltage to the electrolysis cell [35].

While *N. cameroonii* contains PFL it lacks a formate hydrogen lyase complex (FHL) which is present in *Escherichia coli*. FHL catalyzes the reaction of formate to hydrogen. The deletion of a FHL repressor

led to an increase of hydrogen production in the bacterium [255]. The introduction of such an enzyme into *N. cameroonii* could greatly increase the hydrogen yield. A similar effect could be achieved by deletion of the PFL pathway and thereby redirecting the metabolic flux in the fungus towards PFO. Up to now the genetic manipulation of AF has not been established with the best result leading to a transient expression of a β-glucuronidase after biolistic transformation [202]. The availability of such a technology could further enhance the research of these organisms and open the doors for biotechnological applications of these remarkable biomass degraders. While methods of permanent transformation are not available, preliminary studies could be conducted using RNA interference, which was used to knock down the lactate dehydrogenase of the anaerobic fungus *Pecoramyces ruminantium* [23].

6 Characterization of *Neocallimastigomycota* Hemicellulases

This chapter is based on the publication:

Characterization and phylogenetic analysis of a novel GH43 β-xylosidase from *Neocallimastix californiae*

Marcus Stabel[1], Julia Hagemeister[1], Zacharias Heck[1], Habibu Aliyu[1], Katrin Ochsenreither[1]

[1] Karlsruhe Institute of Technology, Process Engineering in Life Sciences 2: Technical Biology, Karlsruhe, Germany

Publishing details:

Frontiers in Fungal Biology

Volume 2

Published on 7 July 2021

DOI: https://doi.org/10.3389/ffunb.2021.692804

Author Contributions: MS conceptualized the study. MS, JH, ZH and HA performed the experiments and analyzed the data. MS wrote the original draft. HA and KO reviewed and edited the draft. HA and KO constructively contributed to the content.

6.1 Introduction

The conversion of lignocellulose containing material into fermentable sugars is an important step towards a CO_2 neutral economy and society [256]. However, microbial accessibility of and sugar release from lignocellulosic materials requires pretreatment, which tends to be expensive, energy intensive and commonly involves the use of hazardous and toxic compounds [5]. In contrast, biological pretreatment involves mild and eco-friendly conditions with the drawback of being time consuming and the used enzymes being expensive.

Although hemicellulose make up around 30 % of the lignocellulose dry weight [5], xylose is far less used as an renewable carbon source, because many of the biotechnological relevant microorganisms are unable to break down hemicelluloses such as xylans or to metabolize xylose [257]. Xylan is the most common polymer of the hemicellulose fraction with its backbone constituting a chain of β-1,4-linked xylopyranose molecules with different possible substitutions (Figure 18). The latter include acetylations, methylations and side chains of glucuronic acid, arabinose, coumaric acid and ferulic acid. The exact composition of these substitutions varies from plant to plant and thereby requires different enzymes for each type [258]. The basic enzymes which are always required are xylanases and xylosidases. Xylanases hydrolyze the backbone releasing xylose polymers which are further depolymerized to xylose by xylosidases. Substitutions of the xylose backbone can inhibit xylanase activity and thereby the whole process [259]. In this case, debranching enzymes like arabinofuranosidases, glucuronidases and acetyl xylan esterases are required [258], which remove the respective substitutions and thereby enable endoxylanase activity. In addition to their application in the degradation of lignocellulose, xylanolytic enzymes can be used in animal feed, food industry, paper production and preparation of textile fibres [260].

Within the fungal kingdom anaerobic fungi of the phylum *Neocallimastigomycota* have been recognized for their highly efficient lignocellulose degradation abilities [17,117]. *Neocallimastigomycota* are native to the digestive system of a huge variety of herbivores, of which a good overview is given by Gruninger *et al.* [16]. Horizontal gene transfer has been an important driver in the evolution of anaerobic fungal carbohydrate active enzymes (CAZymes) with over 50 % of some glycoside hydrolase (GH) families being of non-fungal origin [50]. Although several studies have highlighted the potential of anaerobic fungi for biotechnology [16,17,22,261–263], only limited information about characterized CAZymes from these fungi has been published so far. However, some of the few characterized enzymes have shown promising properties like multiple hydrolase activities [167,177] and competitiveness with

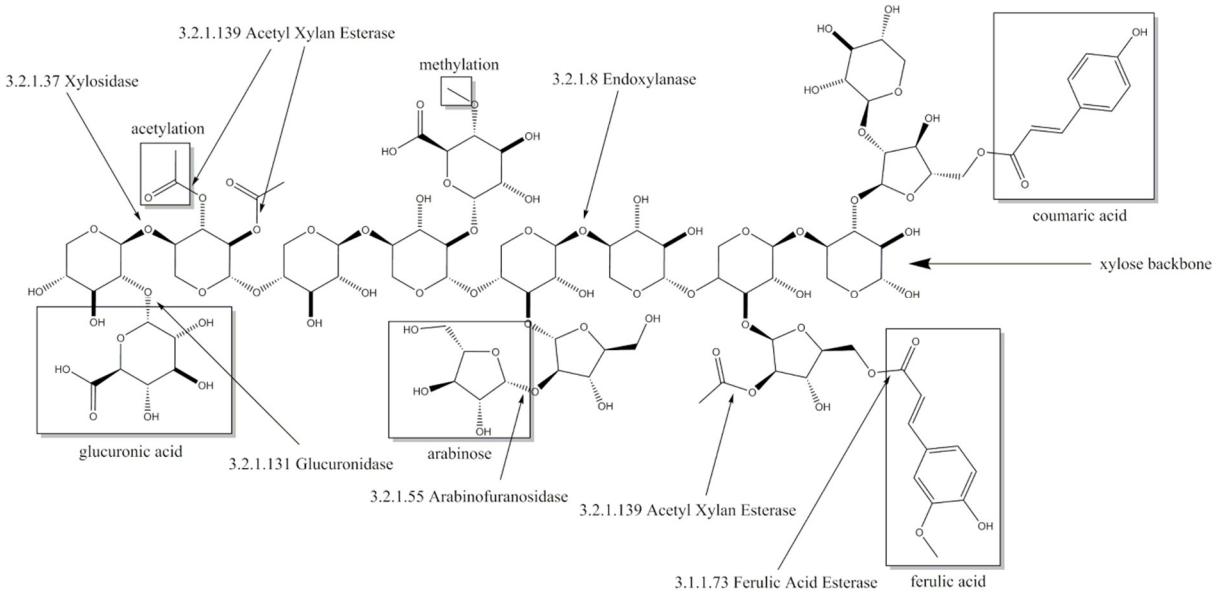

Figure 18: Xylose backbone of xylan with possible substitutions and the cleaving sites of corresponding enzymes including enzyme commission number.

commercial mixtures in terms of activity [119]. Despite these promising properties for lignocellulose degradation, the knowledge about *Neocallimastigomycota* enzymes at a biochemical level is very limited. For example, despite several having been identified just one enzyme with xylosidase activity has been fully characterized [167]. These potential xylosidases include members of the GH family 43 [80,85,118,203]. GH43 is one of the most prominent families containing xylosidases showing some of the highest reported xylosidase activities so far [264–266]. The family is further divided in 37 subfamilies (GH 43_1-GH 43_37) [267] and encompasses enzymes with dual xylosidase and arabinofuranosidase activity [268–270]. Here we report the heterologous expression, purification and characterization of a novel GH43 xylosidase from *Neocallimastix californiae*.

6.2 Material and Methods

6.2.1 *in silico* characterization and phylogenetic analyses

A putative proteome from *Neocallimastix californiae* was downloaded from GenBank (assembly accession: GCA_002104975.1). The totality of known xylosidases (EC 3.2.1.37) and endo-xylanases (EC 3.2.1.8) was downloaded from SwissProt (05.04.2018). From each dataset a local database was created in BioEdit (V. 7.0.5.3) [213]. The respective enzyme databases were searched against the *Neocallimastix californiae* database using the local BLASTp function of BioEdit. The proteome sequence with the highest similarity scores to the local xylosidase (ORY16049) and the local endoxylanase (ORY50654) databases was selected for cloning. The xylosidase and the endoxylanase were further validated via NCBI conserved domain search [271]. Phyre2 [272] was used for additional homology search of the xylosidase including the tertiary structure.

To perform phylogenetic analysis of Xyl43Nc, the protein was queried against the UniProtKB database (03.02.2021) using blastp. The top 100 sequences with the highest similarity score were downloaded, annotated using dbCAN [273,274] and aligned using T-Coffee [275]. Phylogenies were reconstructed using IQ-TREE v2.0.3 [214] with model selection [215] and 1000 ultrafast bootstraps [216]. The resulting tree was rooted using MAD [276]. Tree visualization and editing was done with Evolview V3 [234].

6.2.2 Cloning procedure

Genes were codon optimized and synthesized by GenScript. Cloning into pET21b (Novagen) was performed using the NEBuilder® HiFi DNA Assembly Cloning Kit following the manufacturer's instructions. Colonies were picked and cultured overnight at 37 °C and 120 rpm in LB-Media containing 10 g/l NaCl, 10 g/l tryptone, 5 g/l yeast extract and 50 mg/l ampicillin. Plasmids were extracted from the overnight culture using the Monarch® Plasmid Miniprep Kit from New England Biolabs following the manufacturer's instructions and correctness of the construct was confirmed by sequencing (GATC-Eurofins Genomics). pET21b constructs were transformed into $CaCl_2$ competent *E. coli* BL21 pLysS (DE3) cells by heat shock transformation.

6.2.3 Heterologous enzyme expression and purification

TB-Medium was prepared by dissolving 12 g Trypton, 24 g Yeast extract and 4 ml 100 % glycerol in 900 ml ddH_2O. 100 ml of a sterile solution containing 0.17 M KH_2PO_4 and 0.72 M K_2HPO_4 was added to TB medium after sterilization by autoclaving. 100 ml TB-Medium was inoculated to an OD600 of 0.1 with an overnight culture and grown at 37 °C and 130 rpm until reaching an OD600 of 0.6. To induce heterologous expression, IPTG was added to a final concentration of 1 mM. Subsequently, the culture was incubated overnight at 20 °C and 130 rpm. Cells were centrifuged at 4 °C and 4,000 g for 10 min. The supernatant was discarded and the cell pellet was resuspended in 20 ml Binding Buffer (50 mM NaPP, 0.5 M NaCl, 50 mM Imidazol, pH 6.9). The following steps were performed at 4 °C or on ice: Cells were disrupted by ultrasonification with a 20 kHz ultrasonic homogenizer Sonopuls HD 3100 equipped with the probe MS 72 (Bandelin electronic GmbH & Co. KG) at an amplitude of 60 % for 5 min with intervals of 20 sec pulse and 30 sec pause. Cell debris was removed by centrifugation for 1 h at 4 °C and 100.000 g. The obtained protein crude extract was applied to a HIS Trap HP Column 1 ml from GE Healthcare in a ÄKTA Start System. The target protein was eluted from the column with 70

% Binding Buffer and 30 % Elution Buffer (50 mM NaPP, 0.5 M NaCl, 0.5 M Imidazol, pH 6.9). Obtained fractions containing the target protein were pooled, concentrated with Amicon® Ultra 15 mL Centrifugal Filters (MW 10.000) and further purified by using a HiPrep Sephacryl S-200 HR Column from GE Healthcare in the same ÄKTA system as mentioned above with 0.15 M NaCl, 50 mM NaPP pH 7 as elution buffer. The resulting fraction was concentrated using the same filters described above. Purity of the enzyme was confirmed by SDS-PAGE with a 12.5 % Gel stained with coomassie stain containing 20 % (v/v) methanol, 10 % (v/v) acetic acid and 1 g/l brilliant blue R250 (Carl Roth). Bluestar Protein Ladder from Nippon Genetics (10-180 kDa range) was used as marker.

6.2.4 Activity assays

Activity of β-xylosidase was quantified by reactions with 500 µl 7.5 mM 4-Nitrophenol-xylopyranosides (Megazyme) in 50 mM citrate buffer (pH 5-6) or 50 mM natrium phosphate buffer (pH 6-7.5) as substrate. The reaction was started by adding 5 µl of enzyme with a concentration of 0.3-0.5 mg/ml to the substrate solution. Exact enzyme concentrations were determined using ROTI®Quant universal (Carl Roth) following the manual instructions. The reactions were stopped after 2 min with 1.5 M Na_2CO_3. All reactions were performed in triplicate. Absorption was measured at 405 nm in 96-well plates using Epoch Microplate Spectrophotometer (BioTek Instruments GmbH) and product concentration was calculated based on a calibration curve (linear range between 0 and 0.2 mM). Distribution of samples to the 96-well plate was performed by a Brand Liquid Handling Station.

For determining influences of different ions on the reaction, 1 mM or 10 mM of $BaCl_2$, $MgCl_2$, $MnCl_2$, $NiCl_2$, KCl, LiCl, $ZnCl_2$, $CaCl_2$, $CoCl_2$ or $CuCl_2$ were added prior to the substrate solution.

For temperature stability assays, enzyme solutions were incubated at different temperatures for 1 h and then applied to the activity assay as described above.

For determination of kinetic parameters, substrate concentrations of 0.25-7.5 mM 4-Nitrophenol-xylopyranosides were used. For product inhibition tests xylose concentrations of 0-10 mM were used. The reaction time for the activity assay with 4-Nitrophenolarabinofuranosides (Megazyme) was increased to 4 min due to relatively lower activity. The calculation of K_m, A_{max} and K_i was done by curve fitting with the Enzyme Kinetics add-on (V 1.10) in Origin (OriginLab V. 9.65).

For testing the β-xylosidase under more natural conditions an endoxylanase was needed and identified as described above. The endoxylanase temperature optimum was determined in reactions of 5 g/l purified beechwood xylan in 50 mM NaPP pH 6 as substrate at temperatures between 30 °C and 60 °C. The reactions were started by adding 5 µl purified enzyme (0.3-0.5 mg/ml) to 500 µl of pre-heated substrate. After one hour, a sample was taken for analysis using 3,5-dinitrosalicylic acid (DNS) assay adapted from [277], which also stopped the reaction. Specifically, 233 µl of the reaction assay was mixed with 350 µl DNS-solution (10 g/l DNS, 2 g/l of phenol, 0.5 g/l of sodium sulphite and 10 g/l NaOH in ddH_2O) and incubated for 15 min at 95 °C. 117 µl of Rochelles salt solution (400 g/l sodium tartrate in ddH_2O) was added afterwards and the solution was cooled to RT for 15 min. The resulting solution was dispensed in triplicate to a 96 well plate and absorbance was measured at 540 nm. Substrate solution with xylose concentrations between 0.8-4 mM was used as a reference. The pH optimum was determined analogously with reactions using the same substrate in 50 mM citrate buffer (pH 5, 5.5, 6) or 50 mM NaPP (pH 6, 6.5, 7) at 38 °C.

Combined activity of both enzymes was assayed by reactions of 5 g/l purified beechwood xylan (Megazyme) or wheat arabinoxylan (Megazyme) in 50 mM NaPP pH 6 at 32°C. The reaction was started by adding 5 µl enzyme solution (0.3-0.5 mg/ml) and 5 µl 50 mM NaPP pH 6 for single enzyme activity tests or 5 µl of each enzyme solution for combined activity tests. The reaction was stopped after 24 h by boiling at 95 °C for 10 min and analyzed by thin layer chromatography (TLC) and high-performance liquid chromatography (HPLC). TLC was performed using silica gel plates (Alugram SIL G, Macherey-Nagel GmbH & Co. KG). 10 µl of sample was spotted onto the plate and developed in a chamber with chloroform/acetic acid/water 6:7:1 (v/v) as eluent solution. Afterwards, the plate was dried at RT and

dyed by dipping in acetic acid/sulfuric acid/anisaldehyde 100:1:0.5 (v/v) solution followed by heating with a dryer until bands became visible. Additionally, samples were prepared for HPLC by centrifuging at 15.000 g for 10 min. 10 µl of supernatant were injected to an Rezex ROAorganic acid H+(8%) Column from Phenomenex in a 1100 Series System from Agilent Technologies with 5 mM sulfuric acid as eluent at a flow rate of 0.5 ml/min and a column temperature of 50 °C. The resulting peaks were detected with a refractive index detector.

6.3 Results

6.3.1 Xylosidase characterization

The highest score and e-value in the local BLASTp analysis for the xylosidase was obtained for ORY16049 against P49943, an xylosidase/arabinofuranosidase from *Bacteroides ovatus* [278], sharing 55.8 % sequence identity. P49943 was described and characterized as BoXA [279]. In the following, ORY16049 will be called Xyl43Nc in reference to its putative activity and its organismal origin (*Neocallimastix californiae*). Conserved domain search revealed that the protein consists mainly of a CoXyl43 like GH family 43 domain (311/327 amino acids). CoXyl43 is a calcium dependent xylosidase belonging to the GH 43 family [280]. Xyl43Nc was further categorized as a member of GH 43_1 subfamily using dbCAN2. The highest confidence hits during structure prediction with Phyre2 were RS223-BX and CoXyl43. RS223-BX is another GH43 xylosidase that could also be activated by different ions [281] and shares similarity with CoXyl43 [282] and BoXA [279].

Xyl43Nc comprises 327 amino acids with an estimated molecular weight of 37.4 kDa. Due to the fusion with a 6xHis-Tag and a T7 epitope, the expressed protein has a calculated molecular weight of 39.3 kDa. On SDS-PAGE the purified enzyme was visible as a single band between 35 kDa and 48 kDa in accordance to the predictions (Figure 19). Activity tests using the substrate 4-Nitrophenol-xylopyranoside, revealed a temperature optimum of 32 °C for Xyl43Nc (Figure 20A). On both sides of the optimum, enzyme activity decreases rapidly. For instance, at 32 ± 2 °C, enzyme activity decreased by ~ 50%. In terms of thermal stability, the enzyme was sensitive towards increased temperatures (Figure 20B). An incubation at 30 °C for one hour decreased the activity to 76 %, while at 35 °C the activity was decreased to 52 % and at 40 °C to 20 % of the original activity. Similarly, high activity was detected between pH 5.5 and 7 with pH 6.0 being optimal (Figure 20C). Outside of this pH range activity decreased rapidly. Kinetic parameters were determined for the substrate 4-Nitrophenol-xylopyranosides

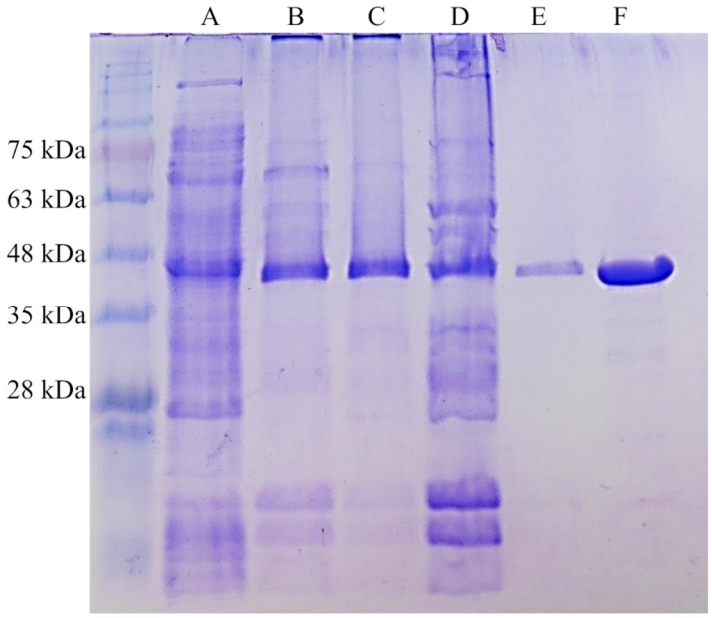

Figure 19: SDS-PAGE of different purification steps of Xyl43Nc. Crude protein extract (A), affinity chromatography fraction 1 (B), affinity chromatography fraction 2 (C), pool of both fractions (D), size exclusion chromatography (E) and concentrated size exclusion chromatography (F). The strong band of Xyl43Nc between 35 kDa and 48 kDa is visible in all samples. Marker: Bluestar Protein Ladder 10-180 kDa (Nippon Genetics).

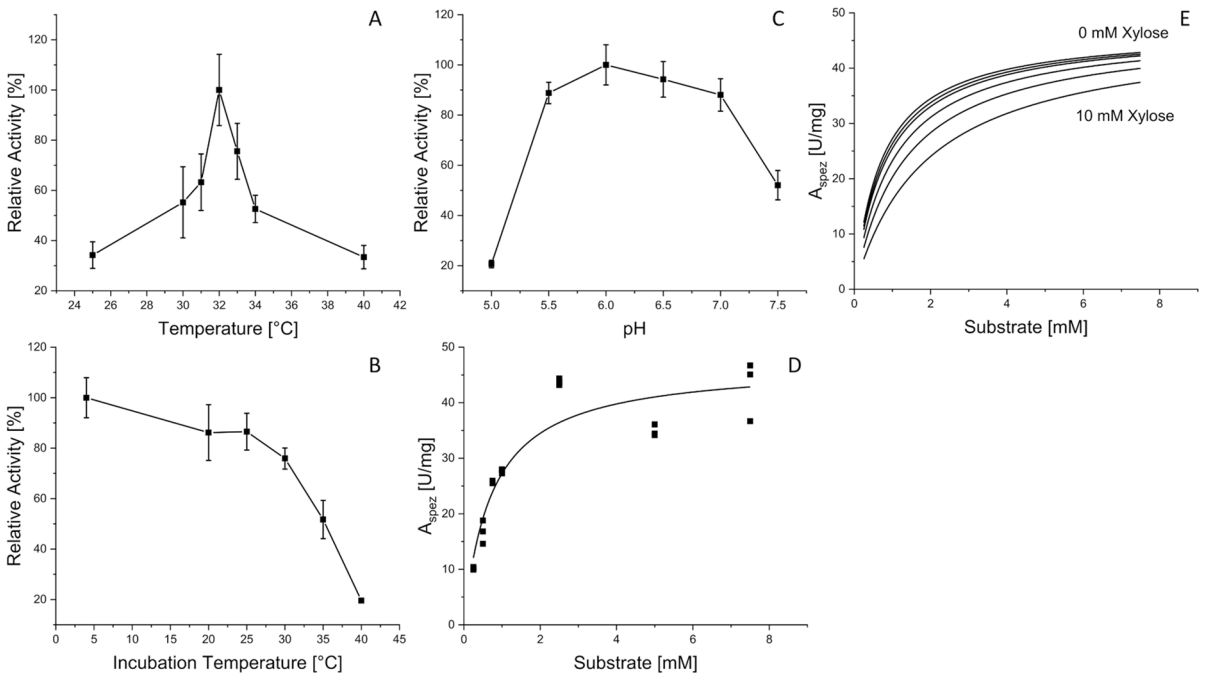

Figure 20: Biochemical characteristics of Xyl43Nc with 4-Nitrophenol-xylopyranoside as substrate. Activities are given in relation to the strongest activity at different reaction temperatures (A), after incubation of the enzyme for one hour at different temperatures (B) and at different pH values (C). Reaction kinetics without product inhibition with measured specific activities and corresponding fitted curve (D). Fitted reaction kinetics with different xylose concentrations between 0 mM and 10 mM (E).

Table 11: Relative activity of Xyl43Nc towards 4-nitrophenol-xylopyranoside after addition of different ion concentrations or EDTA compared to the reaction without additives

Substance	relative activity [%]
Ba 10 mM	90.78±4.63
Ba 1 mM	87.02±1.93
Mg 10 mM	95.19±2.92
Mg 1 mM	94.27±3.94
Mn 10 mM	98.16±1.73
Mn 1 mM	91.17±5.36
Ni 10 mM	90.59±4.19
Ni 1 mM	95.35±2.03
K 10 mM	94.72±1.21
K 1 mM	91.64±7.09
Li 10 mM	88.53±2.38
Li 1 mM	95.93±5.15
Zn 10 mM	101.65±7.32
Zn 1 mM	101.88±3.80
Ca 10 mM	88.17±1.24
Ca 1 mM	93.19±4.58
Co 10 mM	88.22±2.16
Co 1 mM	79.13±10.48
Cu 10 mM	92.30±3.01
Cu 1 mM	88.56±2.21
10 mM EDTA	91.28±9.51
20 mM EDTA	101.59±16.33

(Figure 20D): K_m of 0.72 mM and k_{cat} of 29,28 s^{-1}. The product xylose inhibited the reaction competitively (Figure 20E) with a K_i of 6.11 mM. In addition to xylosidase activity, a low arabinofuranosidase activity with 4-Nitrophenolarabinofuranosides as substrate was detected (K_m 0.1, k_{cat} 1.06 s^{-1}).

In contrast to CoXyl43 and RS223-BX but similar to BoXA, Xyl43Nc activity seemed not to be dependent on metal ions. None of the tested ions (up to 10 mM) led to considerable increase in activity, while most were leading to a slight decrease in activity (Table 11) instead. The maximal decrease was observed with 1 mM Co (activity of 70.13 %). This value had a high deviation and the higher Co concentration of 10 mM led to a smaller decrease of activity. EDTA also didn´t have a great impact on the activity of the enzyme.

6.3.2 Phylogeny of Xyl43Nc

To study the evolutionary history of Xyl43Nc, one hundred and one homologous sequences, occurring only among bacteria and fungi, were identified and a maximum likelihood (ML) phylogeny was generated. The ML phylogenetic analysis revealed the presence of three strongly supported (bootstrap support range: 85 % - 100 %, Figure 28, Appendix) major branches (Figure 21). The first branch comprising the enzymes from *Ascomycota* (fungi) and the second the bacterial sequences from *Firmicutes*, *Bacteroides* and *Proteobacteria*. By contrast, Xyl43Nc clusters distinctly (branch support: 100%) alongside enzymes of other members of the phylum *Neocallimastigomycota* and those of the bacterial phylum *Spirochaetes*, suggesting a separate early evolutionary trajectory for GH43_1 of members of *Neocallimastigomycota* distinct from that of the fungal phylum *Ascomycota*. Interestingly, within the Xyl43Nc branch, A0AV5WKY4 from *Spirochaetes bacterium* formed a monophyletic clade (bootstrap support: 100 %), which diverged earlier from the common ancestor of the rest of the members of *Spirochaetes* and *Neocallimastigomycota*, suggesting that GH43_1 of the latter, including Xyl43Nc, are likely to have been acquired via lateral gene transfer from *Spirochaetes* like enzymes. Horizontal gene transfer has been shown to have played a significant role in the evolution of anaerobic fungi [50,122].

6.3.3 Activity against natural substrate

In order to test the activity of the novel xylosidase in a more natural context, endoxylanase activity was also needed. Therefore, local blast analysis of the *Neocallimastix californiae* proteome was done against an endoxylanase database. The highest score was obtained for ORY50654 against B8YG19, published as XynS20E [177], from *Neocallimastix patriciarum* with 87.44 % identity. ORY50654, renamed X11Nc, has a length of 655 amino acids and conserved domain search detected a GH11 domain (178 amino acids), an alpha/beta-hydrolase super family domain (265 amino acids) and two CBM_10 dockerin domains (38 and 35 amino acids). Conserved domain search of XynS20E yielded in the same quantity and type of domains as for X11Nc. The search results are in accordance to the previously published results describing endoxylanase GH11, acetylesterase and two dockerin domains [177]. X11Nc has an estimated molecular weight of 70.7 kDa and the expressed version of the protein including tags results in a molecular weight of 72.6 kDa, which can be detected on the SDS PAGE between the 63 kDa and 75 kDa marker bands. X11Nc has a temperature optimum of 38 °C (Figure 22A) and a pH optimum of 6 (Figure 22B).

To evaluate synergistic effects, X11Nc and Xyl43Nc were used individually as well as in combination against beechwood xylan and arabinoxylan from wheat. When Xyl43Nc was used alone, only weak activity was observed against beechwood xylan (Figure 23A), whereas the single application of the endoxylanase X11Nc seemed to release polysaccharides of different length. When both enzymes were combined, released oligo-saccharides from the endoxylanase reaction disappeared, substituted by a strong xylose band instead. The amount of released xylose seemed to be higher in the combined reaction compared to the reaction of the xylosidase alone. Longer saccharides from the endoxylanase reaction seemed to remain untouched by the xylosidase activity implying a low or inexistent activity towards them. The activity of the enzymes on arabinoxylan from wheat seemed to follow the same rules but with much fainter saccharide spots. The HPLC analysis confirmed these results. The highest amount of xylose was released after 24 h by the combined action reaching 1.22 g/l on beechwood xylan and 0.26 g/l xylose

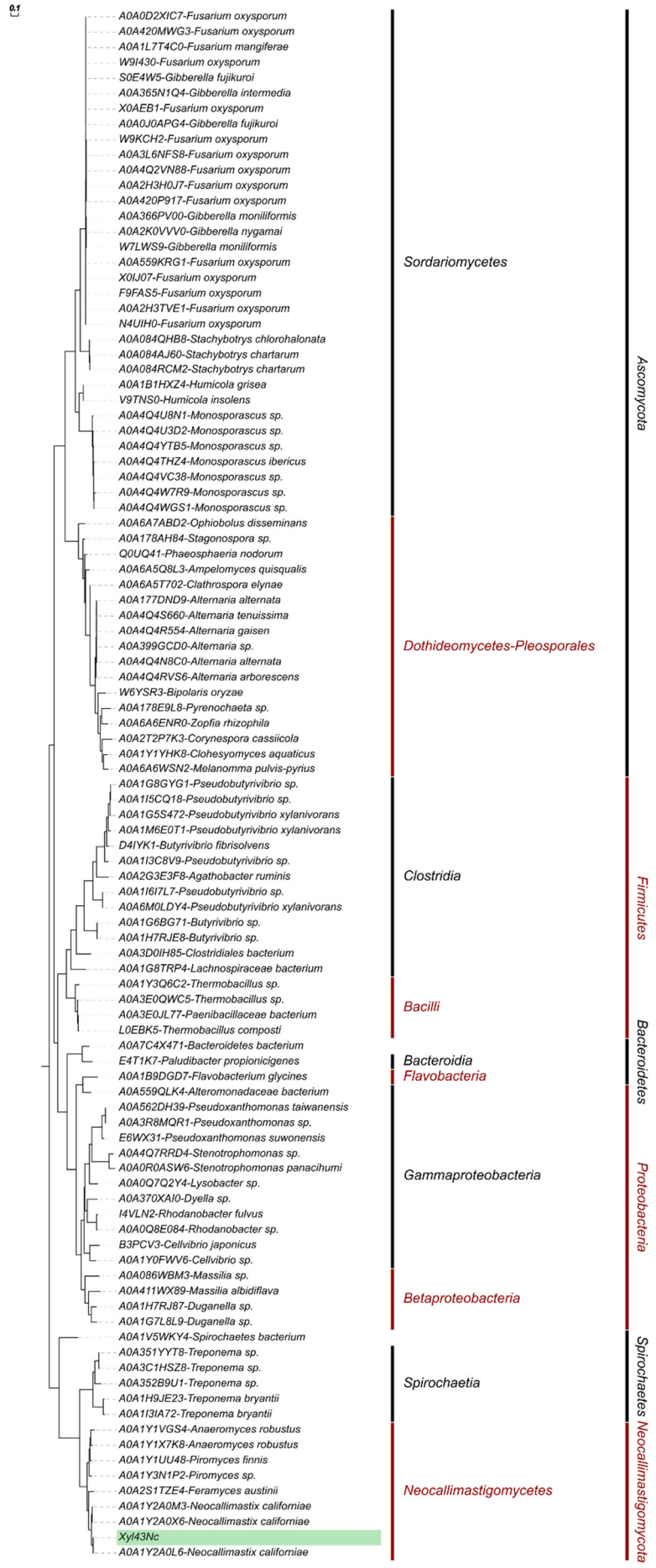

Figure 21: Phylogenetic relationship of Xyl43Nc to other GH43_1 enzymes. Sequences were aligned using T-Coffee [275]. Phylogenies were reconstructed using IQ-TREE v2.0.3 [214] with the automatic model selection (WAG+I+G4) and –bb 1000. The resulting tree was rooted using MAD [276].

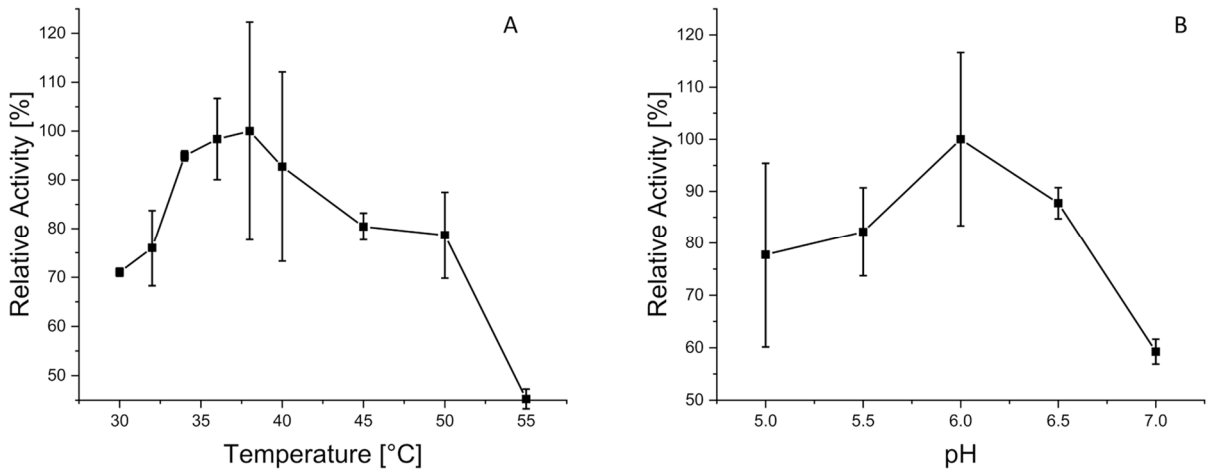

Figure 22: Biochemical characteristics of X11Nc when using purified beechwood xylan as substrate. Activities are given in relation to the strongest activity at different reaction temperatures (A) and at different reaction pH values (B).

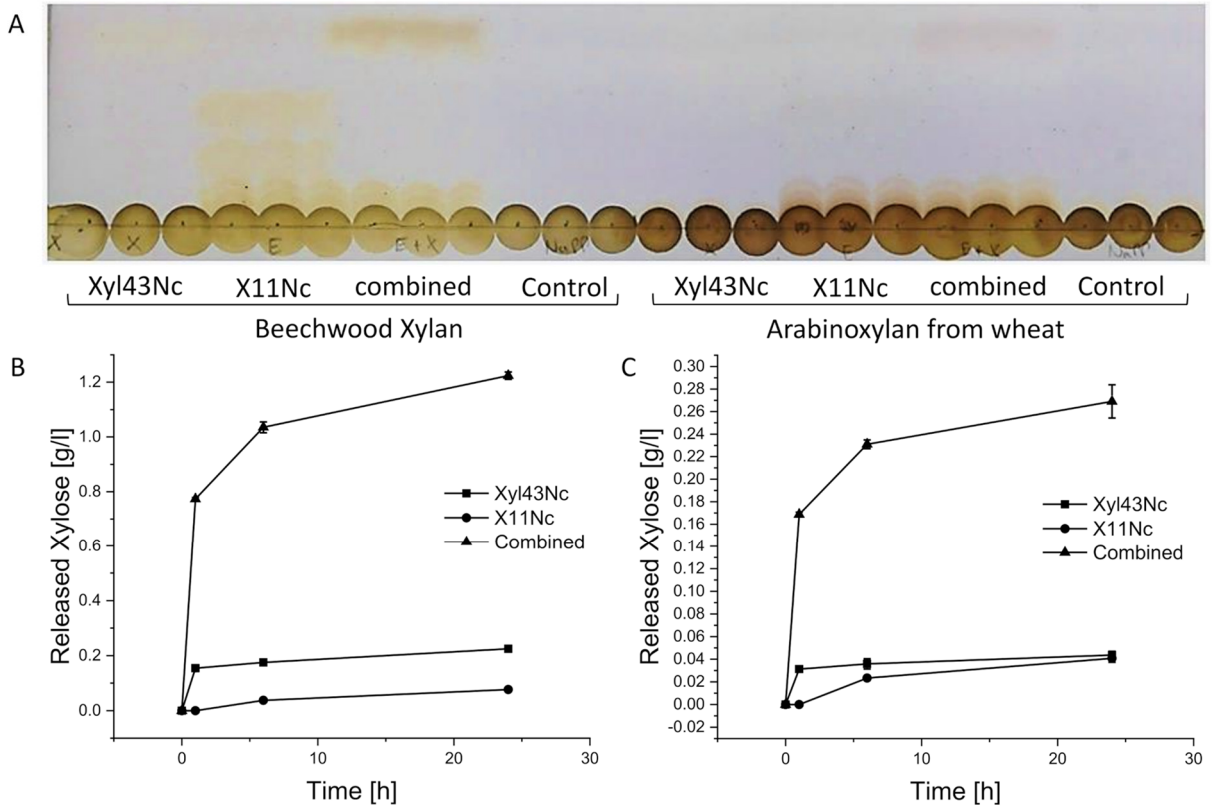

Figure 23: Individual and combined reactions of Xyl43Nc and X11Nc with purified beechwood xylan and arabinoxylan from wheat as substrates. Thin layer chromatography of the triplicate reactions after 24 h (A). Slight bands of xylose can be seen in the reactions of Xyl43Nc alone and much stronger xylose bands in the combined reactions. Concentrations of released xylose during the reactions with purified beechwood xylan (B) and arabinoxylan from wheat (C).

on arabinoxylan from wheat (Figure 23B). Under the same conditions Xyl43Nc alone just released 0.22 g/l on beechwood xylan. On arabinoxylan from wheat the amount of released xylose by Xyl43Nc was calculated to be 0.04 g/l, which is already below the calibration lower limit (Figure 23C).

Despite the low activity against 4-Nitrophenolarabinofuranosides described above, no release of arabinose from the reactions with arabinoxylan could be detected. In all reactions with arabinoxylan from wheat as substrate the amount of released xylose was considerably lower than from beechwood xylan. The HPLC results revealed a strong decrease in activity after the first hour of reaction for both the combined reaction and the reaction of Xyl43Nc alone. Specifically, the combined reaction on beechwood xylan released 0.77 g/l xylose during the first hour, an additional 0.27 g/l during the

following five hours but only 0.19 g/l within another 18 h of reaction time. This decrease in activity is in accordance with the temperature instability of Xyl43Nc described above.

6.4 Discussion

GH43 enzymes have been detected in anaerobic fungi previously [80,85,118,203] but none has been kinetically and thermodynamically characterized to the best of our knowledge. Xyl43Nc showed a very low temperature optimum at 32 °C when compared to the growth optimum of 39 °C for anaerobic fungi [283]. The latter temperature has a clear negative impact on the activity of Xyl43Nc xylosidase (Figure 20B, Figures 23B and 23C). Glycosylation has been shown to increase the stability and activity of other proteins [284], raising the question of our data being influenced by choosing *E. coli* as expression host. However, the only other heterologously expressed xylosidase from anaerobic fungi was also expressed in *E. coli* and had a temperature optimum of 39 °C [167] in accordance to the culture temperature. Future studies will have to reveal potential influence of the host system on the production of anaerobic fungal CAZymes. Another possibility for the lack of stability of Xyl42Nc at the culture temperature of *Neocallimastix californiae* would be the natural occurrence in a protein complex which increases the final stability of the enzyme. These cellulosome named complexes are widely spread throughout the *Neocallimastigomycota* phylum [122]. Enzymes occurring in cellulosomes contain a dockerin domain which allows them to bind to the complex [122]. Conserved domain search did not identify dockerin domains in Xyl43Nc making the absence of a naturally occurring binding partner less likely for the unexpected temperature behavior of the enzyme. Consequently the addition of such a domain to Xyl43Nc could provide a more stable and even active enzyme, as cellulosomes have increased biomass degradability through synergistic enzyme activity and targeting of the substrate through carbohydrate binding modules [120]. Recently a chimeric enzyme consisting of GH5 from *Thermatoga maritima* and a dockerin domain from *Piromyces finnis* was shown to be recruited into native cellulosomes highlighting the potential for the construction of full artificial cellulosomes [123].

The only biochemically characterized xylosidase from *Neocallimastigomycota* is Bgxg1, a multifunctional GH39 encompassing xylosidase, galactosidase and glucosidase activities [167]. The properties for Bgxg1 and other xylosidases are listed in Table 12. When compared to Xyl43Nc, Bgxg1 had a similar pH optimum but was more stable at conditions differing from the optimum for both temperature and pH. Although the turnover number k_{cat} for Bgxg1 was not calculated, it had a lower K_m and a higher V_{max} than Xyl43Nc. The only other anaerobic fungal xylosidases with evidence at protein level were purified from *Neocallimastix frontalis* [285,286]. Both enzymes showed a similar pH (6.4 and 6.5) and temperature optima (35 °C and 37 °C). When comparing Xyl43Nc to the related xylosidase BoXA from *Bacteroides ovatus* the enzyme shows a lower K_m and a higher k_{cat} determined for the artificial substrate 4-Nitrophenol-xylopyranosides. The activity of xylosidases on 4-Nitrophenol-xylopyranosides doesn´t necessarily correlate with the activity on natural substrates like xylobiose with both higher and lower activities being possible [287]. BoXA had an k_{cat} of 69 s^{-1} for xylobiose and of 7.82 s^{-1} for 4-Nitrophenol-xylopyranosides (Jordan et al., 2017; Table 12). Further characterization of

Table 12: Biochemical properties of selected xylosidases on the substrates 4-nitrophenol-xylopyranoside (NPX), xylobiose (X2), xylotriose (X3) and xylotetraose (X4).

GH	Enzyme	Substrate	pH	Temp. [°C]	K_m [mM]	V_{max} [U/mg]	k_{cat} [s-1]	Publication
39	Bgxg1	NPX	6	39	0.00485	127	-	[167]
43	Xyl43Nc	NPX	6	32	0.72	46.97	29.28	here
43	BoXA	NPX	6	25	4.57	-	7.82	[279]
		X2	6	25	0.606	-	69	
		X3	6	25	0.0908	-	19.1	
		X4	6	25	0.124	-	25.9	
43	Wxyn43	NPX	6	37	7.4	-	258	[266]
		X2	6	37	7.2	-	961	
		X3	6	37	6.5	-	900	
		X4	6	37	17	-	770	

Xyl43Nc with xylooligosaccharides is needed to determine the activity of the enzyme against its natural substrate and finally evaluating the enzymes potential for lignocellulose degradation. Up to date the highest xylosidase activity has been reported for Wxyn43 with a k_{cat} of 258 s^{-1} on 4-Nitrophenol-xylopyranosides and a k_{cat} of 961 s^{-1} on xylobiose [266].

The pH optimum of endoxylanase X11Nc was in the same range as reported for the closely related endoxylanase XynS20E [177], but the temperature optimum was much lower (38 °C vs. 49 °C). The combined reaction of Xyl43Nc xylosidase and X11Nc endoxylanase indicated that the xylosidase was able to hydrolyze smaller oligosaccharides resulting in xylose release. This tendency to shorter substrates is a common feature of xylosidases [260]. The reactions with arabinoxylan as substrate revealed the same pattern as the reactions with beechwood xylan but resulted in lower xylose concentrations. The complete degradation of arabinoxylan requires removal of arabinose substitutions by an arabinofuranosidase because they can inhibit xylanase activity sterically [259] leading to the observed lower activity. Although Xyl43Nc exhibited a low arabinofuranosidase activity against 4-Nitrophenolarabinofuranosides, release of arabinose from arabinoxylan was not detected, suggesting a negligible activity for the enzyme against natural substrates.

Interestingly the highest ranked enzymes in the conserved domain search and the highest ranked to be used as model for the structure of Xyl43Nc by Phyre2 are all highly ion dependent. In contrast, Xyl43Nc wasn´t further activated by the addition of different ions and addition of the chelating agent EDTA didn´t decrease enzyme activity. This is in accordance with BoXA, which also shares 80.6 % identical residues with RS223-BX in general and 19/20 residues of the active site [279] but is ion independent despite high overall similarity [288]. Both enzymes also share high identity in the active site with CoaXyl43 [288]. The main difference in the active center between the ion dependent xylosidases RS223-BX and CoaXyl43 is the coordination of the calcium ion. RS223-BX coordinates the ion by His-274 and Asp-85 [289]. While the first amino acid is conserved in CoaXyl43 (His-319) the latter is substituted by Ala-126 [282]. We suppose that during structure prediction the algorithm selected RS223-BX and CoaXyl43 as models because of the lack of a crystal structure of BoXA or a similar enzyme. Xyl43Nc is ion independent in contrast to these models and therefore no tertiary structure could be determined. As proposed before [288] a crystal structure of BoXA could elucidate the reaction mechanisms of this type of ion independent xylosidase. The exact catalytic mechanism of ion independent GH43 xylosidases could be of fundamental interest for future methods of enzymatic xylan degradation.

We investigated the evolution of Xyl43Nc along with similar enzymes from other fungi and bacteria. Our results were consistent with previous studies in highlighting the role of horizontal gene transfer in the evolution of *Neocallimastigomycota* [50,122]. Xyl43Nc and similar proteins from anaerobic fungi cluster with *Spirochaetes* and the phylogeny suggests a common ancestry and horizontal gene transfer from these bacteria to *Neocallimastigomycota*. Previous studies have identified *Proteobacteria*, *Bacteroidetes*, *Firmicutes*, *Spirochaetes* as the main bacterial horizontal gene transfer donors for anaerobic fungi [50]. Outside of the phylum *Neocallimastigomycota*, the evidence for gene transfer of GH from bacteria to fungi is limited [290].

In conclusion, we characterized the first GH43 xylosidase from *Neocallimastigomycota* starting to reveal the untapped xylan degrading resource of this fungal phylum and confirming its potential for future exploitation. Over the last years more genomic and transcriptomic data has become available for various strains of the phylum [19,117,122]. Transcriptomic data could guide the search for potential CAZyme candidates for expression through identifying the enzyme/gene variants which are expressed under certain cultivation conditions. Although the information on the biochemical properties of anaerobic fungal enzymes are limited, there have been promising results [119,167] highlighting the necessity and relevance of biochemical characterization studies. Future efforts should also investigate the influence of the expression system on the activity and stability of heterologous *Neocallimastigomycota* enzymes. Developing novel expression systems for *Neocallimastigomycota*

enzymes could open the way for a more extended heterologous production and characterization of these enzymes. The highly active enzymes of this phylum could promote biomass pretreatment and thereby pave the way towards a bio-based economy.

7 Conclusions

The effects of human-made climate change are becoming more and more obvious and a transition from a fossil-based to a bio-based economy is inevitable. However, this might lead to a conflict when agricultural resources will be used for fuel instead for food production. A viable solution is the use of waste products, e.g. straw or stalks, for the fuel production thereby avoiding the dilemma. These waste products are often composed of lignocellulose, which is highly resistant to any kind of degradation, making the conversion time-consuming and/or energy-intensive. However, anaerobic fungi of the phylum *Neocallimastigomycota* are able to grow on untreated lignocellulose. These fungi are highly understudied making a biotechnological implementation difficult. This thesis tries to pave the way for a future biotechnological implementation of this promising organisms.

In contrast to most other microorganisms, anaerobic fungi cannot be purchased from culture collections. The first aim of this thesis was the establishment of *Neocallimastigomycota* culture at the institute, the gain of fungal strains and a first biochemical characterization of the obtained strains. For this, an isolation from different zoo animal feces was performed. One isolate from alpaca feces belonged to the previously uncultured *Neocallimastigomycota* SK4 lineage. Interestingly, the same strain was isolated at the same time by a second group in Texas, USA from wild aoudad sheep samples. In a cooperation between both institutes the novel fungal species was described as *Aestispascuomyces dubliciliberans*. The other isolates could be identified as *Neocallimastix cameroonii* (from giraffe), *Caecomyces spec.* (from Przewalski's horse), *Orpinomyces joyonii* (from watussi cattle), *Pecoramyces ruminantium* (from scimitar oryx), and *Khoyollomyces ramosus* (from horse). All isolates grew on a variety of monosaccharide, disaccharides and more complex substrates like straw, but differed in their substrate utilization range. During growth hydrogen, acetate, formate, lactate, ethanol and succinate were the main products. *Orpinomyces joyonii* lacked succinate production and *Khoyollomyces ramosus* didn´t produce lactate. Metabolite production also seemed to be sequential with hydrogen, acetate and formate being produced first and the other metabolites following afterwards.

Following up on the results from the first aim, *Neocallimastix cameroonii*, which proved to be the most resistant isolate, was further studied for the second aim of the thesis: The implementation of anaerobic fungi in dark fermentation. During the testing of different nitrogen sources only glutamine and ammonium led to growth of this isolate. In bottle experiments an optimal temperature range of 38.5-41.5 °C and a starting pH range 6.6-6.8 proofed to be optimal. Increasing the initial hydrogen concentration decreased the overall hydrogen production. Inversely, decreasing the partial pressures of hydrogen by increasing the volume of the gas phase and/or increasing the gas transfer from liquid to gas phase by shaking resulted in higher hydrogen production suggesting an end-product inhibition. Since anaerobic fungal culture is almost exclusively performed in static bottle culture, the next aim was the establishment of anaerobic fungi dark fermentation in a stirred tank reactor system in order to be able to control and optimize the culture conditions. These results could be confirmed in stirred tank reactor experiments after establishment of the fungus in this system. By maintaining the pH of the reactor at 6.8 the hydrogen production could be doubled when compared to reactors omitting pH regulation. Increasing the stirring speed increased the hydrogen yield. While intermediate stirring at 250 rpm increased both the amount and the speed of hydrogen production when compared to 0 rpm, increasing the stirring speed further to 600 rpm led to a higher amount but slower hydrogen production.

While these results answer the questions from the beginning of this thesis and pave the way for the usage of anaerobic fungi for dark fermentation or biotechnology in general, many more questions are raised through them and the system needs further improvements. For metabolic analysis the carbonate buffer system used in all fungal experiments isn´t optimal because the release of CO_2 from the carbonate buffer due to acidification impedes measurement of metabolically released CO_2. The establishment of another buffer system in the medium and a possible change from CO_2 to N_2 atmosphere should be prioritized for further metabolic investigations. While some studies suspect a high metabolic similarity between anaerobic fungi [19] in this thesis not all isolates produced every metabolite. As mentioned above lacatate production was lacking in *Khoyollomyces ramosus* and succinate production in

Orpinomyces joyonii. These differences in metabolism should be investigated in future studies as the metabolic understanding will play an essential role in the future biotechnological implementation of anaerobic fungi. Such studies could use genomic and transcriptomic sequencing of the isolates to determine the exact capacities and regulation of the corresponding metabolisms. Especially the mechanism and regulation of electron disposal should be of interest as these have a direct effect on hydrogen productivity. From a more applied point of view, the stirred tank reactor experiments should be followed up by improving the stirrer setup to increase homogenization of the liquid phase and implementing a higher volume for the gas phase as done in bottle experiments. As in bottle experiments only starting pH values could be tested, the bioreactor setup can also be used to determine the pH optima for hydrogen production and the exact effect of pH on the metabolism. Further optimization of the medium could also have some potential, as the needs of anaerobic fungi have just been started to get elucidated in this thesis. Due to their growth as an attached mycelium, the inoculum for *Neocallimastigomycota* is difficult to standardize. This leads to high deviations in some experiments. For other fungi like *Alternaria* or *Aspergillus*, spores, which can be counted, are used to circumvent this problem. Establishment of a similar method in the course of this thesis yielded mixed results. While a spore solution could be collected and led to growth the number of spores was too low for evaluation (data not shown). Last but not least, from a process point of view combining anaerobic fungal dark fermentation with other bio-hydrogen producing processes could lead to success. Especially a follow-up with photofermentation or microbial electrolysis could be of interest, as in these processes organic acids produced by the fungi producing more hydrogen could be consumed.

Parallel to the experiments to establish culture and fermentation processes for anaerobic fungi, the third and last aim of this thesis was to heterologously express and biochemically characterize lignocellulose degrading enzymes from *Neocallimastigomycota*. Therefore, the genome of the anaerobic fungus *Neocallimastix californiae* was explored. Because of the limited knowledge about xylan degrading enzymes when compared to enzymes involved in cellulose degradation the focus was set on the first. A xylosidase, an endoxylanase, an arabinofuranosidase and a glucuronidase were identified and aimed to express them in the yeast *Pichia pastoris*. Although the cloning procedure was successful (data not shown), the expression titers were too low for purification and characterization. In an attempt to overcome this, the genes were cloned and expressed in *Escherichia coli*. While the xylosidase and endoxylanase were highly active this wasn´t the case for the other two enzymes. The arabinofuranosidase had only low activity and no activity was detected for the glucuronidase. The xylosidase, Xyl43Nc, and the endoxylanase, X11Nc, were purified by consecutive HIS-tag affinity and size exclusion chromatography and characterized afterwards. Xyl43Nc was highly active against 4-Nitrophenol-xylopyranosides with a K_m of 0.72 mM, a k_{cat} of 29.28 s^{-1}, a temperature optimum of 32 °C and a pH optimum of 6. X11Nc had a temperature optimum of 38 °C and a pH optimum of 6. The combined activity of both enzymes led to the release of xylose from beechwood xylan and wheat xylan. While the characterization of both enzymes is a first step to increase the biochemical knowledge of the wide array of *Neocallimastigomycota* enzymes, much remains to be done. While the approach taken here to express putative enzymes derived from the genome led to some success, further studies should improve the methodology by including transcriptomic and proteomic data in the process of finding adequate candidate enzymes for expression. Despite many enzymes for lignocellulose degradation from anaerobic fungi being of prokaryotic origin, the effect of eukaryotic and prokaryotic expression hosts on the activity of these promising enzymes should be clarified.

Taken together, this thesis takes the first step towards a biotechnological implementation of anaerobic fungi and their enzymes. The implementation of anaerobic fungi has the potential to substitute expensive biomass pretreatment with lucrative biotechnological production of hydrogen and other valuables.

References

1. Fawzy, S.; Osman, A.I.; Doran, J.; Rooney, D.W. Strategies for mitigation of climate change: a review. *Environ. Chem. Lett.* **2020**, *18*, 2069–2094, doi:10.1007/s10311-020-01059-w.

2. BMBF; BMEL *Nationale Bioökonomiestrategie*; 2020;

3. Mat Aron, N.S.; Khoo, K.S.; Chew, K.W.; Show, P.L.; Chen, W.-H.; Nguyen, T.H.P. Sustainability of the four generations of biofuels – A review. *Int. J. Energy Res.* **2020**, *44*, 9266–9282, doi:https://doi.org/10.1002/er.5557.

4. Tomei, J.; Helliwell, R. Food versus fuel? Going beyond biofuels. *Land use policy* **2016**, *56*, 320–326, doi:https://doi.org/10.1016/j.landusepol.2015.11.015.

5. Rahmati, S.; Doherty, W.; Dubal, D.; Atanda, L.; Moghaddam, L.; Sonar, P.; Hessel, V.; Ostrikov, K. (Ken) Pretreatment and fermentation of lignocellulosic biomass: reaction mechanisms and process engineering. *React. Chem. Eng.* **2020**, *5*, 2017–2047, doi:10.1039/D0RE00241K.

6. Ghaemi, F.; Abdullah, L.C.; Ariffin, H. Lignocellulose structure and the effect on nanocellulose production. In *Lignocellulose for Future Bioeconomy*; Elsevier, 2019; pp. 17–30 ISBN 9780128163542.

7. Scheller, H.V.; Ulvskov, P. Hemicelluloses. *Annu. Rev. Plant Biol.* **2010**, *61*, 263–289, doi:10.1146/annurev-arplant-042809-112315.

8. Ponnusamy, V.K.; Nguyen, D.D.; Dharmaraja, J.; Shobana, S.; Banu, J.R.; Saratale, R.G.; Chang, S.W.; Kumar, G. A review on lignin structure, pretreatments, fermentation reactions and biorefinery potential. *Bioresour. Technol.* **2019**, *271*, 462–472, doi:https://doi.org/10.1016/j.biortech.2018.09.070.

9. Chen, H. Brief Introduction to the Biotechnology of Lignocellulose. In *Biotechnology of Lignocellulose: Theory and Practice*; Springer Netherlands: Dordrecht, 2014; pp. 1–24 ISBN 978-94-007-6898-7.

10. Lewandowski, W.M.; Ryms, M.; Kosakowski, W. Thermal Biomass Conversion: A Review. *Processes* **2020**, *8*, doi:10.3390/pr8050516.

11. Kumar, B.; Bhardwaj, N.; Agrawal, K.; Chaturvedi, V.; Verma, P. Current perspective on pretreatment technologies using lignocellulosic biomass: An emerging biorefinery concept. *Fuel Process. Technol.* **2020**, *199*, 106244, doi:https://doi.org/10.1016/j.fuproc.2019.106244.

12. IEA *The Future of Hydrogen*; Paris, 2019;

13. BMWi *Die Nationale Wasserstoffstrategie*; 2020;

14. European Comisson EU Hydrogen Strategy Available online: https://ec.europa.eu/commission/presscorner/detail/en/FS_20_1296 (accessed on Aug 20, 2020).

15. Lepage, T.; Kammoun, M.; Schmetz, Q.; Richel, A. Biomass-to-hydrogen: A review of main routes production, processes evaluation and techno-economical assessment. *Biomass and Bioenergy* **2021**, *144*, 105920, doi:https://doi.org/10.1016/j.biombioe.2020.105920.

16. Gruninger, R.J.; Puniya, A.K.; Callaghan, T.M.; Edwards, J.E.; Youssef, N.; Dagar, S.S.; Fliegerova, K.; Griffith, G.W.; Forster, R.; Tsang, A.; et al. Anaerobic fungi (phylum Neocallimastigomycota): Advances in understanding their taxonomy, life cycle, ecology, role and biotechnological potential. *FEMS Microbiol. Ecol.* **2014**, *90*, 1–17, doi:10.1111/1574-6941.12383.

17. Seppälä, S.; Wilken, S.E.; Knop, D.; Solomon, K. V.; O'Malley, M.A. The importance of sourcing enzymes from non-conventional fungi for metabolic engineering and biomass breakdown. *Metab. Eng.* 2017, *44*, 45–59.

18. Boxma, B.; Voncken, F.; Jannink, S.; Van Alen, T.; Akhmanova, A.; Van Weelden, S.W.H.; Van Hellemond, J.J.; Ricard, G.; Huynen, M.; Tielens, A.G.M.; et al. The anaerobic chytridiomycete fungus Piromyces sp. E2 produces ethanol via pyruvate:formate lyase and an alcohol dehydrogenase E. *Mol. Microbiol.* **2004**, *51*, 1389–1399, doi:10.1046/j.1365-2958.2003.03912.x.

19. Wilken, S.E.; Monk, J.M.; Leggieri, P.A.; Lawson, C.E.; Lankiewicz, T.S.; Seppälä, S.; Daum, C.G.; Jenkins, J.; Lipzen, A.M.; Mondo, S.J.; et al. Experimentally Validated Reconstruction and Analysis of a Genome-Scale Metabolic Model of an Anaerobic Neocallimastigomycota Fungus. *mSystems* **2021**, *6*, e00002-21, doi:10.1128/mSystems.00002-21.

20. Vinzelj, J.; Joshi, A.; Insam, H.; Podmirseg, S.M. Employing anaerobic fungi in biogas production: challenges & opportunities. *Bioresour. Technol.* **2020**, *300*, 122687, doi:https://doi.org/10.1016/j.biortech.2019.122687.

21. Dollhofer, V.; Dandikas, V.; Dorn-In, S.; Bauer, C.; Lebuhn, M.; Bauer, J. Accelerated biogas production from lignocellulosic biomass after pre-treatment with Neocallimastix frontalis. *Bioresour. Technol.* **2018**, doi:10.1016/j.biortech.2018.05.068.

22. Hooker, C.A.; Lee, K.Z.; Solomon, K. V. Leveraging anaerobic fungi for biotechnology. *Curr. Opin. Biotechnol.* 2019.

23. Calkins, S.S.; Elledge, N.C.; Mueller, K.E.; Marek, S.M.; Couger, M.B.; Elshahed, M.S.; Youssef, N.H. Development of an RNA interference (RNAi) gene knockdown protocol in the anaerobic gut fungus Pecoramyces ruminantium strain C1A. *PeerJ* **2018**, *2018*, e4276, doi:10.7717/peerj.4276.

24. Ni, M.; Leung, D.Y.C.; Leung, M.K.H.; Sumathy, K. An overview of hydrogen production from biomass. *Fuel Process. Technol.* **2006**, *87*, 461–472, doi:https://doi.org/10.1016/j.fuproc.2005.11.003.

25. Brentner, L.B.; Peccia, J.; Zimmerman, J.B. Challenges in Developing Biohydrogen as a Sustainable Energy Source: Implications for a Research Agenda. *Environ. Sci. Technol.* **2010**, *44*, 2243–2254, doi:10.1021/es9030613.

26. Sharma, A.; Arya, S.K. Photobiological Production of Biohydrogen: Recent Advances and Strategy. In *Prospects of Renewable Bioprocessing in Future Energy Systems*; Rastegari, A.A., Yadav, A.N., Gupta, A., Eds.; Springer International Publishing: Cham, 2019; pp. 89–116 ISBN 978-3-030-14463-0.

27. Melis, A.; Zhang, L.; Forestier, M.; Ghirardi, M.L.; Seibert, M. Sustained Photobiological Hydrogen Gas Production upon Reversible Inactivation of Oxygen Evolution in the Green AlgaChlamydomonas reinhardtii. *Plant Physiol.* **2000**, *122*, 127–136, doi:10.1104/pp.122.1.127.

28. Ghiasian, M. Biophotolysis-Based Hydrogen Production by Cyanobacteria. In *Prospects of Renewable Bioprocessing in Future Energy Systems*; Rastegari, A.A., Yadav, A.N., Gupta, A., Eds.; Springer International Publishing: Cham, 2019; pp. 161–184 ISBN 978-3-030-14463-0.

29. Hallenbeck, P.C. Hydrogen Production by Cyanobacteria. In *Microbial Technologies in Advanced Biofuels Production*; Hallenbeck, P.C., Ed.; Springer US: Boston, MA, 2012; pp. 15–28 ISBN 978-1-4614-1208-3.

30. Adessi, A.; De Philippis, R. Hydrogen Production: Photofermentation. In *Microbial Technologies in Advanced Biofuels Production*; Hallenbeck, P.C., Ed.; Springer US: Boston, MA, 2012; pp. 53–75 ISBN 978-1-4614-1208-3.

31. McKinlay, J.B.; Harwood, C.S. Photobiological production of hydrogen gas as a biofuel. *Curr. Opin. Biotechnol.* **2010**, *21*, 244–251, doi:https://doi.org/10.1016/j.copbio.2010.02.012.

32. Oh, Y.-K.; Raj, S.M.; Jung, G.Y.; Park, S. Chapter 3 - Metabolic Engineering of Microorganisms for Biohydrogen Production. In *Biohydrogen*; Pandey, A., Chang, J.-S., Hallenbecka, P.C.,

Larroche, C., Eds.; Elsevier: Amsterdam, 2013; pp. 45–65 ISBN 978-0-444-59555-3.

33. Abo-Hashesh, M.; Hallenbeck, P.C. Fermentative Hydrogen Production. In *Microbial Technologies in Advanced Biofuels Production*; Hallenbeck, P.C., Ed.; Springer US: Boston, MA, 2012; pp. 77–92 ISBN 978-1-4614-1208-3.

34. Kadier, A.; Simayi, Y.; Kalil, M.S.; Abdeshahian, P.; Hamid, A.A. A review of the substrates used in microbial electrolysis cells (MECs) for producing sustainable and clean hydrogen gas. *Renew. Energy* **2014**, *71*, 466–472, doi:https://doi.org/10.1016/j.renene.2014.05.052.

35. Yang, E.; Omar Mohamed, H.; Park, S.-G.; Obaid, M.; Al-Qaradawi, S.Y.; Castaño, P.; Chon, K.; Chae, K.-J. A review on self-sustainable microbial electrolysis cells for electro-biohydrogen production via coupling with carbon-neutral renewable energy technologies. *Bioresour. Technol.* **2021**, *320*, 124363, doi:https://doi.org/10.1016/j.biortech.2020.124363.

36. Liu, H.; Hu, H. Microbial Electrolysis: Novel Biotechnology for Hydrogen Production from Biomass. In *Microbial Technologies in Advanced Biofuels Production*; Hallenbeck, P.C., Ed.; Springer US: Boston, MA, 2012; pp. 93–105 ISBN 978-1-4614-1208-3.

37. Rousseau, R.; Etcheverry, L.; Roubaud, E.; Basséguy, R.; Délia, M.-L.; Bergel, A. Microbial electrolysis cell (MEC): Strengths, weaknesses and research needs from electrochemical engineering standpoint. *Appl. Energy* **2020**, *257*, 113938, doi:https://doi.org/10.1016/j.apenergy.2019.113938.

38. Fukuyama, Y.; Inoue, M.; Omae, K.; Yoshida, T.; Sako, Y. Chapter Three - Anaerobic and hydrogenogenic carbon monoxide-oxidizing prokaryotes: Versatile microbial conversion of a toxic gas into an available energy. In; Gadd, G.M., Sariaslani, S., Eds.; Advances in Applied Microbiology; Academic Press, 2020; Vol. 110, pp. 99–148.

39. Yukesh Kannah, R.; Kavitha, S.; Preethi; Parthiba Karthikeyan, O.; Kumar, G.; Dai-Viet, N.V.; Rajesh Banu, J. Techno-economic assessment of various hydrogen production methods – A review. *Bioresour. Technol.* **2021**, *319*, 124175, doi:https://doi.org/10.1016/j.biortech.2020.124175.

40. Akhlaghi, N.; Najafpour-Darzi, G. A comprehensive review on biological hydrogen production. *Int. J. Hydrogen Energy* **2020**, *45*, 22492–22512, doi:https://doi.org/10.1016/j.ijhydene.2020.06.182.

41. Liebetanz, E. Die parasitischen Protozoen des Wiederkäuermagens. *Arch. für Protistenkd.* **1910**, *19*, 19–83.

42. Orpin, C.G. Studies on the Rumen Flagellate Neocallimastix frontalis. *J. Gen. Microbiol.* **1975**, *91*, 249–262, doi:10.1099/00221287-91-2-249.

43. Orpin, C.G. The Occurrence of Chitin in the Cell Walls of the Rumen Organisms Neocallimastix frontalis, Piromonas communis and Sphaeromonas communis. *J. Gen. Microbiol.* **1977**, *99*, 215–218, doi:10.1099/00221287-99-1-215.

44. Hibbett, D.S.; Binder, M.; Bischoff, J.F.; Blackwell, M.; Cannon, P.F.; Eriksson, O.E.; Huhndorf, S.; James, T.; Kirk, P.M.; Lücking, R.; et al. A higher-level phylogenetic classification of the Fungi. *Mycol. Res.* **2007**, *111*, 509–547, doi:10.1016/j.mycres.2007.03.004.

45. Ebersberger, I.; De Matos Simoes, R.; Kupczok, A.; Gube, M.; Kothe, E.; Voigt, K.; Von Haeseler, A. A consistent phylogenetic backbone for the fungi. *Mol. Biol. Evol.* **2012**, *29*, 1319–1334, doi:10.1093/molbev/msr285.

46. Naranjo-Ortiz, M.A.; Gabaldón, T. Fungal evolution: diversity, taxonomy and phylogeny of the Fungi. *Biol. Rev.* **2019**, *94*, 2101–2137, doi:10.1111/brv.12550.

47. Sekimoto, S.; Rochon, D.; Long, J.E.; Dee, J.M.; Berbee, M.L. A multigene phylogeny of Olpidium and its implications for early fungal evolution. *BMC Evol. Biol.* **2011**, *11*, 331,

doi:10.1186/1471-2148-11-331.

48. Tedersoo, L.; Sánchez-Ramírez, S.; Kõljalg, U.; Bahram, M.; Döring, M.; Schigel, D.; May, T.; Ryberg, M.; Abarenkov, K. High-level classification of the Fungi and a tool for evolutionary ecological analyses. *Fungal Divers.* **2018**, *90*, 135–159, doi:10.1007/s13225-018-0401-0.

49. Wang, Y.; Youssef, N.H.; Couger, M.B.; Hanafy, R.A.; Elshahed, M.S.; Stajich, J.E. Molecular Dating of the Emergence of Anaerobic Rumen Fungi and the Impact of Laterally Acquired Genes. *mSystems* **2019**, *4*, e00247-19, doi:10.1128/mSystems.00247-19.

50. Murphy, C.L.; Youssef, N.H.; Hanafy, R.A.; Couger, M.B.; Stajich, J.E.; Wang, Y.; Baker, K.; Dagar, S.S.; Griffith, G.W.; Farag, I.F.; et al. Horizontal gene transfer as an indispensable driver for evolution of Neocallimastigomycota into a distinct gutdwelling fungal lineage. *Appl. Environ. Microbiol.* **2019**, *85*, doi:10.1128/AEM.00988-19.

51. Heath, I.B.; Bauchop, T.; Skipp, R.A. Assignment of the rumen anaerobe Neocallimastix frontalis to the Spizellomycetales (Chytridiomycetes) on the basis of its polyflagellate zoospore ultrastructure . *Can. J. Bot.* **1983**, doi:10.1139/b83-033.

52. Gold, J.J.; Heath, I.B.; Bauchop, T. Ultrastructural description of a new chytrid genus of caecum anaerobe, Caecomyces equi gen. nov., sp. nov., assigned to the Neocallimasticaceae. *BioSystems* **1988**, doi:10.1016/0303-2647(88)90039-1.

53. Hanafy, R.A.; Lanjekar, V.B.; Dhakephalkar, P.K.; Callaghan, T.M.; Dagar, S.S.; Griffith, G.W.; Elshahed, M.S.; Youssef, N.H. Seven new Neocallimastigomycota genera from wild, zoo-housed, and domesticated herbivores greatly expand the taxonomic diversity of the phylum. *Mycologia* **2020**, doi:10.1080/00275514.2019.1696619.

54. Stabel, M.; Hanafy, R.A.; Schweitzer, T.; Greif, M.; Aliyu, H.; Flad, V.; Young, D.; Lebuhn, M.; Elshahed, M.S.; Ochsenreither, K.; et al. Aestipascuomyces dupliciliberans gen. Nov, sp. nov., the first cultured representative of the uncultured SK4 clade from aoudad sheep and alpaca. *Microorganisms* **2020**, *8*, 1–17, doi:10.3390/microorganisms8111734.

55. Hanafy, R.A.; Youssef, N.H.; Elshahed, M.S. Paucimyces polynucleatus gen. nov, sp. nov., a novel polycentric genus of anaerobic gut fungi from the faeces of a wild blackbuck antelope. *Int. J. Syst. Evol. Microbiol.* **2021**, *71*, 004832, doi:10.1099/ijsem.0.004832.

56. Ozkose, E.; Thomas, B.J.; Davies, D.R.; Griffith, G.W.; Theodorou, M.K. Cyllamyces aberensis gen.nov. sp.nov., a new anaerobic gut fungus with branched sporangiophores isolated from cattle. *Can. J. Bot.* **2001**, doi:10.1139/cjb-79-6-666.

57. Breton, A.; Bernalier, A.; Dusser, M.; Fonty, G.; Gaillard-Martinie, B.; Guillot, J. Anaeromyces mucronatus nov. gen., nov. sp. A new strictly anaerobic rumen fungus with polycentric thallus. *FEMS Microbiol. Lett.* **1990**, doi:10.1016/S0378-1097(05)80035-7.

58. Barr, D.J.S.; Kudo, H.; Jakober, K.D.; Cheng, K.-J. Morphology and development of rumen fungi: Neocallimastix sp., Piromyces communis , and Orpinomyces bovis gen.nov., sp.nov. . *Can. J. Bot.* **1989**, doi:10.1139/b89-361.

59. Dagar, S.S.; Kumar, S.; Griffith, G.W.; Edwards, J.E.; Callaghan, T.M.; Singh, R.; Nagpal, A.K.; Puniya, A.K. A new anaerobic fungus (Oontomyces anksri gen. nov., sp. nov.) from the digestive tract of the Indian camel (Camelus dromedarius). *Fungal Biol.* **2015**, doi:10.1016/j.funbio.2015.04.005.

60. Callaghan, T.M.; Podmirseg, S.M.; Hohlweck, D.; Edwards, J.E.; Puniya, A.K.; Dagar, S.S.; Griffith, G.W. Buwchfawromyces eastonii gen. nov., sp. nov.: A new anaerobic fungus (Neocallimastigomycota) isolated from buffalo faeces. *MycoKeys* **2015**, doi:10.3897/mycokeys.9.9032.

61. Hanafy, R.A.; Elshahed, M.S.; Liggenstoffer, A.S.; Griffith, G.W.; Youssef, N.H. Pecoramyces ruminantium, gen. nov., sp. nov., an anaerobic gut fungus from the feces of cattle and sheep.

Mycologia **2017**, doi:10.1080/00275514.2017.1317190.

62. Joshi, A.; Lanjekar, V.B.; Dhakephalkar, P.K.; Callaghan, T.M.; Griffith, G.W.; Dagar, S.S. Liebetanzomyces polymorphus gen. et sp. nov., a new anaerobic fungus (Neocallimastigomycota) isolated from the rumen of a goat. *MycoKeys* **2018**, doi:10.3897/mycokeys.40.28337.

63. Hanafy, R.A.; Elshahed, M.S.; Youssef, N.H. Feramyces austinii, gen. Nov., sp. nov., an anaerobic gut fungus from rumen and fecal samples of wild barbary sheep and fallow deer. *Mycologia* **2018**, doi:10.1080/00275514.2018.1466610.

64. Kittelmann, S.; Naylor, G.E.; Koolaard, J.P.; Janssen, P.H. A proposed taxonomy of anaerobic fungi (class neocallimastigomycetes) suitable for large-scale sequence-based community structure analysis. *PLoS One* **2012**, doi:10.1371/journal.pone.0036866.

65. Hanafy, R.A.; Johnson, B.; Youssef, N.; Elshahed, M. Assessing anaerobic gut fungal diversity in herbivores using D1 / D2 large ribosomal subunit sequencing and multi-year isolation. *Environ. Microbiol.* **2020**, doi:10.1111/1462-2920.15164.

66. Orpin, C.G.; Munn, E.A. Neocallimastix patriciarum sp.nov., a new member of the Neocallimasticaceae inhabiting the rumen of sheep. *Trans. Br. Mycol. Soc.* **1986**, doi:10.1016/s0007-1536(86)80138-3.

67. Ho, Y.W.; Barr, D.J.S. Classification of Anaerobic Gut Fungi from Herbivores with Emphasis on Rumen Fungi from Malaysia. *Mycologia* **1995**, doi:10.2307/3760810.

68. Wang, X.; Liu, X.; Groenewald, J.Z. Phylogeny of anaerobic fungi (phylum Neocallimastigomycota), with contributions from yak in China. *Antonie Van Leeuwenhoek* **2017**, *110*, 87–103, doi:10.1007/s10482-016-0779-1.

69. Ho, Y.W.; Barr, D.J.S.; Abdullah, N.; Jalaludin, S.; Kudo, H. Neocallimastix variabilis, a New Species of Anaerobic Fungus from the Rumen of Cattle. *Mycotaxon* **1993**, *46*, 241–258.

70. Webb, J.; Theodorou, M.K. Neocallimastix hurleyensis sp.nov., an anaerobic fungus from the ovine rumen . *Can. J. Bot.* **1991**, doi:10.1139/b91-156.

71. Ariyawansa, H.A.; Hyde, K.D.; Jayasiri, S.C.; Buyck, B.; Chethana, K.W.T.; Dai, D.Q.; Dai, Y.C.; Daranagama, D.A.; Jayawardena, R.S.; Lücking, R.; et al. Fungal diversity notes 111–252—taxonomic and phylogenetic contributions to fungal taxa. *Fungal Divers.* **2015**, doi:10.1007/s13225-015-0346-5.

72. Li, G.J.; Hyde, K.D.; Zhao, R.L.; Hongsanan, S.; Abdel-Aziz, F.A.; Abdel-Wahab, M.A.; Alvarado, P.; Alves-Silva, G.; Ammirati, J.F.; Ariyawansa, H.A.; et al. Fungal diversity notes 253–366: taxonomic and phylogenetic contributions to fungal taxa. *Fungal Divers.* **2016**, doi:10.1007/s13225-016-0366-9.

73. Stabel, M.; Schweitzer, T.; Haack, K.; Gorenflo, P.; Aliyu, H.; Ochsenreither, K. Isolation and biochemical characterization of six anaerobic fungal strains from zoo animal feces. *Microorganisms* **2021**, *9*, doi:10.3390/microorganisms9081655.

74. Orpin, C.G. The Rumen Flagellate Piromonas communis: Its Life-history and Invasion of Plant Material in the Rumen. *J. Gen. Microbiol.* **1977**, *99*, 107–117, doi:10.1099/00221287-99-1-107.

75. Li, J.; Heath, I.B.; Bauchop, T. Piromyces mae and Piromyces dumbonica , two new species of uniflagellate anaerobic chytridiomycete fungi from the hindgut of the horse and elephant . *Can. J. Bot.* **1990**, doi:10.1139/b90-129.

76. Breton, A.; Dusser, M.; Gaillard-Martine, B.; Guillot, J.; Millet, L.; Prensier, G. Piromyces rhizinflata nov. sp., a strictly anaerobic fungus from faeces of the Saharian ass: a morphological, metabolic and ultrastructural study. *FEMS Microbiol. Lett.* **1991**, doi:10.1111/j.1574-6968.1991.tb04830.x.

77. Gaillard-Martinie, B.; Breton, A.; Dusser, M.; Julliand, V. Piromyces citronii sp. nov., a strictly anaerobic fungus from the equine caecum: a morphological, metabolic, and ultrastructural study. *FEMS Microbiol. Lett.* **1995**, doi:10.1016/0378-1097(95)00225-T.

78. Chen, Y.C.; Hseu, R.S.; Chien, C.Y. Piromyces polycephalus (Neocallimastigaceae), a new rumen fungus. *Nov. Hedwigia* **2002**, doi:10.1127/0029-5035/2002/0075-0409.

79. Orpin, C.G. Studies on the Rumen Flagellate Sphaeromonas communis. *J. Gen. Microbiol.* **1976**, doi:10.1099/00221287-94-2-270.

80. Henske, J.K.; Gilmore, S.P.; Knop, D.; Cunningham, F.J.; Sexton, J.A.; Smallwood, C.R.; Shutthanandan, V.; Evans, J.E.; Theodorou, M.K.; O'Malley, M.A. Transcriptomic characterization of Caecomyces churrovis: A novel, non-rhizoid-forming lignocellulolytic anaerobic fungus. *Biotechnol. Biofuels* **2017**, *10*, doi:10.1186/s13068-017-0997-4.

81. Chen, Y.C.; Tsai, S. Da; Cheng, H.L.; Chien, C.Y.; Hu, C.Y.; Cheng, T.Y. Caecomyces sympodialis sp. nov., a new rumen fungus isolated from Bos indicus. *Mycologia* **2007**, doi:10.3852/mycologia.99.1.125.

82. Hanafy, R.A.; Johnson, B.; Elshahed, M.S.; Youssef, N.H. Anaeromyces contortus, sp. Nov., a new anaerobic gut fungal species (neocallimastigomycota) isolated from the feces of cow and goat. *Mycologia* **2018**, doi:10.1080/00275514.2018.1465773.

83. Breton, A.; Bernalier, A.; Bonnemoy, F.; Fonty, G.; Gaillard, B.; Gouet, P. Morphological and metabolic characterization of a new species of strictly anaerobic rumen fungus: Neocallimastix joyonii. *FEMS Microbiol. Lett.* **1989**, doi:10.1111/j.1574-6968.1989.tb03065.x.

84. Li, J.; Heath, I.B.; Cheng, K.-J. The development and zoospore ultrastructure of a polycentric chytridiomycete gut fungus, Orpinomyces joyonii comb.nov. . *Can. J. Bot.* **1991**, doi:10.1139/b91-079.

85. Youssef, N.H.; Couger, M.B.; Struchtemeyer, C.G.; Liggenstoffer, A.S.; Prade, R.A.; Najar, F.Z.; Atiyeh, H.K.; Wilkins, M.R.; Elshahed, M.S. The genome of the anaerobic fungus orpinomyces sp. strain c1a reveals the unique evolutionary history of a remarkable plant biomass degrader. *Appl. Environ. Microbiol.* **2013**, doi:10.1128/AEM.00821-13.

86. Hausner, G.; Inglis, G.D.; Yanke, L.J.; Kawchuk, L.M.; McAllister, T.A. Analysis of restriction fragment length polymorphisms in the ribosomal DNA of a selection of anaerobic chytrids. *Can. J. Bot.* **2000**, doi:10.1139/b00-067.

87. Brookman, J.L.; Mennim, G.; Trinci, A.P.J.; Theodorou, M.K.; Tuckwell, D.S. Identification and characterization of anaerobic gut fungi using molecular methodologies based on ribosomal ITS1 and 18S rRNA. *Microbiology* **2000**, *146*, 393–403, doi:10.1099/00221287-146-2-393.

88. Fliegerová, K.; Hodrová, B.; Voigt, K. Classical and molecular approaches as a powerful tool for the characterization of rumen polycentric fungi. In Proceedings of the Folia Microbiologica; 2004.

89. Edwards, J.E.; Kingston-Smith, A.H.; Jimenez, H.R.; Huws, S.A.; Skøt, K.P.; Griffith, G.W.; McEwan, N.R.; Theodorou, M.K. Dynamics of initial colonization of nonconserved perennial ryegrass by anaerobic fungi in the bovine rumen. *FEMS Microbiol. Ecol.* **2008**, doi:10.1111/j.1574-6941.2008.00563.x.

90. Liggenstoffer, A.S.; Youssef, N.H.; Couger, M.B.; Elshahed, M.S. Phylogenetic diversity and community structure of anaerobic gut fungi (phylum Neocallimastigomycota) in ruminant and non-ruminant herbivores. *ISME J.* **2010**, doi:10.1038/ismej.2010.49.

91. Koetschan, C.; Kittelmann, S.; Lu, J.; Al-Halbouni, D.; Jarvis, G.N.; Müller, T.; Wolf, M.; Janssen, P.H. Internal transcribed spacer 1 secondary structure analysis reveals a common core throughout the anaerobic fungi (Neocallimastigomycota). *PLoS One* **2014**, doi:10.1371/journal.pone.0091928.

92. Dollhofer, V.; Callaghan, T.M.; Dorn-In, S.; Bauer, J.; Lebuhn, M. Development of three specific PCR-based tools to determine quantity, cellulolytic transcriptional activity and phylogeny of anaerobic fungi. *J. Microbiol. Methods* **2016**, doi:10.1016/j.mimet.2016.05.017.

93. Milne, A.; Theodorou, M.K.; Jordan, M.G.C.; King-Spooner, C.; Trinci, A.P.J. Survival of anaerobic fungi in feces, in saliva, and in pure culture. *Exp. Mycol.* **1989**, *13*, 27–37, doi:https://doi.org/10.1016/0147-5975(89)90005-4.

94. Paul, S.S.; Kamra, D.N.; Sastry, V.R.B. Fermentative characteristics and fibrolytic activities of anaerobic gut fungi isolated from wild and domestic ruminants. *Arch. Anim. Nutr.* **2010**, *64*, 279–292, doi:10.1080/17450391003625037.

95. Gordon, G.L.R.; Phillips, M.W. Removal of anaerobic fungi from the rumen of sheep by chemical treatment and the effect on feed consumption and in vivo fibre digestion. *Lett. Appl. Microbiol.* **1993**, *17*, 220–223, doi:10.1111/j.1472-765X.1993.tb01451.x.

96. Dey, A.; Sehgal, J.P.; Puniya, A.K.; Singh, K. Influence of an anaerobic fungal culture (Orpinomyces sp.) administration on growth rate, ruminal fermentation and nutrient digestion in calves. *Asian-Australasian J. Anim. Sci.* **2004**, *17*, 820–824, doi:10.5713/ajas.2004.820.

97. Lee, S..; Ha, J..; Cheng, K.-J. Influence of an anaerobic fungal culture administration on in vivo ruminal fermentation and nutrient digestion. *Anim. Feed Sci. Technol.* **2000**, *88*, 201–217, doi:10.1016/S0377-8401(00)00216-9.

98. Tripathi, V.K.; Sehgal, J.P.; Puniya, A.K.; Singh, K. Effect of administration of anaerobic fungi isolated from cattle and wild blue bull (Boselaphus tragocamelus) on growth rate and fibre utilization in buffalo calves. *Arch. Anim. Nutr.* **2007**, *61*, 416–423, doi:10.1080/17450390701556759.

99. Saxena, S.; Sehgal, J.P.; Puniya, A.K.; Singh, K. Effect of administration of rumen fungi on production performance of lactating buffaloes. *Benef. Microbes* **2010**, *1*, 183–188, doi:10.3920/BM2009.0018.

100. Paul, S.S.; Deb, S.M.; Punia, B.S.; Das, K.S.; Singh, G.; Ashar, M.N.; Kumar, R. Effect of feeding isolates of anaerobic fungus Neocallimastix sp. CF 17 on growth rate and fibre digestion in buffalo calves. *Arch. Anim. Nutr.* **2011**, *65*, 215–228, doi:10.1080/1745039X.2011.559722.

101. Paul, S.S.; Kamra, D.N.; Sastry, V.R.B.; Sahu, N.P.; Agarwal, N. Effect of administration of an anaerobic gut fungus isolated from wild blue bull (Boselaphus tragocamelus) to buffaloes (Bubalus bubalis) on in vivo ruminal fermentation and digestion of nutrients. *Anim. Feed Sci. Technol.* **2004**, *115*, 143–157, doi:10.1016/j.anifeedsci.2004.01.010.

102. Hess, M.; Paul, S.S.; Puniya, A.K.; van der Giezen, M.; Shaw, C.; Edwards, J.E.; Fliegerová, K. Anaerobic Fungi: Past, Present, and Future . *Front. Microbiol.* 2020, *11*, 2621.

103. Orpin, C.G.; Bountiff, L. Zoospore Chemotaxis in the Rumen Phycomycete Neocallimastix frontalis. *J. Gen. Microbiol.* **1978**, *104*, 113–122, doi:10.1099/00221287-104-1-113.

104. Wubah, D.A.; Kim, D.S.H. Chemoattraction of anaerobic ruminai fungi zoospores to selected phenolic acids. *Microbiol. Res.* **1996**, *151*, 257–262, doi:https://doi.org/10.1016/S0944-5013(96)80022-X.

105. Bauchop, T. The anaerobic fungi in rumen fibre digestion. *Agric. Environ.* **1981**, *6*, 339–348, doi:10.1016/0304-1131(81)90021-7.

106. Ho, Y.W.; Abdullah, N.; Jalaludin, S. Colonization of guinea grass by anaerobic rumen fungi in swamp buffalo and cattle. *Anim. Feed Sci. Technol.* **1988**, doi:10.1016/0377-8401(88)90083-1.

107. Ho, Y.W.; Abdullah, N.; Jalaludin, S. Penetrating Structures of Anaerobic Rumen Fungi in Cattle and Swamp Buffalo. *Microbiology* **1988**, *134*, 177–181, doi:10.1099/00221287-134-1-177.

108. Wubah, D.A.; Fuller, M.S.; Akin, D.E. Studies on Caecomyces communis: Morphology and

Development. *Mycologia* **1991**, *83*, 303, doi:10.2307/3759990.

109. Orpin, C.G.; Greenwood, Y. The Role of Haems and Related Compounds in the Nutrition and Zoosporogenesis of the Rumen Chytridiomycete Neocallimastix frontalis H8. *Microbiology* **1986**, *132*, 2179–2185, doi:10.1099/00221287-132-8-2179.

110. Orpin, C.G. Isolation of cellulolytic phycomycete fungi from the caecum of the horse. *J. Gen. Microbiol.* **1981**, *123*, 287–296, doi:10.1099/00221287-123-2-287.

111. Struchtemeyer, C.G.; Ranganathan, A.; Couger, M.B.; Liggenstoffer, A.S.; Youssef, N.H.; Elshahed, M.S. Survival of the anaerobic fungus Orpinomyces sp. Strain C1A after prolonged air exposure. *Sci. Rep.* **2014**, *4*, 1–7, doi:10.1038/srep06892.

112. McGranaghan, P.; Davies, J.C.; Griffith, G.W.; Davies, D.R.; Theodorou, M.K. The survival of anaerobic fungi in cattle faeces. *FEMS Microbiol. Ecol.* **1999**, *29*, 293–300, doi:10.1111/j.1574-6941.1999.tb00620.x.

113. Lowe, S.E.; Theodorou, M.K.; Trinci, A.P.J. Isolation of anaerobic fungi from saliva and faeces of sheep. *J. Gen. Microbiol.* **1987**, *133*, 1829–1834, doi:10.1099/00221287-133-7-1829.

114. Wubah, D.A.; Fuller, M.S.; Akin, D.E. Resistant Body Formation in Neocallimastix Sp., An Anaerobic Fungus from the Rumen of a Cow. *Mycologia* **1991**, *83*, 40–47, doi:10.1080/00275514.1991.12025977.

115. Nielsen, B.B.; Zhu, W.Y.; Trinci, A.P.J.; Theodorou, M.K. Demonstration of zoosporangia of anaerobic fungi on plant residues recovered from faeces of cattle. *Mycol. Res.* **1995**, *99*, 471–474, doi:10.1016/S0953-7562(09)80648-5.

116. Brookman, J.L.; Ozkose, E.; Rogers, S.; Trinci, A.P.J.; Theodorou, M.K. Identification of spores in the polycentric anaerobic gut fungi which enhance their ability to survive. *FEMS Microbiol. Ecol.* **2000**, doi:10.1016/S0168-6496(00)00003-9.

117. Solomon, K. V; Haitjema, C.H.; Henske, J.K.; Gilmore, S.P.; Borges-Rivera, D.; Lipzen, A.; Brewer, H.M.; Purvine, S.O.; Wright, A.T.; Theodorou, M.K.; et al. Early-branching gut fungi possess large, comprehensive array of biomass-degrading enzymes. *Science (80-.).* **2016**, *351*, 1192–1195, doi:10.1126/science.aad1431.

118. Couger, M.B.; Youssef, N.H.; Struchtemeyer, C.G.; Liggenstoffer, A.S.; Elshahed, M.S. Transcriptomic analysis of lignocellulosic biomass degradation by the anaerobic fungal isolate Orpinomyces sp. strain C1A. *Biotechnol. Biofuels* **2015**, *8*, 208, doi:10.1186/s13068-015-0390-0.

119. Morrison, J.M.; Elshahed, M.S.; Youssef, N.H. Defined enzyme cocktail from the anaerobic fungus Orpinomyces sp. Strain C1A effectively releases sugars from pretreated corn stover and switchgrass. *Sci. Rep.* **2016**, *6*, doi:10.1038/srep29217.

120. Gilmore, S.P.; Henske, J.K.; O'Malley, M.A. Driving biomass breakdown through engineered cellulosomes. *Bioengineered* **2015**, *6*, 204–208, doi:10.1080/21655979.2015.1060379.

121. Wilson, C.; Wood, T. The anaerobic fungus Neocallimastix frontalis: isolation and properties of a cellulosome-type enzyme fraction with the capacity to solubilize hydrogen-bond-ordered cellulose. *Appl. Microbiol. Biotechnol.* **1992**, *37*, 125–129, doi:10.1007/BF00174216.

122. Haitjema, C.H.; Gilmore, S.P.; Henske, J.K.; Solomon, K. V; de Groot, R.; Kuo, A.; Mondo, S.J.; Salamov, A.A.; LaButti, K.; Zhao, Z.; et al. A parts list for fungal cellulosomes revealed by comparative genomics. *Nat. Microbiol.* **2017**, *2*, 17087, doi:10.1038/nmicrobiol.2017.87.

123. Gilmore, S.P.; Lillington, S.P.; Haitjema, C.H.; de Groot, R.; O'Malley, M.A. Designing chimeric enzymes inspired by fungal cellulosomes. *Synth. Syst. Biotechnol.* **2020**, *5*, 23–32, doi:10.1016/j.synbio.2020.01.003.

124. Henske, J.K.; Wilken, S.E.; Solomon, K. V.; Smallwood, C.R.; Shutthanandan, V.; Evans, J.E.;

Theodorou, M.K.; O'Malley, M.A. Metabolic characterization of anaerobic fungi provides a path forward for bioprocessing of crude lignocellulose. *Biotechnol. Bioeng.* **2018**, *115*, 874–884, doi:10.1002/bit.26515.

125. Solomon, K. V.; Henske, J.K.; Gilmore, S.P.; Lipzen, A.; Grigoriev, I. V.; Thompson, D.; O'Malley, M.A. Catabolic repression in early-diverging anaerobic fungi is partially mediated by natural antisense transcripts. *Fungal Genet. Biol.* **2018**, *121*, 1–9, doi:10.1016/j.fgb.2018.09.004.

126. Henske, J.K.; Gilmore, S.P.; Haitjema, C.H.; Solomon, K. V.; O'Malley, M.A. Biomass-degrading enzymes are catabolite repressed in anaerobic gut fungi. *AIChE J.* **2018**, *64*, 4263–4270, doi:10.1002/aic.16395.

127. Marvin-Sikkema, F.D.; Pedro Gomes, T.M.; Grivet, J.P.; Gottschal, J.C.; Prins, R.A. Characterization of hydrogenosomes and their role in glucose metabolism of Neocallimastix sp. L2. *Arch. Microbiol.* **1993**, *160*, 388–96.

128. Kown, M.; Song, J.; Ha, J.K.; Park, H.S.; Chang, J. Analysis of functional genes in carbohydrate metabolic pathway of anaerobic rumen fungus Neocallimastix frontalis PMA02. *Asian-Australasian J. Anim. Sci.* **2009**, *22*, 1555–1565, doi:10.5713/ajas.2009.80371.

129. Li, Y.; Jin, W.; Mu, C.; Cheng, Y.; Zhu, W. Indigenously associated methanogens intensified the metabolism in hydrogenosomes of anaerobic fungi with xylose as substrate. *J. Basic Microbiol.* **2017**, *57*, 933–940, doi:10.1002/jobm.201700132.

130. Harhangi, H.R.; Akhmanova, A.S.; Emmens, R.; Van Der Drift, C.; De Laat, W.T.A.M.; Van Dijken, J.P.; Jetten, M.S.M.; Pronk, J.T.; Op Den Camp, H.J.M. Xylose metabolism in the anaerobic fungus Piromyces sp. strain E2 follows the bacterial pathway. *Arch. Microbiol.* **2003**, *180*, 134–141, doi:10.1007/s00203-003-0565-0.

131. Cheng, Y.F.; Jin, W.; Mao, S.Y.; Zhu, W.Y. Production of citrate by anaerobic fungi in the presence of co-culture methanogens as revealed by 1H NMR spectrometry. *Asian-Australasian J. Anim. Sci.* **2013**, *26*, 1416–1423, doi:10.5713/ajas.2013.13134.

132. Li, Y.; Li, Y.; Jin, W.; Sharpton, T.J.; Mackie, R.I.; Cann, I.; Cheng, Y.; Zhu, W. Combined Genomic, Transcriptomic, Proteomic, and Physiological Characterization of the Growth of Pecoramyces sp. F1 in Monoculture and Co-culture With a Syntrophic Methanogen. *Front. Microbiol.* **2019**, *10*, 435, doi:10.3389/fmicb.2019.00435.

133. Li, Y.; Jin, W.; Cheng, Y.; Zhu, W. Effect of the Associated Methanogen Methanobrevibacter thaueri on the Dynamic Profile of End and Intermediate Metabolites of Anaerobic Fungus Piromyces sp. F1. *Curr. Microbiol.* **2016**, *73*, 434–441, doi:10.1007/s00284-016-1078-9.

134. van der Giezen, M.; Sjollema, K.A.; Artz, R.R.E.; Alkema, W.; Prins, R.A. Hydrogenosomes in the anaerobic fungus Neocallimastix frontalis have a double membrane but lack an associated organelle genome. *FEBS Lett.* **1997**, *408*, 147–150, doi:10.1016/S0014-5793(97)00409-2.

135. van der Giezen, M.; Slotboom, D.J.; Horner, D.S.; Dyal, P.L.; Harding, M.; Xue, G.P.; Embley, T.M.; Kunji, E.R.S. Conserved properties of hydrogenosomal and mitochondrial ADP/ATP carriers: A common origin for both organelles. *EMBO J.* **2002**, *21*, 572–579, doi:10.1093/emboj/21.4.572.

136. van der Giezen, M.; Birdsey, G.M.; Horner, D.S.; Lucocq, J.; Dyal, P.L.; Benchimol, M.; Danpure, C.J.; Embley, T.M. Fungal hydrogenosomes contain mitochondrial heat-shock proteins. *Mol. Biol. Evol.* **2003**, *20*, 1051–1061, doi:10.1093/molbev/msg103.

137. Akhmanova, A.; Voncken, F.G.J.; Hosea, K.M.; Harhangi, H.; Keltjens, J.T.; op den Camp, H.J.M.; Vogels, G.D.; Hackstein, J.H.P. A hydrogenosome with pyruvate formate-lyase: anaerobic chytrid fungi use an alternative route for pyruvate catabolism. *Mol. Microbiol.* **1999**, *32*, 1103–1114, doi:10.1046/j.1365-2958.1999.01434.x.

138. Marvin-Sikkema, F.D.; Driessen, A.J.M.; Gottschal, J.C.; Prins, R.A. Metabolic energy

generation in hydrogenosomes of the anaerobic fungus Neocallimastix: evidence for a functional relationship with mitochondria. *Mycol. Res.* **1994**, *98*, 205–212, doi:10.1016/S0953-7562(09)80187-1.

139. Seppälä, S.; Solomon, K. V.; Gilmore, S.P.; Henske, J.K.; O'Malley, M.A. Mapping the membrane proteome of anaerobic gut fungi identifies a wealth of carbohydrate binding proteins and transporters. *Microb. Cell Fact.* **2016**, *15*, 212, doi:10.1186/s12934-016-0611-7.

140. Jin, W.; Cheng, Y.F.; Mao, S.Y.; Zhu, W.Y. Isolation of natural cultures of anaerobic fungi and indigenously associated methanogens from herbivores and their bioconversion of lignocellulosic materials to methane. *Bioresour. Technol.* **2011**, *102*, 7925–7931, doi:10.1016/j.biortech.2011.06.026.

141. Leis, S.; Dresch, P.; Peintner, U.; Fliegerová, K.; Sandbichler, A.M.; Insam, H.; Podmirseg, S.M. Finding a robust strain for biomethanation: Anaerobic fungi (Neocallimastigomycota) from the Alpine ibex (Capra ibex) and their associated methanogens. *Anaerobe* **2014**, *29*, 34–43, doi:10.1016/j.anaerobe.2013.12.002.

142. Bauchop, T.; Mountfort, D.O. Cellulose fermentation by a rumen anaerobic fungus in both the absence and the presence of rumen methanogens. *Appl. Environ. Microbiol.* **1981**, *42*, 1103–1110, doi:10.1128/aem.42.6.1103-1110.1981.

143. Swift, C.L.; Brown, J.L.; Seppälä, S.; O'Malley, M.A. Co-cultivation of the anaerobic fungus Anaeromyces robustus with Methanobacterium bryantii enhances transcription of carbohydrate active enzymes. *J. Ind. Microbiol. Biotechnol.* **2019**, *46*, 1427–1433, doi:10.1007/s10295-019-02188-0.

144. Zhu, W.-Y.; Theodorou, M.K.; Nielsen, B.B.; Trinci, A.P.J. Dilution Rate Increases Production of Plant Cell-wall Degrading Enzymes by Anaerobic Fungi in Continuous-flow Culture. *Anaerobe* **1997**, *3*, 49–59, doi:https://doi.org/10.1006/anae.1997.0070.

145. Liu, J.-R.; Yu, B.; Liu, F.-H.; Cheng, K.-J.; Zhao, X. Expression of rumen microbial fibrolytic enzyme genes in probiotic Lactobacillus reuteri. *Appl. Environ. Microbiol.* **2005**, *71*, 6769–75, doi:10.1128/AEM.71.11.6769-6775.2005.

146. Chang, J.-J.; Lin, Y.-J.; Lay, C.-H.; Thia, C.; Wu, Y.-C.; Hou, Y.-H.; Huang, C.-C.; Li, W.-H. Constructing a cellulosic yeast host with an efficient cellulase cocktail. *Biotechnol. Bioeng.* **2018**, *115*, 751–761, doi:https://doi.org/10.1002/bit.26507.

147. Ranganathan, A.; Smith, O.P.; Youssef, N.H.; Struchtemeyer, C.G.; Atiyeh, H.K.; Elshahed, M.S. Utilizing anaerobic fungi for two-stage sugar extraction and biofuel production from lignocellulosic biomass. *Front. Microbiol.* 2017, *8*, 635.

148. Hillman, E.T.; Li, M.; Hooker, C.A.; Englaender, J.A.; Wheeldon, I.; Solomon, K. V Hydrolysis of lignocellulose by anaerobic fungi produces free sugars and organic acids for two-stage fine chemical production with Kluyveromyces marxianus. *Biotechnol. Prog. n/a*, e3172, doi:https://doi.org/10.1002/btpr.3172.

149. Elliott, A.R.; Silvert, P.Y.; Xue, G.P.; Simpson, G.D.; Tekaia-Elhsissen, K.; Aylward, J.H. Transformation of Bacillus subtilis using the particle inflow gun and submicrometer particles obtained by the polyol process. *Anal. Biochem.* **1999**, *269*, 418–420, doi:10.1006/abio.1999.4036.

150. Gilbert, H.J.; Hazlewood, G.P.; Laurie, J.I.; Orpin, C.G.; Xue, G.P. Homologous catalytic domains in a rumen fungal xylanase: evidence for gene duplication and prokaryotic origin. *Mol. Microbiol.* **1992**, *6*, 2065–2072, doi:10.1111/j.1365-2958.1992.tb01379.x.

151. Tamblyn Lee, J.M.; Hu, Y.; Zhu, H.; Cheng, K.J.; Krell, P.J.; Forsberg, C.W. Cloning of a xylanase gene from the ruminal fungus Neocallimastix patriciarum 27 and its expression in Escherichia coli. *Can. J. Microbiol.* **1993**, *39*, 134–139, doi:10.1139/m93-020.

152. Liu, J.-R.; Yu, B.; Lin, S.-H.; Cheng, K.-J.; Chen, Y.-C. Direct cloning of a xylanase gene from the mixed genomic DNA of rumen fungi and its expression in intestinal Lactobacillus reuteri. *FEMS Microbiol. Lett.* **2005**, *251*, 233–241, doi:10.1016/j.femsle.2005.08.008.

153. López-Contreras, A.M.; Smidt, H.; Van der Oost, J.; Claassen, P.A.M.; Mooibroek, H.; De Vos, W.M. Clostridium beijerinckii Cells Expressing Neocallimastix patridarum Glycoside Hydrolases Show Enhanced Lichenan Utilization and Solvent Production. *Appl. Environ. Microbiol.* **2001**, *67*, 5127–5133, doi:10.1128/aem.67.11.5127-5133.2001.

154. Xue, G.P.; Gobius, K.S.; Orpin, C.G. A novel polysaccharide hydrolase cDNA (celD) from Neocallimastix patriciarum encoding three multi-functional catalytic domains with high endoglucanase, cellobiohydrolase and xylanase activities. *J. Gen. Microbiol.* **1992**, *138*, 2397–2403, doi:10.1099/00221287-138-11-2397.

155. Xue, G.P.; Johnson, J.S.; Bransgrove, K.L.; Gregg, K.; Beard, C.E.; Dalrymple, B.P.; Gobius, K.S.; Aylward, J.H. Improvement of expression and secretion of a fungal xylanase in the rumen bacterium Butyrivibrio fibrisolvens OB156 by manipulation of promoter and signal sequences. *J. Biotechnol.* **1997**, *54*, 139–148, doi:10.1016/S0168-1656(97)01671-4.

156. Durand, R.; Rascle, C.; Fèvre, M. Expression of a catalytic domain of a Neocallimastix frontalis endoxylanase gene (xyn3) in Kluyveromyces lactis and Penicillium roqueforti. *Appl. Microbiol. Biotechnol.* **1999**, *52*, 208–214, doi:10.1007/s002530051510.

157. Harhangi, H.R.; Steenbakkers, P.J.M.; Akhmanova, A.; Jetten, M.S.M.; Van der Drift, C.; Op den Camp, H.J.M. A highly expressed family 1 β-glucosidase with transglycosylation capacity from the anaerobic fungus Piromyces sp. E2. *Biochim. Biophys. Acta - Gene Struct. Expr.* **2002**, *1574*, 293–303, doi:10.1016/S0167-4781(01)00380-3.

158. Li, X.L.; Ljungdahl, L.G.; Ximenes, E.A.; Chen, H.; Felix, C.R.; Cotta, M.A.; Dien, B.S. Properties of a recombinant β-glucosidase from polycentric anaerobic fungus Orpinomyces PC-2 and its application for cellulose hydrolysis. In Proceedings of the Applied Biochemistry and Biotechnology - Part A Enzyme Engineering and Biotechnology; Springer, 2004; Vol. 113, pp. 233–250.

159. O'Malley, M.A.; Theodorou, M.K.; Kaiser, C.A. Evaluating expression and catalytic activity of anaerobic fungal fibrolytic enzymes native topiromyces sp E2 inSaccharomyces cerevisiae. *Environ. Prog. Sustain. Energy* **2012**, *31*, 37–46, doi:10.1002/ep.10614.

160. van der Giezen, M.; Kiel, J.A.K.W.; Sjollema, K.A.; Prins, R.A. The hydrogenosomal malic enzyme from the anaerobic fungus Neocallimastix frontalis is targeted to mitochondria of the methylotrophic yeast Hansenula polymorpha. *Curr. Genet.* **1998**, *33*, 131–135, doi:10.1007/s002940050318.

161. Li, X.-L.; Skory, C.D.; Ximenes, E.A.; Jordan, D.B.; Dien, B.S.; Hughes, S.R.; Cotta, M.A. Expression of an AT-rich xylanase gene from the anaerobic fungus Orpinomyces sp. strain PC-2 in and secretion of the heterologous enzyme by Hypocrea jecorina. *Appl. Microbiol. Biotechnol.* **2007**, *74*, 1264–1275, doi:10.1007/s00253-006-0787-6.

162. Poidevin, L.; Levasseur, A.; Païs, G.; Navarro, D.; Heiss-Blanquet, S.; Asther, M.; Record, E. Heterologous production of the *Piromyces equi* cinnamoyl esterase in *Trichoderma reesei* for biotechnological applications. *Lett. Appl. Microbiol.* **2009**, *49*, 673–678, doi:10.1111/j.1472-765X.2009.02734.x.

163. Liu, J.H.; Selinger, L.B.; Cheng, K.J.; Beauchemin, K.A.; Moloney, M.M. Plant seed oil-bodies as an immobilization matrix for a recombinant xylanase from the rumen fungus Neocallimastix patriciarum. *Mol. Breed.* **1997**, doi:10.1023/A:1009604119618.

164. Obembe, O.O.; Jacobsen, E.; Timmers, J.; Gilbert, H.; Blake, A.W.; Knox, J.P.; Visser, R.G.F.; Vincken, J.P. Promiscuous, non-catalytic, tandem carbohydrate-binding modules modulate the cell-wall structure and development of transgenic tobacco (Nicotiana tabacum) plants. *J. Plant*

Res. **2007**, *120*, 605–617, doi:10.1007/s10265-007-0099-7.

165. Denman, S.; Xue, G.P.; Patel, B. Characterization of a Neocallimastix patriciarum cellulase cDNA (celA) homologous to Trichoderma reesei cellobiohydrolase II. *Appl. Environ. Microbiol.* **1996**.

166. Hung, Y.L.; Chen, H.J.; Liu, J.C.; Chen, Y.C. Catalytic efficiency diversification of duplicate β-1,3-1,4-glucanases from Neocallimastix patriciarum J11. *Appl. Environ. Microbiol.* **2012**, *78*, 4294–4300, doi:10.1128/AEM.07473-11.

167. Morrison, J.M.; Elshahed, M.S.; Youssef, N. A multifunctional GH39 glycoside hydrolase from the anaerobic gut fungus Orpinomyces sp. strain C1A. *PeerJ* **2016**, *2016*, e2289, doi:10.7717/PEERJ.2289.

168. Qiu, X.; Selinger, B.; Yanke, L.J.; Cheng, K.J. Isolation and analysis of two cellulase cDNAs from Orpinomyces joyonii. *Gene* **2000**, *245*, 119–126, doi:10.1016/S0378-1119(00)00028-7.

169. Tseng, C.W.; Ko, T.P.; Guo, R.T.; Huang, J.W.; Wang, H.C.; Huang, C.H.; Cheng, Y.S.; Wang, A.H.J.; Liu, J.R. Substrate binding of a GH5 endoglucanase from the ruminal fungus Piromyces rhizinflata. *Acta Crystallogr. Sect. F Struct. Biol. Cryst. Commun.* **2011**, *67*, 1189–1194, doi:10.1107/S1744309111032428.

170. Xue, G.P.; Orpin, C.G.; Gobius, K.S.; Aylward, J.H.; Simpson, G.D. Cloning and expression of multiple cellulase cDNAs from the anaerobic rumen fungus Neocallimastix patriciarum in Escherichia coli. *J. Gen. Microbiol.* **1992**, *138*, 1413–1420, doi:10.1099/00221287-138-7-1413.

171. Zhou, L.; Xue -p., G.; Orpin, C.G.; Black, G.W.; Gilbert, H.J.; Hazlewood, G.P. Intronless celB from the anaerobic fungus Neocallimastix patriciarum encodes a modular family A endoglucanase. *Biochem. J.* **1994**, *297*, 359–364, doi:10.1042/bj2970359.

172. Blum, D.L.; Li, X.L.; Chen, H.; Ljungdahl, L.G. Characterization of an acetyl xylan esterase from the anaerobic fungus Orpinomyces sp. strain PC-2. *Appl. Environ. Microbiol.* **1999**, *65*, 3990–3995, doi:10.1128/aem.65.9.3990-3995.1999.

173. Cybinski, D.H.; Layton, I.; Lowry, J.B.; Dalrymple, B.P. An acetylxylan esterase and a xylanase expressed from genes cloned from the ruminal fungus Neocallimastix patriciarum act synergistically to degrade acetylated xylans. *Appl. Microbiol. Biotechnol.* **1999**, *52*, 221–225, doi:10.1007/s002530051512.

174. Dalrymple, B.P.; Cybinski, D.H.; Layton, I.; McSweeney, C.S.; Xue, G.P.; Swadling, Y.J.; Lowry, J.B. Three Neocallimastix patriciarum esterases associated with the degradation of complex polysaccharides are members of a new family of hydrolases. *Microbiology* **1997**, *143*, 2605–2614, doi:10.1099/00221287-143-8-2605.

175. Fanutti, C.; Ponyi, T.; Black, G.W.; Hazlewood, G.P.; Gilbert, H.J. The conserved noncatalytic 40-residue sequence in cellulases and hemicellulases from anaerobic fungi functions as a protein docking domain. *J. Biol. Chem.* **1995**, *270*, 29314–29322, doi:10.1074/jbc.270.49.29314.

176. Millward-Sadler, S.J.; Hall, J.; Black, G.W.; Hazlewood, G.P.; Gilbert, H.J. Evidence that the Piromyces gene family encoding endo-1,4-mannanases arose through gene duplication. *FEMS Microbiol. Lett.* **1996**, *141*, 183–188, doi:10.1016/0378-1097(96)00219-4.

177. Pai, C.K.; Wu, Z.Y.; Chen, M.J.; Zeng, Y.F.; Chen, J.W.; Duan, C.H.; Li, M.L.; Liu, J.R. Molecular cloning and characterization of a bifunctional xylanolytic enzyme from Neocallimastix patriciarum. *Appl. Microbiol. Biotechnol.* **2010**, *85*, 1451–1462, doi:10.1007/s00253-009-2175-5.

178. Xue, G. ping; Denman, S.E.; Glassop, D.; Johnson, J.S.; Dierens, leanne M.; Gobius, K.S.; Aylward, J.H. Modification of a xylanase cDNA isolated from an anaerobic fungus Neocallimastix patriciarum for high-level expression in Escherichia coli. *J. Biotechnol.* **1995**, *38*, 269–277, doi:10.1016/0168-1656(94)00133-W.

179. Chen, H.L.; Chen, Y.C.; Lu, M.Y.J.; Chang, J.J.; Wang, H.T.C.; Ke, H.M.; Wang, T.Y.; Ruan, S.K.; Wang, T.Y.; Hung, K.Y.; et al. A highly efficient β-glucosidase from the buffalo rumen fungus Neocallimastix patriciarum W5. *Biotechnol. Biofuels* **2012**, doi:10.1186/1754-6834-5-24.

180. Steenbakkers, P.J.M.; Harhangi, H.R.; Bosscher, M.W.; Van Der Hooft, M.M.C.; Keltjens, J.T.; Van Der Drift, C.; Vogels, G.D.; Op Den Camp, H.J.M. β-Glucosidase in cellulosome of the anaerobic fungus Piromyces sp. strain E2 is a family 3 glycoside hydrolase. *Biochem. J.* **2003**, *370*, 963–970, doi:10.1042/BJ20021767.

181. Wang, T.-Y.; Chen, H.-L.; Lu, M.-Y.J.; Chen, Y.-C.; Sung, H.-M.; Mao, C.-T.; Cho, H.-Y.; Ke, H.-M.; Hwa, T.-Y.; Ruan, S.-K.; et al. Functional characterization of cellulases identified from the cow rumen fungus Neocallimastix patriciarum W5 by transcriptomic and secretomic analyses. *Biotechnol. Biofuels* **2011**, *4*, 24, doi:10.1186/1754-6834-4-24.

182. Mingardon, F.; Chanal, A.; López-Contreras, A.M.; Dray, C.; Bayer, E.A.; Fierobe, H.P. Incorporation of fungal cellulases in bacterial minicellulosomes yields viable, synergistically acting cellulolytic complexes. *Appl. Environ. Microbiol.* **2007**, *73*, 3822–3832, doi:10.1128/AEM.00398-07.

183. Jin, X.; Meng, N.; Xia, L. Expression of an Endo-β-1,4-glucanase Gene from Orpinomyces PC-2 in Pichia pastoris. *Int. J. Mol. Sci.* **2011**, *12*, 3366–3380, doi:10.3390/ijms12053366.

184. Hughes, S.R.; Riedmuller, S.B.; Mertens, J.A.; Li, X.L.; Bischoff, K.M.; Qureshi, N.; Cotta, M.A.; Farrelly, P.J. High-throughput screening of cellulase F mutants from multiplexed plasmid sets using an automated plate assay on a functional proteomic robotic workcell. *Proteome Sci.* **2006**, *4*, 10, doi:10.1186/1477-5956-4-10.

185. Tsai, C.F.; Qiu, X.; Liu, J.H. A comparative analysis of two cDNA clones of the cellulase gene family from anaerobic fungus Piromyces rhizinflata. *Anaerobe* **2003**, doi:10.1016/S1075-9964(03)00087-8.

186. Eberhardt, R.Y.; Gilbert, H.J.; Hazlewood, G.P. Primary sequence and enzymic properties of two modular endoglucanases, Cel5A and Cel45A, from the anaerobic fungus Piromyces equi. *Microbiology* **2000**, *146*, 1999–2008, doi:10.1099/00221287-146-8-1999.

187. Liu, J.H.; Tsai, C.F.; Liu, J.W.; Cheng, K.J.; Cheng, C.L. The catalytic domain of a Piromyces rhizinflata cellulase expressed in Escherichia coli was stabilized by the linker peptide of the enzyme. *Enzyme Microb. Technol.* **2001**, *28*, 582–589, doi:10.1016/S0141-0229(00)00349-5.

188. Chu, C.Y.; Tseng, C.W.; Yueh, P.Y.; Duan, C.H.; Liu, J.R. Molecular cloning and characterization of a β-glucanase from Piromyces rhizinflatus. *J. Biosci. Bioeng.* **2011**, *111*, 541–546, doi:10.1016/j.jbiosc.2011.01.009.

189. Liab, K.; Azadi, P.; Collins, R.; Tolan, J.; Kim, J.S.; Eriksson, K.E.L. Relationships between activities of xylanases and xylan structures. *Enzyme Microb. Technol.* **2000**, *27*, 89–94, doi:10.1016/S0141-0229(00)00190-3.

190. Liu, J.R.; Duan, C.H.; Zhao, X.; Tzen, J.T.C.; Cheng, K.J.; Pai, C.K. Cloning of a rumen fungal xylanase gene and purification of the recombinant enzyme via artificial oil bodies. *Appl. Microbiol. Biotechnol.* **2008**, doi:10.1007/s00253-008-1418-1.

191. Xue, H.; Zhou, J.; You, C.; Huang, Q.; Lu, H. Amino acid substitutions in the N-terminus, cord and α-helix domains improved the thermostability of a family 11 xylanase XynR8. *J. Ind. Microbiol. Biotechnol.* **2012**, *39*, 1279–1288, doi:10.1007/s10295-012-1140-y.

192. Ximenes, E.A.; Chen, H.; Kataeva, I.A.; Cotta, M.A.; Felix, C.R.; Ljungdahl, L.G.; Li, X.L. A mannanase, ManA, of the polycentric anaerobic fungus Orpinomyces sp. strain PC-2 has carbohydrate binding and docking modules. *Can. J. Microbiol.* **2005**, *51*, 559–568, doi:10.1139/w05-033.

193. Madhavan, A.; Tamalampudi, S.; Ushida, K.; Kanai, D.; Katahira, S.; Srivastava, A.; Fukuda, H.; Bisaria, V.S.; Kondo, A. Xylose isomerase from polycentric fungus Orpinomyces: Gene sequencing, cloning, and expression in Saccharomyces cerevisiae for bioconversion of xylose to ethanol. *Appl. Microbiol. Biotechnol.* **2009**, *82*, 1067–1078, doi:10.1007/s00253-008-1794-6.

194. Gruninger, R.J.; Cote, C.; McAllister, T.A.; Abbott, D.W. Contributions of a unique β-clamp to substrate recognition illuminates the molecular basis of exolysis in ferulic acid esterases. *Biochem. J.* **2016**, *473*, 839–849, doi:10.1042/BJ20151153.

195. Qi, M.; Wang, P.; Selinger, L.B.; Yanke, L.J.; Forster, R.J.; McAllister, T.A. Isolation and characterization of a ferulic acid esterase (Fae1A) from the rumen fungus Anaeromyces mucronatus. *J. Appl. Microbiol.* **2011**, *110*, 1341–1350, doi:10.1111/j.1365-2672.2011.04990.x.

196. Fillingham, I.J.; Kroon, P.A.; Williamson, G.; Gilbert, H.J.; Hazlewood, G.P. A modular cinnamoyl ester hydrolase from the anaerobic fungus Piromyces equi acts synergistically with xylanase and is part of a multiprotein cellulose-binding cellulase-hemicellulase complex. *Biochem. J.* **1999**, *343*, 215–224, doi:10.1042/0264-6021:3430215.

197. Dollhofer, V.; Callaghan, T.M.; Griffith, G.W.; Lebuhn, M.; Bauer, J. Presence and transcriptional activity of anaerobic fungi in agricultural biogas plants. *Bioresour. Technol.* **2017**, *235*, 131–139, doi:https://doi.org/10.1016/j.biortech.2017.03.116.

198. Procházka, J.; Mrázek, J.; Štrosová, L.; Fliegerová, K.; Zábranská, J.; Dohányos, M. Enhanced biogas yield from energy crops with rumen anaerobic fungi. *Eng. Life Sci.* **2012**, *12*, 343–351, doi:10.1002/elsc.201100076.

199. Ferraro, A.; Dottorini, G.; Massini, G.; Mazzurco Miritana, V.; Signorini, A.; Lembo, G.; Fabbricino, M. Combined bioaugmentation with anaerobic ruminal fungi and fermentative bacteria to enhance biogas production from wheat straw and mushroom spent straw. *Bioresour. Technol.* **2018**, *260*, 364–373, doi:10.1016/j.biortech.2018.03.128.

200. Saye, L.M.G.; Navaratna, T.A.; Chong, J.P.J.; O'Malley, M.A.; Theodorou, M.K.; Reilly, M. The Anaerobic Fungi: Challenges and Opportunities for Industrial Lignocellulosic Biofuel Production. *Microorganisms* **2021**, *9*, doi:10.3390/microorganisms9040694.

201. Swift, C.L.; Louie, K.B.; Bowen, B.P.; Olson, H.M.; Purvine, S.O.; Salamov, A.; Mondo, S.J.; Solomon, K. V; Wright, A.T.; Northen, T.R.; et al. Anaerobic gut fungi are an untapped reservoir of natural products. *Proc. Natl. Acad. Sci.* **2021**, *118*, doi:10.1073/pnas.2019855118.

202. Durand, R.; Rascle, C.; Fischer, M.; Fèvre, M. Transient expression of the β-glucuronidase gene after biolistic transformation of the anaerobic fungus Neocallimastix frontalis. *Curr. Genet.* **1997**, *31*, 158–161, doi:10.1007/s002940050190.

203. Hagen, L.H.; Brooke, C.G.; Shaw, C.A.; Norbeck, A.D.; Piao, H.; Arntzen, M.; Olson, H.M.; Copeland, A.; Isern, N.; Shukla, A.; et al. Proteome specialization of anaerobic fungi during ruminal degradation of recalcitrant plant fiber. *ISME J.* **2021**, *15*, 421–434, doi:10.1038/s41396-020-00769-x.

204. Edwards, J.E.; Forster, R.J.; Callaghan, T.M.; Dollhofer, V.; Dagar, S.S.; Cheng, Y.; Chang, J.; Kittelmann, S.; Fliegerova, K.; Puniya, A.K.; et al. PCR and Omics Based Techniques to Study the Diversity, Ecology and Biology of Anaerobic Fungi: Insights, Challenges and Opportunities . *Front. Microbiol.* 2017, *8*, 1657.

205. Guo, W.; Zhou, M.; Ma, T.; Bi, S.; Wang, W.; Zhang, Y.; Huang, X.; Guan, L.L.; Long, R. Survey of rumen microbiota of domestic grazing yak during different growth stages revealed novel maturation patterns of four key microbial groups and their dynamic interactions. *Anim. Microbiome* **2020**, *2*, 23, doi:10.1186/s42523-020-00042-8.

206. Kittelmann, S.; Seedorf, H.; Walters, W.A.; Clemente, J.C.; Knight, R.; Gordon, J.I.; Janssen, P.H. Simultaneous Amplicon Sequencing to Explore Co-Occurrence Patterns of Bacterial, Archaeal and Eukaryotic Microorganisms in Rumen Microbial Communities. *PLoS One* **2013**,

doi:10.1371/journal.pone.0047879.

207. Calkins, S.; Elledge, N.C.; Hanafy, R.A.; Elshahed, M.S.; Youssef, N. A fast and reliable procedure for spore collection from anaerobic fungi: Application for RNA uptake and long-term storage of isolates. *J. Microbiol. Methods* **2016**, *127*, 206–213, doi:https://doi.org/10.1016/j.mimet.2016.05.019.

208. Hungate, R.E. Chapter IV A Roll Tube Method for Cultivation of Strict Anaerobes. In; Norris, J.R., Ribbons, D.W., Eds.; Methods in Microbiology; Academic Press, 1969; Vol. 3, pp. 117–132.

209. Lowe, S.E.; Theodorou, M.K.; Trinci, A.P.J.; HespelL, R.B. Growth of Anaerobic Rumen Fungi on Defined and Semi-defined Media Lacking Rumen Fluid. *Microbiology* **1985**, *131*, 2225–2229, doi:10.1099/00221287-131-9-2225.

210. Marvin-Sikkema, F.D.; Richardson, A.J.; Stewart, C.S.; Gottschal, J.C.; Prins, R.A. Influence of hydrogen-consuming bacteria on cellulose degradation by anaerobic fungi. *Appl. Environ. Microbiol.* **1990**, *56*, 3793–3797, doi:10.1128/aem.56.12.3793-3797.1990.

211. Kumar, S.; Stecher, G.; Tamura, K. MEGA7: Molecular Evolutionary Genetics Analysis Version 7.0 for Bigger Datasets. *Mol. Biol. Evol.* **2016**, *33*, 1870–1874, doi:10.1093/molbev/msw054.

212. Katoh, K.; Rozewicki, J.; Yamada, K.D. MAFFT online service: Multiple sequence alignment, interactive sequence choice and visualization. *Brief. Bioinform.* **2019**, *20*, 1160–1166, doi:10.1093/bib/bbx108.

213. Hall, T.A. BIOEDIT: a user-friendly biological sequence alignment editor and analysis program for Windows 95/98/ NT. *Nucleic Acids Symp. Ser.* **1999**.

214. Minh, B.Q.; Schmidt, H.A.; Chernomor, O.; Schrempf, D.; Woodhams, M.D.; von Haeseler, A.; Lanfear, R. IQ-TREE 2: New Models and Efficient Methods for Phylogenetic Inference in the Genomic Era. *Mol. Biol. Evol.* **2020**, *37*, 1530–1534, doi:10.1093/molbev/msaa015.

215. Kalyaanamoorthy, S.; Minh, B.Q.; Wong, T.K.F.; von Haeseler, A.; Jermiin, L.S. ModelFinder: fast model selection for accurate phylogenetic estimates. *Nat. Methods* **2017**, *14*, 587–589, doi:10.1038/nmeth.4285.

216. Hoang, D.T.; Chernomor, O.; von Haeseler, A.; Minh, B.Q.; Vinh, L.S. UFBoot2: Improving the Ultrafast Bootstrap Approximation. *Mol. Biol. Evol.* **2017**, *35*, 518–522, doi:10.1093/molbev/msx281.

217. Nicholson, M.J.; McSweeney, C.S.; Mackie, R.I.; Brookman, J.L.; Theodorou, M.K. Diversity of anaerobic gut fungal populations analysed using ribosomal ITS1 sequences in faeces of wild and domesticated herbivores. *Anaerobe* **2010**, *16*, 66–73, doi:https://doi.org/10.1016/j.anaerobe.2009.05.003.

218. Paul, S.S.; Bu, D.; Xu, J.; Hyde, K.D.; Yu, Z. A phylogenetic census of global diversity of gut anaerobic fungi and a new taxonomic framework. *Fungal Divers.* **2018**, doi:10.1007/s13225-018-0396-6.

219. Lowe, S.E.; Griffith, G.G.; Milne, A.; Theodorou, M.K.; Trinci, A.P.J. The Life Cycle and Growth Kinetics of an Anaerobic Rumen Fungus. *Microbiology* **1987**, *133*, 1815–1827, doi:https://doi.org/10.1099/00221287-133-7-1815.

220. Ahrendt, S.R.; Quandt, C.A.; Ciobanu, D.; Clum, A.; Salamov, A.; Andreopoulos, B.; Cheng, J.-F.; Woyke, T.; Pelin, A.; Henrissat, B.; et al. Leveraging single-cell genomics to expand the fungal tree of life. *Nat. Microbiol.* **2018**, *3*, 1417–1428, doi:10.1038/s41564-018-0261-0.

221. Davis, W.J.; Amses, K.R.; James, E.S.; James, T.Y. A new 18S rRNA phylogeny of uncultured predacious fungi (Zoopagales). *Mycologia* **2019**, *111*, 291–298, doi:10.1080/00275514.2018.1546066.

222. James, T.Y.; Stajich, J.E.; Hittinger, C.T.; Rokas, A. Toward a Fully Resolved Fungal Tree of Life. *Annu. Rev. Microbiol.* **2020**, *74*, 291–313, doi:10.1146/annurev-micro-022020-051835.

223. Chen, H.; Liu, J.; Chang, X.; Chen, D.; Xue, Y.; Liu, P.; Lin, H.; Han, S. A review on the pretreatment of lignocellulose for high-value chemicals. *Fuel Process. Technol.* **2017**, *160*, 196–206, doi:https://doi.org/10.1016/j.fuproc.2016.12.007.

224. Behera, S.; Arora, R.; Nandhagopal, N.; Kumar, S. Importance of chemical pretreatment for bioconversion of lignocellulosic biomass. *Renew. Sustain. Energy Rev.* **2014**, *36*, 91–106, doi:https://doi.org/10.1016/j.rser.2014.04.047.

225. Liggenstoffer, A.S.; Youssef, N.H.; Wilkins, M.R.; Elshahed, M.S. Evaluating the utility of hydrothermolysis pretreatment approaches in enhancing lignocellulosic biomass degradation by the anaerobic fungus Orpinomyces sp. strain C1A. *J. Microbiol. Methods* **2014**, *104*, 43–48, doi:https://doi.org/10.1016/j.mimet.2014.06.010.

226. Ho, Y.W.; Abdullah, N.; Jalaludin, S. Penetrating Structures of Anaerobic Rumen Fungi in Cattle and Swamp Buffalo. *Microbiology* **1988**, *134*, 177–181, doi:10.1099/00221287-134-1-177.

227. Wilson, C.A.; Wood, T.M. Studies on the cellulase of the rumen anaerobic fungus Neocallimastix frontalis, with special reference to the capacity of the enzyme to degrade crystalline cellulose. *Enzyme Microb. Technol.* **1992**, doi:10.1016/0141-0229(92)90148-H.

228. Wang, H.-C.; Chen, Y.-C.; Hseu, R.-S. Purification and characterization of a cellulolytic multienzyme complex produced by Neocallimastix patriciarum J11. *Biochem. Biophys. Res. Commun.* **2014**, *451*, 190–195, doi:10.1016/j.bbrc.2014.07.088.

229. Kameshwar, A.K.S.; Qin, W. Genome Wide Analysis Reveals the Extrinsic Cellulolytic and Biohydrogen Generating Abilities of Neocallimastigomycota Fungi. *J. Genomics* **2018**, *6*, 74–87, doi:10.7150/jgen.25648.

230. Ghangas, G.S.; Hu, Y.J.; Wilson, D.B. Cloning of a Thermomonospora fusca xylanase gene and its expression in Escherichia coli and Streptomyces lividans. *J. Bacteriol.* **1989**, doi:10.1128/jb.171.6.2963-2969.1989.

231. Kuiper-Goodman, T.; Scott, P.M. Risk assessment of the mycotoxin ochratoxin A. In *Biomedical and environmental sciences : BES*; 1989; Vol. 2, pp. 179–248.

232. O'Donnell, K.; Reynolds, D.R.; Taylor, J.W. Fusarium and its Near Relatives. In *The fungal holomorph: mitotic, meiotic and pleomorphic speciation in fungal systematics*; CAB International; Wallingford, 1993; pp. 225–236 ISBN 0851988652.

233. Brown, J.L.; Swift, C.L.; Mondo, S.; Seppala, S.; Salamov, A.; Singan, V.; Henrissat, B.; Henske, J.K.; Lee, S.; He, G.; et al. Co-cultivation of the anaerobic fungus Caecomyces churrovis with Methanobacterium bryantii enhances transcription of carbohydrate binding modules. *bioRxiv* **2021**, 2021.07.09.451685, doi:10.1101/2021.07.09.451685.

234. Subramanian, B.; Gao, S.; Lercher, M.J.; Hu, S.; Chen, W.H. Evolview v3: A webserver for visualization, annotation, and management of phylogenetic trees. *Nucleic Acids Res.* **2019**, *47*, W270–W275, doi:10.1093/nar/gkz357.

235. Szenk, M.; Dill, K.A.; de Graff, A.M.R. Why Do Fast-Growing Bacteria Enter Overflow Metabolism? Testing the Membrane Real Estate Hypothesis. *Cell Syst.* **2017**, *5*, 95–104, doi:https://doi.org/10.1016/j.cels.2017.06.005.

236. Teusink, B.; Wiersma, A.; Molenaar, D.; Francke, C.; de Vos, W.M.; Siezen, R.J.; Smid, E.J. Analysis of Growth of Lactobacillus plantarum WCFS1 on a Complex Medium Using a Genome-scale Metabolic Model*. *J. Biol. Chem.* **2006**, *281*, 40041–40048, doi:https://doi.org/10.1074/jbc.M606263200.

237. Sonenshein, A.L. Control of key metabolic intersections in Bacillus subtilis. *Nat. Rev. Microbiol.* **2007**, *5*, 917–927, doi:10.1038/nrmicro1772.

238. de Alteriis, E.; Cartenì, F.; Parascandola, P.; Serpa, J.; Mazzoleni, S. Revisiting the Crabtree/Warburg effect in a dynamic perspective: a fitness advantage against sugar-induced cell death. *Cell Cycle* **2018**, *17*, 688–701, doi:10.1080/15384101.2018.1442622.

239. Singla, M.K.; Nijhawan, P.; Oberoi, A.S. Hydrogen fuel and fuel cell technology for cleaner future: a review. *Environ. Sci. Pollut. Res.* **2021**, *28*, 15607–15626, doi:10.1007/s11356-020-12231-8.

240. van der Giezen, M.; Sjollema, K.A.; Artz, R.R.E.; Alkema, W.; Prins, R.A. Hydrogenosomes in the anaerobic fungus Neocallimastix frontalis have a double membrane but lack an associated organelle genome. *FEBS Lett.* **1997**, *408*, 147–150, doi:10.1016/S0014-5793(97)00409-2.

241. Hackstein, J.H.P.; Baker, S.E.; van Hellemond, J.J.; Tielens, A.G.M. Hydrogenosomes of Anaerobic Fungi: An Alternative Way to Adapt to Anaerobic Environments. In *Hydrogenosomes and Mitosomes: Mitochondria of Anaerobic Eukaryotes*; Tachezy, J., Ed.; Springer International Publishing: Cham, 2019; pp. 159–175 ISBN 978-3-030-17941-0.

242. Theodorou, M.K.; Davies, D.R.; Nielsen, B.B.; Lawrence, M.I.G.; Trinci, A.P.J. Determination of growth of anaerobic fungi on soluble and cellulosic substrates using a pressure transducer. *Microbiology* **1995**, *141*, 671–678, doi:10.1099/13500872-141-3-671.

243. Marvin-Sikkema, F.D.; Lahpor, G.A.; Kraak, M.N.; Gottschal, J.C.; Prins, R.A. Characterization of an anaerobic fungus from llama faeces. *J. Gen. Microbiol.* **1992**, *138*, 2235–2241, doi:10.1099/00221287-138-10-2235.

244. Orpin, C.G.; Greenwood, Y. Nutritional and germination requirements of the rumen chytridiomycete Neocallimastix patriciarum. *Trans. Br. Mycol. Soc.* **1986**, *86*, 103–109, doi:10.1016/S0007-1536(86)80121-8.

245. Soares, J.F.; Confortin, T.C.; Todero, I.; Mayer, F.D.; Mazutti, M.A. Dark fermentative biohydrogen production from lignocellulosic biomass: Technological challenges and future prospects. *Renew. Sustain. Energy Rev.* **2020**, *117*, 109484, doi:https://doi.org/10.1016/j.rser.2019.109484.

246. Lamed, R.J.; Lobos, J.H.; Su, T.M. Effects of Stirring and Hydrogen on Fermentation Products of *Clostridium thermocellum*. *Appl. Environ. Microbiol.* **1988**, *54*, 1216–1221, doi:10.1128/aem.54.5.1216-1221.1988.

247. Rajhi, H.; Puyol, D.; Martínez, M.C.; Díaz, E.E.; Sanz, J.L. Vacuum promotes metabolic shifts and increases biogenic hydrogen production in dark fermentation systems. *Front. Environ. Sci. Eng.* **2016**, *10*, 513–521, doi:10.1007/s11783-015-0777-y.

248. Pawar, S.S.; Nkemka, V.N.; Zeidan, A.A.; Murto, M.; van Niel, E.W.J. Biohydrogen production from wheat straw hydrolysate using Caldicellulosiruptor saccharolyticus followed by biogas production in a two-step uncoupled process. *Int. J. Hydrogen Energy* **2013**, *38*, 9121–9130, doi:https://doi.org/10.1016/j.ijhydene.2013.05.075.

249. Zhang, J.; Kong, C.; Yang, M.; Zang, L. Comparison of Calcium Oxide and Calcium Peroxide Pretreatments of Wheat Straw for Improving Biohydrogen Production. *ACS Omega* **2020**, *5*, 9151–9161, doi:10.1021/acsomega.9b04368.

250. Lopez-Hidalgo, A.M.; Sánchez, A.; De León-Rodríguez, A. Simultaneous production of bioethanol and biohydrogen by Escherichia coli WDHL using wheat straw hydrolysate as substrate. *Fuel* **2017**, *188*, 19–27, doi:https://doi.org/10.1016/j.fuel.2016.10.022.

251. Nasirian, N.; Almassi, M.; Minaei, S.; Widmann, R. Development of a method for biohydrogen production from wheat straw by dark fermentation. *Int. J. Hydrogen Energy* **2011**, *36*, 411–420, doi:https://doi.org/10.1016/j.ijhydene.2010.09.073.

252. Zhu, W.-Y.; Theodorou, M.K.; Longland, A.C.; Nielsen, B.B.; Dijkstra, J.; Trinci, A.P.J. Growth and Survival of Anaerobic Fungi in Batch and Continuous-Flow Cultures: ECOLOGY. *Anaerobe* **1996**, *2*, 29–37, doi:https://doi.org/10.1006/anae.1996.0004.

253. Joblin, K.N.; Naylor, G.E. Inhibition of the rumen anaerobic fungus Neocallimastix frontalis by fermentation products. *Lett. Appl. Microbiol.* **1993**, *16*, 254–256, doi:https://doi.org/10.1111/j.1472-765X.1993.tb01412.x.

254. Liu, H.; Grot, S.; Logan, B.E. Electrochemically Assisted Microbial Production of Hydrogen from Acetate. *Environ. Sci. Technol.* **2005**, *39*, 4317–4320, doi:10.1021/es050244p.

255. Kim, S.; Seol, E.; Oh, Y.-K.; Wang, G.Y.; Park, S. Hydrogen production and metabolic flux analysis of metabolically engineered Escherichia coli strains. *Int. J. Hydrogen Energy* **2009**, *34*, 7417–7427, doi:https://doi.org/10.1016/j.ijhydene.2009.05.053.

256. Bundeministerium für Bildung und Forschung *Nationale Forschungsstrategie BioÖkonomie 2030 Unser Weg zu einer bio-basierten Wirtschaft*; 2010;

257. Horlamus, F.; Wittgens, A.; Noll, P.; Michler, J.; Müller, I.; Weggenmann, F.; Oellig, C.; Rosenau, F.; Henkel, M.; Hausmann, R. One-step bioconversion of hemicellulose polymers to rhamnolipids with Cellvibrio japonicus: A proof-of-concept for a potential host strain in future bioeconomy. *GCB Bioenergy* **2019**, *11*, 260–268, doi:https://doi.org/10.1111/gcbb.12542.

258. Biely, P.; Singh, S.; Puchart, V. Towards enzymatic breakdown of complex plant xylan structures: State of the art. *Biotechnol. Adv.* 2016, *34*, 1260–1274.

259. Pollet, A.; Delcour, J.A.; Courtin, C.M. Structural determinants of the substrate specificities of xylanases from different glycoside hydrolase families. *Crit. Rev. Biotechnol.* **2010**, *30*, 176–191, doi:10.3109/07388551003645599.

260. Polizeli, M.L.T.M.; Rizzatti, A.C.S.; Monti, R.; Terenzi, H.F.; Jorge, J.A.; Amorim, D.S. Xylanases from fungi: properties and industrial applications. *Appl. Microbiol. Biotechnol.* **2005**, *67*, 577–591, doi:10.1007/s00253-005-1904-7.

261. Haitjema, C.H.; Solomon, K. V.; Henske, J.K.; Theodorou, M.K.; O'Malley, M.A. Anaerobic gut fungi: Advances in isolation, culture, and cellulolytic enzyme discovery for biofuel production. *Biotechnol. Bioeng.* **2014**, *111*, 1471–1482, doi:10.1002/bit.25264.

262. Cheng, Y.; Shi, Q.; Sun, R.; Liang, D.; Li, Y.; Li, Y.; Jin, W.; Zhu, W. The biotechnological potential of anaerobic fungi on fiber degradation and methane production. *World J. Microbiol. Biotechnol.* 2018.

263. Podolsky, I.A.; Seppälä, S.; Lankiewicz, T.S.; Brown, J.L.; Swift, C.L.; O'Malley, M.A. Harnessing Nature's Anaerobes for Biotechnology and Bioprocessing. *Annu. Rev. Chem. Biomol. Eng.* **2019**, doi:10.1146/annurev-chembioeng-060718-030340.

264. Jordan, D.B.; Braker, J.D.; Wagschal, K.; Stoller, J.R.; Lee, C.C. Isolation and divalent-metal activation of a β-xylosidase, RUM630-BX. *Enzyme Microb. Technol.* **2016**, *82*, 158–163, doi:10.1016/j.enzmictec.2015.10.001.

265. Jordan, D.B.; Wagschal, K.; Grigorescu, A.A.; Braker, J.D. Highly active β-xylosidases of glycoside hydrolase family 43 operating on natural and artificial substrates. *Appl. Microbiol. Biotechnol.* **2013**, *97*, 4415–4428, doi:10.1007/s00253-012-4475-4.

266. Falck, P.; Linares-Pastén, J.A.; Adlercreutz, P.; Karlsson, E.N. Characterization of a family 43 β-xylosidase from the xylooligosaccharide utilizing putative probiotic *Weissella* sp. strain 92. *Glycobiology* **2016**, *26*, 193–202, doi:10.1093/glycob/cwv092.

267. Mewis, K.; Lenfant, N.; Lombard, V.; Henrissat, B. Dividing the large glycoside hydrolase family 43 into subfamilies: A motivation for detailed enzyme characterization. *Appl. Environ. Microbiol.* **2016**, *82*, 1686–1692, doi:10.1128/AEM.03453-15.

268. Huy, N.D.; Thayumanavan, P.; Kwon, T.H.; Park, S.M. Characterization of a recombinant bifunctional xylosidase/arabinofuranosidase from Phanerochaete chrysosporium. *J. Biosci. Bioeng.* **2013**, *116*, 152–159, doi:10.1016/j.jbiosc.2013.02.004.

269. Yang, X.; Shi, P.; Huang, H.; Luo, H.; Wang, Y.; Zhang, W.; Yao, B. Two xylose-tolerant GH43 bifunctional β-xylosidase/α- arabinosidases and one GH11 xylanase from Humicola insolens and their synergy in the degradation of xylan. *Food Chem.* **2014**, *148*, 381–387, doi:10.1016/j.foodchem.2013.10.062.

270. Zhang, R.; Li, N.; Liu, Y.; Han, X.; Tu, T.; Shen, J.; Xu, S.; Wu, Q.; Zhou, J.; Huang, Z. Biochemical and structural properties of a low-temperature-active glycoside hydrolase family 43 β-xylosidase: Activity and instability at high neutral salt concentrations. *Food Chem.* **2019**, *301*, 125266, doi:10.1016/j.foodchem.2019.125266.

271. Marchler-Bauer, A.; Bo, Y.; Han, L.; He, J.; Lanczycki, C.J.; Lu, S.; Chitsaz, F.; Derbyshire, M.K.; Geer, R.C.; Gonzales, N.R.; et al. CDD/SPARCLE: Functional classification of proteins via subfamily domain architectures. *Nucleic Acids Res.* **2017**, doi:10.1093/nar/gkw1129.

272. Kelley, L.A.; Mezulis, S.; Yates, C.M.; Wass, M.N.; Sternberg, M.J.E. The Phyre2 web portal for protein modeling, prediction and analysis. *Nat. Protoc.* **2015**, *10*, 845–858, doi:10.1038/nprot.2015.053.

273. Yin, Y.; Mao, X.; Yang, J.; Chen, X.; Mao, F.; Xu, Y. DbCAN: A web resource for automated carbohydrate-active enzyme annotation. *Nucleic Acids Res.* **2012**, *40*, W445–W451, doi:10.1093/nar/gks479.

274. Zhang, H.; Yohe, T.; Huang, L.; Entwistle, S.; Wu, P.; Yang, Z.; Busk, P.K.; Xu, Y.; Yin, Y. DbCAN2: A meta server for automated carbohydrate-active enzyme annotation. *Nucleic Acids Res.* **2018**, *46*, W95–W101, doi:10.1093/nar/gky418.

275. Notredame, C.; Higgins, D.G.; Heringa, J. T-coffee: A novel method for fast and accurate multiple sequence alignment. *J. Mol. Biol.* **2000**, *302*, 205–217, doi:10.1006/jmbi.2000.4042.

276. Tria, F.D.K.; Landan, G.; Dagan, T. Phylogenetic rooting using minimal ancestor deviation. *Nat. Ecol. Evol.* **2017**, *1*, 193, doi:10.1038/s41559-017-0193.

277. McCleary, B. V.; McGeough, P. A Comparison of Polysaccharide Substrates and Reducing Sugar Methods for the Measurement of endo-1,4-β-Xylanase. *Appl. Biochem. Biotechnol.* **2015**, *177*, 1152–1163, doi:10.1007/s12010-015-1803-z.

278. Whitehead, T.R. Nucleotide sequences of xylan-inducible xylanase and xylosidase/arabinosidase genes from Bacteroides ovatus V975. *BBA - Gen. Subj.* **1995**, *1244*, 239–241, doi:10.1016/0304-4165(95)00051-C.

279. Jordan, D.B.; Stoller, J.R.; Lee, C.C.; Chan, V.J.; Wagschal, K. Biochemical Characterization of a GH43 β-Xylosidase from Bacteroides ovatus. *Appl. Biochem. Biotechnol.* **2017**, *182*, 250–260, doi:10.1007/s12010-016-2324-0.

280. Matsuzawa, T.; Kaneko, S.; Yaoi, K. Screening, identification, and characterization of a GH43 family β-xylosidase/α-arabinofuranosidase from a compost microbial metagenome. *Appl. Microbiol. Biotechnol.* **2015**, *99*, 8943–8954, doi:10.1007/s00253-015-6647-5.

281. Lee, C.C.; Braker, J.D.; Grigorescu, A.A.; Wagschal, K.; Jordan, D.B. Divalent metal activation of a GH43 β-xylosidase. *Enzyme Microb. Technol.* **2013**, *52*, 84–90, doi:10.1016/j.enzmictec.2012.10.010.

282. Matsuzawa, T.; Kaneko, S.; Kishine, N.; Fujimoto, Z.; Yaoi, K. Crystal structure of metagenomic β-xylosidase/ α-l-arabinofuranosidase activated by calcium. *J. Biochem.* **2017**, *162*, 173–181, doi:10.1093/jb/mvx012.

283. Theodorou, M.K.; Brookman, J.; Trinci, A.P.J. Anaerobic fungi. In *Methods in Gut Microbial*

Ecology for Ruminants; Makkar, H.P.S., McSweeney, C.S., Eds.; Springer Netherlands: Dordrecht, 2005; pp. 55–66 ISBN 978-1-4020-3791-7.

284. Bonzom, C.; Hüttner, S.; Mirgorodskaya, E.; Chong, S.L.; Uthoff, S.; Steinbüchel, A.; Verhaert, R.M.D.; Olsson, L. Glycosylation influences activity, stability and immobilization of the feruloyl esterase 1a from Myceliophthora thermophila. *AMB Express* **2019**, *9*, 126, doi:10.1186/s13568-019-0852-z.

285. Hebraud, M.; Fevre, M. Purification and characterization of an extracellular β-xylosidase from the rumen anaerobic fungus Neocallimastix frontalis. *FEMS Microbiol. Lett.* **1990**, *72*, 11–16, doi:10.1016/0378-1097(90)90336-O.

286. Garcia-Campayo, V.; Wood, T.M. Purification and characterisation of a β-d-xylosidase from the anaerobic rumen fungus Neocallimastix frontalis. *Carbohydr. Res.* **1993**, *242*, 229–245, doi:10.1016/0008-6215(93)80037-F.

287. Jordan, D.B.; Wagschal, K. Properties and applications of microbial β-D-xylosidases featuring the catalytically efficient enzyme from Selenomonas ruminantium. *Appl. Microbiol. Biotechnol.* **2010**, *86*, 1647–1658, doi:10.1007/s00253-010-2538-y.

288. Jordan, D.B.; Stoller, J.R.; Kibblewhite, R.E.; Chan, V.J.; Lee, C.C.; Wagschal, K. Absence or presence of metal ion activation in two structurally similar GH43 β-xylosidases. *Enzyme Microb. Technol.* **2018**, *114*, 29–32, doi:10.1016/j.enzmictec.2018.03.007.

289. Jordan, D.B.; Braker, J.D.; Wagschal, K.; Lee, C.C.; Chan, V.J.; Dubrovska, I.; Anderson, S.; Wawrzak, Z. X-ray Crystal Structure of Divalent Metal-Activated β-xylosidase, RS223BX. *Appl. Biochem. Biotechnol.* **2015**, *177*, 637–648, doi:10.1007/s12010-015-1767-z.

290. Lange, L.; Pilgaard, B.; Herbst, F.A.; Busk, P.K.; Gleason, F.; Pedersen, A.G. Origin of fungal biomass degrading enzymes: Evolution, diversity and function of enzymes of early lineage fungi. *Fungal Biol. Rev.* 2019, *33*, 82–97.

List of Figures

List of Tables

Abbreviations

Acetyl-CoA	acetyl coenzyme A
ADHE	alcohol dehydrogenase E
AF	Anaerobic fungi
ATP	Adenosine triphosphate
CAZyme	carbohydrate active enzymes
CBM	carbohydrate binding modules
C-source	carbon source
DAPI	6 diamidino-2-phenylindole
DNS	3,5-dinitrosalicylic acid
EDTA	Ethylenediaminetetraacetic acid
FHL	formate hydrogen lyase
GC	Gas chromatography
GH	Glycoside hydrolase
HPLC	high-performance liquid chromatography
ITS1	internal transcribed spacer region 1
LSU	large ribosomal subunit (D1/D2-domain)
NAD(P)H	Nicotinamide adenine dinucleotide (phosphate)
NFOR	NADH:ferredoxin oxidoreductase
N-source	nitrogen source
PFL	pyruvate formate lyase
PFO	pyruvate:ferredoxin oxidoreductase
TLC	thin layer chromatography

Appendix

Supplementarys Chapter 4

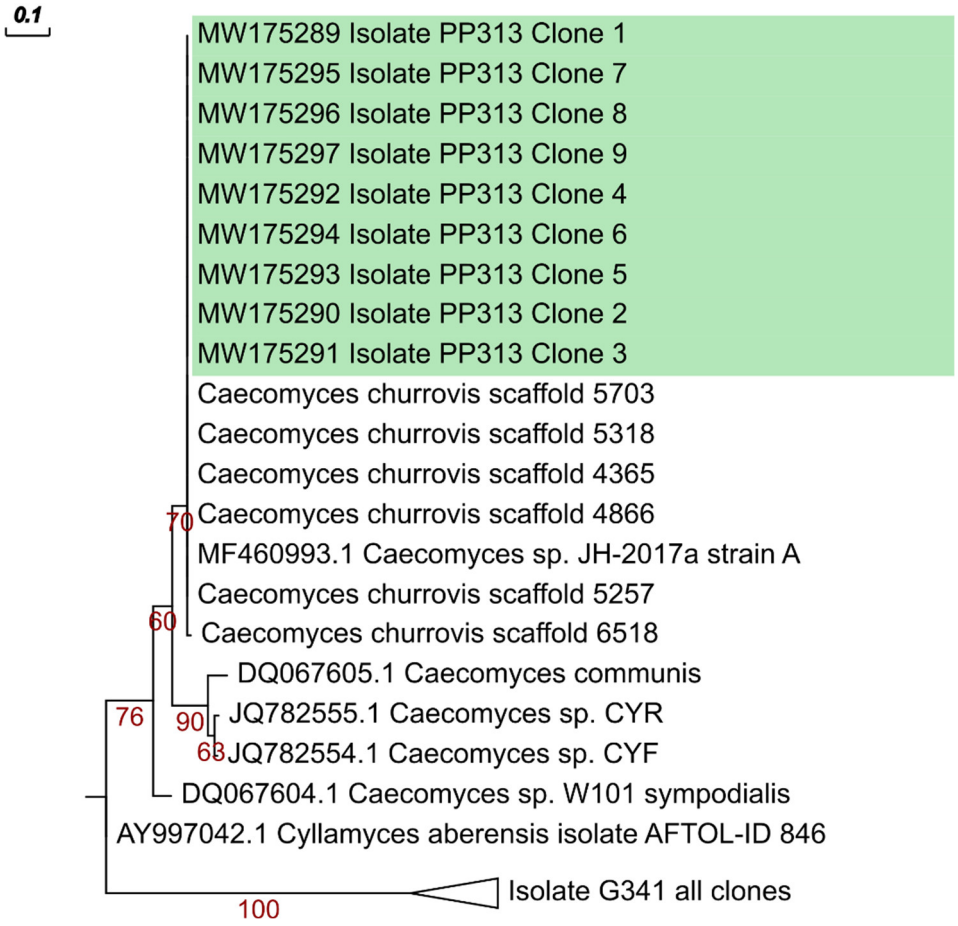

Figure 24: Phylogenetic affiliation of the Isolate PP313 to other *Caecomyces* and *Cyllamyces* based on the nucleotide sequences of the ITS1 from the ribosomal operon. Isolate G341 was used as an outgroup. MAFFT [212] was used for alignment and BioEdit [213] was used for manual curation of the sequences. The ML-tree was constructed through IQTREE [214] with the predicted model HKY+F+G4 and –bb 1000.

Table 13: Residual galactose during growth of different strains on Lactose in g/l and mmol.

	g/l					mmol				
Strain	**1**	**2**	**3**	**Ø**	**SD**	**1**	**2**	**3**	**Ø**	**SD**
G341	0.790	1.017	0.961	0.923	0.096	0.241	0.310	0.293	0.282	0.029
PP313	1.823	2.070	1.982	1.958	0.102	0.556	0.632	0.605	0.598	0.031
W212	1.982	2.008	2.067	2.019	0.035	0.605	0.613	0.631	0.616	0.011
SA222	1.928	1.981	1.868	1.926	0.046	0.589	0.605	0.570	0.588	0.014
X2152	1.501	1.501	0.999	1.334	0.237	0.458	0.458	0.305	0.407	0.072
A252	0.175	0.125	0.118	0.139	0.025	0.053	0.038	0.036	0.043	0.008

Table 14: Produced metabolites from G341 while growing on different c-sources including standard deviation (SD) and excluding ethanol.

	Formate Δ [mmol]	Acetate Δ [mmol]	Lactate Δ [mmol]	Succinate Δ [mmol]	Citrate Δ [mmol]	H2 Δ [mmol]
Cellobiose Ø	1.510	1.251	0.792	0.105	0.000	0.358
Cellobiose SD	0.082	0.067	0.041	0.003	0.000	0.047
Cellulose Ø	1.437	1.073	0.914	0.114	0.000	0.313
Cellulose SD	0.026	0.015	0.038	0.002	0.000	0.030
Fructose Ø	1.503	1.225	0.757	0.133	0.000	0.232
Fructose SD	0.103	0.114	0.071	0.008	0.000	0.007
Glucose Ø	1.398	1.174	0.725	0.126	0.000	0.312
Glucose SD	0.054	0.041	0.037	0.008	0.000	0.023
Inulin Ø	1.138	1.050	0.572	0.112	0.000	0.282
Inulin SD	0.127	0.167	0.102	0.009	0.000	0.032
Lactose Ø	0.607	0.415	0.058	0.000	0.000	0.220
Lactose SD	0.044	0.042	0.009	0.000	0.000	0.010
Maltose Ø	1.356	1.217	0.766	0.125	0.000	0.366
Maltose SD	0.043	0.034	0.064	0.001	0.000	0.007
Mannose Ø	1.309	0.991	0.498	0.108	0.000	0.360
Mannose SD	0.110	0.109	0.095	0.003	0.000	0.036
Pectin Ø	0.138	0.000	0.000	0.000	0.000	0.025
Pectin SD	0.004	0.000	0.000	0.000	0.000	0.005
Starch Ø	1.388	1.161	0.610	0.112	0.000	0.307
Starch SD	0.168	0.112	0.108	0.019	0.000	0.004
Stroh Ø	1.017	0.770	0.140	0.000	0.011	0.352
Stroh SD	0.032	0.053	0.038	0.000	0.000	0.011
Sucrose Ø	1.475	1.327	0.852	0.136	0.000	0.335
Sucrose SD	0.026	0.077	0.067	0.003	0.000	0.033
Trehalose Ø	0.000	0.000	0.000	0.000	0.000	0.008
Trehalose SD	0.000	0.000	0.000	0.000	0.000	0.003
Xylan Ø	1.144	0.848	0.264	0.096	0.064	0.211
Xylan SD	0.017	0.010	0.010	0.003	0.000	0.012
Xylose Ø	1.449	1.368	0.713	0.117	0.000	0.278
Xylose SD	0.063	0.180	0.016	0.003	0.000	0.016

Table 15: Relative produced metabolites from G341 while growing on different c-sources including standard deviation (SD) and excluding ethanol.

	Formate/ total [%]	Acetate/ total [%]	Lactate/ total [%]	Succinate/ total [%]	Citrate/ total [%]	H2/ total [%]
Cellobiose Ø	37.641	31.138	19.710	2.603	0.000	8.908
Cellobiose SD	2.678	1.124	0.642	0.046	0.000	1.062
Cellulose Ø	37.334	27.882	23.718	2.952	0.000	8.115
Cellulose SD	1.148	0.269	0.576	0.046	0.000	0.654
Fructose Ø	39.098	31.754	19.654	3.445	0.000	6.050
Fructose SD	2.952	1.885	1.502	0.196	0.000	0.379
Glucose Ø	37.411	31.432	19.411	3.380	0.000	8.366
Glucose SD	1.277	1.261	0.914	0.208	0.000	0.656
Inulin Ø	36.255	33.187	18.014	3.583	0.000	8.962
Inulin SD	1.134	0.785	0.814	0.307	0.000	0.230
Lactose Ø	46.703	31.874	4.444	0.000	0.000	16.979
Lactose SD	0.487	0.806	0.363	0.000	0.000	0.672
Maltose Ø	35.424	31.794	19.971	3.256	0.000	9.554
Maltose SD	0.598	0.270	1.051	0.123	0.000	0.361
Mannose Ø	40.201	30.348	15.094	3.328	0.000	11.029
Mannose SD	1.046	0.156	1.395	0.318	0.000	0.236
Pectin Ø	84.606	0.000	0.000	0.000	0.000	15.394
Pectin SD	2.213	0.000	0.000	0.000	0.000	2.213
Starch Ø	38.758	32.533	16.906	3.108	0.000	8.695
Starch SD	0.934	1.180	1.263	0.231	0.000	1.026
Stroh Ø	44.424	33.636	6.098	0.000	0.472	15.370
Stroh SD	1.078	2.408	1.629	0.000	0.005	0.634
Sucrose Ø	35.763	32.155	20.653	3.300	0.000	8.130
Sucrose SD	0.902	1.588	1.564	0.098	0.000	0.782
Trehalose Ø	0.000	0.000	0.000	0.000	0.000	100.000
Trehalose SD	0.000	0.000	0.000	0.000	0.000	0.000
Xylan Ø	43.546	32.290	10.063	3.638	2.425	8.038
Xylan SD	0.446	0.309	0.332	0.140	0.009	0.480
Xylose Ø	36.993	34.695	18.224	2.996	0.000	7.092
Xylose SD	1.036	2.291	0.942	0.242	0.000	0.095

Table 16: Produced metabolites from PP313 while growing on different c-sources including standard deviation (SD) and excluding ethanol.

	Formate Δ [mmol]	Acetate Δ [mmol]	Lactate Δ [mmol]	Succinate Δ [mmol]	Citrate Δ [mmol]	H2 Δ [mmol]
Cellobiose Ø	1.319	1.005	0.676	0.194	0.000	0.547
Cellobiose SD	0.043	0.024	0.074	0.002	0.000	0.026
Cellulose Ø	0.000	0.000	0.071	0.000	0.000	0.022
Cellulose SD	0.000	0.000	0.052	0.000	0.000	0.006
Fructose Ø	1.195	0.892	0.608	0.140	0.000	0.475
Fructose SD	0.119	0.072	0.069	0.011	0.000	0.047
Glucose Ø	1.165	0.647	0.711	0.156	0.000	0.488
Glucose SD	0.086	0.136	0.052	0.017	0.000	0.019
Inulin Ø						
Inulin SD						
Lactose Ø	0.850	0.703	0.143	0.106	0.000	0.344
Lactose SD	0.037	0.062	0.023	0.016	0.000	0.018
Maltose Ø	0.000	0.000	0.053	0.000	0.000	0.027
Maltose SD	0.000	0.000	0.038	0.000	0.000	0.002
Mannose Ø						
Mannose SD						
Pectin Ø	0.000	0.228	0.116	0.000	0.000	0.009
Pectin SD	0.000	0.162	0.007	0.000	0.000	0.003
Starch Ø	0.000	0.107	0.080	0.000	0.000	0.017
Starch SD	0.000	0.151	0.001	0.000	0.000	0.001
Stroh Ø	0.592	0.527	0.115	0.000	0.009	0.322
Stroh SD	0.004	0.007	0.009	0.000	0.006	0.008
Sucrose Ø						
Sucrose SD						
Trehalose Ø						
Trehalose SD						
Xylan Ø	1.098	0.891	0.310	0.160	0.046	0.337
Xylan SD	0.019	0.043	0.019	0.014	0.001	0.012
Xylose Ø	1.093	0.836	0.772	0.130	0.000	0.400
Xylose SD	0.068	0.056	0.157	0.017	0.000	0.008

Table 17: Relative produced metabolites from PP313 while growing on different c-sources including standard deviation (SD) and excluding ethanol.

	Formate/total [%]	Acetate/total [%]	Lactate/total [%]	Succinate/total [%]	Citrate/total [%]	H2/total [%]
Cellobiose Ø	35.251	26.875	18.036	5.177	0.000	14.661
Cellobiose SD	0.144	0.365	1.396	0.122	0.000	1.069
Cellulose Ø	0.000	0.000	56.384	0.000	0.000	43.616
Cellulose SD	0.000	0.000	40.128	0.000	0.000	40.128
Fructose Ø	36.033	26.932	18.402	4.226	0.000	14.406
Fructose SD	0.941	0.486	1.709	0.121	0.000	1.548
Glucose Ø	36.839	20.222	22.509	4.918	0.000	15.511
Glucose SD	0.794	2.503	0.828	0.322	0.000	1.067
Inulin Ø						
Inulin SD						
Lactose Ø	39.633	32.711	6.638	4.974	0.000	16.043
Lactose SD	0.559	1.265	0.795	0.977	0.000	0.102
Maltose Ø	0.000	0.000	49.627	0.000	0.000	50.373
Maltose SD	0.000	0.000	35.097	0.000	0.000	35.097
Mannose Ø						
Mannose SD						
Pectin Ø	0.000	49.338	46.641	0.000	0.000	4.020
Pectin SD	0.000	34.946	31.316	0.000	0.000	3.634
Starch Ø	0.000	25.467	61.337	0.000	0.000	13.197
Starch SD	0.000	36.015	29.593	0.000	0.000	6.580
Stroh Ø	37.809	33.694	7.333	0.000	0.568	20.596
Stroh SD	0.487	0.165	0.475	0.000	0.415	0.551
Sucrose Ø						
Sucrose SD						
Trehalose Ø						
Trehalose SD						
Xylan Ø	38.647	31.334	10.886	5.642	1.625	11.866
Xylan SD	0.322	0.957	0.496	0.498	0.015	0.673
Xylose Ø	33.870	25.886	23.821	4.030	0.000	12.394
Xylose SD	2.648	1.657	4.450	0.594	0.000	0.458

Table 18: Produced metabolites from W212 while growing on different c-sources including standard deviation (SD) and excluding ethanol.

	Formate Δ [mmol]	Acetate Δ [mmol]	Lactate Δ [mmol]	Succinate Δ [mmol]	Citrate Δ [mmol]	H2 Δ [mmol]
Cellobiose Ø	1.890	1.191	0.314	0.000	0.000	0.211
Cellobiose SD	0.081	0.058	0.015	0.000	0.000	0.031
Cellulose Ø	1.729	1.413	0.552	0.000	0.000	0.367
Cellulose SD	0.030	0.018	0.042	0.000	0.000	0.024
Fructose Ø	1.803	1.175	0.437	0.000	0.000	0.194
Fructose SD	0.026	0.022	0.057	0.000	0.000	0.016
Glucose Ø	1.901	1.118	0.214	0.000	0.000	0.114
Glucose SD	0.092	0.076	0.031	0.000	0.000	0.002
Inulin Ø						
Inulin SD						
Lactose Ø	0.952	0.784	0.277	0.000	0.000	0.414
Lactose SD	0.020	0.010	0.032	0.000	0.000	0.008
Maltose Ø	1.947	1.145	0.343	0.000	0.000	0.108
Maltose SD	0.060	0.017	0.020	0.000	0.000	0.009
Mannose Ø						
Mannose SD						
Pectin Ø	0.132	0.113	0.000	0.000	0.000	0.024
Pectin SD	0.008	0.092	0.000	0.000	0.000	0.001
Starch Ø	2.026	1.355	0.401	0.000	0.000	0.151
Starch SD	0.081	0.208	0.020	0.000	0.000	0.018
Stroh Ø	0.871	0.910	0.143	0.000	0.014	0.375
Stroh SD	0.010	0.061	0.007	0.000	0.002	0.012
Sucrose Ø	2.227	1.388	0.234	0.000	0.000	0.129
Sucrose SD	0.026	0.163	0.051	0.000	0.000	0.017
Trehalose Ø						
Trehalose SD						
Xylan Ø	1.293	0.837	0.141	0.000	0.068	0.216
Xylan SD	0.033	0.030	0.002	0.000	0.001	0.012
Xylose Ø	1.581	0.948	0.644	0.000	0.000	0.097
Xylose SD	0.089	0.046	0.067	0.000	0.000	0.020

Table 19: Relative produced metabolites from W212 while growing on different c-sources including standard deviation (SD) and excluding ethanol.

	Formate/total [%]	Acetate/total [%]	Lactate/total [%]	Succinate/total [%]	Citrate/total [%]	H2/total [%]
Cellobiose Ø	52.414	33.027	8.696	0.000	0.000	5.864
Cellobiose SD	0.533	0.223	0.217	0.000	0.000	0.840
Cellulose Ø	42.577	34.796	13.597	0.000	0.000	9.030
Cellulose SD	0.712	0.569	0.975	0.000	0.000	0.620
Fructose Ø	49.978	32.562	12.100	0.000	0.000	5.361
Fructose SD	1.146	0.719	1.465	0.000	0.000	0.376
Glucose Ø	56.810	33.384	6.377	0.000	0.000	3.428
Glucose SD	0.745	0.356	0.659	0.000	0.000	0.195
Inulin Ø						
Inulin SD						
Lactose Ø	39.211	32.302	11.409	0.000	0.000	17.078
Lactose SD	0.404	0.829	1.161	0.000	0.000	0.516
Maltose Ø	54.946	32.334	9.675	0.000	0.000	3.045
Maltose SD	0.493	0.478	0.332	0.000	0.000	0.329
Mannose Ø						
Mannose SD						
Pectin Ø	55.941	34.396	0.000	0.000	0.000	9.663
Pectin SD	22.254	25.256	0.000	0.000	0.000	3.002
Starch Ø	51.652	34.262	10.248	0.000	0.000	3.838
Starch SD	1.993	2.783	0.836	0.000	0.000	0.249
Stroh Ø	37.708	39.304	6.185	0.000	0.595	16.208
Stroh SD	0.812	1.419	0.483	0.000	0.120	0.292
Sucrose Ø	56.142	34.787	5.823	0.000	0.000	3.247
Sucrose SD	2.879	2.041	1.003	0.000	0.000	0.340
Trehalose Ø						
Trehalose SD						
Xylan Ø	50.585	32.748	5.524	0.000	2.679	8.464
Xylan SD	0.686	0.961	0.161	0.000	0.018	0.565
Xylose Ø	48.327	28.997	19.722	0.000	0.000	2.954
Xylose SD	0.939	0.606	1.983	0.000	0.000	0.524

Table 20: Produced metabolites from SA222 while growing on different c-sources including standard deviation (SD) and excluding ethanol.

	Formate Δ [mmol]	Acetate Δ [mmol]	Lactate Δ [mmol]	Succinate Δ [mmol]	Citrate Δ [mmol]	H2 Δ [mmol]
Cellobiose Ø	1.537	0.883	0.820	0.000	0.000	0.279
Cellobiose SD	0.074	0.081	0.078	0.000	0.000	0.025
Cellulose Ø	0.620	0.375	0.000	0.000	0.000	0.186
Cellulose SD	0.027	0.063	0.000	0.000	0.000	0.022
Fructose Ø	1.534	0.914	0.577	0.068	0.000	0.193
Fructose SD	0.002	0.016	0.041	0.048	0.000	0.017
Glucose Ø	1.451	0.858	0.846	0.031	0.000	0.213
Glucose SD	0.072	0.035	0.058	0.044	0.000	0.027
Inulin Ø						
Inulin SD						
Lactose Ø	0.786	0.589	0.465	0.000	0.000	0.328
Lactose SD	0.008	0.014	0.085	0.000	0.000	0.013
Maltose Ø	1.469	0.881	0.722	0.000	0.000	0.208
Maltose SD	0.040	0.023	0.028	0.000	0.000	0.019
Mannose Ø	1.142	0.729	1.230	0.000	0.000	0.238
Mannose SD	0.024	0.024	0.006	0.000	0.000	0.011
Pectin Ø	0.199	0.162	0.000	0.000	0.005	0.027
Pectin SD	0.023	0.008	0.000	0.000	0.005	0.001
Starch Ø	1.510	0.933	0.772	0.032	0.000	0.275
Starch SD	0.302	0.183	0.210	0.045	0.000	0.017
Stroh Ø	0.735	0.609	0.058	0.000	0.003	0.303
Stroh SD	0.002	0.010	0.006	0.000	0.005	0.013
Sucrose Ø	1.463	0.925	1.025	0.062	0.000	0.245
Sucrose SD	0.075	0.051	0.039	0.044	0.000	0.009
Trehalose Ø	0.000	0.000	0.000	0.000	0.000	0.005
Trehalose SD	0.000	0.000	0.000	0.000	0.000	0.000
Xylan Ø	1.153	0.765	0.317	0.038	0.055	0.212
Xylan SD	0.015	0.005	0.071	0.053	0.002	0.007
Xylose Ø	1.367	0.869	0.860	0.000	0.000	0.260
Xylose SD	0.049	0.022	0.106	0.000	0.000	0.015

Table 21: Relative produced metabolites from SA222 while growing on different c-sources including standard deviation (SD) and excluding ethanol.

	Formate/total [%]	Acetate/total [%]	Lactate/total [%]	Succinate/total [%]	Citrate/total [%]	H2/total [%]
Cellobiose Ø	43.707	25.044	23.286	0.000	0.000	7.964
Cellobiose SD	0.606	0.898	1.371	0.000	0.000	0.798
Cellulose Ø	52.734	31.573	0.000	0.000	0.000	15.693
Cellulose SD	2.592	2.248	0.000	0.000	0.000	0.362
Fructose Ø	46.704	27.819	17.557	2.041	0.000	5.879
Fructose SD	1.262	0.523	1.117	1.448	0.000	0.395
Glucose Ø	42.681	25.260	24.890	0.894	0.000	6.275
Glucose SD	1.847	1.019	1.726	1.264	0.000	0.912
Inulin Ø						
Inulin SD						
Lactose Ø	36.272	27.191	21.386	0.000	0.000	15.150
Lactose SD	1.167	1.333	3.425	0.000	0.000	1.001
Maltose Ø	44.801	26.860	22.006	0.000	0.000	6.333
Maltose SD	0.839	0.186	0.566	0.000	0.000	0.477
Mannose Ø	34.192	21.813	36.862	0.000	0.000	7.133
Mannose SD	0.288	0.330	0.583	0.000	0.000	0.200
Pectin Ø	50.517	41.331	0.000	0.000	1.210	6.942
Pectin SD	2.429	2.416	0.000	0.000	1.308	0.442
Starch Ø	42.854	26.495	21.741	0.709	0.000	8.200
Starch SD	1.913	1.135	2.508	1.003	0.000	2.021
Stroh Ø	43.009	35.659	3.396	0.000	0.192	17.744
Stroh SD	0.551	0.175	0.330	0.000	0.271	0.638
Sucrose Ø	39.288	24.845	27.587	1.688	0.000	6.591
Sucrose SD	1.357	0.961	1.567	1.198	0.000	0.141
Trehalose Ø	0.000	0.000	0.000	0.000	0.000	100.000
Trehalose SD	0.000	0.000	0.000	0.000	0.000	0.000
Xylan Ø	45.440	30.167	12.438	1.429	2.154	8.372
Xylan SD	1.297	1.021	2.488	2.021	0.017	0.588
Xylose Ø	40.767	25.908	25.575	0.000	0.000	7.750
Xylose SD	1.723	0.881	2.679	0.000	0.000	0.257

Table 22: Produced metabolites from X2152 while growing on different c-sources including standard deviation (SD) and excluding ethanol.

	Formate Δ [mmol]	Acetate Δ [mmol]	Lactate Δ [mmol]	Succinate Δ [mmol]	Citrate Δ [mmol]	H2 Δ [mmol]
Cellobiose Ø	1.971	1.419	0.000	0.177	0.000	0.416
Cellobiose SD	0.038	0.000	0.000	0.123	0.000	0.033
Cellulose Ø	1.562	1.214	0.000	0.242	0.000	0.392
Cellulose SD	0.128	0.070	0.000	0.045	0.000	0.020
Fructose Ø	1.937	1.409	0.000	0.237	0.000	0.282
Fructose SD	0.211	0.073	0.000	0.101	0.000	0.009
Glucose Ø	1.985	1.381	0.000	0.324	0.000	0.236
Glucose SD	0.021	0.091	0.000	0.015	0.000	0.019
Inulin Ø						
Inulin SD						
Lactose Ø	1.115	0.824	0.000	0.098	0.000	0.366
Lactose SD	0.198	0.149	0.000	0.070	0.000	0.026
Maltose Ø	0.000	0.000	0.000	0.000	0.000	0.035
Maltose SD	0.000	0.000	0.000	0.000	0.000	0.002
Mannose Ø						
Mannose SD						
Pectin Ø	0.086	0.302	0.000	0.000	0.000	0.020
Pectin SD	0.061	0.069	0.000	0.000	0.000	0.002
Starch Ø	0.000	0.000	0.000	0.000	0.000	0.008
Starch SD	0.000	0.000	0.000	0.000	0.000	0.001
Stroh Ø	0.919	0.367	0.000	0.000	0.011	0.411
Stroh SD	0.056	0.046	0.000	0.000	0.000	0.017
Sucrose Ø	0.169	0.000	0.027	0.000	0.000	0.050
Sucrose SD	0.004	0.000	0.038	0.000	0.000	0.001
Trehalose Ø	0.000	0.000	0.000	0.000	0.000	0.006
Trehalose SD	0.000	0.000	0.000	0.000	0.000	0.000
Xylan Ø	1.260	0.969	0.000	0.217	0.027	0.309
Xylan SD	0.100	0.116	0.000	0.012	0.010	0.007
Xylose Ø	1.714	1.257	0.000	0.186	0.000	0.321
Xylose SD	0.090	0.073	0.000	0.020	0.000	0.034

Table 23: Relative produced metabolites from X2152 while growing on different c-sources including standard deviation (SD) and excluding ethanol.

	Formate/total [%]	Acetate/total [%]	Lactate/total [%]	Succinate/total [%]	Citrate/total [%]	H2/total [%]
Cellobiose Ø	49.501	35.633	0.000	4.399	0.000	10.466
Cellobiose SD	1.610	0.463	0.000	3.040	0.000	0.968
Cellulose Ø	45.748	35.649	0.000	7.103	0.000	11.500
Cellulose SD	1.773	2.192	0.000	1.406	0.000	0.459
Fructose Ø	50.048	36.663	0.000	5.926	0.000	7.363
Fructose SD	1.187	2.529	0.000	2.197	0.000	0.726
Glucose Ø	50.602	35.139	0.000	8.250	0.000	6.010
Glucose SD	1.596	1.556	0.000	0.220	0.000	0.506
Inulin Ø						
Inulin SD						
Lactose Ø	46.374	34.249	0.000	3.622	0.000	15.755
Lactose SD	1.290	0.340	0.000	2.583	0.000	3.135
Maltose Ø	0.000	0.000	0.000	0.000	0.000	100.000
Maltose SD	0.000	0.000	0.000	0.000	0.000	0.000
Mannose Ø						
Mannose SD						
Pectin Ø	20.767	74.228	0.000	0.000	0.000	5.005
Pectin SD	15.261	15.541	0.000	0.000	0.000	1.028
Starch Ø	0.000	0.000	0.000	0.000	0.000	100.000
Starch SD	0.000	0.000	0.000	0.000	0.000	0.000
Stroh Ø	53.787	21.401	0.000	0.000	0.643	24.169
Stroh SD	0.226	1.582	0.000	0.000	0.033	1.780
Sucrose Ø	70.336	0.000	8.678	0.000	0.000	20.986
Sucrose SD	9.324	0.000	12.272	0.000	0.000	2.952
Trehalose Ø	0.000	0.000	0.000	0.000	0.000	100.000
Trehalose SD	0.000	0.000	0.000	0.000	0.000	0.000
Xylan Ø	45.309	34.735	0.000	7.820	0.940	11.196
Xylan SD	0.180	1.443	0.000	0.489	0.294	1.237
Xylose Ø	49.297	36.159	0.000	5.347	0.000	9.197
Xylose SD	0.664	0.141	0.000	0.360	0.000	0.483

Table 24: Produced metabolites from A252 while growing on different c-sources including standard deviation (SD) and excluding ethanol.

	Formate Δ [mmol]	Acetate Δ [mmol]	Lactate Δ [mmol]	Succinate Δ [mmol]	Citrate Δ [mmol]	H2 Δ [mmol]
Cellobiose Ø	1.717	1.308	0.590	0.216	0.000	0.603
Cellobiose SD	0.044	0.054	0.057	0.023	0.000	0.044
Cellulose Ø	1.268	1.052	0.321	0.131	0.000	0.466
Cellulose SD	0.078	0.080	0.172	0.024	0.000	0.036
Fructose Ø	1.460	1.199	0.615	0.164	0.000	0.430
Fructose SD	0.082	0.077	0.034	0.023	0.000	0.020
Glucose Ø	1.559	1.211	0.576	0.194	0.000	0.500
Glucose SD	0.077	0.055	0.047	0.007	0.000	0.010
Inulin Ø	0.092	0.165	0.021	0.000	0.000	0.037
Inulin SD	0.130	0.234	0.030	0.000	0.000	0.025
Lactose Ø	1.434	1.307	0.317	0.152	0.000	0.549
Lactose SD	0.020	0.043	0.123	0.009	0.000	0.024
Maltose Ø	1.523	1.436	0.651	0.153	0.000	0.438
Maltose SD	0.025	0.176	0.014	0.007	0.000	0.024
Mannose Ø	1.362	1.157	0.508	0.148	0.000	0.323
Mannose SD	0.042	0.168	0.046	0.011	0.000	0.047
Pectin Ø	0.092	0.214	0.049	0.000	0.069	0.020
Pectin SD	0.066	0.185	0.035	0.000	0.002	0.004
Starch Ø	1.501	1.338	0.535	0.168	0.000	0.491
Starch SD	0.144	0.130	0.071	0.011	0.000	0.065
Stroh Ø	0.902	1.054	0.086	0.084	0.013	0.543
Stroh SD	0.008	0.063	0.016	0.008	0.000	0.012
Sucrose Ø	1.611	1.343	0.666	0.194	0.000	0.494
Sucrose SD	0.048	0.067	0.085	0.000	0.000	0.039
Trehalose Ø	0.000	0.000	0.000	0.000	0.000	0.007
Trehalose SD	0.000	0.000	0.000	0.000	0.000	0.005
Xylan Ø	1.325	0.982	0.298	0.124	0.074	0.398
Xylan SD	0.176	0.154	0.063	0.015	0.015	0.011
Xylose Ø	1.405	1.081	0.549	0.187	0.000	0.442
Xylose SD	0.153	0.136	0.079	0.019	0.000	0.011

Table 25: Relative produced metabolites from A252 while growing on different c-sources including standard deviation (SD) and excluding ethanol.

	Formate/total [%]	Acetate/total [%]	Lactate/total [%]	Succinate/total [%]	Citrate/total [%]	H2/total [%]
Cellobiose Ø	38.717	29.499	13.315	4.871	0.000	13.599
Cellobiose SD	0.424	0.908	1.453	0.582	0.000	0.779
Cellulose Ø	39.318	32.561	9.489	4.008	0.000	14.624
Cellulose SD	1.631	0.791	4.454	0.335	0.000	2.571
Fructose Ø	37.725	30.991	15.899	4.221	0.000	11.164
Fructose SD	0.342	0.899	0.571	0.441	0.000	1.011
Glucose Ø	38.581	29.981	14.239	4.801	0.000	12.397
Glucose SD	0.571	0.871	0.890	0.293	0.000	0.652
Inulin Ø	10.128	18.220	2.330	0.000	0.000	69.322
Inulin SD	14.324	25.767	3.295	0.000	0.000	43.386
Lactose Ø	38.209	34.785	8.324	4.037	0.000	14.646
Lactose SD	1.377	0.455	2.886	0.190	0.000	1.151
Maltose Ø	36.309	34.061	15.549	3.668	0.000	10.412
Maltose SD	1.478	2.686	1.012	0.320	0.000	0.137
Mannose Ø	39.075	32.927	14.505	4.281	0.000	9.210
Mannose SD	1.998	2.733	0.566	0.614	0.000	0.760
Pectin Ø	29.110	38.030	9.245	0.000	18.005	5.609
Pectin SD	24.858	30.234	6.750	0.000	7.740	3.403
Starch Ø	37.187	33.251	13.251	4.179	0.000	12.132
Starch SD	1.079	3.000	1.197	0.395	0.000	0.674
Stroh Ø	33.649	39.274	3.198	3.129	0.480	20.271
Stroh SD	0.864	1.195	0.604	0.216	0.024	0.565
Sucrose Ø	37.420	31.154	15.430	4.510	0.000	11.486
Sucrose SD	1.162	0.728	1.665	0.136	0.000	1.155
Trehalose Ø	0.000	0.000	0.000	0.000	0.000	100.000
Trehalose SD	0.000	0.000	0.000	0.000	0.000	0.000
Xylan Ø	41.392	30.587	9.218	3.880	2.284	12.639
Xylan SD	0.689	0.885	0.766	0.166	0.163	1.665
Xylose Ø	38.338	29.441	14.927	5.112	0.000	12.183
Xylose SD	0.047	0.598	0.643	0.087	0.000	1.096

Supplementarys Chapter 5

Table 26: Stock concentrations and final concentrations of different N-sources during the testing of these.

N-source	MW [g/mol]	N-Atoms/Molecule	Final concentration [g/l]	Stock 10x [g/l]
Glutamine	146.15	2	1.459	14.590
Ammonium sulfate	132.14	2	1.319	13.192
Urea	60.06	2	0.560	5.996
Sodium nitrate	84.99	1	1.697	16.969
Arginin	174.2	4	0.870	8.695
Cystein/HCl	157.62	1	3.147	31.471
Ammonium nitrate	80.04	2	0.799	7.991
Glycin	75.07	1	1.499	14.989

Table 27: Residual glucose and produced hydrogen after growth of N. cameroonii in dependence from the amount of hydrogen added pre inoculation and the pressure inside the bottle at the beginning of the experiment. All values are mean values of a triplicate with standard deviation.

initially added hydrogen [ml]	initially added hydrogen [mmol]	initial pressure [bar]	residual glucose [mmol]	produced hydrogen [mmol]
0	0.000±0.000	1.227±0.009	0.291±0.030	0.221±0.016
2.5	0.093±0.001	1.207±0.012	0.081±0.047	0.222±0.032
5	0.188±0.000	1.213±0.059	0.123±0.050	0.191±0.027
7.5	0.277±0.005	1.293±0.017	0.188±0.106	0.201±0.015
10	0.381±0.005	1.310±0.024	0.076±0.060	0.170±0.023
12.5	0.458±0.004	1.360±0.008	0.081±0.040	0.169±0.029
15	0.565±0.007	1.387±0.031	0.050±0.065	0.136±0.034
20	0.736±0.009	1.453±0.033	0.026±0.011	0.112±0.020

Table 28: Output from the multiple linear regression in Origin evaluating the effects of the parameters hydrogen start (mmol) and pressure start (bar) on the dependent variable produced hydrogen (mmol).

Number of Points	48
Degrees of Freedom	45
Residual Sum of Squares	0.02027
R-Square (COD)	0.73165
Adj. R-Square	0.71973

	Value	Standard Error	t-Value	Prob>|t|
Intercept	0.29548	0.01371	21.55487	2.37948E-25
Pressure start	-0.05299	0.00836	-6.34155	9.70107E-8
Hydrogen start	-0.1415	0.01354	-10.45109	1.28198E-13

Table 29: Final pressure and produced hydrogen during growth on different N-sources with 0.5 mM Na2S as reducing agent. For Ammonium sulfate* 1 g/l cysteine was used as reducing agent. All values are mean values of a triplicate with standard deviation.

N-source	Pressure [bar]	Produced hydrogen [mmol]
Glutamine	1.857±0.164	0.261±0.049
Ammonium sulfate	1.790±0.216	0.203±0.053
Urea	1.163±0.009	0.002±0.002
Sodium nitrate	1.163±0.005	0.000±0.000
Arginin	1.170±0.008	0.000±0.000
Cysteine	1.167±0.012	0.000±0.000
Ammonium nitrate	1.603±0.287	0.169±0.088
Glycine	1.150±0.014	0.002±0.002
Straw	1.157±0.005	0.000±0.000
Water	1.200±0.078	0.000±0.000
Ammonium sulfate*	2.053±0.009	0.273±0.006

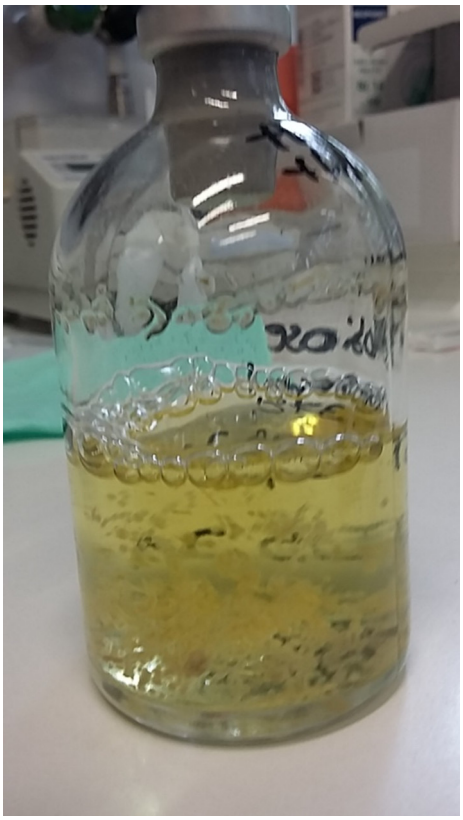

Figure 25: Morphology of *Neocallimastix cameroonii* during growth on cellobiose while agitated.

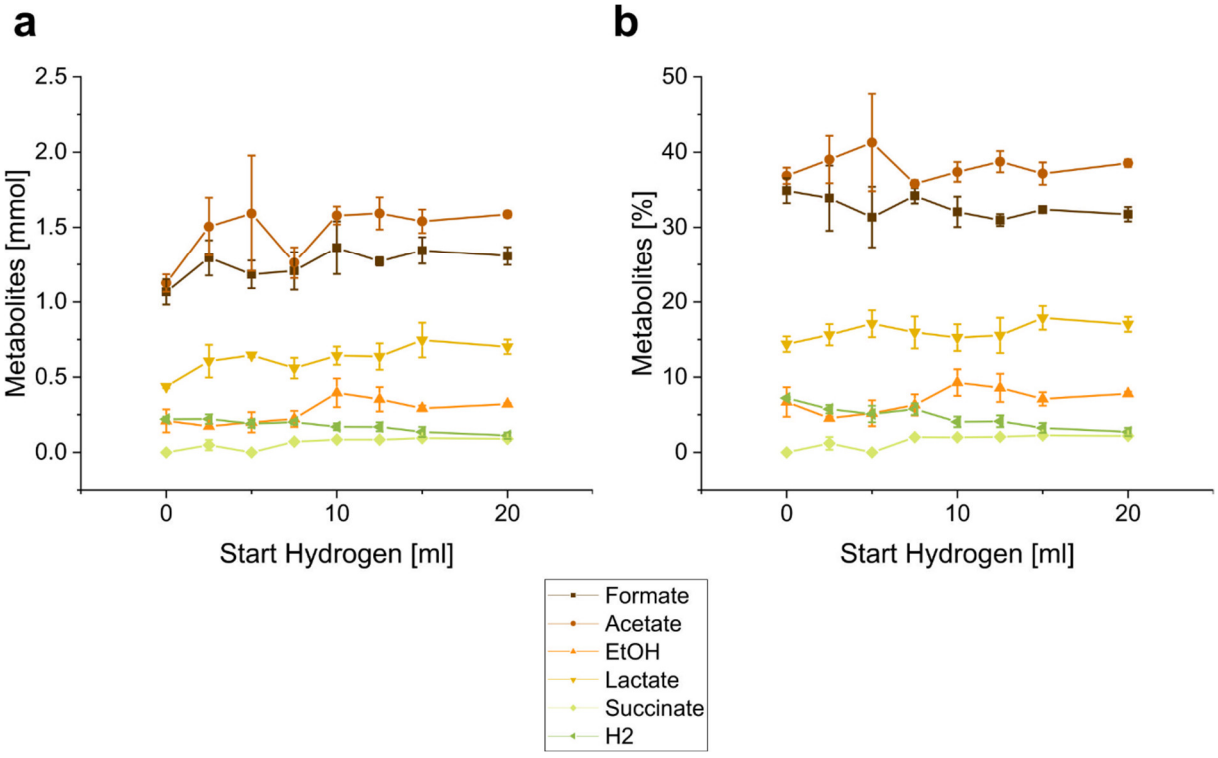

Figure 26: Effect of hydrogen addition on the metabolism of *Neocallimastix cameroonii*. a: absolute amounts of the produced metabolites; b: relative amount of the produced metabolites in relation to the total amount of produced metabolites.

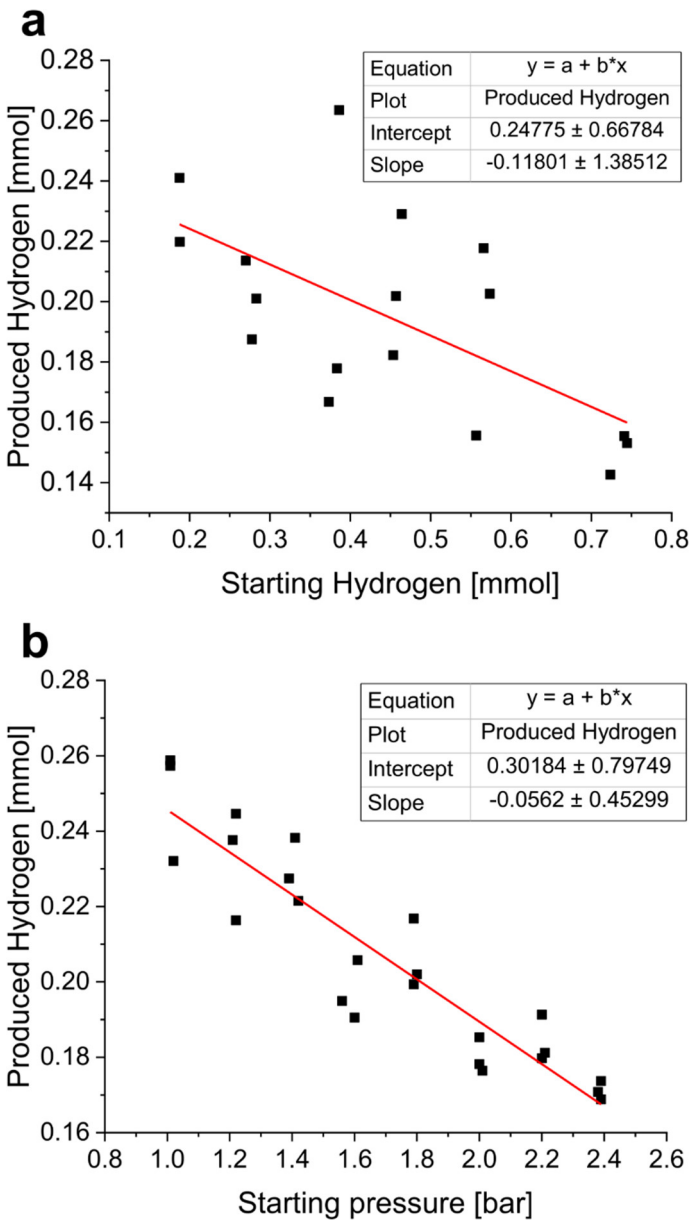

Figure 27: Effect of initial hydrogen and pressure on hydrogen production of *Neocallimastix cameroonii*. a: Effect of initial hydrogen; b: effect of initial pressure. Linear fitting was performed with Origin (OriginLabs).

Supplementarys Chapter 6

DNA sequence of Xyl43Nc as used for expression:

ATGGTAACCATCGAGAAAAGGCCTTTGGTAACAGATACTTACACGGCGGATCCCAGTGCACACGTT
TTTAATGGTAAAATCTACATTTATCCTAGCCATGATCGGGACATCGAGACTATCGACAACGATAAC
GGAGACCAGTATGATATGAAGGATTATCACGTATACGAGATGGACGATGAGAACACACTGCCTCG
CGACTGCGGCAAGGTTTTGGATATCAAGGATATTCCGTGGGTCTCTAAACAATTGTGGGCTCCGGA
CTGCGTTGAAAAAGACGGGAAGTATTATTTTTTCTACCCCGCAAGAGACAAAGAAGGCTTCTTCAG
AATAGGGGTGGCGATAGGAGATAAACCTGGCGGACCGTTCAAGCCGGAGCCCAACTACATCCAGG
GAACTTACTCGATAGATCCTTGCATCTTTCCTGACACCGACAAGAATTTCTACCTCACCTTTGGAGG
CATCTGGGGTGGCCAGCTTGATAAATATAGAAATAACGTTTACGACGAGAAAAACGAGGAACCCA
CAGGAGAGACCCCTGCAGTGTGCGCTAAGATAGCCAAGATGAACCCTGACATGAAAACGTTAGCA
GAAGCACCGCGCGATATTGTGATACTCGATGAAAATGGCAAACCCCTTACAGGGAAGGACCACGA
CCGACGTTATTTTGAAGACCCATGGCTATATAAAAAGGGCGACACGTACTATTTTACATACTCGAC
CGGTGACACGCACTTCTTGTGCTGGTCCACTAGCAAGAATGTCTATGGGCCGTATACGTATGGAGG
AAAAATATTAACACCCGTGTTGGGGTGGACAACCCACCATTCCATCCTAGAGTACCACGGAAAATG
GTGGCTGTTTTACCACGATTGCGAAATTAGTAAGGGTGTTAATCATAAGCGGAACGTGAAGTTCCG
GGAGCTGAAGTACGACGACAAGGGCGGTATTATCACAATGGACGGTACCCTAGGGGCA

DNA sequence of X11Nc as used for expression

ATGAGACTGGGAATTGCGTTAAGTACCATCGCAGTATTGCTGACTGCTACAAGTGCTAGAAATTTG
GACAAGAGACAATGGGGTTGGGGGGGTTTTGGTGGCGGTGGAAATGGTGGTGGTAAGACTATAAA
TGATTATAAACGTGAGCAAGTTAGCGGTCGTGATATCCACGTTTACGCCCCGTCAAATCTTGCCCC
AAACTCACCTCTTCTGTTGTCCTTACATGGCATGGATCAGGATCCAAATTATCAACAATCAAATACT
CATTGGGAAACATTGGCCGATAAAGAAGGATTTGTAGTAGTTTATCCCAGAGGAGGAACTGGAAT
GAGCACTTGGGACATTCAAGGTACCAAAGACACTCAATGGGTTTCACAGATTATCGACCAAATGAA
GAAAGAATACAATATAGATACTAAACGTGTTTATCTTTCTGGGTTTAGTATGGGAGGAATGTTCAC
ATATCATGCAATGTCACAAATTGCAAACAAAATTGCAGCCTTCGCCCCGTGTTCCGGTCCGAATGT
TTTCGGTGCCTCCAAGGCTCAGCGTCCAGTTCCTATCTTCCATGTTCATGGCACTAACGATGATGTT
CTAAACTATAACCAGGTGGAGGGGTTCCTGAAGAATTACCGAGATCAGTTCCACTGCCCCTCACAA
GCTGACACTAAGACAAACTACCCAAACAGAGAGAATCCTAATGCAACCCTGTATAGCTGGGGTCC
ATGCGATAAAGGGGTTTACATTAAACATTTAAAATTGCAAGGGAGAGGCCACTCCCCTTCTAGTGC
GGACATTGAGGACATCTGGAACTTTCTGAAGGAATACACTGTTGATGGACCAGTCTCAGCTAGCGG
TAATACCAACCCAACAACAGGAGGTAACGGCGGTAACGGAGGCAATGGTGGTAACGGTGGAAACG
GTAATTCAAACGCGAAGTGTAGTTCAAATATAACTAAACAGGGGTATAAGTGCTGTTCGTCTAACT
GTGAAGTGGTCTACACTGACACCGACGGAGACTGGGGTGTTGAAAATGACCAATGGTGTGGATGT
GGAAACAGAGTCACTGTTGGAAATGGGACCTGTTCAGCTAAGATTACCTCCCAGGGATATAAGTGT
TGCCCAAACGGTTGTATCATTTATTATACTGACGATGATGGTACTTGGGGTGTTAACAACGACGAG
TGGTGTGGTTGCGGAGGCGGATCTAATAACGGCCAATCAAACGGCGGCTCTAGCTCCAATGGTGGT
TCTTCCTCCAATGGTGGTTCTTATCAAGGTGCCGGCAATACAAATTTCTGCTCTAATGCCAAGCACT
CGGGTAAGTCCGAAAAAGTAACCTCCAACAAAGTTGGTTCGATTAATGGGATAGGTTACGAGCTTT
GGTCAGACTCTGGTAACAATTCAGCAACTTTCTATGAGGACGGATCGTTCTCCTGTTCATTTCAGTA
CGCTAAAGACTACCTATGTAGATCGGGTCTGTCATTTGACTCCACCAAAACTCACCAACAGATCGG
ACATATATACGCTGAATTTAAATTAGTCAAGCAAAACATTCAGAACGTTGATTATTCTTACGTTGG
AATATATGGCTGGACACGAAACCCTTTAGTTGAATTTTACGTTGTTGATAACTGGTTGTCTCAATAT
CGGCCTGGAGACTGGGTTGGGAACAAAAAACACGGAGATTTCACTATTGACGGAGCCAAGTACAC
AGTGTATGAAAATACAAGATATGGCCCTAGTATAGATGGAAACACCAACTTCAAACAATACTTCTC
AATAAGACAACAGCCTAGGGACTGTGGTACTATAGATATTACTGCACATTTTCAACAATGGGAGAA
ATTAGGGATGACTATGGGTAAAATGCATGAGGCTAAAGTGTTGGGAGAGGCAGGTTCAAACGGAG
GAGGTACGTCTGGTACCGCCGATTTTCCATATGCGAAAGTTTACGTTAAGAAT

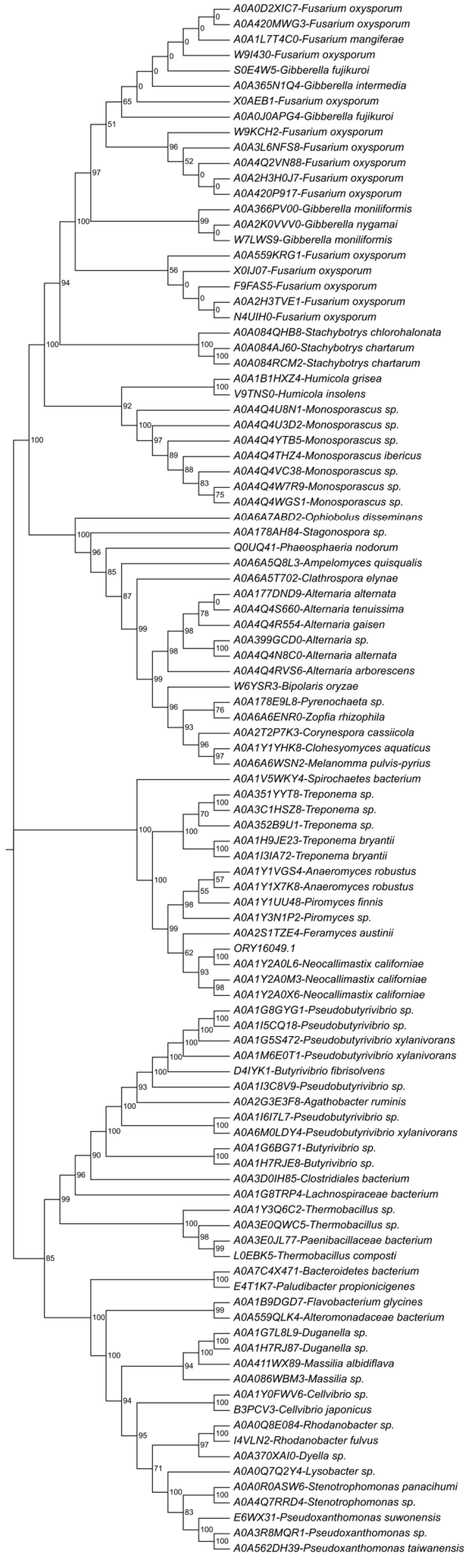

Figure 28: Phylogenetic relationship of Xyl43Nc to other GH43_1 enzymes with bootstrap values. Sequences were aligned using T-Coffee [275]. Phylogenies were reconstructed using IQ-TREE v2.0.3 [214] with the automatic model selection (WAG+I+G4) and –bb 1000. The resulting tree was rooted on midpoint.